Drug development and immunological characterization of Acinetovax, a prophylactic vaccine against resistant nosocomial bacteria *Acinetobacter baumannii*.

Carlos Berrio Íñigo

Ph.D. thesis

Advanced Immunology Ph.D. Program

Co-directors: Elisabet Rosell i Vives and Carme Roura i Mir

Department of Cellular Biology, Physiology, and immunology

Faculty of Biosciences

Universitat Autònoma de Barcelona

2022

UAB
Universitat Autònoma de Barcelona

Memoria presentada por Carlos Berrio Íñigo para optar al grado de Doctor en el Programa de Doctorado en Inmunología Avanzada por la Universidad Autónoma de Barcelona

Carlos Berrio Íñigo

Trabajo realizado bajo la dirección de las doctoras Elisabet Rosell i Vives y Carme Roura i Mir

Elisabet Rosell i Vives

Directora

Carme Roura i Mir

Directora

30 de noviembre de 2021

Este proyecto de investigación se ha elaborado en colaboración con la empresa Laboratorios Reig Jofre en el Plan de Doctorados Industriales, convocatoria DI 2017.

Responsable y tutor del proyecto en la empresa:

ELISABET ROSELL VIVES - DNI 46323853J	Digitally signed by ELISABET ROSELL VIVES - DNI 46323853J Date: 2022.01.14 09:22:32 +01'00'

Dra. Elisabet Rosell i Vives,

Bellaterra, 12/01/2022

Agradecimientos:

Esta tesis doctoral se ha realizado gracias al financiamiento de las siguientes instituciones y empresas:

Me gustaría comenzar los reconocimientos agradeciendo profundamente a todas las personas que han permitido que haya podido experimentar este proceso de investigación en Reig Jofre ya que mucho más allá del título, lo que me llevo es sobre todo un crecimiento personal y profesional tremendo.

Durante estos años de tesis he aprendido a luchar, a valorarme más a mí mismo, a mi trabajo y, sobre todo, a entender que el éxito de cualquier proyecto pasa siempre por

cuidar al equipo humano que lo confecciona. Todo esto lo he aprendido gracias a haber podido llevar una parte importante de la organización de un proyecto tan grande como el desarrollo de una vacuna innovadora en un entorno farmacéutico.

Quiero agradecer en especialmente el tiempo dedicado a la Dra. Rosell por la oportunidad que me brindó hace 5 años, permitiéndome hacer el máster de industria farmacéutica y biotecnológica y posteriormente confiando en mí para desarrollar este proyecto del que he aprendido tantísimo.

También quería agradecer profundamente a la Dra. Roura todas las horas dedicadas para sacar adelante la investigación centrada en la inmunología. Contigo he podido profundizar en mi conocimiento sobre la inmunología y entender que aún me queda mucho por aprender, lo que en parte me asusta, pero a la vez me emociona. Gracias de verdad por tu paciencia y tu tiempo durante estos años.

Marina, no podrás leer esto porque te has ido demasiado pronto, pero te puedo asegurar que todos los que trabajamos contigo te llevamos en el corazón. Si puedo sacar un aprendizaje sobre lo que te pasó, es que hay que disfrutar del tiempo que tenemos en este mundo con la gente a la que queremos y alejarnos de las cosas que nos hagan infelices. La vida es demasiado corta como para pasarla amargado.

De entre todas con las personas con las que he trabajado en Reig Jofre, quería agradecer especialmente a Sandra, Marimar y Mariona. Muchas gracias a las tres por estar ahí para superar las trabas que supone la tesis doctoral y el apoyo que me habéis brindado durante estos años.

equipo de LEITAT por ayudarnos con la producción de los anticuerpos con los que se han desarrollado los ensayos inmunológicos.

Gracias a Ramon, Toni y Xevi por apoyarme durante los momentos más difíciles de la tesis. Habéis estado conmigo durante todos mis años en Barcelona y me habéis acogido con los brazos abiertos. Durante este tiempo hemos construido una pequeña familia que ha sobrevivido entre otras cosas a una pandemia mundial y a un confinamiento en conjunto. Después de esto, sé que nos tenemos los unos a los otros para superar todo lo que nos venga.

Gracias también a Josepo, Elso, Manu, David, Jorge, Cristian y Martin por haberme ayudado a ser la persona que soy hoy. Ya han pasado 9 años desde que nos conocemos y espero que esta amistad perdure por siempre. Gracias a vosotros aprendí a confiar en mí mismo y a valorar la importancia de elegir bien a personas con las que puedas contar. Aunque vivamos muy lejos los unos de los otros, sabéis que me iré a donde haga falta para ayudaros si tenéis cualquier problema.

También quería agradecer a Isa, Inés y Lluís todas las conversaciones haciendo "terapia" juntos, solucionando los problemas del mundo o simplemente disfrutando de una buena conversación. Sois las tres unas personas increíbles de las que aprendo cada día. Me alegro mucho de haberos conocido y espero seguir compartiendo con vosotros pequeños momentos.

Gracias también a mi familia, que a pesar de la distancia me han apoyado en los momentos más duros de la tesis. Siempre habéis apoyado todas las decisiones que he tomado en mi vida, me habéis entendido con todas mis rarezas y me habéis escuchado cuando lo he necesitado, no hay mucha gente que pueda decir eso de su familia así que gracias de corazón.

Por último, me gustaría agradecer a Elena, por estar aquí siempre para escucharme y apoyarme. Has pasado conmigo los mejores y peores momentos durante estos años y lo has hecho sin esperar nada a cambio. Tengo muy claro que eres mi prioridad en mi vida y que todo lo que haga, pasará primero por tenerte a mi lado. Además, tu familia me ha acogido y tratado como uno más desde que empezamos a salir y ellos también me han hecho sentir como en casa, así que gracias de corazón.

Index

1. List of abbreviations and acronyms

A. baumannii: *Acinetobacter baumannii.*

Ab: Antibody.

APC: Antigen Presenter Cell.

ATTC: American Type Culture Collection.

ANOVA: Analysis of Variance.

AuNP: Gold Nanoparticles.

BCA: Bicinchoninic acid Assay.

BCR: B Cell Receptor.

BSA: Bovine Serum Albumin.

BLAST: Basic Local Alignment Search Tool.

CD: Cluster of Differentiation.

CFU: Colony Forming Units.

CMO: Contract Manufacturer Organizator.

CNM: *Centro Nacional de Microbiología*.

CRAB: Carbapenem Resistant *Acinetobacter baumannii*.

CSIC: *Consejo Superior de Investigaciones Científicas.*

CV: Coefficient of Variance.

DC: Dendritic Cell.

DMSO: Dymetilsulfoxide.

DNA: Deoxyribonucleic Acid.

DP: Drug Product.

DS: Drug Substance.

DSC: Differential scanning calorimetry.

DTT: Dithiothreitol.

ECL: Electrochemiluminescence.

EDC: 5-Ethynyl-2'-deoxycytidine.

EMA: European Medical Agency.

ELISA: Enzyme Linked Immunosorbent Assay.

FDA: Food and Drug Association.

FSC:	Forward Scatter.
GMP:	Good Manufacturing Practices.
HRP:	Horseradish Peroxidase.
IAA:	Iodoacetamide.
ICH:	The International Council for Harmonization of Technical Requirements for Pharmaceuticals for Human Use.
ICU:	Intensive Care Unit.
IFN:	Interferon.
Ig	Immunoglobulin.
IL:	Interleukin.
kDa:	kilodalton.
LDS:	Lithium Dodecyl Sulfate.
LPS:	Lipopolysaccharide.
MALDI-TOF/TOF:	Matrix-Assisted Laser Desorption/Ionization Time Of Flight/ Time Of Flight.
MDR:	Multi-Drug Resistance.
MHC:	Major Histocompatibility Complex.
NCBI:	National Center for Biotechnology Information.
NHS:	N-Hydroxy succinimide.
NK:	Natural Killer.
OD:	Optical Density.
Omp:	Outer membrane protein.
PAMP:	Pathogen-Associated Molecular Patterns.
PBS:	Phosphate Buffer Solution.
PCR:	Polymeric Chain Reaction.
PDR:	Pan-Drug Resistances.
.PEG:	Polyethylene Glycol.
PMA:	Phorbol 12-myristate 13-acetate.
PMDA:	Pharmaceuticals and Medical Devices Agency.
PRR:	Pattern Recognition Receptor.
REA:	Recombinant Antibodies.

RH:	Relative Humidity.
ROS:	Reactive Oxygen Species.
rpm:	revolution per minute.
RPMI:	Roswell Park Memorial Institute.
SD:	Standard Deviation.
SDS:	Sodium Dodecyl Sulfate.
SOP:	System Of Procedure.
SSD:	Side Scatter.
TAP:	Transporter associated with Antigen Processing.
TCR:	T Cell Receptor.
TG:	Thioglycolate Broth.
TEM:	Transmission Electron Microscopy.
TGF:	Tumor growth Factor.
Th:	Helper T cell.
TLR:	Toll-Like Receptor.
TMB:	3,3',5,5'-Tetramethylbenzidine.
TNF:	Tumor Necrosis Factor.
TSB:	Tryptic Soy Broth.
USP:	United States Pharmacopeia.
UTI:	Urinary Tract Infections.
WB:	Western Blot.
WHO:	World Health Organization.
XDR:	Extensive-Drug Resistances.

2. Summary

This industrial Ph.D. thesis aimed to transfer the vaccine Acinetovax from a biotechnological company to a pharmaceutical company where it could be industrialized. This vaccine has been developed to prevent infections by *A. baumannii* resistant strains in nosocomial environments. This is an opportunistic bacterium that has developed antibiotic resistances and is nowadays a real problem in hospitals worldwide.

Therefore, to improve the protection to *A. baumannii* infections in these environments, an innovative vaccine, Acinetovax, was developed by the company Vaxdyn and was transferred to the pharmaceutical company Reig Jofre in order to develop the final formulation of the drug product that could be tested and eventually administered.

Prophylactic vaccines have countless issues during their development and their market phases because they are inoculated into healthy individuals to prevent infections and can provoke, in some cases, adverse effects. This scenario forces these products to be safer and more effective than other drugs.

The tools to study the effectiveness of the vaccines are limited, and most of them are centered on characterizing the immune response induced. The use of animal models in pre-clinical assays using vaccines to prevent infections allows scientists to monitor survival after infection, to analyze the cellular immune response induced in spleen and the lymph nodes, or to study the humoral response through immunoglobulin determination. On the contrary, in the clinical stage, the only way to evaluate the immune response is on sera samples, so it is essential to develop robust ELISA methods.

The first step in the transference process consisted of developing a battery of analytical techniques based on the humoral response induced by the vaccine and validate the method following international guidelines. The main analytical method developed was a sandwich ELISA to quantify in the pharmaceutical product, the immunodominant protein identified, Omp22.

A second objective was to develop and characterize the pharmaceutical formulation of the vaccine. Several batches were designed to optimize the formula and were tested with the developed techniques. The main objective of the new formulation was to achieve a stable drug product that could maintain its protective capacity. The stability of the developed formulation was demonstrated with evidence obtained through the analytical techniques validated.

The third objective was to study the immune response induced by the vaccine. The humoral immune response was studied in an *in vivo* mice model of sepsis measuring survival and specific antibody production in serum. ELISA determination of the different IgG and IgM isotypes, in addition to showing robust results, is essential for the initiation of the clinical phase of the vaccine. The cellular immune response was analyzed by flow cytometry, where cytokines produced by splenocytes of immunized mice were determined.

In summary, most of the objectives of the thesis were achieved and the work conducted to a vaccine formulation better prepared to enter the clinical phase, the next step of the developmental procedure.

3. General hypothesis and objectives

3.1 Hypothesis

Acinetovax is a vaccine that can be transferred from a research stage of development to an industrialized production environment which will allow it to achieve a closer step towards clinical phases.

3.2 Objectives

The general objective of this thesis project was to develop a new vaccine against *A. baumannii* infections and take the development process closer to the clinical phase. Therefore, the specific objectives were:

- Characterize the humoral response produced by the vaccine Acinetovax, detect the immunodominant proteins and develop analytical methods to characterize the vaccine following international guidelines.

- Develop and optimize a galenical formula that maintains the vaccine-induced protection in an *in vivo* sepsis mouse model against *A. baumannii* infections and improve the stability of the formula.

- Characterize the cellular response produced by the vaccine Acinetovax in a sepsis mice model.

4. General introduction

4.1 *A baumannii*

4.1.1 Taxonomy

Acinetobacter is a taxonomical genus identified in early 20th century. Although, in 1954 Brisou and Prévot designed this group as *Acinetobacter* (1). This name refers to the characteristic of the bacteria of being a non-motile genus (1). In 1972 were settled the main characteristics of the genus, and four years later, in 1976, this genus was related to the *Neisseriaceae* family of bacteria (2,3). After developing different new techniques to improve the study of the bacterial phenotype, one of the most robust taxonomy classifications of the history of this genus was created, and 12 different species of *Acinetobacter* were identified (4). The *Acinetobacter* genus was reclassified into the *Moraxacelacea* family inside the Gammaproteobacterial Order in the '90s decade and has not been changed since then (5–7).

Nowadays, *Acinetobacter* is a bacterial genus characterized as a non-highly virulent and ubiquitous bacteria in water and soil (8). Currently, this genus is composed of 50 species of bacteria, including *Acinetobacter baumannii*, the focus of this thesis project (9).

4.1.2 Biology

The *Acinetobacter* genus is a group of gram-negative bacteria between 1 and 2.5 μm in length. They have a variable morphology during the reproduction cycle, acquiring a bacillar form (figure 1) during the exponential phase and creating a colloidal form during the stationary phase, in which they get grouped. The differentiation between species based on phenotype is difficult because of the similarities between different species of *Acinetobacter* (10).
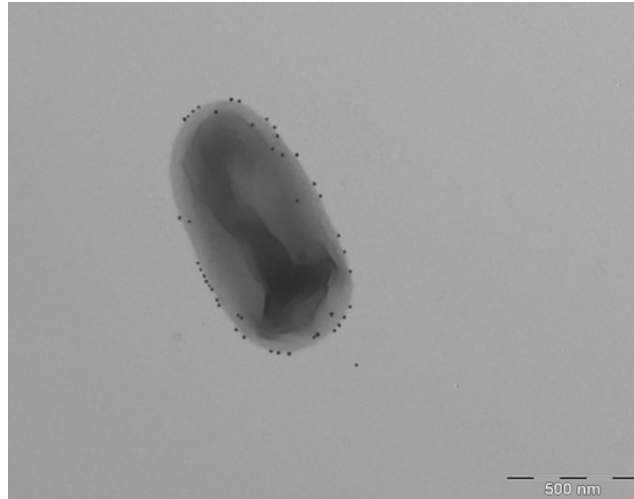
Figure 1. Coccobacillus *A. baumannii* obtained in this thesis, TEM analysis.

All species of the genus are non-motile, non-colored, encapsulated, strictly aerobic, oxidase and indol negative, positive catalase, and non-fermenting. (11). *Acinetobacter* is a mesophilic genus of bacteria that lives at temperatures around 37ºC even though environmental bacteria may prefer lower temperatures than 37ºC (12). *Acinetobacter* is also a versatile genus that can quickly grow in a simple medium that facilitates the survival in a wild environment (8).

Species of this genus might be present in human mucosa and open wounds. Some studies show that a 43% of non-hospitalized individuals are carriers of *Acinetobacter* strains (13,14) and it is also present in the general population (15).

One of the main characteristics of the bacteria included in this genus is that they are gram-negative. These bacteria have an internal membrane formed by a double layer of waterproof phospholipids surrounding the cytoplasm. The lipidic bilayer regulates the entrance of nutrients, metabolites, and macromolecules into the cell. This layer is surrounded by the periplasmatic space in which a bacterial wall can be found. Finally, there is an external membrane composed of phospholipids and the lipopolysaccharide which is in contact with the exterior of the cell. The external membrane has an essential function for the bacteria, and it is crucial for the cell's survival in different environments. The virulence and pathogenicity of gram-negative bacteria are mainly due to components of the lipopolysaccharide.
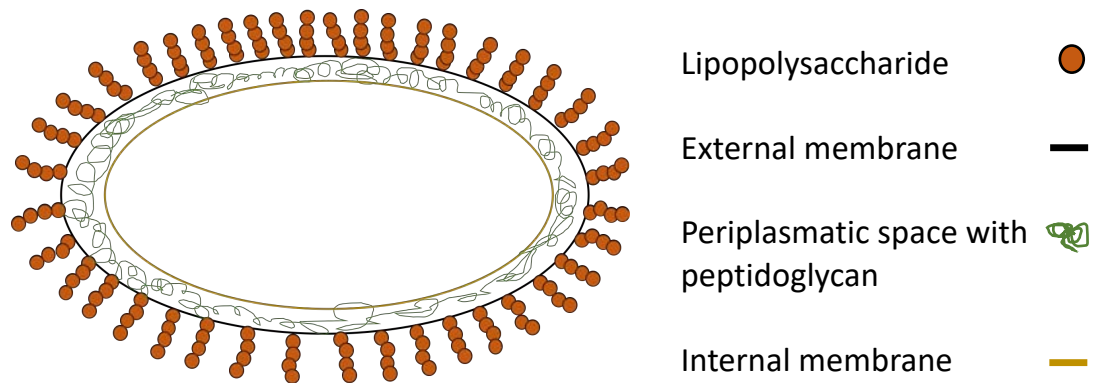
Figure 2. General composition of gram-negative bacteria.

<u>Biofilm formation</u>

A. baumannii can survive extreme conditions due to its capability to change its state between planktonic and biofilm production. Biofilms are extracellular matrix of protein, polysaccharides, and other small molecules. In its planktonic form, bacteria can proliferate but are also susceptible to environmental changes. Though, the biofilm state protects bacteria from environmental challenges and promote their survival under extreme conditions. Further, in this biofilm state bacteria communicate with each other through quorum sensing (16).

Biofilms can easily attach to almost any kind of surface, such as plastic, glass, and metals. In hospitals, biofilms bind to catheters, mechanical ventilators, and other medical fungible materials (17). Biofilm risks long and medium-term ICU patients and those under mechanical ventilation, aged, going to surgery, under dialysis treatment and parenteral nutrition and also low birth weight newborns (18–20).

4.2 Virulence factors and host interaction

A. baumannii has several specific and non-specific virulence factors which help bacterium to colonize an infect the host. These virulence factors play an important role in: resistance against innate immunity, bacterial replication, cell adhesion, biofilm formation or interaction with other bacteria, among others (21).

Of the different virulence factors, OmpA is one of the most studied and characterized. This is a highly conserved protein among different *A. baumannii* strains and plays an important role in the pathogenesis of other gram-negative bacteria, it interacts with host cells inducing inflammatory and innate immune responses. Also, iron plays an important role in the bacteria pathogenesis, it elicits the bacterial dissemination in the blood of the host during pneumonia (21).

Also, regarding the interaction with the host, *A. baumannii* is not a threat to healthy individuals, but causes problems to ICU patients or immunocompromised patients. This bacterium interacts with the host early during infection, being recognized by host pattern recognition receptors, leading to a proinflammatory cytokine and chemokines production. These responses generate the attraction of macrophages and neutrophils. *A. baumannii* infections are successful when the immune system response of the host is avoided (21).

Although, the interaction of *A. baumannii* with the host and the immune response elicited has not been characterized yet (21).

4.3 Pathogenesis

Gram-negative opportunistic bacterial pathogens are responsible for 2–10% of all Gram-negative hospital infections despite that *A. baumannii* was considered to have lower virulence compared to other gram-negative bacteria such as *Pseudomonas* aeruginosa or *Klebsiella pneumoniae* (22,23). Although, this pathogen's incidence has increased in the last decades, *A. baumannii* has become the main infectious agent affecting intensive care unit

(ICU) patients. Further, *A. baumannii* has been classified by the Infectious Diseases Society of America as one of the six most relevant multidrug-resistant (MDR) microorganisms in hospitals worldwide (24,25). The estimated global incidence of *A. baumannii* infections is approximately 1.000.000 cases annually (6,26).

Most *A. baumannii* infections affect to one of these four groups of patients: 1) infections acquired by ICU patients; 2) healthcare-associated infections acquired outside ICU setting; 3) infections in trauma patients often following natural disasters such as earthquakes or war outbreaks and finally, 4) general population acquired infections leading to pneumonia, bacteremia or meningitis (27). Most of the infections and deaths occur in ICU settings (28) and nowadays, the mortality rates have increased in Europe and the USA between 8 and 14% (20). These rates have also increased in other parts of the world, such as Central and South America (20).

A. baumannii can cause diseases in any system and organ of the host, especially after invasive treatments that disrupt the body's natural barriers (29). Infections are common in patients suffering from an underlying disease or who have undergone major surgical procedures. *A. baumannii* can quickly enter the body through open wounds, intravascular catheters, and mechanical ventilators. Infections caused by *A. baumannii* are associated mainly with extended periods of hospitalization (13). However, the most acute infections, with the highest mortality rates, are ventilator-associated pneumonia and bloodstream infection (30).

Some studies suggest that these nosocomial infections produced by *A. baumannii* are starting to spread outside the ICU environment (31,32). Due to the antibiotic resistances, biofilm production, and their capacity to survive prolonged periods in the environment, this bacterium has become one of the most successful pathogens in healthcare systems, becoming endemic. This alarming situation of *A. baumannii* incidence must be considered a significant threat to hospital patients, and new treatments should be developed to stop the spreading of nosocomial multidrug *A. baumannii* infections.

4.3.1 Respiratory infections

A. baumannii is responsible for pneumonia and tracheobronchitis in some patients (27,33). A significant proportion of these patients are colonized, but some develop clinically significant respiratory tract infections (27). Some studies suggest that *A. baumannii* infections are directly associated with an increase in death ratios (34). The patients who have to use mechanical ventilation are the most significant group at risk of suffering these infections, increasing the incidence up to a 27% (35).

Different epidemiologic studies have determined that *A. baumannii* is the fifth cause of pneumonia right behind *P. aeruginosa* in ICU patients (36). This specific illness has a bad prognosis with an attributable mortality between 8-23%, increased in cases of ventilation-associated pneumonia to 40% (37–39).

4.3.2 Bloodstream infections

Bacteremia is the second most frequent nosocomial infection produced by *A. baumannii* (40). The most common clinical cause of bacteremia is pneumonia (41), but the next principal cause is intravenous catheters. Some other causes are urinary tract infection, skin infections, or burns (42). The mortality rate of bloodstream infection is around 40% (43).

Bacteremia caused by *A. baumannii* used to be polymicrobial infections caused by various genotypes of bacteria. In this kind of infection, the bacterial synergy is essential in the invasion mechanism and the mortality cannot easily be attributed to *A. baumannii* (44). A study performed in the US presented *A. baumannii* as the cause of the incidence of 1.3% in nosocomial bacteremia, the 10th most frequent pathogen, but with the 3rd highest mortality after *P. aeruginosa* and *Candida spp.* (43). In general, the mortality produced by *A. baumannii* is considered high, and some studies show mortalities between 20% and 70% (45). This percentage was determined by risk factors related to the mortality of this infection.

4.3.3 Urinary tract infection

Urinary tract infections are sporadic in hospitals. Most of the isolated strains of *A. baumannii* obtained in urine biologic samples are the product of colonization that has not become an infection yet (46). The highest risk groups are elderly patients that use urinary catheters permanently.

4.3.4 Central nervous infections

The most frequent central nervous infection caused by *A. baumannii* is acute meningitis. Nowadays, most meningitis cases have a nosocomial origin, usually derived from direct interventions in the central nervous system such as surgeries (40). A study performed in 1997 showed that *A. baumannii* meningitis-associated mortality was around 20-27% (47). Although, mortality rates have increased until 70% in a study performed more recently (48).

4.4 Antibiotic resistance:

Acinetobacter baumannii is the most representative species of this genus of bacteria, because it has recently started causing opportunistic nosocomial infections and throughout the last 25 years has become significantly important becoming a world-threatening pathogen (13). Most of *A. baumannii* virulence is also due to its capacity to form biofilms that help bacteria to survive under extreme conditions and show antibiotic resistance (16).

Generally, patients such as ICU patients using automatic ventilators and critical patients with compromised skin integrity are the population with higher risk (13). The two main clinical manifestations of *A. baumannii* infection are pneumonia and bacteremia. Other infections include urinary tract infections (UTIs) related to biofilm formation in urinary catheters or percutaneous nephrostomy. (6)

Compared with other clinical bacteria, *A. baumannii* has an excellent capacity to develop drug resistance in short periods. This characteristic is due to the evolutionary history of these species which lives in the soil, and is in contact to antibiotics present in fungus, animals, and plants(49,50). This was increased due to the selective pressure after the administration of broad-spectrum antibiotic and transmission of strains among patients (49,50).

In 1970 most antibiotic treatments were effective against *A. baumannii*, but nowadays, there are some *A. baumannii* strains resistant to all kinds of antibiotics (51). Therefore it has been included in the Multiple drug-resistant (MDR) bacteria group known as ESKAPE (52). The name of this group references the acronyms of *Enterococcus faecium, Staphylococcus aureus, Klebsiella pneumoniae, Acinetobacter baumannii, Pseudomonas aeruginosa,* and the *Enterobacter genus* (52).

Antibiotic resistances are separated into different threatening levels; multiple drug resistant (MDR) is milder and implies non-susceptibility to ≥1 agent in ≥3 antimicrobial categories. The next step of susceptibility is extensive drug-resistant (XDR), which implies resistance to ≥1 agent in all but ≤2 antimicrobial categories. The most threatening category is pan-resistances (PDR), composed by strains non-susceptible to any kind of antibiotic used nowadays (50,53,54).

This situation has forced the World Health Organization (WHO) to classify *A. baumannii as* one of the top priorities to develop new treatments (55). *A. baumannii* is nowadays one of the six most relevant multidrug-resistant microorganisms in hospitals worldwide (56,57).

4.4.1 Treatment for *A. baumannii* infections due to resistances

Carbapenems have been historically the best therapeutic option for treating MDR *A. baumannii* (28,50). Carbapenem-resistant *A. baumannii* (CRAB) can be treated with tigecycline and colistimethate as alternative agents. For example, colistin and polymyxin B are used to treat XDR *A. baumannii* (50). *A. baumannii* strains have shown a 95% of susceptibility to colistin (50,58). However, a recent *in vitro* study on colistin resistance showed that, even though the effectiveness against this bacteria was high, a re-growth was observed in the next 3 hours and it was confirmed after 24 hours (59).

Due to the limitations of treatments against PDR *A. baumannii*, new combinations of antibiotics are being tested worldwide. These new combinations are more expensive, toxic, and less efficient (34,50,60,61). One of these antibiotic combinations is ampicillin-sulbactam. This specific combination, tested in Detroit from 2003 to 2008 showed a decrease in susceptibility to *A. baumannii* strains from 90% to approximately 40% (62).

The increase of resistant *A. baumannii* strains reduces the therapeutic options and makes the comparison difficult between clinical trials for MDR, XDR, or PDR. Also it reduces the available therapeutic option to prevent *A. baumannii* infections (6,50).

4.4.2 Mechanisms of antibiotic resistances

The fight against *A. baumannii* infections requires the understanding of resistance mechanisms developed by theses bacterial species. Many different studies were performed to understand the different kinds of resistances in order to develop new possible treatments.

Membrane transporters:

Membrane transporters are one of the critical resistance mechanisms allowing the expulsion of the antibiotic from the bacterium. The expelling of the antibiotic is usually

mediated by efflux pump proteins present in the membrane of both antibiotic-sensible and non-sensible strains of bacteria (63,64). Core antibiotic resistance-related efflux pump families are Superfamily ABC, Superfamily MF, family SMR, Superfamily MATE, and superfamily RND. Among these families, the most common transporters are *Ade*ABC, which confer resistance to β-lactams, and Tet A/B, related to tetracyclines resistance (64).

Inactivator enzymes:

Bacteria can produce enzymes that eliminate antibiotics to protect themselves and this is one of the main strategies of bacteria to survive to antibiotic treatment. One of the group of enzymes used to hydrolyze antibiotics is that of carbapenemases. This group of enzymes hydrolyzes phenazines, cephalosporins, monobactams, and carbapenems, and they belong to the groups A, B, and D of β-lactamases (65).

Nowadays, >50% of *A. baumannii* from the USA and European ICUs are carbapenem-resistant (6,66). Based on published hospital-acquired infections, 22,950 cases of CRAB infection occur annually in the United States and 75,000 cases globally (between USA, Europe and Japan). CRAB costs healthcare systems an excess of 389 million dollars and 4,590 deaths in the United States, and an annual cost of 742 million dollars globally. Also, CRAB produce and 15,000 deaths globally (26).

Membrane permeability alteration

Another method used by bacteria to increase antibiotic resistance consist of reducing the permeability of the membrane through a decrease in porins in the outer membrane. Porins are integral outer membrane proteins (OMPs) allowing the transport of molecules through the lipid bilayer membranes. A reduction on the production of porins helps bacteria to reduce antibiotic concentration in the cytoplasm (67).

Antibiotic target modification

Some bacteria change the composition of their molecular structures to achieve protection from antibiotics. For example, *A. baumannii* develops resistance to a polymyxin called colistin which was not used in hospitals for 50 years and was recovered to treat MDR bacterial infections (68). The target modification mechanism of resistance to colistin is based on the deletion of the antibiotic binding target on the lipopolysaccharide (LPS), the lipid A.(69). This structural change is the result of the deletion of the genes *lpxA, lpxB,* or *lpxC*. This genetic modification leads to the absence of lipopolysaccharide (LPS). LPS is a molecule contained in bacteria that provokes a nonspecific and uncontrolled immunological reaction. The reaction helps the bacteria to survive slipping past (70,71). However, LPS modifications forces the bacteria into a more vulnerable state to other antibiotics due to the changes produced on its membrane (69).

4.5 New approaches

The data reported in this thesis show the critical situation generated by nosocomial infections and more specifically how *A. baumannii* spreading is becoming a more significant problem in hospitals worldwide. The most straightforward conclusion obtained from all the efforts to study resistances is that bacterial evolution and adaptation are faster than human antibiotic development capacity. Recently, the World Health Organization has categorized *A. baumannii* as a top priority pathogen against which new treatments must be developed (55). Some of the new approaches undertaken to stop *A. baumannii* burden are as follows.(72).

A prophylactic vaccine to prevent the infection of MDR, XDR, and PDR are one of the most remarkable ways to stop the increase of cases worldwide. Vaccination against drug-resistant bacteria would prevent infections, reduce antibiotic use and stop the increase.

Different strategies have been proposed to develop experimental vaccines based on single purified antigens (73) or multi-component vaccines. The first group is that of vaccines composed of protein OmpA (74), Bap biofilm-associated protein (75) or the membrane

transporter Ata (76). All these approaches elicited a good immune response although survival was achieved exclusively with the OmpA protein-based vaccine, which showed partial protection. The second group uses multi-component vaccines such as outer membrane complexes (73), outer membrane vesicles (77) or formalin-inactivated whole cells (78). All vaccines from the second group developed a potent immune response and generated high protection against an *A. baumannii* murine infection model using both ATCC 19606 strains and clinical isolates (72). However, this kind of vaccines have to deal with high endotoxin levels due to the presence of LPS (72).

4.6 Strategy and design of the Acinetovax vaccine

To overcome this problem a new vaccine against *A. baumannii*, Acinetovax, was developed and constitutes the focus of this thesis. Acinetovax was shown to maintain the protective capacity of multi-component vaccines against *A. baumannii* and was LPS endotoxin free*.

4.6.1 Acinetovax vaccine development

This vaccine was developed by a biotechnology company called Vaxdyn specifically created to further characterize the vaccine and make it commercially available. The vaccine Acinetovax contains an *A. baumannii* genetically modified strain lacking LPS- due to a genetic modification and it is protected by the patent PCT/EP2015/059870. The vaccine developed in this is based on an antibiotic-resistant strain of *A. baumannii* that lacks LPS due to the inactivation of genes *lpxA, lpxB,* and *lpxC.* For this vaccine, the genes were genetically inactivated, producing the absence of LPS in the bacteria with this modification.

The vaccine showed a high protective capacity that was maintained on the different assays performed afterwards. As an example, figure 3 shows the results of an assay in which two groups of mice were immunized with two doses of the LPS(-) strain IB010 vaccine (predecessor of Acinetovax vaccine) and seven days after the administration of the second dose, were inoculated with two types of bacterial isolate, a wild type LPS(+) *A. baumannii* strain (ATCC 19606) and an LPS(-) clinically resistant isolate (Ab-154). Also, there was a

control group immunized with aluminum hydroxide (negative control) and a positive control group previously vaccinated with the ATCC 19606 (LPS+) strain. It is worth mentioning that LPS(+) bacteria cannot be used in human vaccines production because of the nonspecific immune response induced.
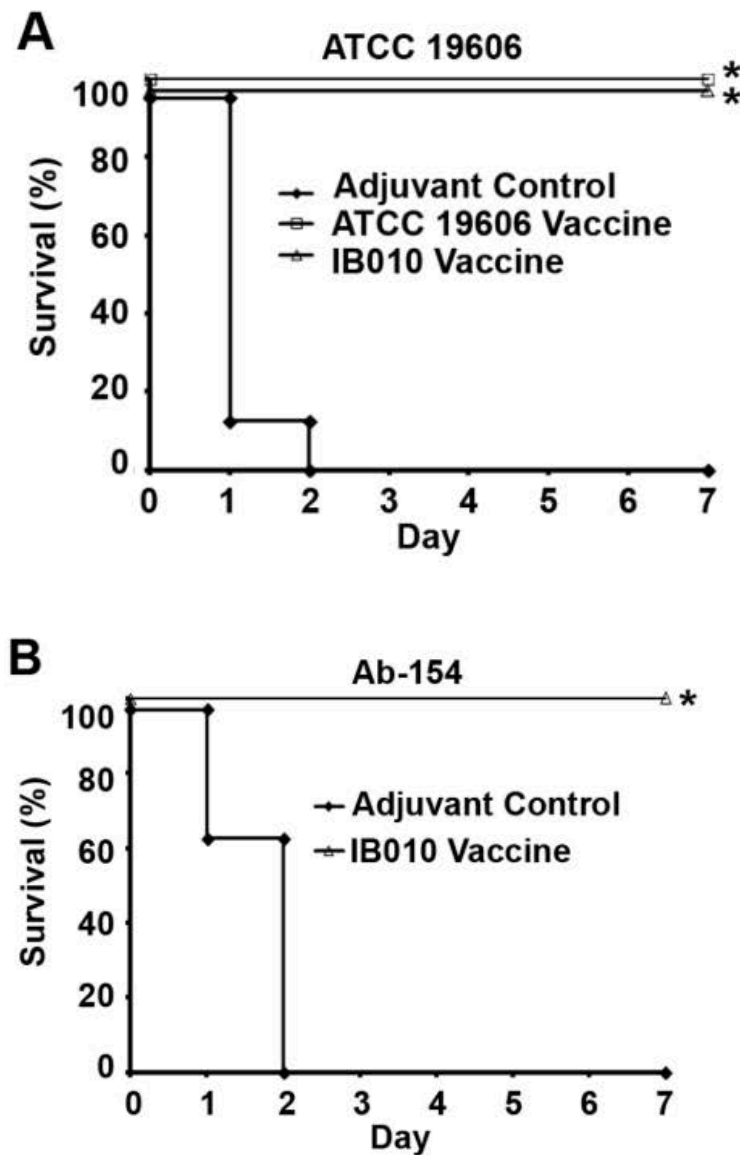
Figure 3. Effect of vaccination on a murine sepsis model of disseminated *A. baumannii* infection. Vaccinated (IB010 vaccine) and control mice were inoculated with 2.2 CFU (340.96 LD50) of the ATCC 19606 strain LPS(+) (A) or 1.056106 CFU (2.186 LD50) of the *A. baumannii* clinical isolate Ab-154 (LPS-) (B), and survival was monitored for seven days (n= 58 mice/group). * p=0.05 compared to control mice (72).

The results show that the vaccine can protect mice in a murine sepsis model of *A. baumannii* with a high protection capacity.

To develop the Acinetovax vaccine, Vaxdyn generated by genetic engineering an *A. baumannii* strain mimicking those lacking LPS.

As mentioned before, gram-negative bacteria LPS induces a strong innate immune response that can even evolve to a septic shock (79). Further, once LPS is removed the immune response changes dramatically and is mainly targeting exposed proteins of the bacteria. Vaxdyn inactivated by heat at 75ºC for 30 minutes, and the newly generated *A. baumannii* bacterial strain was administered as a vaccine together with the adjuvant aluminum hydroxide. This vaccine was tested as described for vaccine IB010 in figure 3 in a sepsis model in which vaccinated mice were infected with a clinical isolate of *A. baumannii*. The survival rate observed indicated that the vaccine can protected the animals in this sepsis model against clinical isolate Ab-154 (72).

After the development of this potential commercially interesting vaccine, Vaxdyn looked for a partner company to perform a large-scale production of the vaccine. This partner company is called Reig Jofre, a pharmaceutical company located in Sant Joan Despí, in Barcelona. It is a pharmaceutical company focused on the production of generic and biosimilar products that creates partnerships to support small biotechnological companies such as Vaxdyn.

4.6.2 Vaccine target population

As mentioned before, *A. baumannii* is an opportunistic pathogen present in nosocomial environments and has developed antibiotic resistances. The foremost affected collectives are ICU patients, especially those who use ventilator assistance, patients who go through invasive procedures, and patients who have to use parenteral administrations (41). Acinetovax vaccine has been developed thinking on patients going through these procedures.

4.7 Immune response

Thousands of microbe species, both pathogenic and non-pathogenic can be found worldwide. Pathogenic microbes are described as those with capacity to threaten normal organism functions. When this happens a pathogen specific immune response is induced in normal conditions, avoiding self-damage production (80).

A general feature of the immune system is that it detects structural features that compose the pathogen, which allows the immune system to differentiate it from self-components (80,81).

The first response triggered by infection is known as the innate immune response. This response is rapid and nonspecific. Meanwhile, the adaptive immune response depends on specific antigen recognition through receptors expressed by B and T cells, the two most important cell types of the adaptive response. Both innate and adaptive immune responses work together to stop infections produced by pathogens (80).

Cells of the immune system come from hematopoietic stem cells from the bone marrow. These cells differentiate into myeloid and lymphoid cells precursors. A scheme of these cells is shown hereafter (82).
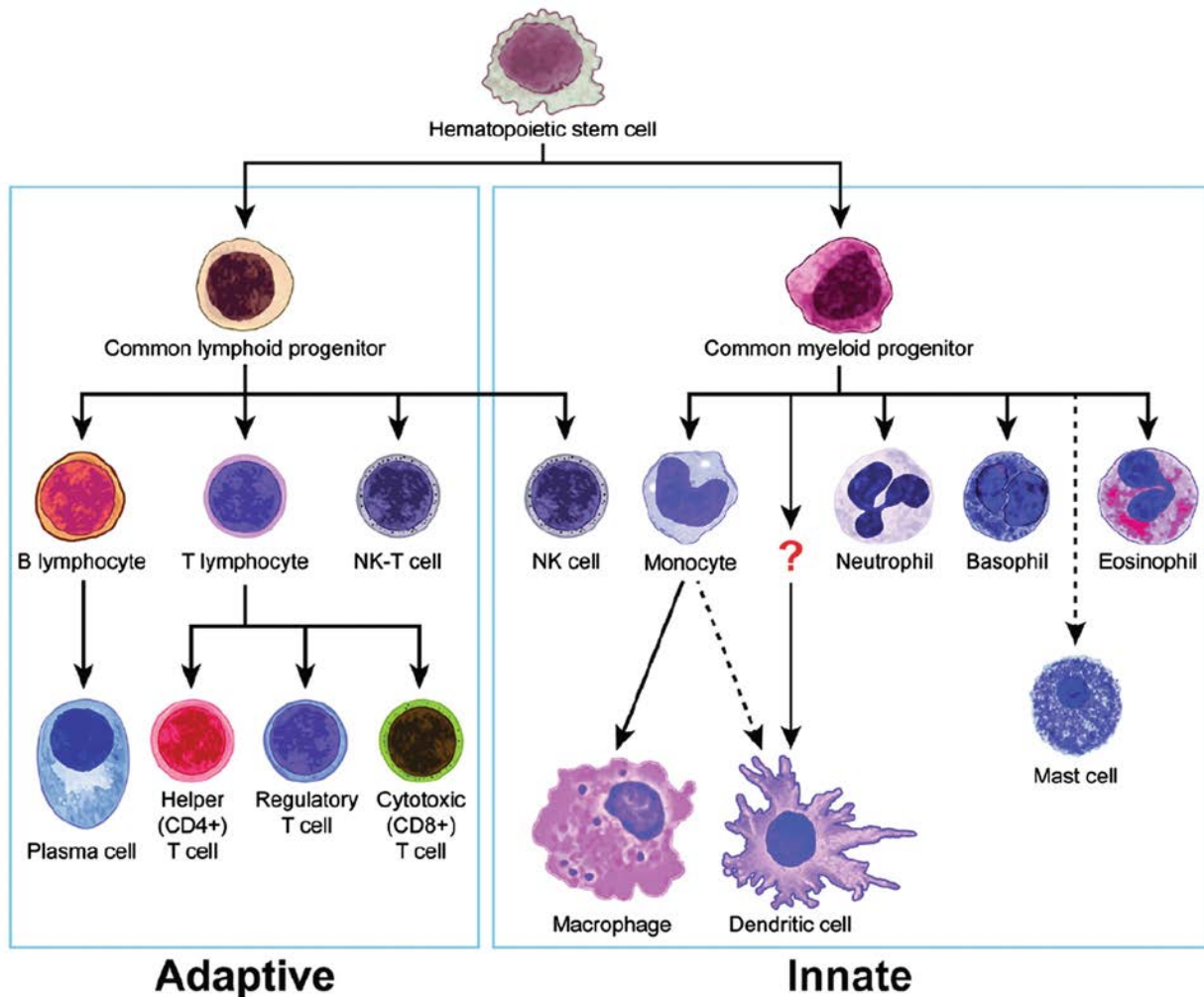
Figure 4. Myeloid and lymphoid cell strains (83).

The common myeloid progenitors give rise to many cell types such as red blood cells, platelets, granulocytes (eosinophils, neutrophils basophils and mast cells) (82). These cell types have several mechanisms to attack and eliminate pathogens. Macrophages and neutrophils phagocyte microorganisms and form the phagosomes. These are merged with cytoplasmic granules containing lytic enzymes that degrade microorganisms in a low pH and oxidative conditions with the presence of reactive species of oxygen (ROS) and nitrogen (NO). All these components degrade the microorganisms performing an essential function for host survival (82). Granulocytes immunological activity, on the other hand, consists mainly in the liberation of enzymes, oxygen reactive species that are cytotoxic to bacterial pathogens (82).

4.8 Innate immune response

The innate immune response is composed of all mechanisms of host's defense ready to act when pathogens appear. These mechanisms are physical and chemical barriers (epithelial cells, mucosa, antimicrobial peptides, among others), detection by pattern recognition receptors (PRRs) of pathogen associated molecular patterns (PAMP) and Complement System activation (80,81,84).

The innate immune response is therefore essential for host survival because it can stop the rapid spread of pathogens and it also modulates the adaptive immune response.

4.9 Adaptive immune response

Lymphoid cells precursors give rise to B and T cells, which are the basis of the adaptive immune response development. They respond to pathogens through the adaptation of B receptors and T effector cells to detect specific antigens present in pathogens (81,85).

The adaptive immune response produces specific protection and is effective after the innate immune response. Briefly, when a pathogen crosses the innate immune response barriers, tissue-resident immune cells phagocyte the pathogen and start to degrade it. Some cells, such as macrophages or dendritic cells (DCs), are known as professional antigen-presenting cells (APC) (81,84). APCs have the function to fractionate pathogens and their proteins into peptides that will be loaded onto Major Histocompatibility Complex (MHC) molecules. When dendritic cells capture the antigen they travel to the proximal lymph node. During the journey, DCs process the antigens cleaving the proteins into peptides that can be loaded onto MHC molecules, either MHC-class I or MHC-class II (85).

The peptide-MHC molecules will be recognized by T cells through the T cell receptor or TCR to start the cellular adaptive immune response.

APCs that captured exogenous antigens will present them loaded onto MHC-class II molecules to T CD4 cells. APCs will present peptides derived from cytosolic antigens loaded onto MHC-class I molecules to T CD8 cells (85).

Upon antigen recognition, T cells will become activated and differentiate to effector T cells to fight the infection. (81).

4.9.1 B cell response

Circulating naïve B cells recognize either soluble or membrane-bound antigens through their antigen-specific receptor (BCR). The BCR at this stage is an IgM and/or an IgD anchored to the membrane. Once B cells recognize the antigen, they internalize and degrade it and can present antigenic peptides loaded onto MHC-II molecules to T cells and start the T-dependent B cell activation in the follicles of secondary lymphoid organs. The antigen is recognized by T cells in the follicles specifically activated against this antigen. As a result of this interaction, together with co-stimulation through CD40-CD40L and the production of cytokines by the T cell (i.e., IL2, IL4, and IL5), B cells become fully activated (86). Cytokines are molecules of small size secreted by many cells, especially cells related to the immune system. Cytokines take part in many immunological processes, acting as mediators and regulators of the hematopoiesis.
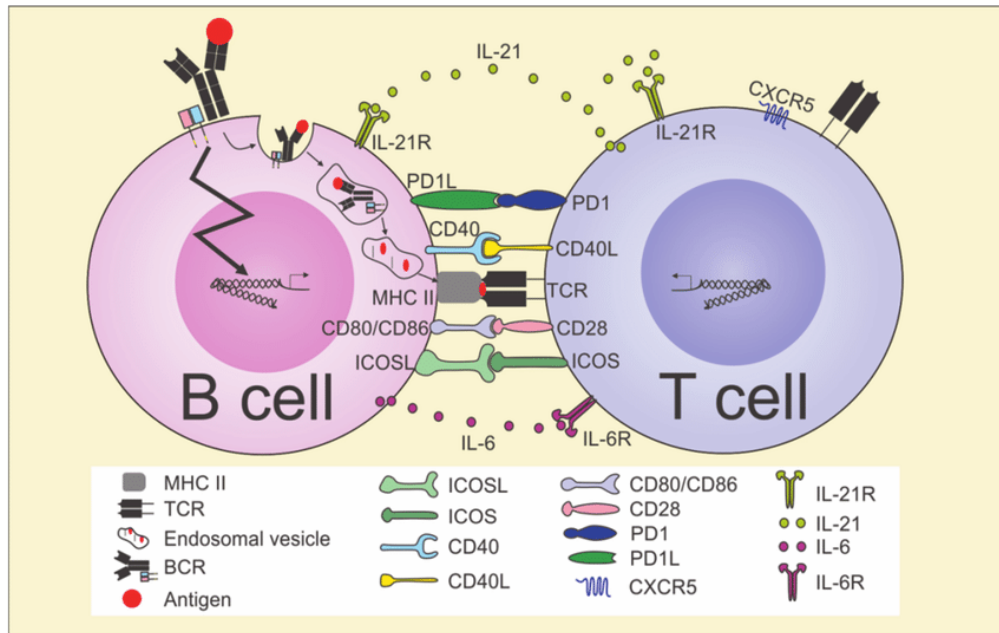
Figure 5. Scheme of B cell activation by T helper cell (87).

This activation is essential for the correct function of B cells because they induce cell proliferation, possibly isotype switch recombination, and favors BCR affinity maturation.

Further, B cell activation can lead to the differentiation to antibody-secreting plasma cells and/or to memory B cells (81).

Affinity maturation is a consequence of the acquisition of mutations on the CDR3 of the variable region of the Ig and the subsequent selection of the B cells bearing a BCR with the higher affinity for the antigen (81). As mentioned, the activation process consists of a primary response with the generation of soluble IgM short-lived plasma cells mostly. After a second contact with the antigen a secondary response based on IgG production mainly, takes place. (see figure 7) (81).
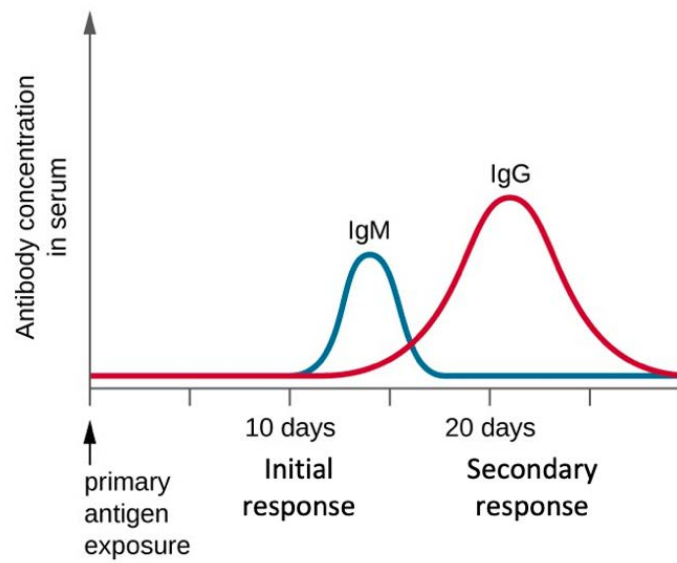
Figure 6. B cell antibody curve production (86)

Antigen-specific B cells might switch from an IgM to an IgG isotype, but also to IgA, or IgE. The isotypes generated depend on the cytokines produced during the T cell-B cell interaction. Isotype change implies changes in the effector capacity of the immunoglobulin due to their interaction with different Fc receptors expressed on different cell types. Furthermore, the affinity of the antibodies for the objective antigen can be improved upon selection in the germinal centers. (86).

45
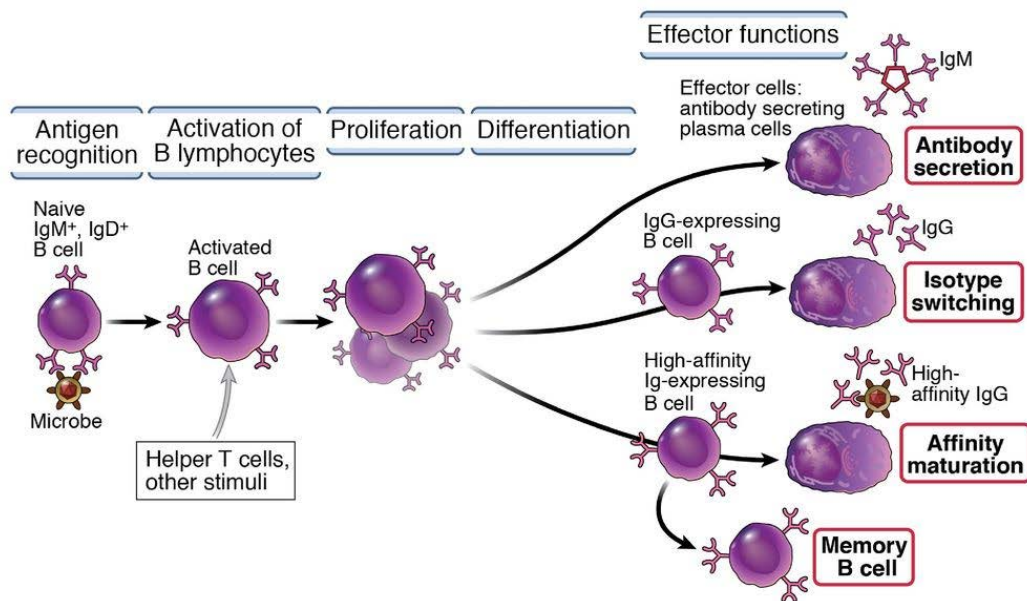
Figure 7. B cell development process (81).

Cytokines produced by T helper follicular cells (Thf) determine the isotype switch. For instance, IL-10 (humans) or IFNγ (mice) induce the switch to IgG. By contrast, switching to the IgE class is stimulated by IL-4 (81).

Also, IgG subtype production is dependent on the underlying T helper response. The four subclasses present in mice IgG1, IgG2a, IgG2b and IgG3, are related to cytokines produced by the different T helper classes (81,88).

Usually, B cells responding to T-independent antigens produce IgG3 and IgG2b antibodies that detect carbohydrates (89). Meanwhile, IgG1 production is related to Th2 responses and the cytokine IL4. In the case of IgG2a, its production is increased by a Th1 response mediated by IFN   (90). Finally, Th17 have been shown to induce a switch to IgG1, IgG2a, IgG2b, and IgG3. Interleukin IL17 secreted by Th17 cells is related to IgG2a and IgG3 production, whereas IL-21 is related to the production of IgG2b and IgG3 (88). 4.9.2 T cell response

T lymphocytes are core adaptive immune cells and have a central role in developing the immune response. This cell population expresses a TCR associated to a CD3 complex in their membrane. Further, they express either the CD4 or the CD8 coreceptor. CD4+ T cells are T helper cells, and CD8+ T cells are cytotoxic (81).

DC and other professional APCs present pathogen-derived peptides loaded onto their MHC-I or MHC-II molecules to T cells in the secondary lymphoid organs. There, multiple naïve CD4+ and CD8+ T cells with different antigenic specificities can recognize the peptide-MHC complexes through their TCR (91). CD4+ T cells will give rise to effector T helper cells while CD8 T cells will become cytotoxic effector cells (84).
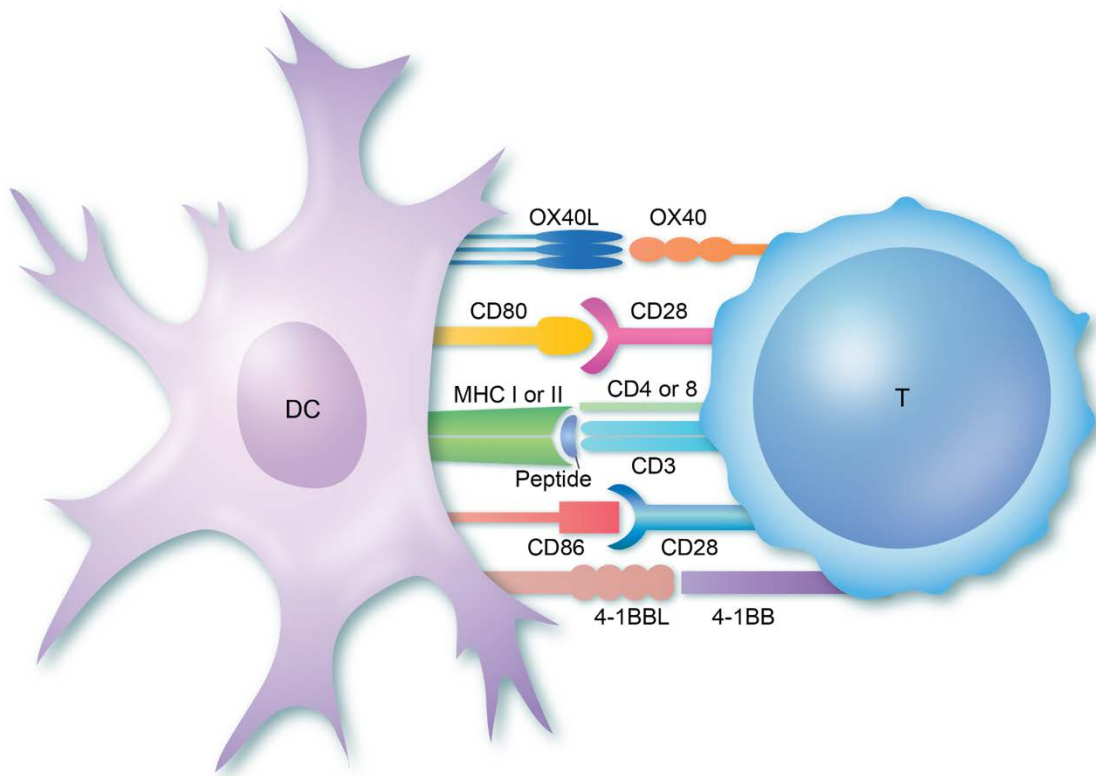
Figure 8. Antigen presentation by the dendritic cell to a Naïve T cell (92).

<u>T cell receptor</u>

T cells contain on their membrane a molecule known as T cell receptor (91). The function of this receptor, similarly to the immunoglobulins forming the B cell receptor , is to recognize antigens through their variable binding site. These receptors are generated by somatic recombination of gene segments coding for the variable, (diversity), junction and the constant gene segments of the receptor chains generating a very diverse repertoire of T and B cells with different antigen specificities (81).

Although BCR and TCRs they both recognize antigen specific epitopes, they function differently. In contrast to B cell receptors, T cell receptors recognize antigenic peptides only when loaded onto MHC molecules as described in figure 9 (81). Although, T cell receptors cannot bind free soluble antigens as B cell receptors do, they can recognize a wide variety of antigens (93). Millions of gene segment rearrangements leading to T cell receptors production allow these receptors to detect millions of antigens. (93)

<u>CD4$^+$ T Lymphocytes</u>

T helper cells can differentiate into several subtypes of effector cells, Th1, Th2 and Th17, among others (94) upon activation in the antigen recognition site, impelling the conversion of the cells into different T helper subtypes (94). Cytokines secreted during the effector phases of the innate and the adaptive immune responses participate on the differentiation of T helper effector cell subtypes (95).

CD4$^+$ T cells turn into Th1 effectors when activated in the presence of IL-12 or IFNγ. They become Th2 in the presence of IL-4 and Th17 when they are in contact of IL-6 or TGF-β. The secretion of different cytokines characterizes these T cell subtypes upon activation. Th1 cells will secret TNFα and IFNγ, Th2 cells will secrete IL4 and IL13 and Th17 will produce IL17 mainly.

The activation of these T cells gives rise to CD4 effector and memory cells. Memory cells with a lower threshold for activation will be maintained allowing the production of a faster and stronger secondary immune response.

The classical differentiation of T helper immune responses has always been that Th1 cells respond to intracellular pathogens and Th2 to extracellular pathogens. Further, it has usually been described that the two responses are mutually exclusive. However, immune responses are complex, and other T helper cell types have been described, such as Th17, Treg, Th22, Th9, and Thf cells (96).

	Signature cytokines	Immune reactions	Host defense	Role in diseases
T$_H$1 cell	IFNγ	Macrophage activation; IgG production	Intracellular microbes	Autoimmune diseases; tissue damage associated with chronic infections
T$_H$2 cell	IL-4 IL-5 IL-13	Mast cell, eosinophil activation; IgE production; "alternative" macrophage activation	Helminthic parasites	Allergic diseases
T$_H$17 cell	IL-17A IL-17F IL-22	Neutrophilic, monocytic inflammation	Extracellular bacteria; fungi	Autoimmune inflammatory diseases

Figure 9. Properties of different T cell subtypes such as Th1, Th2, and Th17 (81).

Th1 response:

In response to intracellular bacteria, and viruses, some cells such as dendritic cells and macrophages produce IL12 while NK cells secrete IFN-γ (97,98) inducing a predominant Th1 response as it was shown *in-vitro* (97,98). Also, IFN-γ is known to inhibit the induction of Th2 and Th17 responses (99).

Activated Th1 cells secrete IFN-γ, a cytokine that activates macrophages and boosts their antimicrobial activity (97). Further, Th1 cells favor the activation of TCD8 and NK cells that clear intracellular pathogens infections (81).

Th2 response:

Upon activation Th2 cells secrete IL4, IL5, IL9 and IL13 (100). The Th2 response is induced mainly against extracellular pathogens contributing to the production of specific antibodies. The immune response against parasites such as helminths requires the activation of B cells and the generation of IgE secreting plasma cells. The cytokine IL4 is responsible for the antibody isotype switching to IgE, an immunoglobulin that activates the degranulation of innate immune cells such as basophils or mast cells by cross-linking Fc receptors for IgE. Basophils and mast cells secrete different molecules that elicit inflammatory cell recruitment. In the intestinal mucosa Th2 cells also activate eosinophils by producing IL-5 and mast cells by IL9. Also, Th2 increases the production of mucus by epithelial cells (98,100).

Th17 response:

The secretion of IL17 characterizes Th17 cells (101). The Th17-mediated response induces intense tissue inflammation that contribute to the clearance of extracellular bacteria and fungi from skin and the mucosa (101). Specifically, there have been studies showing a Th17 immune response induced after the infection of Gram-positive *Propiniobacterium acnes*; gram-negative *Citrobacter rodentium, Klebsiella pneumoniae, Bacteroides spp., Borrelia spp.*, acid-fast *Mycobacteria tuberculosis* and other bacteria such as *Pneumocystis carinii.* Also after the infection by *Candida albicans* (102–108)*.
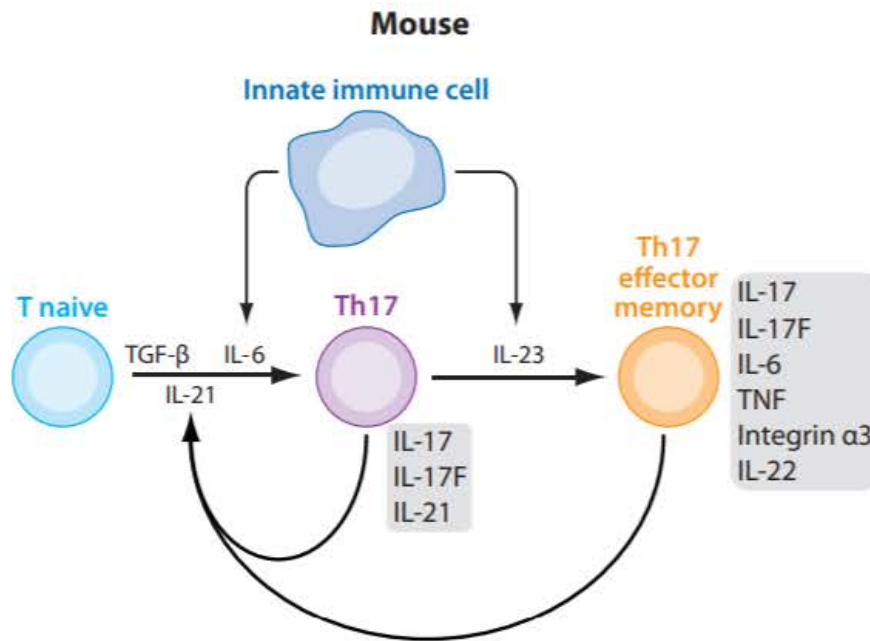
Figure 10. Th17 subset cytokine production(101).

Th17 cells secrete IL17 mainly but also they can secrete IL21 and IL22, cytokines that promote a neutrophil response at the infection site (109). Infection by *Pseudomonas aeruginosa* and *Aspergillus fumigatus* for example induce IL-17 production and, even though the infection is controlled thanks to neutrophil infiltration, IL-17 driven inflammation stops being protective and increases the risk of immunopathologies such as autoimmune diseases (101).

CD8^{+} T Lymphocytes

T CD8^{+} lymphocytes are effector cytotoxic cells mainly targeting cells infected by intracellular pathogens such as viruses or intracellular bacteria. They get activated after the recognition of MHCI-presented peptides by APCs (110). . Upon activation TCD8^{+} cells liberate the content of their cytolytic granules and induce the apoptosis of the target cell which help to avoid the propagation of the infection (81).

MHC molecules:

MHC molecules are cell membrane proteins that display mainly peptide antigens which can be recognized by T lymphocytes. There are two types of MHC molecules, MHC class I and MHC class II (84).
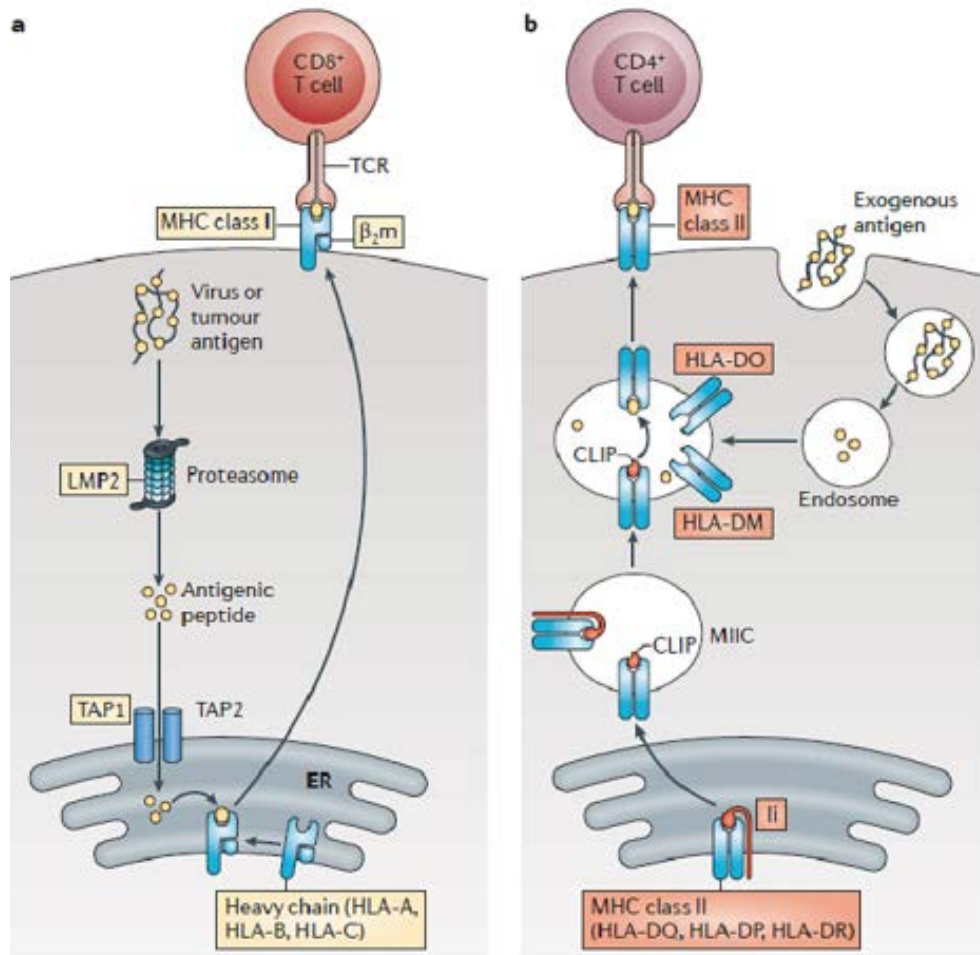
Figure 11. MHCI and MHCII antigen presentation processes(81).

MHC class I

Classical MHC class I molecules are expressed in all nucleated cells where they expose peptides derived from cytosolic proteins mainly both self or derived from intracellular pathogens (i.e., viruses). These pathogens evade some of the mechanisms of the immune system that work for extracellular pathogens such as antibodies (81).

Cytosolic proteins are cut down thanks to a multi enzymatic complex called proteasome generating peptides transported to the endoplasmic reticulum by the transporter TAP. There they can be loaded onto MHC class I molecules that are being generated there. The peptide-MHC complexes migrate to the cell membrane, where can be recognized by TCD8^{+} lymphocytes (84).

MHC class II

Classical MHC class II molecules are constitutively expressed only on the membrane of professional APCs (111). These molecules present peptides mainly derived from exogenous proteins that are internalized and degraded in the endosomal pathway (111). In this case, when a pathogen is phagocytosed it goes through a degradation pathway during which endosomal compartments containing pH specific proteolytic enzymes will generate peptides suitable to be loaded onto MHC-class II molecules (111). The peptide-MHC complexes will migrate to the membrane and be recognized by CD4+ T lymphocytes (111).

Chapter 1. Development and validation of analytical methods to study the vaccine effectivity.

5. Introduction

5.1 Development of analytical method in a pharmaceutical context

The development of analytical methods in the biotechnological products must be based on the characteristics of the pharmaceutical products, this is not always the case in small molecule products for which the techniques are limited and already fixed. The biotechnological guidelines suggest specific techniques to study the quality of the products, but they must be highly adapted.

Analytical methodology must detect when a product has lost its capacity to improve patients' heath at their disease stage. In the case of this vaccine, it is crucial to understand the immune response generated because it is responsible for the protection elicited against *A baumannii* infection. That is why most of the developed methods during this thesis use antibodies to evaluate the quality of the product.

Also, it is essential to understand the pharmaceutical environment in which the methods are being developed. Analytical methods in the pharmaceutical industry must be parametrized. Parametrization of the analytic methods consists of the definition with a high level of detail of all the steps used to perform an analytical assay. Parametrization allows scientists to define which are the critical parameters of analytical methods reducing variability, increasing robustness and therefore, improving the quality method assay.

This high delimitation of the assay methods is performed under international regulations that are followed by all pharmaceutical laboratories. There are two key regulations: Good Manufacturing Practices (GMPs) and The International Council for Harmonization of Technical Requirements for Pharmaceuticals for Human Use (ICH). Both regulations enable

scientists to control every subtle parameter of the assays performed under these regulations.

5.2 Good manufacturing practices (GMPs)

GMPs are essential for the pharmaceutical industry. These regulations help the companies to achieve compliance with the basic quality standards. GMPs ensure the quality of all pharmaceutical products during their production (112). GMPs regulation defines that every assay performed in a pharmaceutical laboratory must have traceability. Meaning that every detail has to be described and every step must be annotated (112). Therefore, it is essential to train the personnel in the different GMP regulations (112). Personnel must be qualified and must have experience, both according to their position. Also, the tasks performed by every employee must be defined and registered in a system operator procedure (SOP) (112).

The companies need to implement continuing education programs to keep their employees up to date on possible changes in the production processes. In addition, the company must train its workers on the basic rules of the use of laboratory uniform, personal protection equipment and risk management. Every product, reagent or assay solution must be correctly labeled with all the information necessary about its content and handling precautions (112).

Any equipment used for any activity inside the pharmaceutical laboratory or production area must be qualified and calibrated to assure its correct functioning. Also, all the processes and procedures performed must be validated and correctly documented. The companies must ensure adequate resources and infrastructures for the correct production of the pharmaceutical products (112).

Also, the documentation must be correctly registered to assure its traceability. For example, during the performance of an assay, the batches, and the expiration date of all the reagents and the equipment used must be registered *in situ*. These rules are essential

steps to avoid errors and to track any problem detected in the future. If there is any deviation in the procedure, the Quality Assurance department must be notified to start an investigation in which deviation effect is scrutinized (112).

5.3 The International Council for Harmonization of Technical Requirements for Pharmaceuticals for Human Use (ICH)

Pharmaceutical products are one of the most regulated products in the world due to the nature of the products manufactured. They are one of the first necessities in our world because they can cure diseases but also the treatment can damage the organism.

Therefore, regulation of medicines is essential to assure quality in health systems. During the last century, all countries worldwide have developed regulatory agencies to control safety, quality, and efficacy of the pharmaceutical products sold inside their frontiers (113)

Regulations were created after tragedies caused by poorly tested drugs such as thalidomide in Europe in the 1960s. In the first stages of the regulatory development, countries created different regulations that were sometimes divergent about the technical requirements of the products. This obliged companies to duplicate time-consuming and expensive efforts to reach the market (113).

The harmonization was therefore essential to facilitate drug products access to the international markets. In the 1990s, harmonization started to facilitate drug business between 3 entities that were leading drug pharmacopeias: FDA (EEUU), EMA (Europe), and PMDA (Japan). Harmonization was centered on the three main topics: safety, quality and efficacy. The new basis for approving and authorizing medicinal products worldwide was finally created, and it was called International Council for Harmonization (ICH). ICH was afterward accepted as the standard regulation by companies as a base to study their products and facilitate their commercialization worldwide (113). ICH has continuously evolved since then to adapt to new drugs such as antibodies, gene therapy and other biological products (113).

5.3.1 Assay development under ICH guidelines:

Regulation related to the pharmaceutical products is implemented at all stages of development, including the most initial ones. In the case of this thesis, ICH Q2 and ICH Q6B were followed to select and develop the analytical methods needed to study the product at the different stages (113). ICH Q6B is a guideline that defines the most critical parameters to be selected and studied which are:

A. The potency is defined as the capacity of a method to detect the activity of the product. In this specific case, it would be the capacity of the vaccine to elicit an immune response (113). The vaccine Acinetovax potency was determined through an *in-vivo* assay in a murine sepsis model induced by infection by *A. baumannii* in immunized mice.

B. The quantity is determined by a chosen specific parameter related to the content of the drug substance (113). In this specific case, total protein is the selected parameter. Total protein concentration is also related to the number of bacteria present in the product quantified through μBCA. A protein chosen to evaluate the stability of the product known as Omp22 was quantified by an ELISA method.

C. The identity is a qualitative parameter which is described as the ability of a method to detect a selected protein of the product. In this case, the protein Omp22, which is related with the immune response produced by of *A. baumannii* was selected as an identity marker(114). This protein can be identified through western blot. (113)

Finally, physicochemical characteristics of the drug product were also determined. Specifically, pH, osmolarity, visual appearance, reconstitution time, and residual water (the last two were explicitly used for lyophilized products) were determined (113).

5.4 Analytical development

5.4.1 Importance of antibodies in the Acinetovax vaccine development

As mentioned before, antibodies are a key tool for the analytical evaluation of the vaccine. Antibodies are molecules produced by B cells during the immune response. These molecules have a high affinity and specificity for a particular epitope, detecting it with high sensitivity. A simplified scheme of antibodies structure can be found hereafter (81).
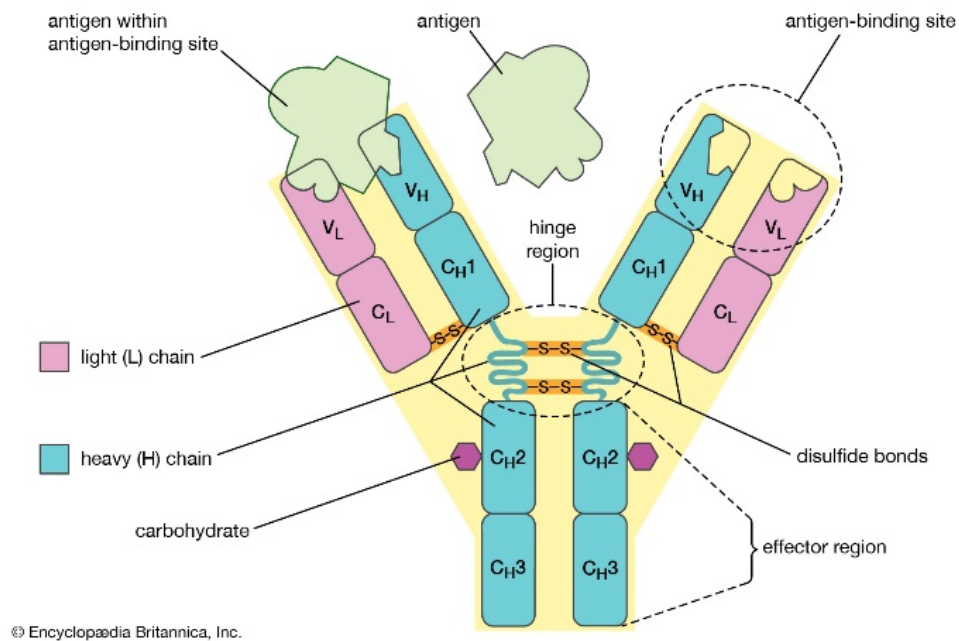
Figure 12. Antibody scheme description(115).

Antibodies are used to detect proteins in analytical methodologies such as ELISA, western blots, or flow cytometry. These techniques have been used in different ways in this thesis (81,116).

The antibodies produced in this thesis were monoclonal antibodies obtained by Vaxdyn in collaboration with LEITAT investigation center (117).

5.4.2 ELISA

Enzyme-linked immunoassay (ELISA) is an analytical technique used in molecular biology since 1941 (118,119). This method consists on the detection of the soluble antigens using antibodies conjugated to an enzyme to quantify the enzymatic response in the presence of the corresponding substrate (119). Many possible enzymes can be used to perform the ELISA: peroxidase, alkaline phosphatase, galactosidase and glucose oxidase (119). One of the most used is peroxidase, that oxidizes 3,3',5,5'-tetramethylbenzidine (TMB) into 3,3',5,5'-tetramethylbenzidine diamine (119). This product reaction is stopped with sulfuric acid, and the reaction produces a colorimetric response that can be measured by analyzing the absorbance of the product at 450 nm with a spectrophotometer (119).

There are many options to perform an ELISA assay, but they can be categorized into three main types: direct ELISA (120,121), indirect ELISA (122) and sandwich ELISA (123). See the different types in figure 13.
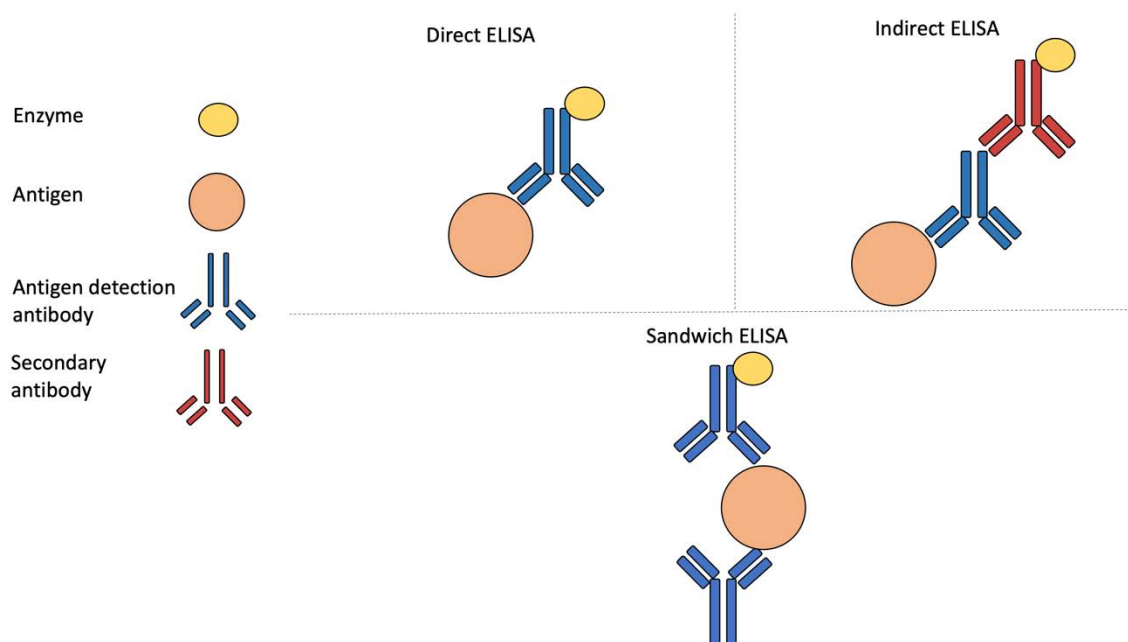
Figure 13. Main types of ELISA

Direct ELISA:

This ELISA is used to measure the amount of protein, usually for high-weight antigens. In this case, antigens are directly attached to the plate wells and then an antibody specific for this antigen, directly conjugated to an enzyme, is added (120). This procedure is followed by buffer solution washes to eliminate non-bound antibodies. Next, an enzyme specific substrate is added and the colored signal generated is quantified. With this signal, the amount of antigen present in the assay can be measured (120,121).

Indirect:

This ELISA was denominated indirect because a primary antibody recognizes the antigen however its detection is based on a secondary antibody, conjugated to an enzyme, specific for the constant region of the primary antibody. Then, the substrate that is transformed by the enzyme is added to produce a colored signal. With this signal, the amount of antigen can be measured. This method is more often used on qualitative rather than quantitative assays (122).

Sandwich ELISA:

Sandwich ELISA is a method in which the capture antibody (coating antibody) bound to the plate capture the antigens added to it. Afterwards, a second antibody (detection antibody) specific for a different epitope and conjugated to an enzyme is used to detect the different epitope of the protein. Finally, the enzymatic colored product is measured (123). This ELISA is more specific than other kinds of ELISA because, from a sample containing different proteins, the only protein captured by antibodies in the plate is the target protein. This ELISA has been described as 2-5 times more sensitive than previous ELISA methods (118,123).

In the ELISA developed to study the vaccine Acinetovax, the sandwich ELISA option has been chosen because the drug substance contains complete bacterial cells. This ELISA will

ensure that the response measured is exclusively from bacteria. This ELISA has been developed to quantify the protein Omp22 expressed on the bacteria membrane. If the selected assay had been direct or indirect ELISA not only bacteria would be attached, but also all suspended proteins and molecules. This event would be a method to quantify the protein in the whole drug product, but it was decided to focus on the bacteria.

ELISA sandwich method was also selected to be used later in the project as an *in vitro* potency assay because ELISA detection is based on the capacity of antibodies to bind to the protein Omp22, one of the immunodominant protein and target of the immune response (114). If this protein is degraded and non-detected by the antibody, this could reduce the protection induced by the vaccine.

5.4.3 μBCA

While analyzing biotechnological products, it is necessary to quantify the protein present in the sample on many occasions. One of the most used methods to quantify the protein content of a sample is the Bicinchonic acid (BCA) assay (124). This technique was developed in 1985 to determine the concentration of protein present on samples avoiding the drawbacks of other techniques such as Biuret reaction or Lowry assay. These techniques showed high variability between analyzed proteins, interference with reagents or compounds used for protein purification and problems with the analysis of hydrophobic proteins (124–127).

The BCA assay is based on the transformation of $Cu2^+$ to $Cu1^+$ due to the interaction with proteins of the sample. $Cu1^+$ reacts with bicinchoninic acid forming the BCA2 complex (124). Under alkaline conditions, the complex has an absorption at 562 nm (125). The method is simple, sensible, and does not have many interferants. This thesis uses the methodology called μBCA based on identical principles of BCA but with higher sensitivity than the BCA (124).

5.4.4 Western blot and protein profile

Western blot is a technique used in molecular biology and developed in 1979. This technique has been widely used in laboratories worldwide as a tool to detect proteins in complex or straightforward samples. (128,129).

The first step consist of running sample proteins on a polyacrylamide gel electrophoresis (PAGE) (130). Electrophoresis separates proteins primary by their molecular weight and charge in the gel. Once separated by electrophoresis proteins are transferred to a membrane for detection by western blot. In the membrane, proteins are detected with antibodies. These antibodies, as in ELISA, can be bound to different enzymes that react with the substrate. This reaction can be measured in several ways depending on the enzyme (130).

5.4.5 *In vivo* assay

The development of a pharmaceutical products usually takes several years, the average time for a product to reach the market is around ten years. This amount of time requires a considerable investment for companies and if the products fall in the process, it can mean significant losses for the company. This situation forces the companies to develop predictive *in-vivo* testing assays based on animal model research that helps to decide whether the products are suitable to proceed to the next step or not.

In-vivo assays are the key to better understand several product parameters, such as its effectivity, dose-response, toxicity, or other parameters that help to characterize the product.

The results obtained in the i*n-vivo* assays are used as a model to predict the effect of the pharmaceutical product once administered in patients.

5.5 Hypothesis:

The hypothesis of this chapter is that vaccine Acinetovax produces a potent and protective humoral response targeting specific *A. baumannii* immunodominant proteins. Antibodies isolated from splenocytes of immunized mice can be purified to develop different analytical techniques to study the quality of the vaccine Acinetovax

5.6 Technical objectives:

Characterize the humoral response induced by the vaccine Acinetovax, determine the immunodominant proteins and develop methods for studying the vaccine at different stages of the production process. To achieve this objective, we had to:

- Demonstrate that the formulations produced in Reig Jofre protect against *A. baumannii* infection in a sepsis mouse model.
- Characterize the humoral response induced by the vaccine Acinetovax.
- Detect and characterize the immunodominant proteins present in the vaccine.
- Develop and validate an ELISA test method to quantify Omp22 protein, following ICH validation guidelines.
- Develop a µBCA method to quantify total protein contained in Acinetovax formulation following ICH validation guidelines.
- Develop an electrophoresis staining method to identify the proteins that compose the vaccine.
- Develop a reproducible Western blot method to identify Omp22 contained in Acinetovax following ICH validation guidelines.

6. Material and methods

6.1 Material

Bacterial strains *A. baumannii* 167R (LPS negative and colistin-resistant), *A. baumannii* 167S, (LPS positive and colistin susceptible) (131–133) *P. aeruginosa* (ATCC27853) (28), and *E. coli* (ATCC25922) (132) were kindly gifted by and Instituto de Biomedicina de Sevilla (IBIS). Mutant LPS negative *A. baumannii* is the drug substance (VXD-001) of Acinetovax that was reported previously in an article as IB010 (72) was kindly gifted by Vaxdyn S.L (Sevilla, Spain)(72). All strains were inactivated by temperature (75ºC for 30 minutes). All vaccine Acinetovax batches were produced with drug substance VXD-001 in Reig Jofre. The difference between VXD-001 and Acinetovax was that VXD-001 just contained bacteria and Acinetovax had bacteria and other excipients such as aluminum hydroxide. Monoclonal antibodies (N1-N8 at 5 mg/mL) were obtained from hybridomas produced by LEITAT technological center (Barcelona, Spain) in association with Vaxdyn S.L (Sevilla, Spain). These hybridomas were obtained from mice previously immunized with drug substance VXD-001 (72). The rest of the reagents can be found in table 1.

Table 1. Chapter 1 reagents

General use		
Reagent	*Reference*	*Brand*
Tween 20	P2287	Sigma-Aldrich, Sant Louis, USA
Skimmed milk	2543453	Nestle, Vevey, Switzerland
PBS	524650-1EA	Merk, Darmstadt, Germany
NaCl	S7653-250G	Sigma-Aldrich, Sant Louis, USA
Alhydrogel 2%	113943	CRODA, Frederikssund, Denmark
Trehalose	T-104-4	Pfantiehl, Waukegan, USA
Sucrose	S8501	Merk, Darmstadt, Germany
ELISA		
Reagent	*Reference*	*Brand*
High binding protein 96 well plate	44-2404-21	ThermoFisher, Waltham, USA
TMB (3,3',5,5'-Tetramethylbenzidine)	T0440	ThermoFisher, Waltham, USA
Streptavidin/peroxidase	P0397	Agilent, Santa Clara, United States
µBCA		

Reagent	Reference	Brand
KIDS Solulink	SP-2002	Vector, Burlingame, USA
BSA standard (2mg/mL)	23209	ThermoFisher, Waltham, USA
µBCA reagent A	RQC3979	ThermoFisher, Waltham, USA
µBCA reagent B	RQC3980	ThermoFisher, Waltham, USA
µBCA reagent C	RQC3981	ThermoFisher, Waltham, USA
Electrophoresis and WB		
Reagent	Reference	Brand
Lithium dodecyl sulfate (LDS)	P0007	ThermoFisher, Waltham, USA
Dithiothreitol (DTT)	B0009	ThermoFisher, Waltham, USA
Electrophoresis running buffer	LC2675	ThermoFisher, Waltham, USA
Transference solution	LC3675	ThermoFisher, Waltham, USA
Electrochemiluminescence (ECL)	32209	ThermoFisher, Waltham, USA
Polyacrylamide tris-glycine gels	XP10200BOX	ThermoFisher, Waltham, USA
Goat anti-mouse-HRP antibody	10094724	ThermoFisher, Waltham, USA
nitrocellulose membranes	88018	ThermoFisher, Waltham, USA
Whatman filter paper	WHA1003917	Sigma-Aldrich, Sant Louis, USA
Simply a blue staining kit	LC6065	ThermoFisher, Waltham, USA
MALDI TOF/TOF		
Reagent	Reference	Brand
CNBr (Cyano-gen bromide-activated)-Sepharose	17043002	Cytiva, Chicago, USA
Poly-prep columns	7311550	Biorad, Hercules, USA
Mobicol	M2210	Boca scientific, Westwood, USA
MALDI-TOF MS	NC1254234	Bruker, Billerica, Massachusetts
TEM microscopy		
Reagent	Reference	Brand
Gold nanoparticles	777099	Sigma-Aldrich, Sant Louis, USA
Mercapto-ω-carboxy-PEG (Mw 5000 Da)	712523	Aldrich, Sant Louis, USA
1-etil-3-(3-dimetilaminopropil) carbodiimida (EDC)	T511307	Sigma-Aldrich, Sant Louis, USA
N-Hydroxysuccinimide NHS	130672	Sigma-Aldrich, Sant Louis, USA
Cutoff dialysis	PIER68035	VWR international Eurolab, Barcelona, Spain
Higher cutoff (100 KDa)	PIER68036	VWR international Eurolab, Barcelona, Spain

The equipment used to develop the different techniques of this thesis are summarized hereafter in table 2.

Table 2. Equipment

Equipment	Brand	Use
Victor 2030	Perkin Elmer, Waltham, USA	ELISA, µBCA
Imagequant LAS 4000 Mini	Cytiva, Chicago, USA	Western blot, Coomassie staining
speed back	Thermo Fisher, Waltham, USA	MALDI-TOF/TOF
Di-gestPro MS,	CEM, Charlotte, USA	MALDI-TOF/TOF
MALDI-TOF/TOF mass spectrometer (4800 AB)	Sciex, Framingham, USA	MALDI-TOF/TOF
Mascot database	Matrix Science, Boston, MA, USA	MALDI-TOF/TOF
Zetasizer Nano ZS	Malverns Instruments, Malvern, UK	DLS
Jeol JEM 1010 100 kv	Jeol, Tokyo, Japan	Microscopy

6.2 Animals

All experiments involving the use of animals were approved by the general director of "*Agricultura, ganadería y alimentación*" of the "*Comunidad de Madrid*" (Evaluation code: ES280800000015). In all experiments, efforts were made to minimize suffering and animals showing signs of pain and suffer during experimentation were immediately euthanized using thiopental.

The animals used to perform the in-vivo assays were C57BL/6 mice obtained from the *Centro Nacional de Microbiología* (CNM) animal facility.

6.3 *In vivo* assay

6.3.1 Mice immunization:

The immunization protocol for this assay consisted of the following steps. First, 6 to 8 weeks old female C57BL/6 mice were inoculated intramuscularly in the quadriceps muscle. Animals received 2E+09 bacteria and 1 mg of aluminum in a volume of 200µL (100 µL

injected in each leg). Animals received two doses, on day 0 and on day 14. The serum of the animals was obtained to be analyzed on day 21.

6.3.2 Mice infection model

On day 21, after the first inoculation, the sepsis model was initiated. It consisted of the intravenously administration of 100μL of the *A. baumannii LPS(-)* clinical isolate Ab-154 (134) (10^8 cfu/mL). Mice were monitored to evaluate survival for seven days. This method was described previously (135).

6.4 ELISA development method

High binding protein plates were used to bind bacteria to the plate, briefly 100 μL/well of 5E+08 bacteria/mL in PBS 1x were incubated overnight at 4ºC. Plates were washed three times with HT-PBS (PBS x1 + 137 mM NaCl), and 250 μL/well of blocking solution (PBS + 1% skimmed milk) was added for 90 minutes. Plates were washed with HT-PBS and 100 μL/well of antibodies N1 and N7 (1 μg/mL) were added to the corresponding wells and incubated for 60 minutes at 37ºC. Plates were washed with HT-PBS. Then, 100 μL/well of goat anti-mouse HRP antibody diluted 1:10.000 in blocking solution were added for 30 minutes and washed with HT-PBS. Then, Substrate, 100 μL/well of TMB peroxidase, was added. Finally, the reaction was stopped with 50 μL/well of H_2SO_4 (0.16M) and plates were read in a spectrophotometer at 450 nm.

6.4.1 Sandwich ELISA pre-validation method

The High binding protein plate was used to bind the antibody to the plate. Briefly, 100 μL/well of chosen capture antibody was added to each well of the plate, and the plate was incubated overnight at 4ºC. The plate was washed with TPBS (PBS 1X + 0.05% Tween 20). Afterward, 100 μL/well of standard and sample containing *A. baumannii* were added to the plate. Plates were washed with TPBS, and 250 μL/well of blocking solution (PBS + 1% skimmed milk) were added for 90 minutes. Plates were washed with TPBS and 100 μL/well

biotinylated detection antibodies were added to correspondent wells at 1 μg/mL for 60 minutes at 37ºC. Plates were washed with TPBS. Then, 100 μL/well of streptavidin/peroxidase reagent prepared as manufacturer indicates were incubated for 30 minutes and washed with TPBS. Then, 100 μL/well of TMB peroxidase substrate was added. Finally, the reaction was stopped after 7 minutes with 50 μL/well of STOP solution (Dilution 1:17 of H_2SO_4), and plates were read in a spectrophotometer at 450 nm.

6.4.2 Sandwich ELISA validation method

Linearity was assessed with eight calibration dilutions (n = 3) between 1.27E+07 and 1.56E+06 bacteria/mL in triplicate. Non-linear regression analysis of absorbance versus concentration was carried out, regression coefficient (R2), model fit residuals, and % coefficient of variation. (CV = (standard deviation x100)/mean) were studied.

Specificity was determined by elimination one-by-one of capture antibody, detection antibody, bacteria, and streptavidin, and no response should appear in any of the tested conditions. The blank threshold established was that all values should be below 0.100 OD. The raw absorbance of each condition was compared with the threshold.

Intermediate precision (precision between different assays) was determined at three concentration levels (4.78E+06, 7.96E+06, and 1.11E+07 of *A. baumannii*) per triplicate on two separate days. One analyst performed the analysis on two different days, and a second analyst performed one analysis on day one. Also, a blank control with no bacteria was added to the plate to eliminate the background response. Firstly, mean blank absorbances were calculated and subtracted from the rest of the plate. Then, the standard curve was calculated, as explained in the linearity paragraph in this section. Results were analyzed interpolating the samples with the standard curve, and CV of each parameter at each concentration level was obtained (the established threshold was 15%). In addition, ANOVA analysis was carried out at a significance level α = 5% for intermediate precision between different days and analysts. Also, CV between different plates was measured, and the established threshold was 20%.

The method's robustness was assessed by preparing two plates, each with two standard curves and two samples. One curve and its corresponding samples were stopped at two times: 5 minutes (1 curve and 1 sample) and 7 minutes in one plate. The other plate was stopped at 7 minutes and 9 minutes. Then, the two plates were compared to study the differences 5 minutes, 7 minutes, and 9 minutes.

The accuracy of the method was calculated by measuring the 3 different preparations with the standard curve. The mean of each preparation was compared to the theoretical value to calculate the recovery. The theoretical initial concentration is 1.58 E+10 bacteria/mL, and the recovery was indicated as a percentage of similarity. The acceptance criteria were stablished between 75 - 125%.

6.5 µBCA

µBCA assay consisted on preparing a standard curve for the BSA standard (n = 3) diluted in NaCl 0.9% or drug product buffer of concentration between 32 µg BSA/mL to 4 µg BSA/mL. Afterward, samples containing *A. baumannii* bacteria were prepared at 5E+07 and 2.5E+07 bacteria/mL in NaCl 0.9% or drug product buffer. Also, a QC control was prepared at 25 µg BSA/mL in NaCl 0.9% or drug product buffer and was used as system suitability for the plate.

Afterwards, 150 µL of standard, samples or control were added to the wells of the plate and mixed with 150 µL of µBCA reagent. This reagent was prepared following producer guideline: mix 9 mL of reagent A, 8.64 mL of reagent B and 0.36 of reagent C. Plates were incubated for 2 hours at 37ºC and the absorbance emitted at 562 nm measured.

6.5.1 µBCA Validation method

Linearity was assayed for the BSA standard (n = 3) with eight calibration dilutions between 32 µg BSA/mL to 4 µg BSA/mL. In the case of VXD-001 bacterial curve, eight dilutions

between 1.27E+07 and 1.56E+06 bacteria/mL. In both cases, curves contained eight concentration levels by triplicate. Mean of triplicates absorbance was calculated, and linear regression analysis of absorbance versus concentration was carried out and regression coefficient (R^2), model fit residuals, and % coefficient of variation were studied.

The specificity was determined by analyzing NaCl 0.9%, sample diluent, and the excipients used to produce the drug product (trehalose and aluminum hydroxide). The threshold established was that all blank values must be below 0.150 OD. The raw absorbance of each condition was compared with the threshold.

Intermediate precision was determined at two concentration levels (5E+07 and 2.5E+07 bacteria/mL). Its results were interpolated with the standard curve. Obtained CV of 12 replicates of each concentration was calculated, and the established threshold was 10%.

Method precision was determined at two concentration levels (5E+07 and 2.5E+07 bacteria/mL) per triplicate in each plate. Three plates were performed on two separate days. One analyst performed the analysis on two different days, and another analyst performed one analysis. Also, a blank control with no bacteria was added to the plate to eliminate the background response in each plate. Firstly, mean blank absorbances were calculated and subtracted from the rest of the plate. Then, standard curve calculations were performed as explained in linearity calculations. Results were interpolated with the standard curve, and calculations were performed with treated data. CV of each parameter at each concentration level was obtained, the established threshold was 10%.

Method precision plates were compared to measure intermediate precision through an ANOVA analysis at significance level α = 5%. Also, CV between different plates was measured, and the established threshold was 15%.

The method's robustness was assessed by preparing one plate analyzed during the reagent reaction at three different times (1.5, 2, and 2.5 hours). Results were analyzed as mentioned previously and were compared with a statistical analysis ANOVA.

The method's accuracy was calculated by adding a spike of BSA over a known bacteria concentration with different concentrations of protein. The method must be able to achieve measuring the BSA spike correctly. In this case, a basal quantity of 2.5E+07 bacteria/mL was spiked with three different concentrations of BSA (C1, C2, and C3). Each spiked concentration had four replicates in 3 different plates. Spike result was compared with theoretical concentration, obtaining a % similarity between 80% and 120%.

6.6 Coomassie Blue staining method

Briefly, 100 μL of *A. baumannii* LPS(-) (6.3E+08 bacteria/mL) were incubated with LDS and DTT (see table 1) for 10 min at supplier recommended indications and heated at 95ºC for 10 minutes. 25 μL of solution containing 6.3E+07 bacteria/mL were loaded on a polyacrylamide Tris-glycine gel in running buffer solution (see table 1). Electrophoresis was carried out for 2 hours at 100 V. Afterwards, the gel was stained with Simply Blue staining buffer following producer instructions (see table 1). The stained consisted on heating the gel for 40 seconds with 100 mL of mili-Q water (three consecutive times changing the water) at 700 W with a microwave. Then, gel was heated inside 100 mL Simply Blue buffer for 40 seconds at 700 W with a microwave. The gel and staining solution were incubated for ten minutes and afterwards staining solution was discarded. Afterwards, 3 periods of 30 minutes of washing of the gel were performed in mili-Q water. Then, stained gel was analyzed with Imagequant LAS.

6.7 Western blot method

Antibodies specific for the immunodominant proteins of the vaccine Acinetovax N1-N8 were used to characterize them. The general western blot method used in this thesis is described hereafter with the addition of the slight changes applied in each batch analysis for adaptation to batch requirements. Upon gel electrophoresis proteins were transferred to a nitrocellulose membrane. Transference was performed adding Whatman filter papers incubated for half an hour with transference solution prepared following manufacturer

instructions above and below the nitrocellulose membrane. Whatman filter papers were used to conduct the electrical current during transference. Transference was performed at 310 mA for 30 minutes in transference solution. The membrane was incubated overnight at 4ºC in blocking solution and washed with TPBS solution (PBS 1X + 0.05% Tween 20) for 1 hour (all washes are performed this way). Next, the membrane was incubated with antibodies N1 (5 µg/mL) and N5 (5 µg/mL) in MPBS (PBS + 0.2% skimmed milk). Antibodies were used together or separated depending on the assay. This membrane was incubated for 1 hour at room temperature and washed with TPBS solution. Then, membranes were incubated with anti-mouse antibody conjugated with HRP secondary antibody diluted 1:20.000 in MPBS. Membranes were washed. Finally, membranes were incubated with ECL solution according to supplier indications. Sample chemiluminescence was recorded in Imagequant LAS 4000 Mini.

6.8 Immunoprecipitation (IP)

Antibodies N1 and N7 were coupled to CNBr (Cyano-gen bromide-activated)-Sepharose beads following manufacturer specifications. Then, the mixture was transferred to Poly-prep columns, used as a holder, where the non-coupled antibodies flowed through out of the column by gravity and were collected and stored at -40ºC. A control column with beads and no antibody was used as a negative control for coupling and following IP.

VXD-001 aliquot, with 2E+10 bacteria/mL was lysed with lysis buffer (30 mM Tris pH 7.4, 150mM NaCl, 1% Octylphenoxy poly (ethyleneoxy) ethanol (Igepal®) and the protein content quantified. Aliquots of 650 µg of lysate were combined with 100 µL of N1 or N7 antibody- coated beads. Samples were incubated at 4ºC in a rotating mixer for 3.5 hours.

Samples were loaded on an affinity chromatography column with a 10 µm filter (Mobicol column) and centrifuged. The non-retained fraction of the lysate was collected and stored. The Mobicol column was washed with 0.1% TFA to elute the proteins that interacted with the antibodies. Eluate was stored at -40ºC until used. At this point eluates were evaporated on a SpeedVac following manufacturer specifications to eliminate water and they were

reconstituted in 1X LDS sample buffer and 50 mM DTT. A volume containing 5μg of the eluted fraction was analyzed by electrophoresis on polyacrylamide tris glycine gel (see table 1) and subsequently stained with Coomassie Blue. Bands detected were further analyzed by MALDI-TOF/TOF.

6.8.1 Matrix-assisted laser desorption/ionization/Time of flying (MALDI-TOF/TOF)

Bands observed on the SDS-PAGE gel of the eluates were cut and digested using an automatic device. Sample processing included reducing with DTT, derivatization with iodoacetamide (IAA) and enzymatic digestion with trypsin (37ºC, 8h). The resulting mixture of peptides was analyzed to obtain their sequences. Samples were treated with CHCA (α-Cyano-4-hydroxycinnamic acid) matrix in the MALDI plate with Starter kit for MALDI-TOF MS following manufacturer specifications. Samples were analyzed using a MALDI-TOF/TOF mass spectrometer. TOF spectra were interpreted by the Mascot database. The database used for identification was NCBIprot, taxonomy bacteria. All identifications were manually validated.

6.9 Bacteria, Antibody and Gold nanoparticles (AuNPs) conjugation and characterization

The aim was to confirm the expression of protein Omp22 in the bacterial membrane of VXD-001. TEM was carried out using AuNPs linked to the antibody N7. Reactant free AuNPs of 15 nm diameter stabilized in 0.1 mM PBS (1.64E+12 nanoparticles/mL) were linked to antibody N7with ligand α-Mercapto-ω-carboxy-PEG (Mw 5000 Da), based on previous studies (136,137). Firstly, the ligand was coupled to gold nanoparticles. The AuNPs were incubated with a 200 mM equivalent of ligand solution at room temperature under mechanical stirring for 2 h. A 10 kDa cutoff dialysis was performed in 2 L of PBS at 4°C overnight to remove the ligand not bound to nanoparticles. The next day the purified Carboxy-terminated nanostructures were selectively activated using 200 mM 1- ethyl-3- (3-dimethyl aminopropyl) carbodiimide (EDC) / and 50 nM N-hydroxy-succinimide (NHS) coupling chemistry. Once the carboxyl groups were activated, they were incubated with

200 mM equivalents of the N7 antibody for 3 h under Ferris Wheel shaking at room temperature. It was dialyzed overnight at 4°C in 2 L of PBS, but this time with a higher cutoff (100 kDa) to purify EDC, NHS, and antibody residues not bound to the carboxyl group of the ligand. The surface charge (mV) or Z-potential of AuNPs, ligand-AuNPs, antibody N7 and bacteria was characterized in a Zetasizer Nano ZS in PBS at pH 7.4.

Once the nanoparticle-antibody complex was purified, it was incubated with VXD-001 at ratio (100:1) for 1h with gentle mechanical shaking at room temperature. The Bacteria and nanoparticles suspension were centrifugated at 5000xg twice, and two washes with PBS were carried out to eliminate the nanoparticles not bound to bacteria. Finally, the suspension was deposited on TEM carbon grids coated with formvar for later observation using a Jeol JEM 1010 100 kv.

7. Results and discussion

7.1 Characterization of the humoral response induced produced by the vaccine Acinetovax:

7.1.1 *In vivo* dose/response:

An *in vivo* assay was performed to study the potency of the immune response induced by the vaccine, the IgG response, and a dose-response to demonstrate the correlation between bacterial load and survival in a murine sepsis model.

Tested doses contained 0.83 mg of aluminum in 4 different bacterial doses and a control with a dose of 1 mg of aluminum was included. 1 mg of aluminum was the previous concentration used by Vaxdyn in the *in vivo* assays. Doses are summarized in table 3 *and the in vivo* sample methodology was described the section 6.3.1.

The aluminum dose of 0.83 was selected because it is the aluminum limit stablished by international authorities to be the maximum allowed dose administered in humans. Ten animals were immunized with the different doses listed in the table 3.

Table 3. Dose-response *in vivo* samples preparation. The bacteria and aluminum dose composition were different between the different groups.

Group	VXD-001/dose (bacteria)	Aluminum/dose (mg)
Acinetovax control	1E+09	1
Group A (n = 10)	1E+09	0.83
Group B (n = 10)	1E+08	0.83
Group C (n = 10)	1E+07	0.83
Group D (n = 10)	1E+06	0.83
Naïve (C-) (n = 10)	-	-

Sera samples were obtained at day 21 after the first vaccination dose, and they were analyzed by ELISA as explained in section 6.4.1. Results are summarized hereafter:

IgG analysis for Acinetovax dose selection
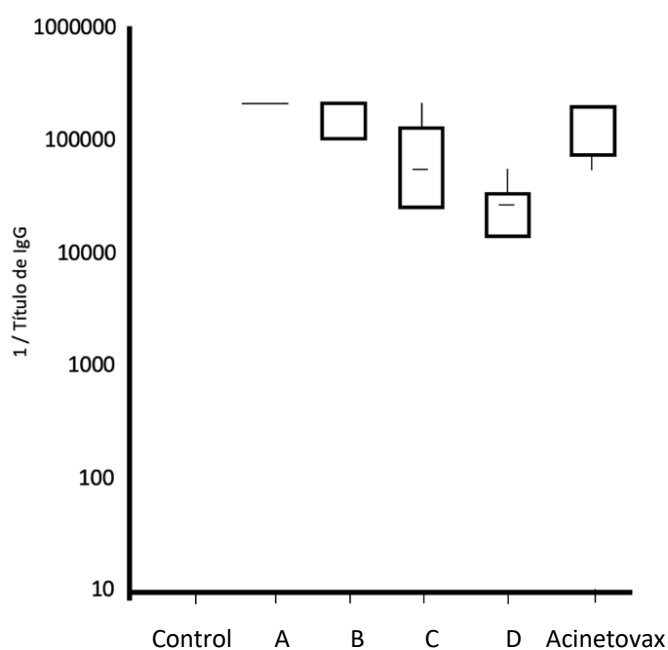
Figure 14. IgG response of serum obtained from mice immunized with different bacteria concentrations. Control (0 bacteria/mL), Group A (1E+09 bacteria/mL), Group B (1E+08 bacteria/mL) Group C (1E+07 bacteria/mL) Group D (1E+06 bacteria/mL) and Acinetovax (1E+09 bacteria/mL).

There was an IgG response in all the immunized groups that was comparable to that of the original Acinetovax at the highest immunogen dose. These data indicated a clear humoral response to the vaccine in immunized animals and points to the involvement of B cells on

the vaccine's protective effect demonstrated in the sepsis assay. The ELISA test was performed with a plate coated with *A. baumannii* bacteria, which means that IgGs detected in the ELISA were specific for *A. baumannii*. Further, specific IgG was not detected in non-immunized animals (negative control), indicating that the results were reliable and specific.

Also, there was a correlation between bacterial dose and IgG concentration at 21 days after the first immunization. The lower the bacterial dose administered, the lower the IgG response produced at day 21.

To analyze the protective effect of the different doses of the vaccine immunized mice were inoculated with Acinetovax as described in section 6.3.3. and there was a correlation between vaccine dose and protection against the infection. Results can be shown hereafter.

In vivo analysis with Acinetovax for dose selection
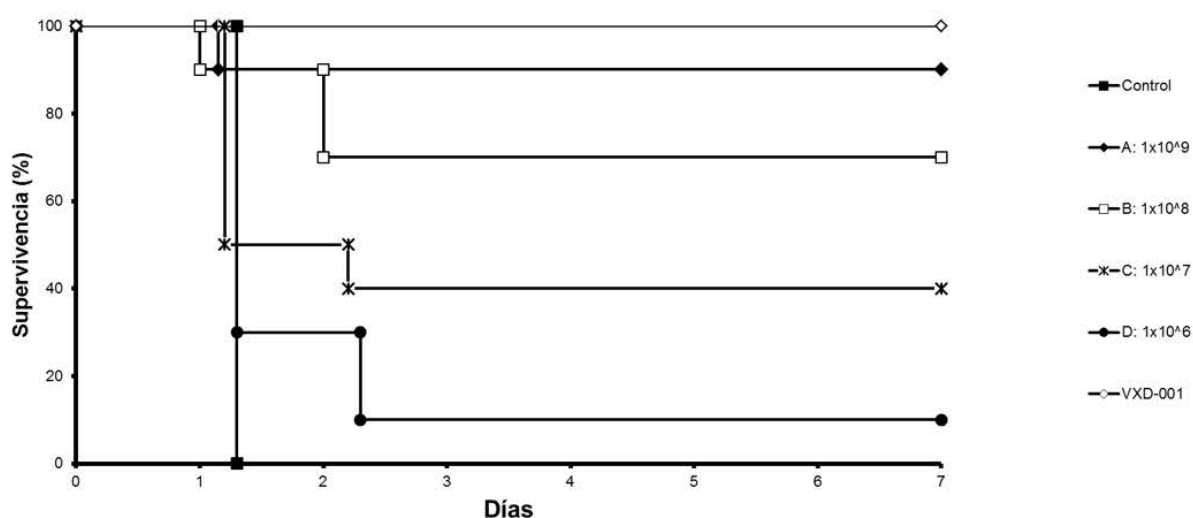
Figure 15. Survival assay of immunized mice with the positive control (in situ prepared Acinetovax), new proposed aluminum dose (Group A), different doses (Groups B, C, and D), and negative control.

Results showed a survival rate of 100% and 90% in mice immunized with VXD-001 (positive control) and group A (1.10E9 bacteria) respectively. This result demonstrates that the drug substance developed by Vaxdyn and the newly formulated vaccine are both protective. Survival decreased considerably in groups B, C, and D according with the bacterial dose reduction. In fact, survival of group D mice that received the lowest bacterial dose was

similar to that of non-immunized mice (naïve mice) considered the negative control. This result indicates a correlation between bacterial dose and elicited protection, indicative that the vaccine is responsible for mice's survival. Further, it suggests that protection is achieved through the induction of a humoral response producing *A. baumannii*-specific IgG.

This study also determined that the aluminum dose (0.83 mg) used as vaccine adjuvant did not show any effect and therefore it could be used in vaccine production.

7.1.2 Antibody selection for assay method development.

B cells from immunized mice were screened to identify those able to produce *A. baumannii* specific antibodies. These cells were used to generate hybridomas producing monoclonal antibodies. Once purified the antibodies were analyzed by ELISA and western blot in order to select the best antibodies to be used in the development of different quality assay methods.

From a total of 32 *A. baumannii* specific monoclonal antibodies obtained, eight were selected, based on their *A. baumannii* specificity, to be used in the development of the different analytical tests to characterize the newly formulated vaccine Acinetovax. They were also used to develop quality control assays such as an ELISA to quantify proteins related to the immune response and Western blot to identify these proteins for its in-depth characterization.

The notation used for these antibodies is N1 to N8. Antibodies will be cited with these names in the rest of the document. All procedures until purifications were performed by Vaxdyn and LEITAT, partners of Reig Jofre in this project.

7.1.3 Development of an ELISA test to analyze the specificity of the antibodies.

This assay was designed to study the antigen specificity of the eight different monoclonal antibodies against *A. baumannii*. Bacterial strains of *P. aeruginosa and E. coli* were used in the assay as non-specific targets. Both bacteria were chosen for being pathogenic gram-negative bacteria. The samples analyzed were *A. baumannii* present in VXD-001, *A. baumannii* strain 167R (resistant to colistin) (131–133), *A. baumannii* 167S (LPS(+) susceptible to colistin), an *E. coli* strain ATCC25922 LPS(+) and a *P. aeruginosa* strain ATCC27853 LPS(+) (132).

To study the specificity of antibodies, N1 to N8, they were tested in an ELISA against the different bacteria mentioned before as described in section 6.4. Results can be found hereafter:
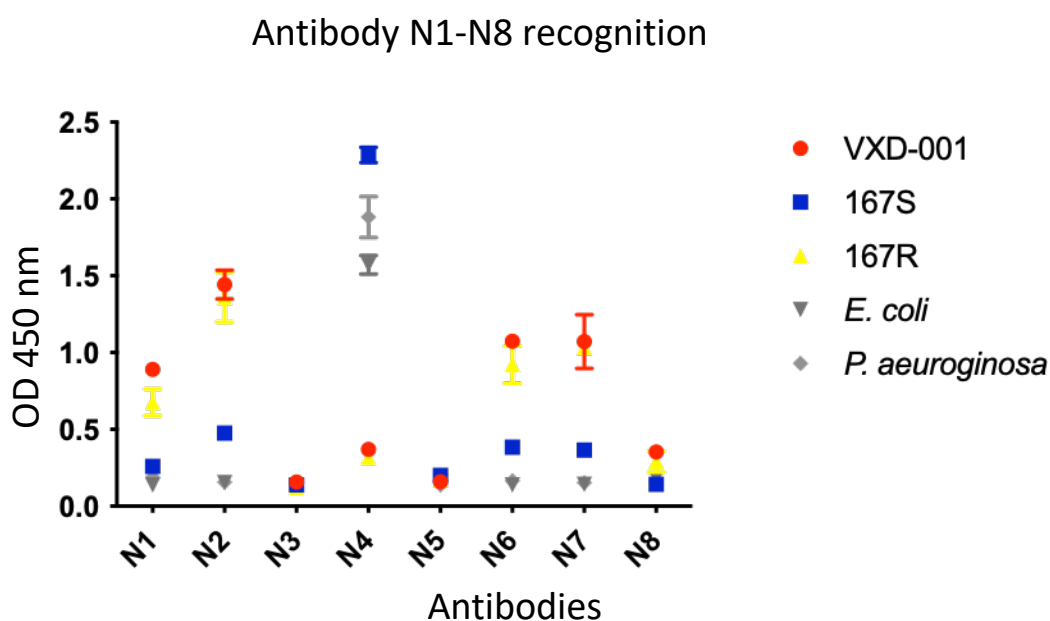
Figure 16. Specificity of the monoclonal antibodies generated. Direct ELISA analysis of the recognition of multiple bacterial strains by antibodies N1 to N8.

The antibodies N1, N2, N6, and N7 detected *A. baumannii* VXD-001 and 167R both LPS(-) but not the other bacterial strains tested. Antibody N4 recognized LPS(+) *A. baumannii* 167S and showed a low response to LPS(-) *A. baumannii* 167R. Also, it recognized *P. aeruginosa* and *E.coli*. Finally, antibodies N3 and N5 cannot recognize *A. baumannii.*

As Acinetovax vaccine is composed of an LPS(-) *A. baumannii,* the antibodies showing the highest capacity to detect the bacteria were N1, N2, N6, and N7. Lack of recognition by some of the antibodies might be explained because of their specificity for intracellular antigens not exposed on the cell membrane

7.1.4 Sandwich ELISA

During ELISA development process it was decided that sandwich ELISA was more suitable than indirect ELISA because sandwich ELISA was more specificity. Capture antibodies allow this method to attach to the plate just the bacteria present in VXD-001 and avoid attaching free protein or floating lipids.

Therefore, eight antibodies were tested against each other to establish which antibodies pairs could be used. The sandwich ELISA steps were as described: 1) capture antibody, 2) LPS(-) *A. baumannii*, 3) biotinylated detection antibody, 4) streptavidin-peroxidase and, 5) peroxidase substrate. The result is shown in figure 17.
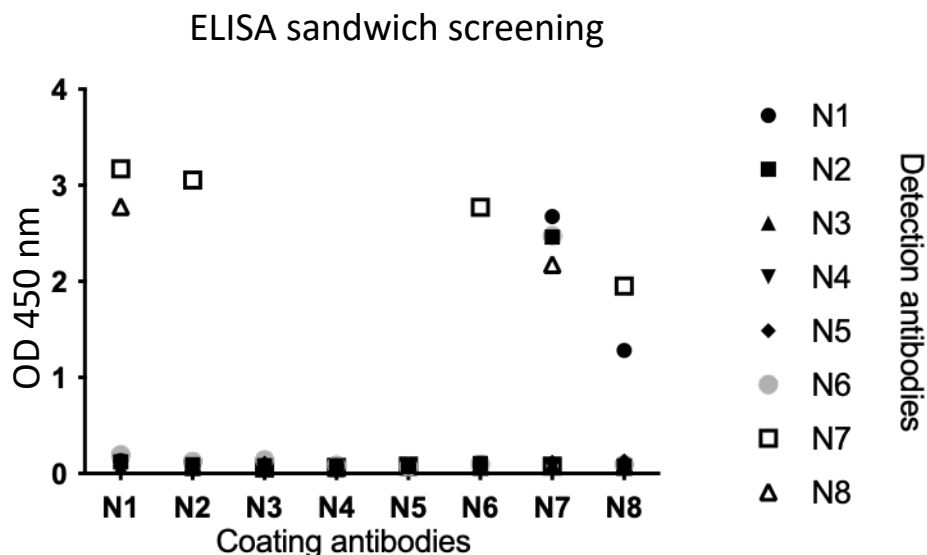
Figure 17. Sandwich ELISA results performing all possible combinations of capture and detection antibodies for monoclonal antibodies N1-N8.

Results suggest that there were different possible combinations to develop an ELISA sandwich. Even though, exclusively one sandwich ELISA method could be developed. The

antibody pair with the best recognition capacity, antibody N1 for antigen capture and N7 for detection, was chosen.

7.1.5 Western blot analysis of the eight *A. baumannii* specific antibodies.

Because some of the ELISA tested antibodies did not show any specificity for *A. baumannii* whole cells, a western blot analysis was performed to determine if some of the epitopes being recognized by antibodies N1-N8 corresponded to intracellular proteins.

The first step to develop this method was to study the optimal concentration of bacteria to be loaded in the gel. Therefore, bacteria were solubilized and prepared as described in section 6.6 and loaded on an SDS-PAGE gel. The gel was subsequently stained with Coomassie Blue to detect all the proteins. (see figure 18).
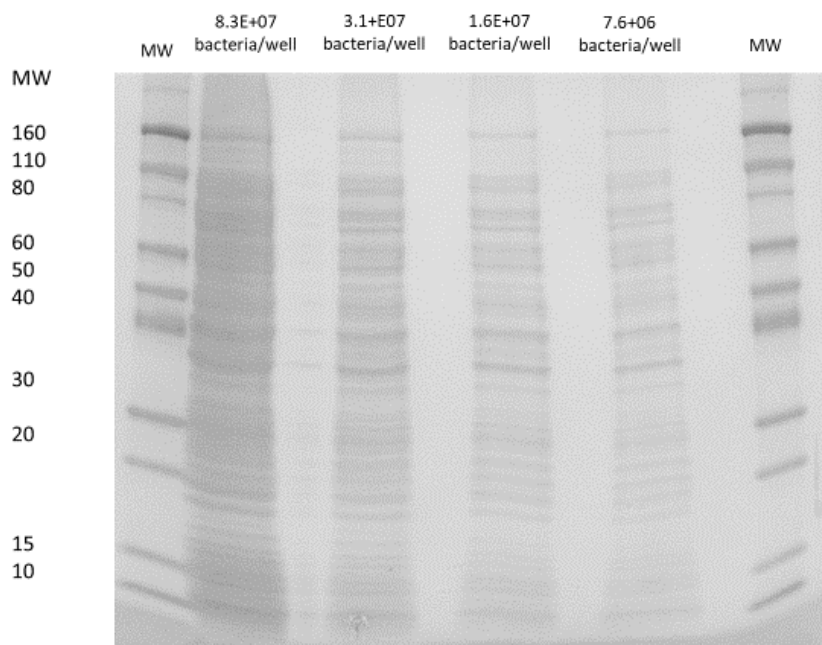
Figure 18. Selection of the best *A. baumannii* bacterial concentration for routine electrophoresis-based analysis. Coomassie Blue stained SDS-PAGE gel.

The optimal concentration determined for SDS-PAGE was 1.6E+07 bacteria/well because the bands were more separated than in 8.3E+07, where no band could be differentiated and were clear enough to see them and detect them. This is the bacterial concentration

used for the western blot analysis of the N1-N8 antibodies. Samples were prepared as described above.

The results are shown in figure 19.
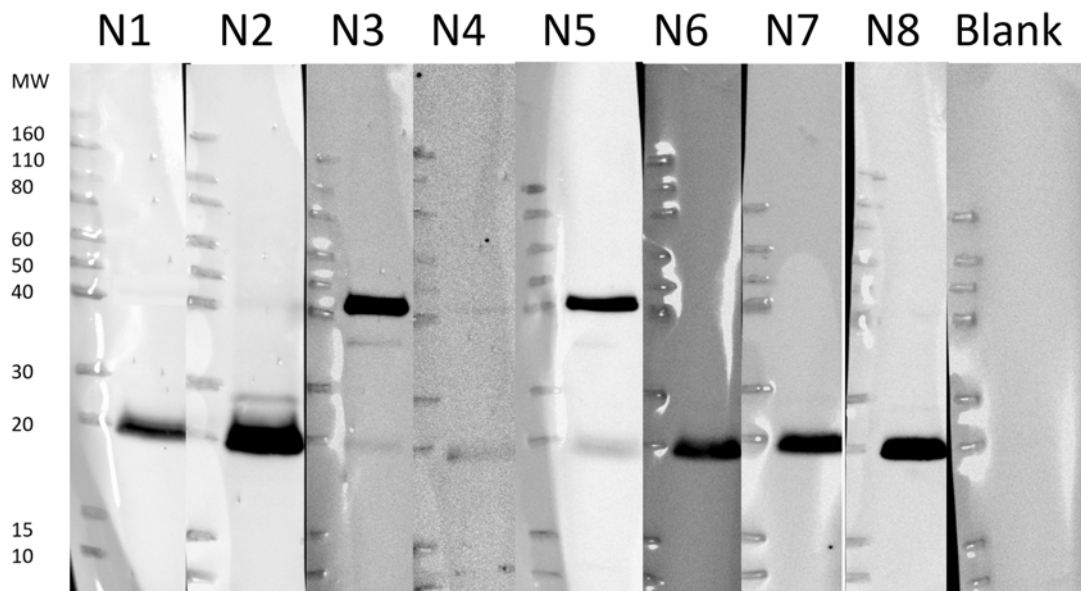
Figure 19. Western blot analysis of *A. baumannii* LPS(-) specificity of antibodies N1-N8

Results of figure 19 show prominent bands of proteins recognized by antibodies N1, N2, N6, N7 and N8, which have a molecular weight of 20 kDa. Antibodies N3 and N5 recognize a protein of around 40 kDa and with lower affinity, a band of 20 kDa. Antibody N4 shows a similar recognition pattern to that of N3 and although with lower intensity. These results show some differences with those of the ELISA test. This is the case of antibodies N3 and N5 that in contrast to the western blot results did not show any reactivity to *A. baumannii* in the ELISA test. In western blot, bacteria were heated and treated with LDS and DTT, degrading the membrane. After this process, all proteins were exposed to electrophoresis and could be recognized in western blot. Meanwhile, in ELISA, the recognized proteins were membrane proteins because the bacteria were complete. The differences observed suggest that antibodies N3 and N5 either recognize an intracellular bacterial protein or an intracellular epitope of this protein.

7.1.6 Immunoprecipitation to analyze the proteins detected by N1 and N7.

To evaluate which specific proteins were recognized by antibodies N1 and N7, immunoprecipitation of an *A. baumannii* protein extract followed by MALDI TOF/TOF analysis was carried out. Bacteria were lysed and incubated with the different antibody-coated beads. The tandem antibody + protein was precipitated and resolved by electrophoresis (figure 20). Eluate control (with no antibody, no bacteria) and a fraction of bacterial free antibody were also analyzed.
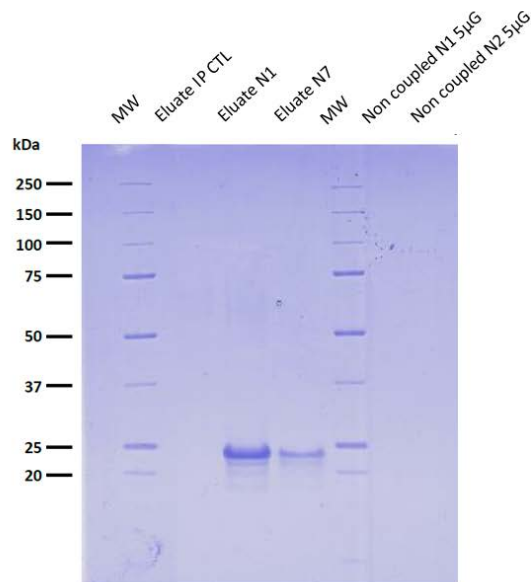
Figure 20. Electrophoresis gel stained with Coomassie staining showed eluates of the immunoprecipitated samples from N1, N7, IP control, and eluates of non-coupled antibodies.

The results show that antibodies N1 and N7 immunoprecipitated proteins of the *A. baumannii* extract. On the other hand, bacterial free fractions of antibodies N1 and N7 showed no bands, indicating that antibody coupling to the beads was performed correctly. Further, eluate IP control prepared with the eluate of a column with no antibodies-beads was included to check that the column procedure did not contaminate the proteins detected in eluates of N1 and N7. Results suggest that a protein of 20-25 kDa is recognized by antibodies N1 and N7, which confirm the results obtained in WB analysis in section 7.1.5.

An analytical MALDI-TOF assay was performed to identify the protein detected in the IP procedure. Results are shown in Table 4. The exact mass of the protein immunoprecipitated with antibodies N1, and N7 was 22 kDa. After searching in the NCBIprot database, the best match to the protein recognized either with Ab N1 and N7, based on the protein score obtained by Mascot database comparison is shown in table 4. The sequences of the two proteins were compared between them and with that of protein Omp22 previously characterized (114) through a BLAST alignment analysis (NCBI, Rockville pike, USA).

Table 4. Identification of proteins immunoprecipitated with antibodies N1 and N7 by MALDI TOF/TOF.

	RefSeq	Protein score	Protein mass (Da)	Coverage**
Protein detected by Ab. N1	WP_002058566.1	209	22480	99%
Protein detected by Ab. N7	WP_001202415.1	283	22529	100%
Omp22*	WP_001202415.1	-	22485	-
*Protein detected by W. Huang *et al*. 2016 scientific report(114).				
**Sequence coverage of immunoprecipitated proteins concerning Omp22				

The similarity of the three proteins was determined to be around 99-100%, which suggests that the antibodies N1 and N7 recognize the protein Omp22. It was previously shown that mice immunization with Omp22 elicited a strong immune response, increased the survival rate and lowered the bacterial burden on *A. baumannii* infections (114). It has been considered therefore a target antigen for the development of vaccines to this pathogen. This result also suggests that the protein detected, Omp22, is probably related to the protective immune response induced by Acinetovax in the murine sepsis model (72).

7.1.7 Cellular localization of protein Omp22

Gold colloidal nanoparticles (colloidal AuNPs) are used in electron microscopy as molecular tracers due to their small size and high electrical contrast. Naked g gold nanoparticles can passively adsorb molecules (also known as physisorption) such as antibodies. The adsorption mechanism is based on the Van der Waals interactions between the molecules and the surface of the particles. Thiol moieties (-SH) are often used as end groups in gold

surface functionalization due to the high affinity of sulfide for metals. The process to obtain a successful ligand exchange between thiol groups and gold surfaces can be controlled with few parameters. The reaction is completed when there is a thiol excess of 200 mM equivalents (137,138). Typically, the pH is kept close to 7 to avoid the decomposition of Gold at acidic pHs (below 5) and the formation of the disulfide that interferes with the ligand exchange performance at basic pHs (above 8). For this analysis AuNPs were coated with antibody N7.

In addition to the hydrophobicity and the specificity between the Omp22 protein and the N7 antibody epitope, the Zeta-potential could influence the adhesion of nanoparticles to the bacteria and give false information about the specificity of the antibody (139). However, as shown in table 6, the Z-potential values were negative for all cases, meaning that the electrostatic forces between AuNPs-Ligand-N7 and VXD-001 were repulsive, and the interaction would be mainly influenced by the antigen and the antibody specifically. Zeta potential is defined as the electrical potential at the shear plane (140). The shear plane boundary between stationery and diffuse layers of charges at the solid-liquid interface (140).

Table 5. Z-potential of AuNPs, AuNPs ligands, N7 antibody, and VXD-001.

Formulation	Z-potential (mV)
AuNPs	-1.25 ± 0.15
AuNPs-Ligand	-11.50 ± 2.00
N7 Antibody	-3.08 ± 0.55
VXD-001	-13.23 ± 1.20

The N7-AuNPs were used to visualize the affinity of the N7 antibody for the protein Omp22 on the bacterial membrane by TEM microscopy. The results are shown in figure 21
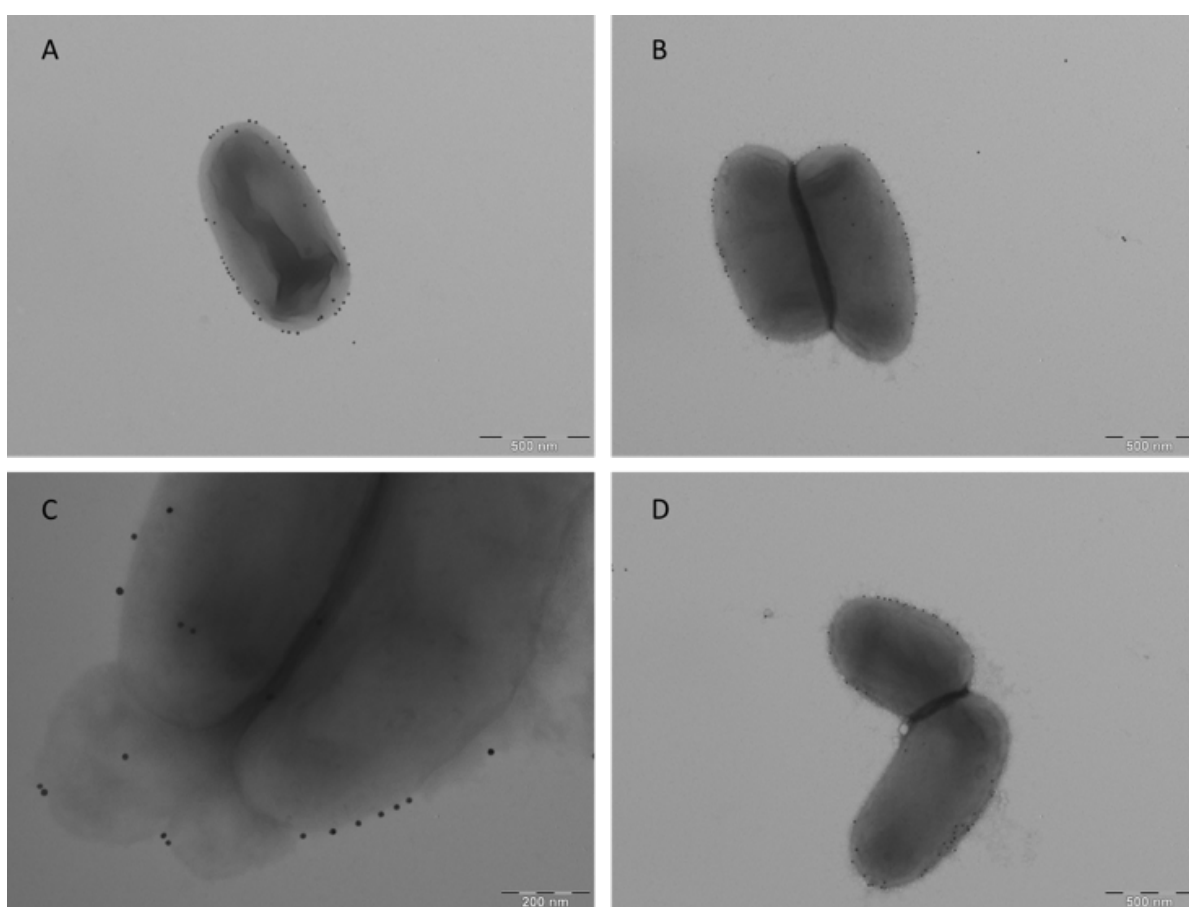
Figure 21. Transmission electron microscopy analysis (TEM) of *A baumannii* labelled with N7-coated gold nanoparticles. Images A, B, C and D show different Bacteria-Ab-Ligand-AuNPs complexes

As shown in figure 21, N7-AuNPs recognize an epitope of protein Omp22 on the bacterial membrane. Black dots observed on the surface correspond to the high electron density of gold nanoparticles, confirming the proper functionalization of the particles with ligand and antibody. It also shows that antibody N7 (which is one of the antibodies produced during

the immune response against Acinetovax) recognizes the bacteria and might be eliciting protection since it can attach to *A. baumannii* (72). This antibody is recognizing a protein on the bacterial membrane of LPS- *A. baumannii,* so it can also be concluded that the specificity of the antibody is maintained after being covalently bound to the hydroxyl groups of the ligand Au.

7.2 Development of an analytical method for quality control of Omp22 ELISA

7.2.1 Obtention of a synthetic peptide part of Omp22:

It was decided to use an ELISA test to quantify the protein Omp22 on the membrane. The first approach consisted on synthesizing a peptide based on Omp22 protein sequence to build up a standard curve. With this standard curve with a known quantity of peptides, the number of Omp22 proteins in the bacterial membrane could be measured. The peptide chosen corresponded to an Omp22 protein domain(?) found in a loop that is potentially facing the outside of the cell. The sequence of the synthesized peptide is the following one (141):

Omp22 (fragment)	c-myc

N-term **VGAAVVLSGCQTTGNNLGGVEYD**EQKLISEEDL C-term

Aminoacids 1-23 corresponded to the Omp22 protein. Aminoacids 24-33 (N term-EQKLISEEDL- C term) corresponded to a *myc* tag sequence which allowed its detection in the analytic assay. This tag is detected with a commercially available antibody and is used as a positive control confirm that the protein is present.

7.2.2 Omp22 standard curve peptides

Monoclonal antibodies N1 and N7 that recognized the protein Omp22 were used to try to detect the Omp22 synthetic peptide in an ELISA assay. The results obtained are shown in figure 22.
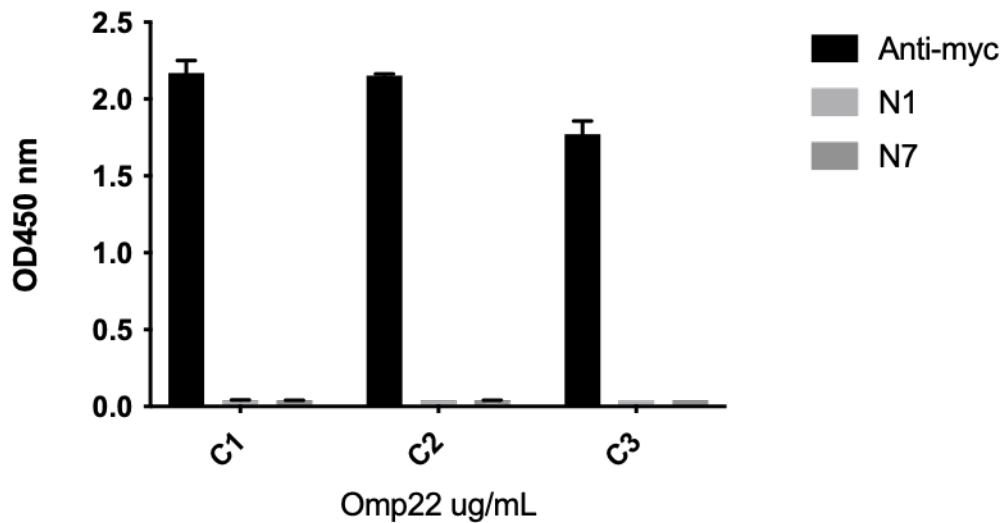
Figure 22. Direct ELISA performed coating the plate with Omp22 synthetic peptide detected by antibodies anti-myc, N1, and N7 antibodies

Figure 22 shows that the peptide Omp22 was recognized by the anti-myc antibody but not by the antibodies N1 and N7. This ELISA has been studied with 5 different peptides have been produced to try to obtain the standard curve, but the results have not been obtained yet.

7.2.3 ELISA sandwich optimization

While the synthetic peptide is produced, that would allow us to have an independent standard, the sandwich ELISA that uses VXD-001 drug substance as a standard was selected to study the potency of vaccine Acinetovax.

The Sandwich ELISA developed consisted on the antibody N1 as a capture antibody, the bacteria, the biotinylated antibody N7 as a detection antibody. Biotin was linked to a streptavidin-peroxidase complex that transformed the substrate on a colored measurable substance. The method was developed to detect the Omp22 protein in drug substance and drug product of the vaccine.

ELISA sandwich method was selected because it is more specific than direct or indirect ELISA due to the capacity of the sandwich ELISA of bounding specifically *A. baumannii* to the plate, avoiding the attachment of any other floating particle in the drug substance which might cause interaction with the antibody reaction.

Following a similar method to the one described in section 6.4.2, several experiments were carried out to optimize the technique and most of all to reduce variability. Two different wash solutions were tested, HT-PBS and TPBS, to evaluate their effect on assay variability. Figure 23 shows the CV% of 3 different plates for each condition containing eight concentrations between 3E+07 and 5E+05 bacteria/mL with three replicated each. Because the data followed a non-normal distribution (Shapiro Wilk normality test, $p<0.05$), a Mann-Whitney non-parametric test was used. The comparison of the results obtained showed that there were statistically significant differences ($p<0.05$) between both treatments.
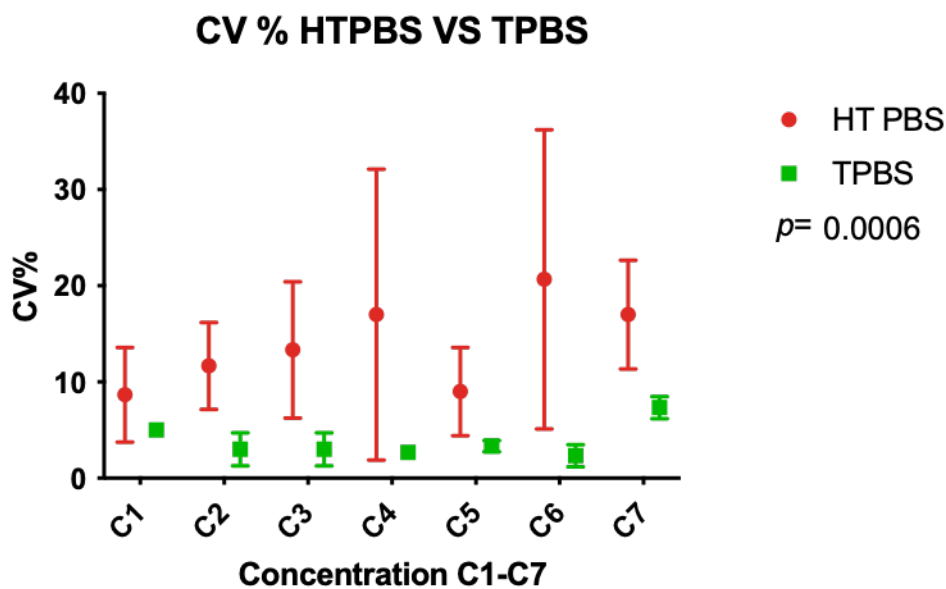
Figure 23. CV% differences between the performance of the ELISA with washing solution HT-PBS and TPBS.

Figure 23 shows that the use of washing solution TPBS clearly improved the result, reducing method's variability from a maximum CV of 40% with HT-PBS to a maximum of 15% with TPBS.

Another modification was related to the concentration of capture antibody. The antibody concentration was an essential factor because the ELISA aimed to add enough capture antibody to completely cover the de well surface, helping to attach as much bacteria as possible. Finally, a detection antibody must be added in excess to detect all bacteria attached to the plate, but too much could cause the background response to increase. Thus, different capture antibody concentrations were assayed (1 and 2 µg/mL) based on the previous experimental setup (data not shown). Four different curves, coming from the linear combination of two factors (2k, being k, each antibody concentration), were prepared from 5E+05 to 5E+08 bacteria/mL.

Figure 24 shows the complete sigmoidal curve of measured optical density (OD) against the proposed concentration range. A similar pattern is observed with the different combinations of antibodies concentrations.
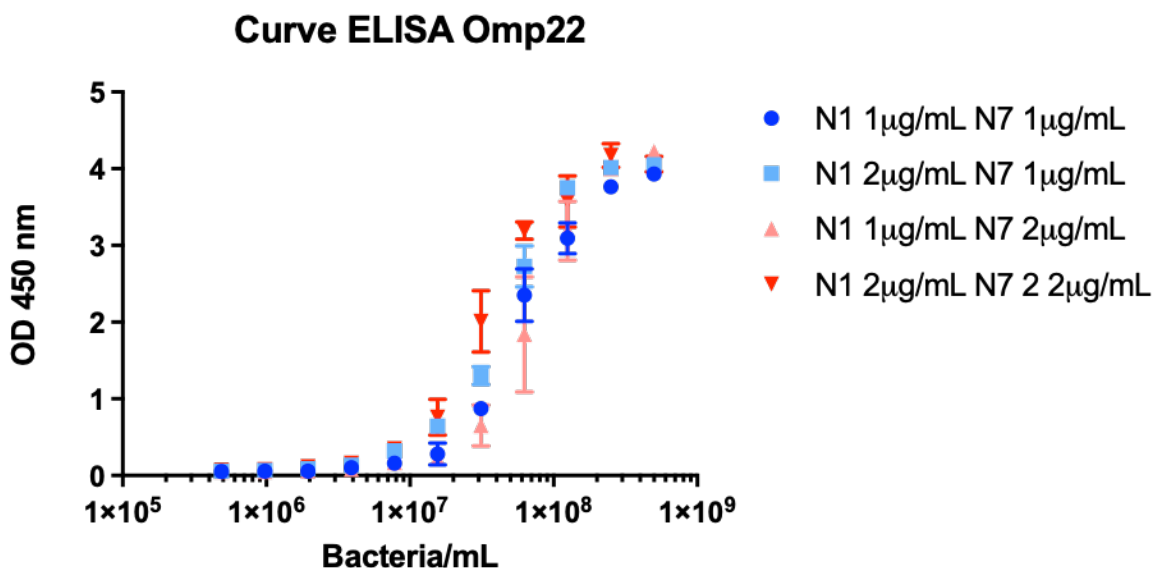
Figure 24. Sandwich ELISA testing different concentrations of capture (N1) and detection (N7) antibodies on a bacteria standard curve.

Drug quantification is usually carried out in the linear segment of the sigmoidal curve, then figure 25 shows the linear coefficient of determination (R^2) of the linear portion (from 6.25E+07 to 9.77E+05 bacteria/mL).
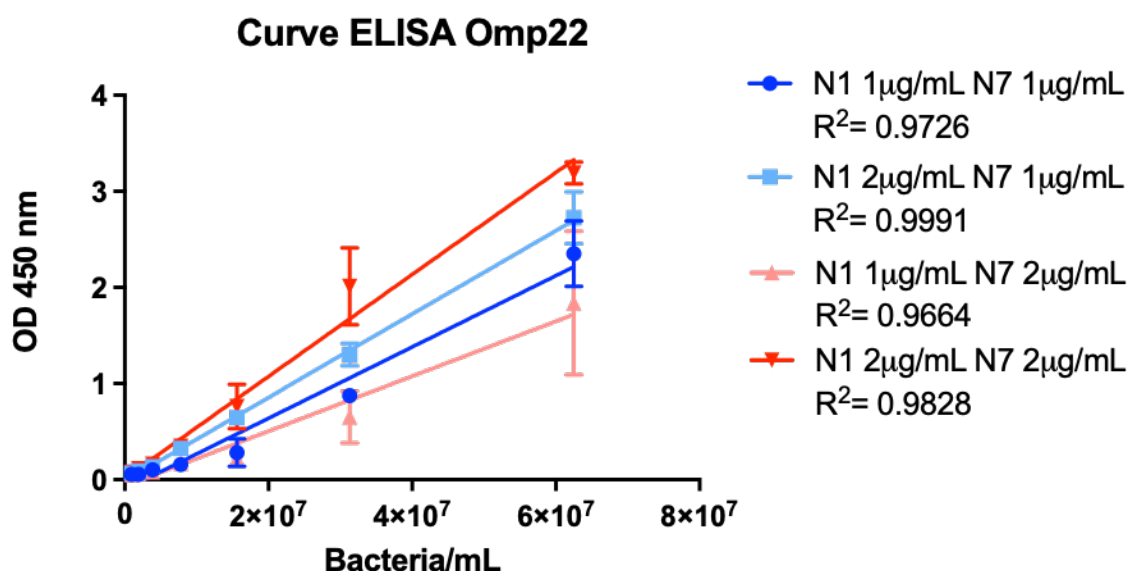
Figure 25. Sandwich ELISA testing different concentrations of capture (N1) and detection (N7) antibodies on a bacteria standard. The linear segment is being shown.

Figure 25 shows differences between different antibody concentrations. According to the ICH Q2 (R1) guideline, the minimum recommended R^2 value should be 0.98, and considering that the higher value was obtained when capture antibody N1 was 2 µg/mL and when detection antibody N7 was 1 µg/mL (both in 100 µL), these were the final concentrations selected for further validation. Results of curves with antibody N1 at 1 µg/mL had curves with R^2 below 0.98, which might be produce because maybe, the wells were not correctly coated at this concentration. Additionally, detection antibody N7 concentration at 1 µg/mL showed lower CV% as described in table 6, probably attributed to the higher noise derived from higher N7 concentration.

Table 6. Comparison between CV% using the selected concentration of antibody N1 and the two concentrations tested for antibody N7.

Maximum CV% replicate in the curve (n = 3)	
N1 2 µg/mL (capture) N7 1 µg/mL (detection)	N1 2 µg/mL(capture) N7 2 µg/mL (detection)
15%	31%

Results observed in table 6 suggest that the concentrations of 2 µg/mL for antibody N1 and 1 µg/mL for antibody N7 is the best combination because they produce results with lower variability.

The optimization performed resulted on a considerably improved method suited to be used for validation and routine analysis of the quality of the product.

Other factors about the method variability optimization were that since the product contains a bacterial suspension, it was essential to establish a mixing routine. Its implementation was a vast improvement.

The small methodological changes introduced along procedure development leaded to a more robust assay with reduced variability achieving a method ready to be validated. Validation consisted of 6 Sandwich ELISA plates in which the following parameters were tested.

7.3 Quantification: ELISA Omp22 validation

Validation consisted of 6 plates in which the following parameters were tested. ELISA sandwich had a capture antibody N1 and detection antibody N7 detected Omp22 on the membrane of *A. baumannii* LPS(-) of Acinetovax drug substance, as mentioned previously, and it was used to study drug product samples.

One of the most challenging steps to optimize this method was reducing variability, thanks to the evidence shown in section 7.2.3 it was improved.

7.3.1 Specificity:

In this part, the different components of the Sandwich ELISA assay were tested to study if they produced any interference. The results shown in table 7 indicate that there is no significant interference in the different blanks analyzed.

Table 7. Validation ELISA specificity results.

Parameter	Acceptance limit	Results	Standard deviation
Blank raw Absorbance	<0.100 OD	0.038	0.001
Absence of capture Ab	<0.100 OD	0.039	0.001
Absence of detection Ab	<0.100 OD	0.040	0.002
Absence of sample	<0.100 OD	0.038	0.003
Absence of streptavidin	<0.100 OD	0.035	0.003
Trehalose BLANK	<0.100 OD	0.035*	0.004
Sucrose BLANK	<0.100 OD	0.037*	0.006

*Individual values can be found in table 8.

Also, two different possible excipients for other drug product development processes were tested: trehalose and sucrose. The results of the possible interference produced by them are shown in the following table.

Table 8. Validation ELISA individual results Blank parameter.

Parameter	Plate 2	Plate 3	Plate 4	Mean	SD
Trehalose BLANK	0.034	0.032	0.039	0.035	0.004
Sucrose BLANK	0.034	0.033	0.043	0.037	0.006

None of the studied conditions of blanks and interferences show a high response in ELISA sandwich assay results of tables 7 or 8.

7.3.2 Range:

For ELISA analytical method, it is essential to work in a concentration range with a correlation between bacterial concentration and OD to develop the ELISA as it will be used to quantify Omp22 concentration. There is a turning point in most analytical methods from which more concentration does not translate into a higher OD response.

Serial concentrations were prepared to determine the range of the sample to study the colorimetry reaction produced by them. In the following figure, bacteria concentration was plotted against the absorbance at 450 nm measured on the ELISA assay.
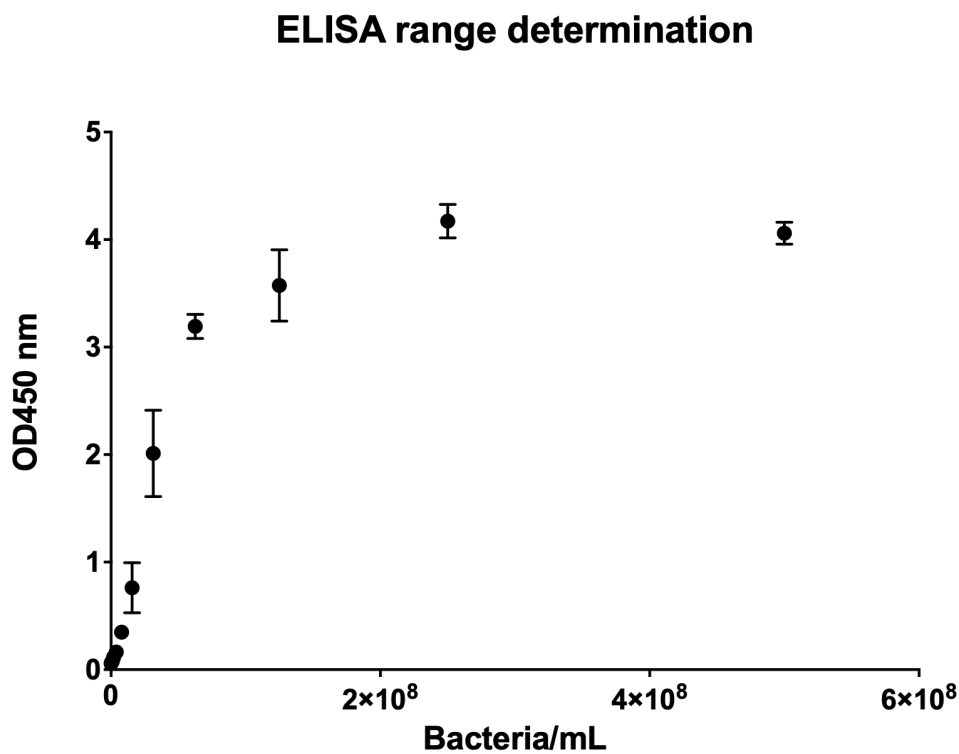
Figure 26. Validation ELISA sandwich concentration range analysis.

Figure 26 shows a turning point in which the correlation between bacteria concentration and OD measured disappears, and this might be the limit in which the method is saturated. From these same data, the linearity of the data below the turning point was represented:

ELISA range determination
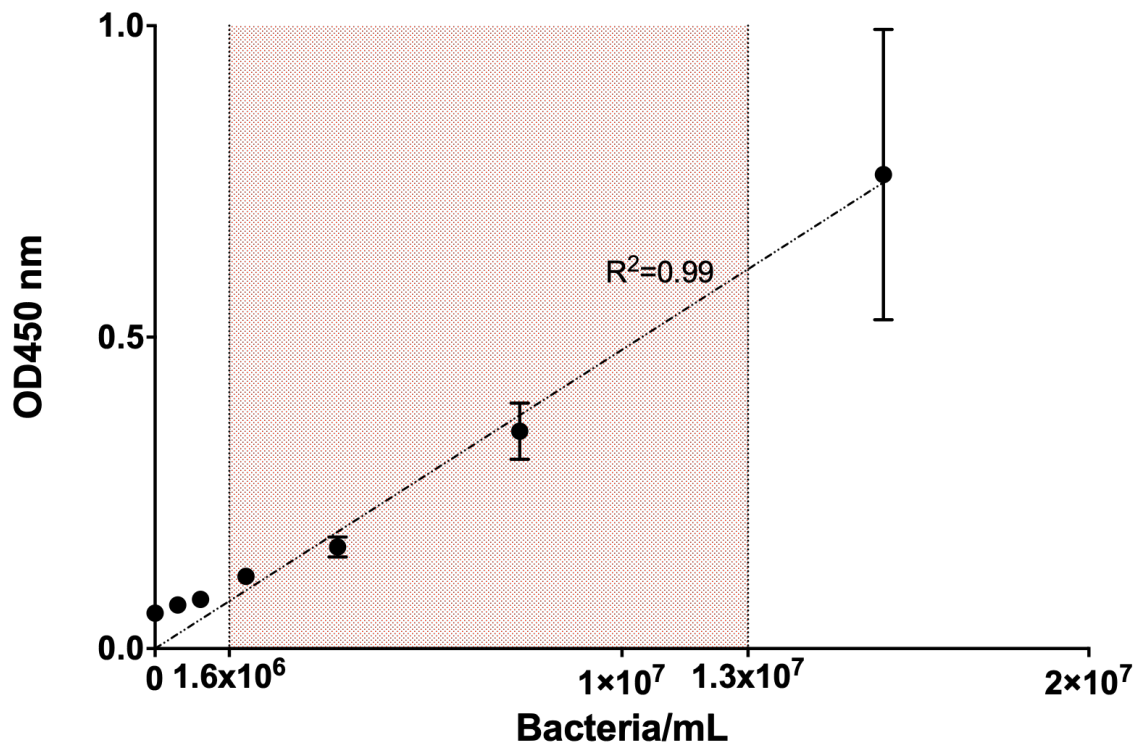
Figure 27. Validation of Sandwich ELISA range study, zoom in the linear part of the curve.

Figure 27 shows the linear part of the curve between the blank and the turning point. The regression line is represented in the graph with a dotted line. The R^2 determination coefficient suggests that the linear regression is correctly adjusted, and, in this concentration range, there is a correlation with OD. As observed in figure 27 the lower the bacteria concentration, the lower the variability of the result. The red area represents the range established to validate the method that was established between 1.6E+06 to 1.3 E+07 bacteria/mL.

This result helped to determine the range to continue working and to study linearity of the method.

7.3.3 Linearity:

Linearity was investigated by contrasting the experimental response provided by the method fitted to a linear model for a set of standard solutions with known increasing concentrations of analyte covering the range from 1.3E+07 to 1.6E+06 bacteria/mL. Three independent assays were performed to analyze this parameter, by the same analyst, on different days. Standard panels consisted of eight different concentration levels (1.27E+07, 1.11E+07, 9.53E+06, 7.94E+06, 6.35E+06, 4.76E+06, 3.18E+06 and 1.59E+06 bacteria/mL). These concentration levels were prepared and analyzed in triplicate for each plate. Results for each standard panel at each plate are summarized in table 9. Mean, SD, and %CV for each concentration level tested and R^2 were calculated. These results are shown hereafter:

Table 9. Validation ELISA sandwich standard curve method descriptive statistics.

Concentration (bacteria/mL)	Plate 1 (n = 3)			Plate 2 (n = 3)			Plate 4 (n = 3)		
	Mean OD	SD	CV%	Mean	SD	CV%	Mean	SD	CV%
1.27E+07	2.125	0.049	2%	1.806	0.036	2%	2.172	0.062	7%
1.11E+07	2.051	0.097	5%	1.635	0.051	3%	1.190	0.045	7%
9.53E+06	1.793	0.049	3%	1.482	0.015	1%	1.716	0.061	7%
7.94E+06	1.500	0.055	4%	1.188	0.021	2%	1.490	0.065	6%
6.35E+06	1.266	0.018	1%	0.994	0.024	2%	1.171	0.047	2%
4.76E+06	0.901	0.051	6%	0.766	0.027	4%	0.887	0.036	1%
3.18E+06	0.624	0.007	1%	0.496	0.023	5%	0.584	0.026	4%
1.59E+06	0.308	0.013	4%	0.250	0.006	2%	0.297	0.002	3%
R^2	0.99			0.99			1.00		

Results of the three standard curves complied with the established criteria defined before the validation. Criteria were established based on replicates variability and linear regression (evaluated through R^2). Results are shown in the following figure.
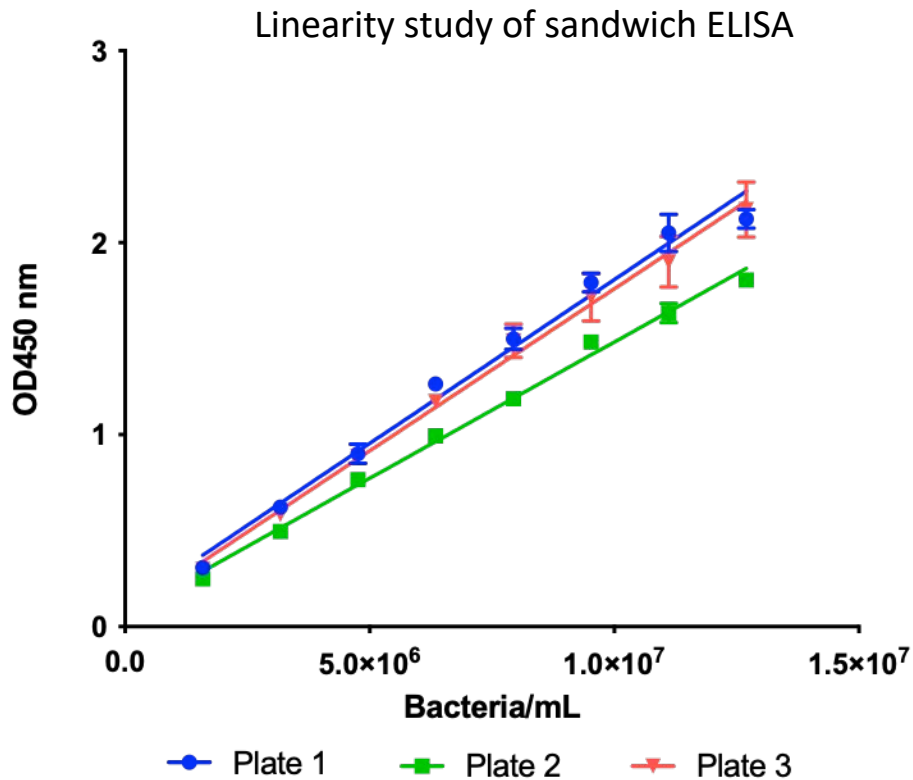
Figure 28. Validation ELISA standard curve of plates 1, 2, and 4.

The results show slight differences between the three curves, the slope is equal between two curves, and one is different. Differences were associated with the intrinsic variability of the assay and the nature of the vaccine.

Also, another quality control of the assay consisted of a residual analysis of the three standard curves of linearity determination. Therefore, a residual plot was created to study how the concentration differed from the theoretical value. Results are shown hereafter:
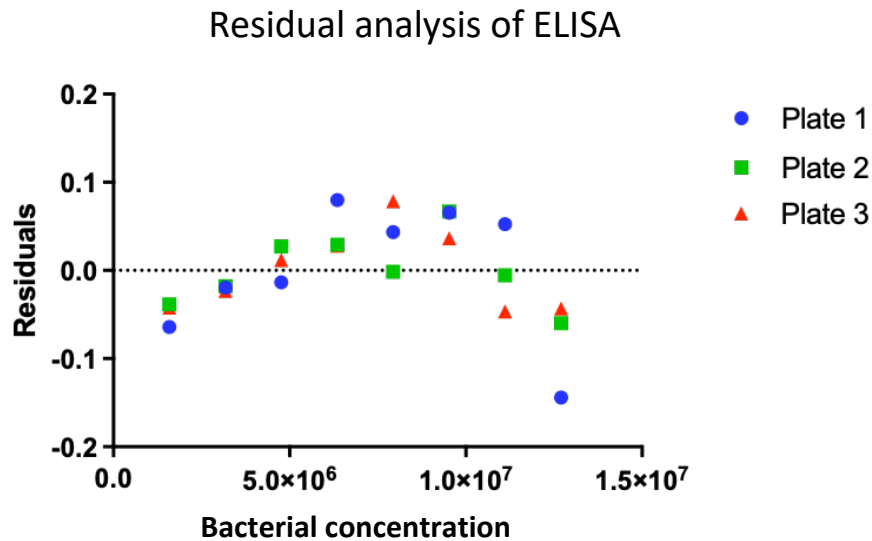
Figure 29. Residuals of the linearity data of plates 1, 2, and 4.

The residual plot of the estimated value shows a slight tendency at the lower and the higher concentrations. This tendency is not relevant in terms of the data obtained.

These results suggest that the range established to develop the standard curve composed with bacteria was linear and reproducible in different conditions.

7.3.4 Precision:

-Instrument repeatability:

Three different concentrations of bacteria were added to the plate to study the reliability of the method. These concentrations are distributed at different levels of response inside the standard curve range. Twelve replicates of each concentration are determined to study the variability due to the instrument, measured as the CV%. Hereafter the results are shown determined at OD 450 nm.

Table 10. Summary for Instrumental repeatability.

	R1	R2	R3	R4	R5	R6	R7	R8	R9	R10	R11	R12	Mean	SD	%CV
C1	2.143	2.390	2.202	2.386	2.266	2.148	2.261	2.278	2.194	2.321	2.352	2.262	2.267	0.085	4%
C2	1.767	1.714	1.716	1.679	1.593	1.527	1.657	1.738	1.739	1.703	1.626	1.588	1.671	0.073	4%
C3	1.032	1.053	1.124	1.071	1.041	0.983	1.000	1.052	1.011	1.128	1.049	1.034	1.048	0.044	4%

These results suggest that variability between different sample replicates at different concentrations was low and similar between them in the established range.

-Method repeatability:

Each plate contained a standard curve and three samples with three different concentrations of the samples. Also, three different plates were performed by different analyst and different days:

Day 1:

-Plate 2: Operator A prepares three samples prepared independently (A1D1)

-Plate 3: Operator B prepares three samples prepared independently (A2D1)

Day 2:

-Plate 4: Operator A prepares three samples prepared independently (A1D2)

Calculations performed in this case were the interpolation of the OD with the standard curve and then, the multiplication of the result to the different dilutions performed to achieve the data normalization. These calculations allowed all the concentrations of all the samples to be compared with each other. Results for method repeatability for the three plates are summarized in the following tables:

Table 11. Validation ELISA method repeatability of plates 2, 3, and 4.

Plate 2 (A1D1)	Sample 1	Sample 2	Sample 3	Sample 4
C1	1.48E+10	1.30E+10	1.70E+10	1.53E+10
C2	1.50E+10	1.24E+10	1.68E+10	1.59E+10
C3	1.47E+10	1.27E+10	1.62E+10	1.47E+10
X	1.48E+10	1.27E+10	1.67E+10	1.53E+10
S	1.78E+08	3.17E+08	3.84E+08	6.01E+08
CV (%)	1.%	2%	2%	4%

Mean	Sr^2	CV $_{plate}$
1.49E+10	2.32E+18	10%

Plate 3 (A2D1)	Sample 1	Sample 2	Sample 3	Sample 4
C1	1.76E+10	2.02E+10	1.75E+10	1.75E+10
C2	1.94E+10	2.22E+10	1.80E+10	1.89E+10
C3	1.86E+10	2.36E+10	1.96E+10	1.97E+10
X	1.85E+10	2.20E+10	1.83E+10	1.87E+10
S	9.30E+08	1.73E+09	1.09E+09	1.14E+09
CV (%)	5%	8%	6%	6%

Mean	Sr^2	CV $_{plate}$
1.94E+10	3.63E+18	10%

Plate 4 (A1D2)	Sample 1	Sample 2	Sample 3	Sample 4
C1	1.40E+10	1.53E+10	1.59E+10	1.93E+10
C2	1.46E+10	1.55E+10	1.63E+10	1.92E+10
C3	1.42E+10	1.44E+10	1.51E+10	1.95E+10
X	1.43E+10	1.51E+10	1.58E+10	1.93E+10
S	2.77E+08	6.07E+08	5.73E+08	1.63E+08
CV (%)	2%	4%	4%	1%

Mean	Sr^2	CV $_{plate}$
1.61E+10	4.21E+18	13%

The results show that CV between the concentration levels each all samples of all plates were below the stablished threshold (15% of CV). Therefore, the analytical method was precise, and variability fitted the established acceptance criteria in the 3 plates.

-Intermediate precision:

In this case, the objective was to compare the result obtained between different days of the same operator, and a different operator. Hereafter the comparison between plates all plates can be found in tables 12 and 13.

Table 12. Validation ELISA intermediate precision day.

Plate 2. (A1D1)					Plate 4, (A1D2)			
	Sample 1	Sample 2	Sample 3	Sample 4		Sample 1	Sample 2	Sample 3	Sample 4
C1	1.48E+10	1.30E+10	1.70E+10	1.53E+10	C1	1.40E+10	1.53E+10	1.59E+10	1.93E+10
C2	1.50E+10	1.24E+10	1.68E+10	1.59E+10	C2	1.46E+10	1.55E+10	1.63E+10	1.92E+10
C3	1.47E+10	1.27E+10	1.62E+10	1.47E+10	C3	1.42E+10	1.44E+10	1.51E+10	1.95E+10
X	1.48E+10	1.27E+10	1.67E+10	1.53E+10	X	1.43E+10	1.51E+10	1.58E+10	1.93E+10
S	1.78E+08	3.17E+08	3.84E+08	6.01E+08	S	2.77E+08	6.07E+08	5.73E+08	1.63E+08
CV (%)	1%	2%	2%	4%	CV (%)	2%	4%	4%	1%

Var plate	2.32E+18
Mean Plate	1.49E+10
CV plate	**10%**

Var plate	4.21E+18
Mean Plate	1.61E+10
CV plate	**13%**

Intermediate Day	
Mean	1.55E+10
SD	1.88E+09
%CV	**12%**

Results suggest that the plates performed by the same analyst in different days had no differences. The intermediate precision between the same analyst in different days was 12%.

Table 13. Intermediate precision operator

Plate 2. (A1D1)					Plate 3, (A2D1)			
	Sample 1	Sample 2	Sample 3	Sample 4		Sample 1	Sample 2*	Sample 3	Sample 4
C1	1.48E+10	1.30E+10	1.70E+10	1.53E+10	C1	1.76E+10	2.02E+10	1.75E+10	1.75E+10
C2	1.50E+10	1.24E+10	1.68E+10	1.59E+10	C2	1.94E+10	2.22E+10	1.80E+10	1.89E+10
C3	1.47E+10	1.27E+10	1.62E+10	1.47E+10	C3	1.86E+10	2.36E+10	1.96E+10	1.97E+10
X	1.48E+10	1.27E+10	1.67E+10	1.53E+10	X	1.85E+10	2.20E+10	1.83E+10	1.87E+10
S	1.78E+08	3.17E+08	3.84E+08	6.01E+08	S	9.30E+08	1.73E+09	1.09E+09	1.14E+09
CV (%)	1%	2%	2%	4%	CV (%)	5%	8%	6%	6%

Var plate	2.32E+18
Mean Plate	1.49E+10
CV plate	**10%**

Var plate	8.63E+17
Mean Plate	1.85E+10
CV plate	**5%**

Intermediate Operator	
Mean	1.64E+10
SD	2.25E+09
%CV	**14%**

* Sample 2 in plate 3, as an individual result, was an outlier. Analysis of variance of plate 3 shows that sample 2 can be considered different from the other samples and be removed for the result. Considering that all samples come from the same original sample, the discordant value may be due to an error in the pipetting during sample 2 preparation.
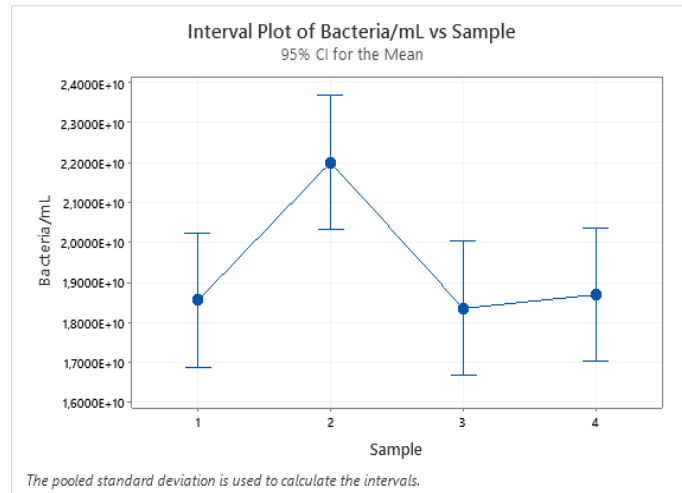
Figure 30. Validation ELISA compares samples 1, 2, 3, and 4 of ELISA assay validation in plate 3.

Results suggest that sample 2 of this plate was different from the rest of the samples and was excluded from further calculations.

Intermediate precision studied between different operators in plate 2 and 3 showed that the CV was 14%, which was also below the previously stablished threshold.

The results of tables 12 and 13 suggest that there were no significant differences between plates prepared by different analyst or different plates prepared by the same analyst.

7.3.5 Accuracy:

In this case, the objective was to assess how different were the results obtained in the different plates from the theoretical value (1.58E+10 bacteria). This determination was performed by dividing the results of the sample between the theoretical value and then obtaining the percentage called recovery. Results of recovery for each plate are shown in table 14.

Table 14. Validation ELISA, recovery calculation for plates 2, 3, and 4.

	Plate 2 (A1D1)				Plate 3 (A1D2)			
	Sample 1	Sample 2	Sample 3	Sample 4	Sample 1	Sample 2*	Sample 3	Sample 4
C1	1.48E+10	1.30E+10	1.70E+10	1.53E+10	1.76E+10	2.02E+10	1.75E+10	1.75E+10
C2	1.50E+10	1.24E+10	1.68E+10	1.59E+10	1.94E+10	2.22E+10	1.80E+10	1.89E+10
C3	1.47E+10	1.27E+10	1.62E+10	1.47E+10	1.86E+10	2.36E+10	1.96E+10	1.97E+10
Media	**1.48E+10**	**1.27E+10**	**1.67E+10**	**1.53E+10**	**1.85E+10**	**2.20E+10**	**1.84E+10**	**1.87E+10**
Std. Dev.	1.53E+08	3.00E+08	4.16E+08	6.00E+08	9.02E+08	1.71E+09	1.10E+09	1.11E+09
CV%	1%	2%	2%	4%	5%	8%	6%	6%
Recovery	94%	80%	105%	97%	117%	139%	116%	118%
Mean	**94%**				**117%**			

	Plate 4 (A1D2)			
	Sample 1	Sample 2	Sample 3	Sample 4
C1	1.40E+10	1.53E+10	1.59E+10	1.93E+10
C2	1.46E+10	1.55E+10	1.63E+10	1.92E+10
C3	1.42E+10	1.44E+10	1.51E+10	1.95E+10
Mean	**1.43E+10**	**1.51E+10**	**1.58E+10**	**1.93E+10**
Std. Dev.	2.77E+08	6.07E+08	5.73E+08	1.63E+08
CV%	2%	4%	4%	1%
Recovery	90%	95%	100%	122%
Mean	**102%**			

As an individual result, the recovery of sample 2 in plate was eliminated as explained previously. Recovery for all plates was within the parameters established (75-125%). Therefore, the three plates complied with the expectations. The method can be considered accurate enough to be used as a quantification method.

7.3.6 Robustness

Robustness was tested in two different plates in which two different times for the colorimetric reaction were compared (7 and 9 minutes in plate 5, and 7 and 5 minutes in plate 6). All samples in this study complied with the expectations regarding its accuracy. Therefore, the data used to assess robustness was analyzed to assure that it complied with accuracy results. Recovery was evaluated in samples of plates 5 and 6 as quality control of the plate.

Table 15. Validation ELISA recovery robustness results for plates 5 and 6.

	Plate 5		Plate 6	
	7 minutes	9 minutes	7 minutes	5 minutes
Theoretical value	1.58E+10	1.58E+10	1.58E+10	1.58E+10
Experimental value	1.49E+10	1.53E+10	1.79E+10	1.98E+10
p value (ANOVA)	0.5164			
Recovery	94%	97%	113%	125%

After achieving the minimum quality requirements, data was analyzed through an ANOVA test to measure the differences between the different colorimetric reaction times. Results of the plate can be found in table 15.

ANOVA analysis shows that time in of TMB substrate exposition is a parameter that does not affect the robustness of the analytical method between 7±2 minutes (p >0.05).

All data from the ELISA analysis suggest that the test is suitable for quantifying Omp22 protein on the bacteria membrane.

7.3.7 ELISA validation summary:

ELISA validation results suggested that the method was working in a linear area, it is precise, accurate, robust and has complied all requirements proposed in the method section. This method was used afterward to study the vaccine Acinetovax in different conditions.

In the table 17, a summary of validation can be found.

Table 16. Validation ELISA summary

PARAMETERS	ACCEPTANCE CRITERIA	RESULTS	Complies/ No Complies
CV Absorbance replicates	-≤10%	See ANNEX results for each plate	Complies
-Standard curve			
-Samples			
SPECIFICITY	-OD raw absorbance < 0.100	Complies	
Blank raw Absorbance	0.038		
Abscence of capture Ab	0.039		
Abscence of detection Ab	0.04		
Abscence of sample	0.038		
Abscence of streptavidine	0.035		
Trehalose BLANK	0.035		
Sucrose BLANK	0.037		
LINEARITY	-R^2 ≥ 0.98	Plate 1: 0.99	Complies
		Plate 2: 0.99	
		Plate 4: 1.00	
	-Residuals non tendency	Residuals non tendency	
PRECISION	-Instrumental precision (n=12) CV%≤ 10%	C1 = 4% C2 = 4% C3 = 4%	Complies
	-Method precision (n=3) CV%≤ 15%	-Plate 2 = 11%	Complies
		-Plate 3 = 1%	
		-Palte 4 = 14%	
	-Intermediate precision (n=3) CV% ≤ 20%	-Intermediate precision (days) Total CV (%) = 12%	Complies
		-Intermediate precision (analysts) Total CV (%) =14%	
ACCURACY	-Recovery between 75%-125% (n=3)	-Plate 2 = 94%	Complies
		-Plate 3 = 117%	
75%-125%		-Plate 4 = 102%	
ROBUSTNESS	-No significant difference between experimental conditions detected by t test (p>0.05)	ANOVA P= 0.5164	Complies
	-Recovery samples between 70% and130%	Recovery:	
		-Plate 5 7 minutes (94%)	
		-Plate 5 5 minutes (97%)	
		-Plate 6 7 minutes (113%)	
		-Plate 6 5 minutes (125%)	

7.4 Quantification: µBCA method validation

This method was validated following the ICH guidelines. Parameters determined in the materials and methods were tested. See method procedure in section 6.5.2.

7.4.1 Specificity:

Specificity is the ability of an analytical method to assess the analyte unequivocally in the presence of components that may be expected to be present. In this case, it consisted on analyzing the diluent of the product that was NaCl 0.9% and the possible excipients used to produce the final product (trehalose and sucrose dilution).
Blanks should not have any reaction with the reagents, and the OD should be below 0.150 as observed in pre validation assays (data not shown).

Table 17. µBCA validation, specificity results calculated from plate 1.

	Blank absorbances results		
	Sample blank	Trehalose	Sucrose
	0.112	0.115	0.119
	0.113	0.116	0.114
	0.113	0.117	0.119
	0.112	0.118	0.118
	0.116		
	0.113		
	0.114		
	0.117		
Average	0.114	0.117	0.118
SD	0.002	0.001	0.002
CV%	2%	1%	2%

The results show no significant interference in the different blanks analyzed in this validation (see table 18). The main conclusions were that neither NaCl nor trehalose or sucrose produced a response above the established limit of 0.150.

7.4.2 Range

The working range was defined for the standard in pre-validation experiments between 32 µg BSA /mL to 4 µg BSA /mL. In plate 1, standard panels of eight different concentration levels were prepared: 32, 28, 24, 20 16, 12 8 and 4 µg/mL.

For the drug product VXD-001, the range was studied in pre-validation experiments between 1E+08 and 1.56E+07 bacteria/mL (data not shown). Linearity was studied in plate 1 with panels of seven different concentration levels: 1E+08, 6.25E+07, 5.47E+07, 4.69E+07, 3,91E+07, 3.13+07, 2.34+07 and 1.56E+07 bacteria/mL. Results for each standard panel at each plate are summarized in figure 31. Mean, SD, and %CV for each concentration level tested, and R^2 were calculated. Results can be found hereafter:
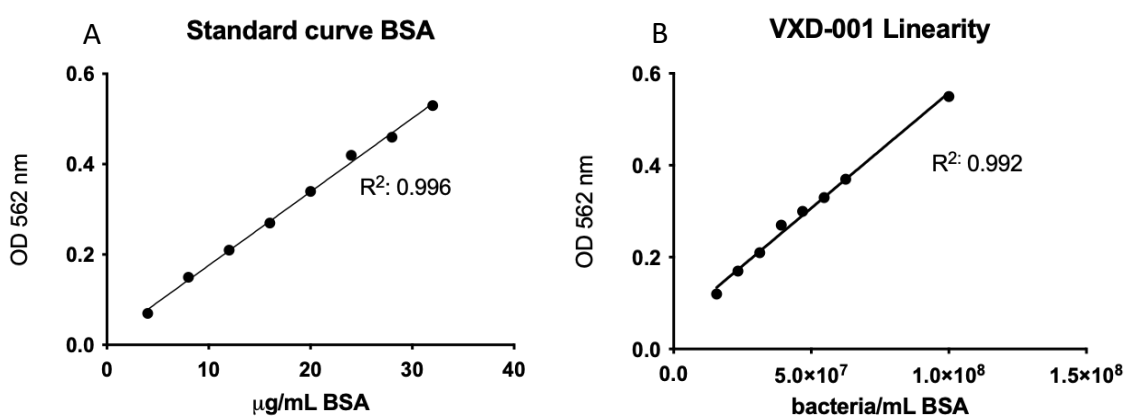
Figure 31. linearity studied for BSA standard (A) and VXD-001 curve (B)(n = 3).

These results have also been represented in the following table:

Table 18. Validation µBCA, linearity of BSA standard, and VXD-001 curve for plate 1.

	BSA Standard curve (n = 3)				VXD-001 curve (n = 3)		
	Average	Standard deviation	CV%		Average	Standard deviation	CV%
C1	0.529	0.010	2%	C1	0.552	0.002	0%
C2	0.462	0.006	1%	C2	0.369	0.005	1%
C3	0.424	0.006	1%	C3	0.329	0.004	1%
C4	0.343	0.004	1%	C4	0.298	0.009	3%
C5	0.269	0.003	1%	C5	0.269	0.006	2%
C6	0.209	0.001	0%	C6	0.209	0.008	4%
C7	0.146	0.002	1%	C7	0.170	0.006	4%
C8	0.074	0.002	2%	C8	0.120	0.007	6%
R^2	0.996			R^2	0.992		

Both BSA and VXD-001 standard curves were correct because R^2 was higher than 0.98, and CV was lower than 10% in all standard curve levels.

-Residual normality:

Residual normality is tested at all points of the curve to look for tendencies and avoid specific concentrations.
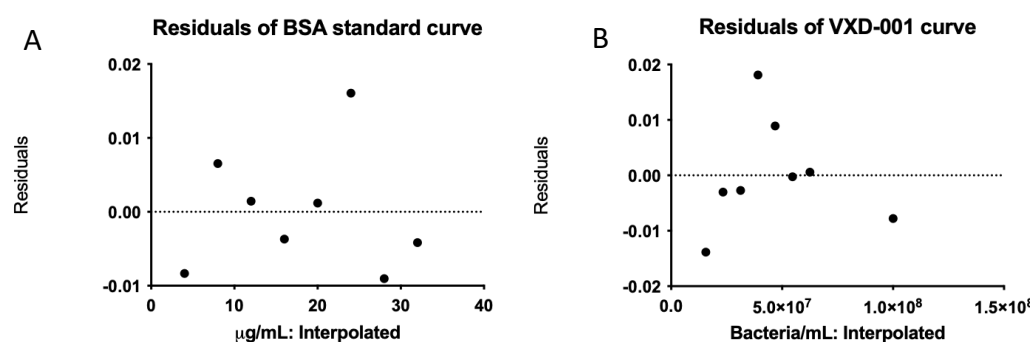
Figure 32. Validation µBCA, residuals of BSA standard (A) and VXD-001 curve(B).

Results of figure 32 had low residuals that were distributed randomly, showing no tendencies.

111

Linearity results suggest that the method was working in a linear range and the correlation between protein and OD could be correlated from figures 31 and 32 and table 19.

7.4.3 Precision

The precision of an analytical procedure expresses the closeness of agreement (degree of scattering) between a series of measurements obtained from multiple sampling of the same homogeneous sample under the prescribed conditions. Three different levels of precision were studied.

Method repeatability:

Method repeatability was meant to determine the variability due to the preparation of different samples inside the same plate. It was assessed using two concentrations (each with six replicates) in 3 independent samples. Results for method repeatability for the three plates are summarized in table 20. The plates were performed as it follows:

Day 1:
-Plate 2: Operator A prepares three samples prepared independently (A1D1)
-Plate 3: Operator B prepares three samples prepared independently (A2D1)

Day 2:
-Plate 4: Operator A prepares three samples prepared independently (A1D2)

Table 19. Validation µBCA, method repeatability plate 2, 3, and 4.

Plate 2 (A1D1)			
	Sample 1	Sample 2	Sample 3
C1	5751	5944	5885
C2	5712	6002	6189
X	5731	5973	6037
S	27	41	215
CV	0%	1%	4%

Plate 3 (A1D2)			
	Sample 1	Sample 2	Sample 3
C1	6473	6440	6451
C2	6561	6461	6604
X	6517	6451	6528
S	63	14	108
CV	1%	0%	2%

Plate 4 (A2D1)			
	Sample 1	Sample 2	Sample 3
C1	6320	6002	6041
C2	6538	6036	6213
X	6429	6019	6127
S	154	24	122
CV	2%	0%	2%

S^2	X	CV
26063	5914	3%

S^2	X	CV
1736	6498	1%

S^2	X	CV
45196	6191	3%

The results of table 19 show that the analytical method was accurate , and that the variability fitted the acceptance criteria established before the validation for the three plates analyzed.

Instrumental repeatability

Instrumental repeatability was studied in plate 1 of µBCA validation. The scope was to see the variability induced by the analytical method instruments and how they interfere. Twelve replicates (R1-R12) of C1 and C2 were applied in Plate 1. Hereafter are shown the results of instrumental repeatability. See table 20 for the results for the %CV at each concentration tested.

Table 20. Validation ELISA, summary for Instrumental repeatability

	R1	R2	R3	R4	R5	R6	R7	R8	R9	R10	R11	R12	Mean	SD	CV%
C1	0.307	0.308	0.304	0.303	0.301	0.301	0.311	0.314	0.305	0.306	0.300	0.304	0.306	0.004	1%
C2	0.167	0.167	0.169	0.169	0.174	0.176	0.172	0.172	0.172	0.168	0.165	0.170	0.170	0.003	2%

Intermediate precision

Intermediate precision is a parameter that measures the variability between different days and different analysts. The precision study was performed with three independent assays (plates 2, 3, and 4) on different days and performed by different analysts.

Plates 2, 3, and 4 used in the method repeatability were analyzed for intermediate precision. Calculation of the mean, variance, and %CV between plates 2 and 3 and plates 3 and 4 was performed.

Table 21. Validation µBCA, intermediate Precision Operator and Day

Plate 2 (A1D1)			
	Sample 1	Sample 2	Sample 3
C1	5751	5944	5885
C2	5712	6002	6189
X	5731	5973	6037
S	27	41	215
CV	0%	1%	4%

Plate 3 (A1D2)			
	Sample 1	Sample 2	Sample 3
C1	6473	6440	6451
C2	6561	6461	6604
X	6517	6451	6528
S	63	14	108
CV	1%	0%	2%

S^2	26063
X	5914
CV	3%

S^2	1736
X	6498
CV	1%

Intermediate day	
Mean	6206
SD	330
CV%	**5%**

Table 22. Validation µBCA, intermediate Precision analyst.

Plate 3 (A1D2)			
	Sample 1	Sample 2	Sample 3
C1	6473	6440	6451
C2	6561	6461	6604
X	6517	6451	6528
S	63	14	108
CV	1%	0%	2%

Plate 4 (A2D1)			
	Sample 1	Sample 2	Sample 3
C1	6320	6002	6041
C2	6538	6036	6213
X	6429	6019	6127
S	154	24	122
CV	2%	0%	2%

S^2	1736
X	6498
CV	1%

S^2	45196
X	6191
CV	3%

Intermediate analyst	
Mean	6345
SD	219
CV%	**3%**

Results show that the variability between plates performed by different analysts and different days fits the criteria decided before the validation. These results are shown in table 21 and 22.

Precision results suggest that the µBCA method was highly precise regarding instrumental, method and intermediate precision. Thresholds determined to stablish if the method was precise were selected based in previous experience with other µBCA methods developed in the laboratory. The obtention of a precise method allow the method to study further drug products.

7.4.4 Accuracy

Accuracy was checked spiking the sample with different known concentrations of a protein. In this case, a basal quantity of 2.5E+07 bacteria/mL was spiked with three different

concentrations of BSA protein concentration (C1, C2, and C3). Each spiked concentration had four replicates in plates 2, 3, and 4.

Accuracy was studied in plates 2-4. Results of recovery for each plate are shown in table 23.

Table 23. Validation µBCA, recovery results of plates 2, 3, and 4.

Plate 2					
	MSC concentration (µg/mL)	MC2 concentration	MSC-MC2 µg/mL	Theoretical spike µg/mL	Recovery %
C1	21.2		11.7	12	98%
C2	17.5	9.4	8	8	100%
C3	13.8		4.3	4	108%

Plate 3					
	MSC concentration (µg/mL)	MC2 concentration	MSC-MC2 µg/mL	Theoretical spike µg/mL	Recovery %
C1	23.2		12.8	12	107%
C2	18.9	10.4	8.5	8	106%
C2	15.1		4.7	4	117%

Plate 4					
	MSC concentration (µg/mL)	MC2 concentration	MSC-MC2 µg/mL	Theoretical spike µg/mL	Recovery %
C1	22.1		12.2	12	102%
C2	18.3	9.9	8.4	8	104%
C2	14.2		4.3	4	106%

Mean accuracy from all plates	
C1	102%
C2	103%
C3	110%

Results suggest that the method recovered around 100% BSA in the three concentrations spiked. All of them were enclosed in the threshold specification between 80% and 120%. This method was accurate enough to be used in pharmaceutical quality control environment.

7.4.5 Robustness

Robustness is a parameter to study the reliability of the analysis with respect to deliberate variations in method parameters. In this case, plate two was evaluated at three different times: 1.5, 2 and 2.5 hours. This step is necessary to understand how critical incubation with μBCA reagents is. The three analyses of plate 2 were compared through an ANOVA and the result can be found hereafter.

Table 24. ANOVA result between μBCA plate 2 was analyzed at 1.5, 2, and 2.5 hours.

ANOVA summary	
p value	0.7404

ANOVA analysis shows (table 24) that the results obtained with revelation times of 1.5, 2 and 2.5 hours are equivalent, meaning that the μBCA method is suitable to be used in routine analysis with 2 hours of reaction.

7.4.6 Assay suitability

Before the validation, it was established that the quality control QC3 must fit the criteria for a plate to be considered suitable. All plates tested in the validation contained a quality control prepared with BSA, a replica of the third dilution of the standard curve. The results of the control in all plates evaluated can be found hereafter:

Table 25. Validation *μBCA*, system suitability responses of plates 1, 2, 3, and 4.

System suitability QC3 (µg/mL)					
Plate 1	Plate 2 (1,5 h)	Plate 2 (2 h)	Plate 2 (2,5 h)	Plate 3	Plate 4
25.1	26.9	26.8	26.5	25.6	25.3

According to the results obtained, the analytical method for total protein quantification, μBCA, is suitable for analyzing the drug substance VXD-001 because the limits for the QC3 were ≥ 20.4 µg/mL and ≤ 27.6 µg/mL.

7.4.7 µBCA summary

Validation of this method was achieved, and the different assays performed suggested that this method was precise, accurate, and could be used to evaluate the quality of a product in pharmaceutical industry. A summary of all validation results can be found hereafter:

Table 26. µBCA validation summary

Parameter	Acceptance limit	Results	Complies
CV Absorbance replicates	CV		
· Standard curve	≤10%	2%	Complies
· Samples	≤10%	5%	Complies
Specificity			
· Blank raw Absorbance NaCl 0.9%	<0.150 OD	0.114	Complies
· Blank trehalose		0.117	Complies
· Blank sucrose		0.118	Complies
Linearity			
· R^2 Standard	R^2 ≥0.98	1	Complies
· R^2 VXD-001		1	Complies
· Residual's standard	Non-tendency visible in the residual plot	Non-tendency visible in the residual plot	Complies
· Residuals VXD-001			Complies
Precision	CV		
· Instrumental precision C1	≤10% (n = 12)	1%	Complies
· Instrumental precision C2		2%	Complies
· Method precision plate 2	≤15%	3%	Complies
· Method precision plate 3		1%	Complies
· Method precision plate 4		3%	Complies
· Intermediate precision day	≤20%	5%	Complies
· Intermediate precision analyst		3%	Complies
Accuracy, recovery			
· Recovery C1	80% – 120 %	102%	Complies
· Recovery C2		103%	Complies
· Recovery C3		110%	Complies
Robustness	No difference between experimental conditions was detected by ANOVA (p>0.05).	p = 0.7404	Complies
System suitability			
· Plate 1	System suitability values must be between 20.4 mg/mL and 27.6 mg/mL	25.1 mg/mL	Complies
· Plate 2		26.9 mg/mL	Complies
· Plate 3		25.6 mg/mL	Complies
· Plate 4		25.3 mg/mL	Complies

7.5 Summary of chapter 1

Results obtained in this chapter were essential to continue with the project. The initial hypothesis was accepted because it could be shown that the vaccine elicited a potent humoral immune response. The humoral immune response was characterized by analyzing the IgG response by an ELISA, the protein characteristics by western blot. Also, the immunodominant protein Omp22 was identified.

The different analytical techniques such as ELISA sandwich, Western blot, Coomassie staining, or µBCA were developed and validated following ICH guidance. With these techniques the different batches of the Acinetovax vaccine can be studied. Therefore, the first objective of the thesis was accomplished.

7.6 Technical achievements

In this chapter, the main objectives have been achieved:

- The formulations developed by Reig Jofre can induce protection against *A. baumannii* in a sepsis model.
- The response induced by the vaccine showed a solid humoral response with high levels of specific IgGs.
- An immunodominant protein present in the vaccine was characterized.
- An ELISA assay method to quantify Omp22 has been developed following ICH validation guidelines.
- Furthermore, following ICH validation guidelines, a µBCA method was developed to quantify the total protein contained in the drug product formulation.
- Also, a robust Western blot assay method to identify the protein Omp22 contained in Acinetovax has been developed following ICH validation guidelines.

    .

Chapter 2. Galenical product development.

8. Introduction:

The second objective of this thesis was to develop an optimized galenical formula of the Acinetovax vaccine. The development and optimization of the formula was a complex process for which trial-error steps have been performed.

In this chapter, different factors considered related to the characteristics of the drug substance, adjuvant, drug product, regulation, lyophilization, and sterility, will be explained.

8.1 Acinetovax vaccine:

The drug substance VXD-001, as indicated previously, consists of a suspension of an LPS negative *A. baumannii* strain. VXD-001 bacterial strain was heat inactivated at 70ºC for 30 minutes. Pharmacopeias establishes the sterilization temperature at 121ºC for 10 minutes but the drug substance VXD-001 is degraded at this temperature. Therefore, a protocol had to be developed to test the sterility of the product through a sterility assay based on pharmacopeia. This step is essential because no microorganism can be alive after the inactivation and even though *A. baumannii* is inactivated at this temperature possible contaminants may be alive after heat treatment.

The second objective of the thesis was therefore to study this drug substance analyzing physicochemical parameters such as pH, osmolarity, visual aspect or reconstitution time.

During drug product scale up some milestones were established. The most important milestone was related to the precipitation time of the bacteria. To ensure that precipitation was not a limitation, time determination assays were performed to evaluate the implications of this fact, such as turbiscan analysis. Also, a minimum mixing time was

determined to ensure the homogeneity of the drug substance during all production processes.

8.2 Aluminum hydroxide:

Initially, when first vaccines were developed, they contained whole bacteria, combinations of lipids, proteins and nonspecific elements that reached the final product due to the lack of tools to detect or eliminate them (142). These uncontrolled elements caused unexpected and uncontrolled reactions (142). Nowadays, vaccines are developed from *in silico* selection, where one specific antigen is selected and the pharmaceutical production controls every molecule found in the final product. Even though this is a significant improvement of the quality and safety it has led to the development of vaccines that cannot induce a strong memory immune response by themselves (142). This problem cannot be solved by increasing the concentration, because it might lead to adverse reactions (143). Therefore, the use of adjuvants to boost and redirect the immune response induced by the vaccine has become essential to obtain effective vaccines.

The adjuvants are used to enhance immune responses through physical-chemical association with antigens. They induce a boost during the specific immune response against the vaccine immunogen (144,145).

Many substances have been inoculated as adjuvants, such as mineral surfactants, nucleic acids, liposomes, polysaccharides and lipopolysaccharides (146–150). New adjuvants are being developed and some are being accepted by regulatory entities, such as MF59 (151). However, the most used adjuvants are still composed of aluminum salts, being the aluminum hydroxide the most commonly used adjuvant (142).

These kinds of adjuvants have been used for decades and have shown excellent safety at a low cost. Also, aluminum is found in our environment abundantly and is ingested through water and food with no secondary effects (142,152).

Although aluminum-based adjuvants have been intensely studied, the immunology behind their effectiveness has not been discovered yet. Immunologically, it has been determined to enhance both Th1 and Th2 immune response depending on the initial immune response induced by the associated antigen (142).

There are different aluminum-based adjuvants such as aluminum hydroxide or aluminum phosphate. Specifically, for Acinetovax, aluminum hydroxide was chosen. Aluminum hydroxide adsorb the antigens, and inside of it, the molecules aggregate, and their physical and chemical characteristics are maintained (142). This adsorption produces a strong local immune response when the vaccine is administered, leading to a better response against the immunogen (142).

Acinetovax vaccine is composed of whole inactivated bacteria and has been administered together with aluminum hydroxide. In this case, the use of an adjuvant might seem inadequate or unnecessary because it is not composed of a single antigen However, the efficacy of the vaccine was shown to decrease if it was administered without the adjuvant. Vaxdyn used their murine model of *A. baumannii* infection to study the efficacy of the vaccine with and without adjuvant. The results obtained are shown hereafter:
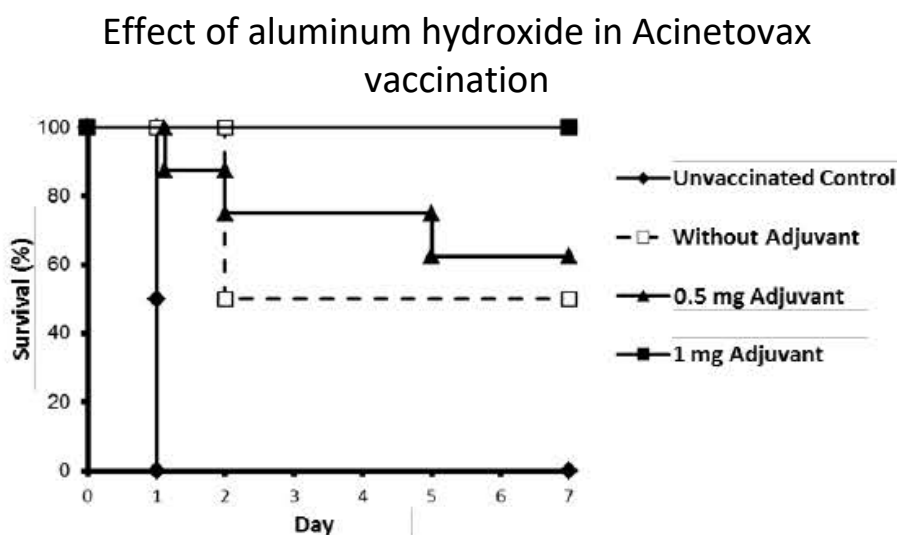
Figure 33. Survival assay performed by Vaxdyn comparing adjuvanted and non-adjuvanted vaccine in a murine sepsis model. (Graphic handed over by Vaxdyn)

The survival graph indicates that the efficacy of the vaccine in the sepsis model decreased if it was administered without the adjuvant. It also decreased as the adjuvant dose used was reduced. The difference in survival rates of mice receiving adjuvanted or non-adjuvanted vaccines might be related, not to their capacity to generate an immune response but to the type of T helper cell response induced. So, in this case, the adjuvant is indispensable to develop a protective immune response that changes the original response produced just by the bacterium.

Aluminum hydroxide clinical issues:

Due to its nature, and depending on the dose administered, aluminum hydroxide can have adverse events. Thus it can cause erythema, subcutaneous nodules, allergic reactions and granuloma (142).

Also, aluminum hydroxide can boost allergies increasing IgE production (142), meaning that it is essential to control the concentration of aluminum hydroxide administered in humans. For these reasons, the European pharmacopeia has limited the concentration of aluminum to a maximum of 1.25 mg per vaccine dose and the FDA to maximum of 0.85 mg per dose (153).

Analytical aluminum hydroxide issues:

Some problems that appeared during the development of the vaccine required the development of new strategies to overcome them.

After a thorough bibliographic review on Aluminum hydroxide one most crucial factor for the efficacy of aluminum hydroxide is that it is easily degraded when exposed to freezing temperatures. When this happens, it loses the capacity to adsorb the vaccine antigens and therefore to produce a protective immune response (154).

Lyophilization is a process in which water contained in a solution is sublimated with a combination of low pressure and freezing temperature. The elimination of water protects the products from degradation and so improves vaccine conservation (155). Therefore, research was performed to determine how the lyophilization could be performed and it was found that the use of trehalose could prevent the degradation of aluminum hydroxide, allowing the vaccine to extend its expiration time (154).

8.3 Drug product:

Acinetovax produced with the VXD-001 drug substance contained an adjuvant known as aluminum hydroxide. During the development of the vaccine, several batches have been tested. These batches have been produced considering several criteria that are explained hereafter.

8.3.1 Terminal sterilization

Regarding pharmacopeia, pharmaceutical companies must incorporate terminal sterilization of the pharmaceutical product (156,157). It is accepted that sterilized articles or devices can be considered sterile when containing less than 10^{-6} live microorganisms present in the final drug product (158). The procedures to sterilize the product were: 1) temperature, already discarded because could cause product degradation; 2) filtration through a 0.22 μm membrane, impossible to be performed with bacteria and aluminum hydroxide; 3) EtO gas-based approach that might produce toxic residuals and finally, 4) irradiation, the method that was thought to be the most feasible for this vaccine.

Irradiation has its risks and effects on the product that might be studied. This treatment could cause denaturalization and degradation of the bacteria, so one of the intentions of this study was to determine the effect of irradiation at sterility level and the rest of the techniques (156,157).

Even though many materials have this gamma-irradiative emission during their degradation process, Cobalt-60 is one of the limited possibilities that might be indicated for sterilization processing in pharmaceutical product development (159,160).

Cobalt-60 is produced specifically for the gamma-irradiation process and housed in specially designed rooms under national regulations (UNE-EN ISO 13485:2018). This kind of gamma irradiation produced by Cobalt-60 is a process that does not generate a radioactive product and kills microorganisms(160).

8.3.2 Galenical product development and stability:

The galenical development is the process in which a pharmaceutical product is optimized from an initial formula used to be tested in pre-clinical development stages to a formula that can be administered into humans. New formulation might include the addition of new excipients to improve the stability, control the pH and the osmolarity among others. Selected excipients might be regulated by different pharmacopeias and its concentration must be controlled to be accepted for human use. Furthermore, this process must be leaded to a scalable production process

Also, it is necessary to study the stability of the formula in different conditions. The stability studies must follow ICH guidelines, based on different pharmacopeias. ICH was also essential for the galenical consideration because the several produced batches had to be studied based on stability guidelines. Specifically, the purpose of guideline Q1A(R2) is to test the stability to provide evidence on how the pharmaceutical product quality varies with time under the influence of environmental factors, such as temperature, humidity, or light. This evaluation is headed to define recommended storage conditions for the product.

The guideline has been created for countries included in the EU, Japan, and the USA, considering the climate conditions of these regions. Also, the guideline establishes that for studying the behavior of the product, the defined methods (defined previously in the analytical development) must be used for studying long term stabilities in the following

periods: every three months during the first year, every six months in the second year and from then on, every year.

8.3.3 Osmolarity

The equilibrium of water electrolytes is a factor that has a central position in clinical sciences (161). This is debt to semi-permeable membrane cells, and the molecule interchange between cells and the media is based on the osmosis process (162).

The osmosis process is based on a solution divided into two different compartments, separated by a membrane that allows the interchange of water molecules but not the flow of solutes, usually known as semi-permeable membranes. When the concentration of solutes in both compartments is different, the water travels from the more concentrated side to the less concentrated side to compensate for the concentration differences (163). This process is known as water osmosis (163).

This measurement is essential while producing a pharmaceutical parenteral product because a wrong osmolarity could cause either hypertonicity or hypotonicity, leading in some cases to the death of cells near the injection, which might mean irritation or less effectivity. To avoid this effect, all products formulated in parenteral development must be isotonic that equals an osmolarity of 0.300 Osmol/L.

The osmolarity of the 37 batches produced in Reig Jofre was tested been to assure that the solution is injectable in mice and, in the future, in humans. To achieve this, the drug substance and excipients of the vaccine must be at adequate concentrations for parenteral injection, and combined, must achieve 0.300 Osmol/L.

8.3.4 Lyophilization:

Lyophilization, also known as freeze-drying, is a method that consists of removing the water by sublimation from frozen material, converting solid water into gas. This procedure allows

pharmaceutical companies to manufacture products with longer expiration dates, especially for unstable products for long periods in their liquid form. Lyophilization improves this elongation of the degradation times because water produces hydrolysis in the product, and also, liquid state is the media in which many chemical reactions occur, and degradation of the product are several degradation interactions (164–166).

The lyophilization process of a drug product in the pharmaceutical industry consists of the following main steps: Freezing, primary drying, and secondary drying. During the freezing, water is turned into ice due to the effect of low temperatures, primary drying consist of the sublimation of the ice thanks to the conditions obtained with a vacuum that reduces the pressure allowing the sublimation, and the last step is known as secondary drying when unfrozen water is removed by desorption (164–166).

The following figure explains the importance of working under low pressure conditions during lyophilization. The chart presents the temperature vs. pressure and, in this figure, the frontiers between different states of the mass.

Water state regarding pressure and temperature
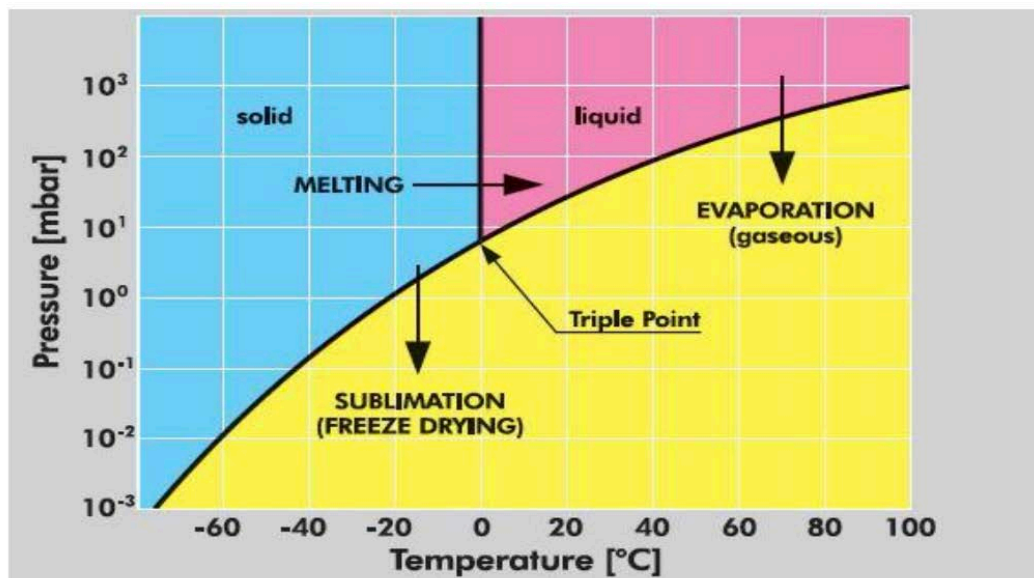
Figure 34. Representation of mass state of water depending on a combination of temperature and pressure (165).

There is a combination of pressure and temperature regarding the figure where it is physically possible to skip the liquid phase, obtaining a steam phase from a solid product.

Lyophilization is a standard procedure but, due to the required energy used in the process, it is an expensive one. Some simple products might take some hours to be lyophilized, but the process could last one entire week in some cases. Therefore, the objective in many cases is to reduce the time required for the process, especially primary drying that is the longest step (160,164). Although increasing the temperature in secondary drying before all the ice is removed will probably cause collapse or eutectic melt, meaning that one of the most important steps is to detect the end of the primary drying (160,164,166).

The development of lyophilized products in the pharmaceutical industry was based on trial and error a few decades ago (155,166). However, nowadays, the methodology behind the development of lyophilization processes has been refined and is based nowadays on the study of thermodynamic conditions of the samples to decide the lyophilization formula instead of using trial-error (155,166).

The DSC method has been used to measure the thermodynamic characteristics of the Acinetovax vaccine. This method measures the heat flow as a function of the temperature added to a sample. The DSC instrument consists of a cabinet with two cells; one is used as a standard and the other to introduce the assayed sample (160,166).

During DSC, both cells are cooled following the selected conditions. The difference in heat flow is also compared to an empty cell that is used as a control. The result is a graphic known as the DSC curve. (160,166). Hereafter, a theoretical thermodynamic figure is being shown.

Lyophilization phases
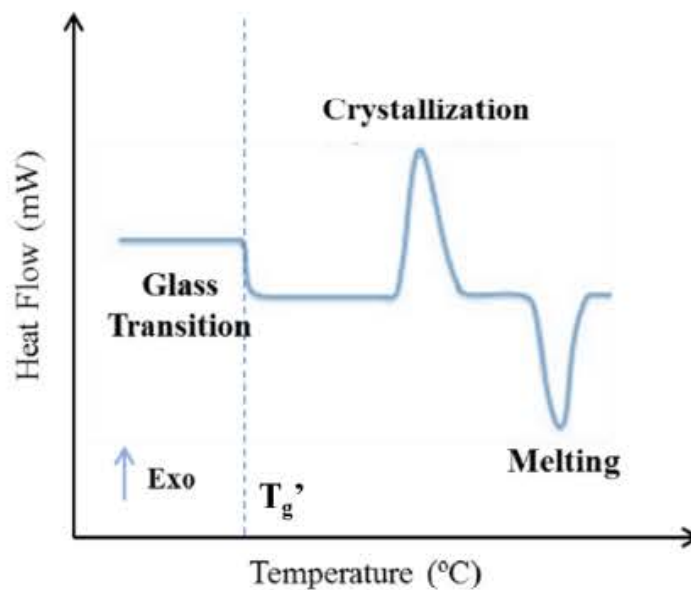
Figure 35. Thermodynamic representation of mass stated facing heat flow (mW) against temperature (166).

Reference and sample have similar behavior with a constant heat flow until sample reaction deviates, creating a curve that shows thermal infections due to the intrinsic characteristics of the sample. These possible thermal events are crystallizations, melting's, and glass transitions (See figure 35).

DSC also shows crystallization temperatures, and amorphous forms are created during the freezing process, known as glass transition temperature (Tg') and eutectic temperature (Te). This temperature is different between different samples, and the product is not frozen until the sample temperature is below Tg' and Te. Therefore, the freezing temperature should be below both temperatures to guarantee solidification.

Once with DSC are establish all thermal events of a possible drug product, the temperature at which these events occur are selected as critical temperatures, and therefore, the lyophilization cycle must be adapted considering these temperatures. Usually, thermal events are produced at specific temperatures and pressures, and therefore, once the vacuum is activated and no pressure affects the product, the events do not show up. This is why that after freezing the drug product, the temperature can be elevated to primary

drying temperature with no risk of the product suffering a collapse due to these thermal events (160,167).

8.3 Hypothesis:

-The galenic formulation produced in Reig Jofre shows improved stability from the non-formulated vaccine and maintains the protection capacity against *A. baumannii* murine sepsis model.

8.4 Technical objectives:

-Develop and optimize a stable galenical formulation that shows the same protection as the *in-situ* galenic preparation produced by Vaxdyn:

- Improve the stability with a lyophilization process.
- Improve the adsorption capacity of the product by controlling the pH of the solution.
- Ensure that galenical changes do not interfere with *in vivo* efficacy of the drug product.
- Maintain the protection capacity after all produced changes.

9. Material and methods

9.1 Material

Material used in this chapter can be found in tables 27 and 28.

Table 27. Chapter 2 material

Product	Reference	Brand
Thioglycolate broth (TG)	70157	Sigma Aldrich, San Luis, USA
Tryptic soy broth (TSB)	22092	Merk, Darmstadt, Germany)
Sterile Petri Dishes	1160960	Hampton, New Hampshire, USA
300 Osmol/L	30.9.0020	Gonotech, Berlin, Germany
Vial clase I 3 mL, boca 13	997F358	VSantos SA
Tapón Bromobutil	1779/4023/50B13	West Pharmaceutical Hispania
Standard solution pH at 4.01, 7.00 and 9.21	LZW9463.99 / LZW9464.98 / LZW9465.99	Crison

The necessary equipment used for chapter 2 can be found in the following table:

Table 28. Chapter 2 equipment

Equipment	Brand
Heater	Memmert, Schwabach, Germany
Tube revolver	Thermo Fisher, Waltham, USA
Osmomat 3000	Gonotech Berlin, Germany
Crison PH25	Crison, L'hospitalet, Spain
Turbiscan	IESMAT, Alcobendas, Spain
Scale 821e	Metler-Toledo, Spain
Class II cabinet Bio II Advance Plus 2020	Telstar, Terrasa, Spain
Lyobeta20 laboratory	Telstar, Terrassa, Spain

9.2 Drug substance and aluminum hydroxide

9.2.1 Drug substance origin

Vaccine Acinetovax *A baumannii* strain was genetically modified by Vaxdyn, which created a research cell bank that was analyzed to assure homogeneity/identification by MALDI-TOF and insertional mutation LPS biosynthesis gene by PCR, viability by colony-forming units, and absence of phages. These four tests assure the presence of *A. baumannii* and no other microorganism in the original process. Then the product was frozen and, afterward, sent to a contract manufacturer organization (CMO) to create large-scale productions. During the scale-up process, the bacteria is expanded until they reach a fixed concentration around 2E+10 bacteria/mL. After this process, the product is inactivated at 70ºC ± 2.5ºC for 30 minutes and is analyzed to determine sterility and endotoxin levels. Sterility is confirmed following pharmacopeia requirements and endotoxins below the pharmacopeia requirements. In the last step, bacteria were suspended in a NaCl 0.9% solution and sent to Reig Jofre, where it was conserved at 4ºC.

In total, two different batches were produced in this project following the previous indications:

-VXD-001 first batch: C1602-003-ABA-P01; (production date: 10/05/2017); concentration: 2E+10 bacteria/mL

-VXD-001 second batch: C1602-003-ABA-P04; (production date: 29/02/2019); concentration: 1.58E+10 bacteria/mL

9.2.2 Drug substance handling method

The drug substance is composed of a bacterial suspension with billions of bacteria, and this number of bacteria produces precipitation after the pass of time. So, every time a drug substance was handled as it follows: The drug substance (and drug product) must be gently mixed by inversion with tube revolver for 10 minutes at 10 RPM. This protocol was followed every time the drug substance was used.

Also, it was established that Acinetovax could not be frozen because the integrity of the dead bacteria might be compromised in the process.

9.2.3 Drug substance sterility

During drug product production, the drug substance was handled specially. The bottles used for drug product productions are different (sharing the exact batch origin) and were always opened in sterile conditions inside a class II microbiological handling cabinet. Maintaining the sterility of the product during its production was mandatory. Drug substance sterility was tested before using it inside the laboratory.

9.2.4 Aluminum hydroxide origin and handling

Aluminum hydroxide was bought to CRODA Denmark with the banded name Alhydrogel 2%. CRODA was a chemical company with expertise in adjuvant production, in which aluminum hydroxide could be found.

The composition of this product is $AlOH_3$, and the most important part is the control of aluminum dose. Alhydrogel 2% contains 10 mg/mL of aluminum.

Aluminum hydroxide is a sensitive adjuvant that can never be stored below 0ºC because it loses its capacity of adsorbing the antigens of the drug substance. This product is sterile and does not precipitate until the antigen is added and adsorbed by the aluminum hydroxide. It must be stored at room temperature in a condition that was never exposed to temperatures below 0ºC.

9.3 Sterility

As mentioned before, the product's sterility is a priority step for the product's scalability and must be assured.

The sterility was determined for drug substance batch VXD-0014-001 and drug product batch 27 at different irradiation times following European Pharmacopeia 2.6.1.

9.3.1 Method:

The sterility of drug substance and drug product was measured following pharmacopeia considerations that consist of the following bases:

- For pharmaceutical product container volumes greater than 100 mL, the required volume to be tested was 10% of the container but not less than 20 mL.
- For pharmaceutical product production of less than 100 containers per batch, the required number of articles to be tested was 10% of the total, or four containers (whichever was higher).

The sterility was tested in 400 mL of the second batch of VXD-001 (P04) and 10 vials of batch 27 for every irradiation condition of 8, 15, and 25 kGy of the drug product.

The preparation of the bacteria was performed in an insulator cabin. The drug product vials have been sterilized exteriorly with alcohol 70%. 4 vials of each sample were reconstituted, if necessary, with water for injections and then, they are incubated in tryptic soy broth (TSB) (30-35ºC) and thioglycolate broth (TG) (20-25ºC) media determined at the start, at day eight and day 13. Negative controls of TSB and TG were also introduced. TSB was used for aerobic bacteria, fungus, and yeast, and TG is used for aerobic and non-aerobic bacteria.

9.4 Physic-chemical properties

9.4.1 Osmolarity

The osmometer is calibrated and verified following pharmaceutical industry regulation, and samples are analyzed while the equipment is prepared. Firstly, the standard is analyzed. This standard of 0.300 Osmol/L was composed of NaCl 0.9% with isotonic composition. Samples were analyzed after the standard was measured as a verification. Then, samples were analyzed in the same way. The method was simple, 50 µL of standard or sample are introduced in Eppendorf and afterward in the equipment. Then the analyte was introduced to the equipment that lowers the temperature of the sample, measuring the freezing point. The freezing point depends on the osmolarity inside the sample. Each sample was analyzed with three replicates to increase the n of the analysis. Osmolarity analysis was performed following European pharmacopeia 2.2.35.

9.4.2 pH

Ph-meter was calibrated at pH 4.01, 7.00, and 9.21, then was verified at 4.00, 7.00, and 9.00 pH. Afterward, they were analyzed with the equipment. When the equipment measure was stabilized, the pH is registered. pH analyses were performed following European Pharmacopeia 2.2.3.

9.4.3 Turbiscan analysis of the drug product and drug substance.

With this method, the objective is to study the precipitation time of the vaccine Acinetovax. This vaccine's drug substance and drug product precipitate due to their nature, but both can be resuspended afterward with gentle mixing. This precipitation can be observed visually, but the precipitation starts probably before the visual separation. In this assay, the precipitation time of the product is determined through equipment known as Turbiscan. This procedure is performed because drug products containing bacteria and aluminum hydroxide have precipitation times incompatible with scalation to industrial batches. This

method assay's main comparison was between a drug product with aluminum hydroxide and no aluminum hydroxide.

If the formula significantly elongates the precipitation time, the final formulation might be separated into two vials: one containing bacteria and excipients and aluminum hydroxide in a second vial.

Material and equipment:

The drug product and drug substance of the vaccine Acinetovax were analyzed through the equipment Turbiscan, a luminescent diode was used to analyze the samples at a wavelength of λ = 880 nm.

Samples sent for the analysis had a volume of 4 mL and are the following: M1 is a sample that imitates the drug product without aluminum hydroxide to assess if the extraction of aluminum hydroxide from the formulation would improve the scalability of the drug product. M2 contained bacteria at the same dose as batch 27 described in section 10.8, trehalose at 5% concentration, NaCl 0.9%, and water for injections. M3 contained the same as M2, but part of the volume was substituted with aluminum hydroxide. This would be the current formula developed nowadays. M3 contained VXD-001 drug substance and as a control.

Table 29. Composition of Acinetovax samples studied in turbiscan.

Sample name	Alhydrogel		VXD-001		Trehalose		NaCl 0.9 (µL)	WFI (µL)	Final volume (µL)
	(µL)	mg	(µL)	bacteria	(µL)	mg			
M1	-		506.4	8E+09	508	0.2	2986	-	4000
M2	664	6.64	506.4	-	508	0.2	2322	-	4000
M3	-		4000	6.32E+10	-	-	-	-	4000

Method:

The homogeneity is measured by quantifying the vaccine turbidity along the vertical axes of the formulation. Samples are analyzed through vertical sweeps of their sample turbidity at different heights using a technique that combines light intensity transmission and the retro dispersed light. This disposition allows the simultaneous characterization in two situations: diluted system analysis using the light transmission and concentrated light transmission through light retro-dispersion.

The Turbiscan equipment has an electroluminescent diode as a light source that emits light at 880 nm. The instrument has two optical sensors, a transmission sensor (180º respect from the light source) and backscattering (45ºC respect from the light). Due to this disposition, transparent samples can be studied thanks to the transmission variance (ΔT) and the study of opaque samples thanks to the backscattering analysis (ΔBS). Both analyses were performed at different heights of the sample, obtaining a measure every 40 μm, allowing to measure concentration changes along with the sample.

9.4.4 Differential scanning calorimetry (DSC).

This procedure is performed as described in section 8.3.4 to develop an optimized lyophilization recipe that considered the critical temperatures of the drug product during the lyophilization.

Method:

DSC was performed at the Service Thermal Analysis and calorimetry service of CSIC (Barcelona, Spain). The analysis was performed with DSC 821e equipped with a liquid N_2 cooling device to achieve low temperatures.

This method is a thermo-analytic method in which the heat flow needed to produce temperature changes is measured and compared between a sample and a reference

standard. Sample and reference were maintained at the same temperature throughout the experiment.

The analytic method was designed to produce a linear increase in the temperature throughout time. Standard had a defined and previously measured calorific capacity well defined in the temperature interval in which the temperature was studied. Sample and standard were cooled and/or heated according to a selected temperature program.

The result of the experiment was a plot in which heat flow was faced against temperature. This curve is known as the DSC curve (see figure 35). The different heat flows showed in the previous chart were usual and were due to phase changes or other thermal events.

Standard and sample had a similar behavior until sample reaction occurs and creates a heat flow thermal inflection. The thermodynamic structural changes that appear in the sample translate into the release or absorption of heat. Apart from state changes, other events showing changes in the sample were crystallization, melting, and glass transitions.

Analysis was performed in DSC equipment. 30 mg of sample were introduced in aluminum pans and were sealed before the analysis. An experimental condition such as temperature ranges were the following ones:

First, during the analysis, the temperature decreased to study the freezing point of the sample from 25ºC until a freezing temperature goal (previously determined) with a temperature change of -10ºC per minute. Afterward, samples were maintained at the determined temperature for one minute. Then samples were heated from the freezing temperature to a primary drying temperature (previously determined) with a temperature change of 10ºC per minute. The exact temperatures can be found specified in batch preparation.

9.4.5 Irradiation procedure:

As mentioned in the introduction of this chapter, the drug product must be sterile for its parenteral injection, and the only possibility with this product was to use gamma-irradiation with Cobalt-60 to achieve this sterility (158).

The method consists of exposing the sample to high-energy photons that result in free radical production and ionization. The main effect is the cleavage of the DNA of microorganisms. This process could cause drug substance degradation, so *in-vitro* and *in vivo* testing was performed to assure that the drug product does not lose its capacity to induce a protective immune response (section 10.3) (158).

Samples were sent to Aragogamma, where the drug product was treated with a gamma-irradiation dose with cobalt 60. The different batches produced during the thesis were treated with different gamma-irradiation doses. Three irradiation doses were tested: 25 kGy, 15 kGy, and 8 kGy of gamma-irradiation. The standard gamma irradiation used in the pharmaceutical industry is 25 kGy, which is why this was the highest dose used for Acinetovax.

The sterility of the product treated with three irradiation doses was determined through microbiology sterility testing (section 9.2). If the three doses achieved sterility, the lowest dose, 8 kGy, would be selected as the standard dose used for industrial production.

9.5 Drug product and stabilities

During the thesis, 37 batches of different sizes and complexities were produced to study different excipients to control the pH, to obtain a stable lyophilized and to study the effect of different conditions such as temperature or irradiation and their effect on stability. The composition, the aim of each batch and the stability studies description can be found in result section 10.

10. Results and discussion

10.1 Homogeneity

<u>Visual aspect and µBCA</u>

Drug substance VXD-001 is a bacterial suspension that separates in 2 different phases after few days. To ensure that the homogeneity could be confirmed while working with it, first, the batch P01 of drug substance was left for two weeks in the refrigerator. After this time, the 2 phases were wholly separated.

Figure 36. Drug substance VXD-001 batch P01 visual aspect after one week of precipitation.

The time until visual homogeneity was achieved was determined around 5 minutes, and afterward, to prove that this homogeneity was real, a group of assays was performed studying product response to µBCA assay from different aliquots obtained from drug substance bottles mixed for 10 minutes.

Three µBCA plates were performed each with four aliquots of the mixed drug substance, each diluted to be introduced in the assay in three different concentrations (see µBCA procedure in section 6.5). Sample concentration was studied interpolating samples with the standard curve as explained in section 6.5. The mean, the standard deviation, and the CV% of the results from the 12 aliquots were calculated. Afterwards, original concentration of the sample was calculated multiplying the result for the dilution factor and obtaining the protein concentration contained in each mL of the drug substance.

Table 30. Total protein quantification means-result of 12 aliquots of the drug substance.

Mean (µg/mL)	SD (µg/mL)	CV%
9765	233	2%

Results suggested that the variability found between the different aliquots of the drug substance mixed it for 10 minutes was low (CV = 2%), and it can be assured that the product after this amount of time was homogenous. Ten minutes of mixing was established for every process step of the drug substance manipulation with this information.

10.2 Drug substance evaluation:

The drug substance P04 was analyzed and evaluated in multiple situations as quality control. In this section, a summary of the results is shown to evaluate its stability and to show that after a long period of time this batch could still stable.

10.2.1 Drug substance P04 in the *in vivo* assays

Since the production of batch P04 of VXD-001, Vaxdyn has performed 6 *in vivo* assays. In all cases, the positive control performed to measure the survival of immunized mice produced a 100% of protection to mice tested in murine model assays, while non-vaccinated controls obtained ≥20% of protection. Four of these assays have been presented in this thesis in figure 37, figure 15 of section 7.1.1, figure 44 of section 10.3 and figure 65 of section 10.10. The assay of figure 15 was performed right after batch P04 production to obtain a result at the initial stability time and the assay of the figure 65 was performed more than two years after its production.

As an example of efficacy of the drug substance in an *in vivo* assay hereafter can be found a comparation between animals vaccinated with batch P04 with GMP and non GMP aluminum hydroxide. This assay was performed 2 years after its production, so a secondary objective consisted of checking its stability.

All the *in vivo* test performed by Vaxdyn before working with Reig Jofre were performed with non-GMP adjuvant, and main objective of this assay was to prove that GMP adjuvant could produce similar *in vivo* response than non-GMP adjuvant. This assay was performed following the procedure described in section 6.3. In this assay, three groups of animals were studied each with five animals. A non-vaccinated negative control and two groups vaccinated with Acinetovax besides GMP and non-GMP adjuvant. Afterward, these animals were infected following indications in section 6.3.2, and their survival can be checked hereafter:
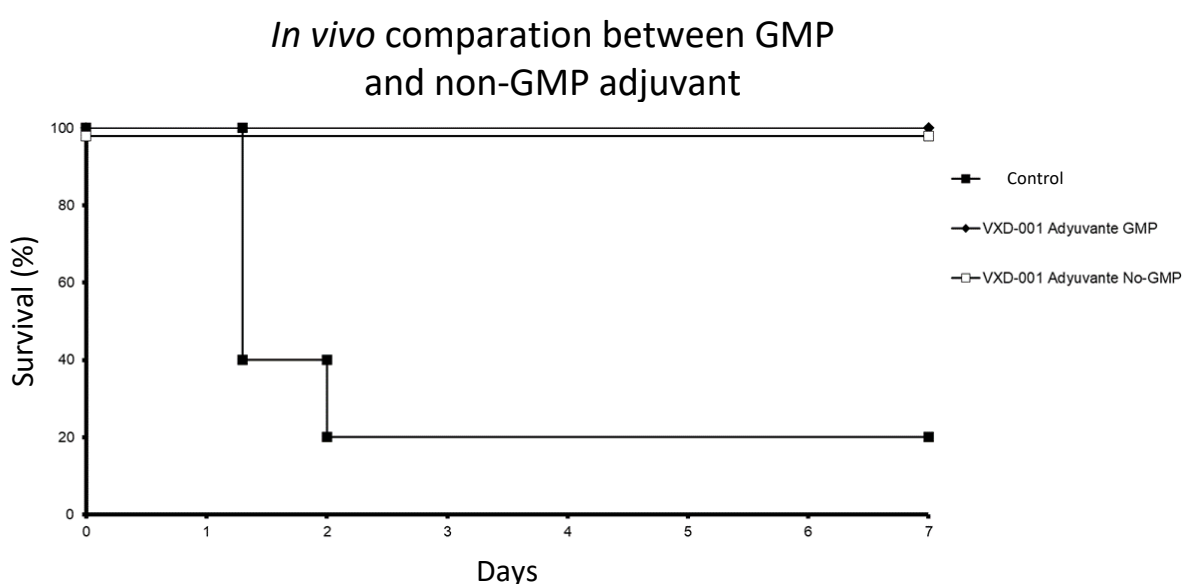
Figure 37. *In vivo* assay testing seven mice per group immunized with GMP and non-GMP aluminum hydroxide besides VXD-001 drug substance in a murine sepsis model. Also, a negative control of naïve animals was studied

As it can be observed, in both vaccinated groups, 100% of the animals survived. Meanwhile, 80% of animals in the control group died during the infection. Regarding the results of figure 37, no differences could be found between GMP and non-GMP immunization because both produced protection of 100% in the murine sepsis model. After this assay, all *in vivo* tests were performed with GMP adjuvant.

Drug substance VXD-001 (Batch P04) was stored at 5ºC for 2 years after this assay, so its efficacy in this *in vivo* study suggests that this product has at least 2 years of stability after being produced and being conserved at 5ºC as shown in results of figure 65 of section 10.10.

10.2.2 API P04 control µBCA historic results

The drug substance VXD-001 has been tested as a control inside all µBCA plates performed in the laboratory. The correlation performed between bacteria dose and protein content shows that 1.58E+10 bacteria/mL corresponded to 6400 µg/mL. This evaluation was performed in more than 30 different assays, and no tendencies were observed. Quality controls produced for more than a year were plotted to show the accuracy of the method and the stability of the drug product:
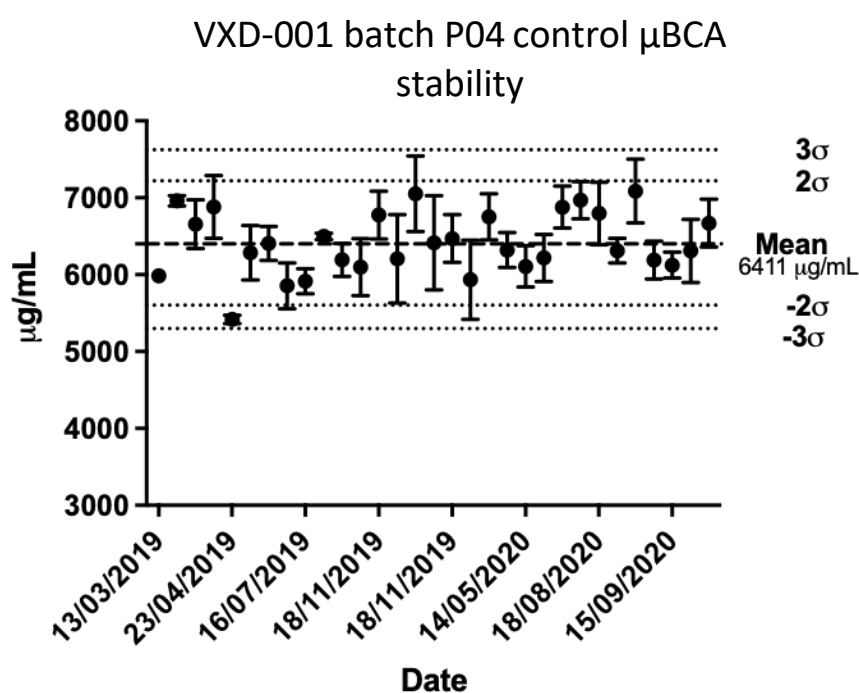
Figure 38. Historic µBCA drug substance control VXD-001 batch P04(API.

Results show a mean of 6411 µg/mL and data distribution suggest no tendency in the µBCA results throughout the time. Therefore, the drug substance P04 was stable during its conservation at 5ºC for 2 years in terms of µBCA results.

In previous testing (data not shown) it was observed that different conditions could provoke the degradation of the sample and the increase of its response to µBCA (such as elevated temperatures or irradiation), therefore, results of figure 38 suggest that the conservation of the product at 5ºC prevented its degradation for at least 2 years.

Furthermore, the results show that the batch P04 was stable and robust control to be included in the assays to study drug product batches.

Data of the figure 38, also proved the robustness and reliability of the µBCA method throughout the time that was previously validated in section 7.4.

10.2.3 API P04 control ELISA historic results

For the last three years, in each ELISA plate, a control conformed by the same drug substance was used in the standard curve, the drug substance batch P04, was used as quality control of the product. ELISA method was improved after qualification to reduce variability and to increase the precision of the method (section7.3).

After these improvements, the method was used in multiple situations to study different drug product conditions. Hereafter, a summary of all drug substance controls performed with the ELISA sandwich method has been plotted.
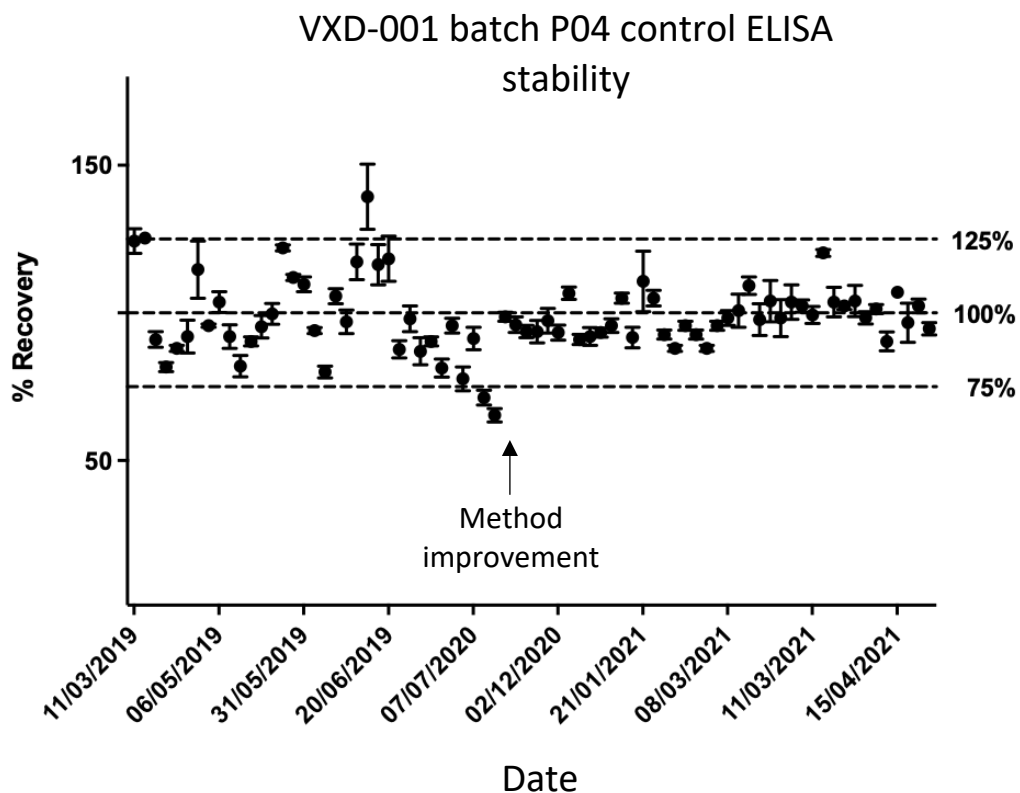
Figure 39. Historic ELISA standard control evolution

Each dot showed in figure 39 represents a drug substance control in an ELISA plate. As it can be observed, the method dramatically improved regarding the accuracy, and variability was considerably reduced. After July 2020, due to the high variability of the method, a risk assessment was performed to parametrize all steps from the method. It was determined that the time spent by samples in the Eppendorf before introducing its content in the plate was critical. After that moment, samples, curves, and control were prepared and immediately introduce in the plate.

Also, this method assured that the drug substance was still stable and that after two years of being produced. Batch P04 of VXD-001 drug substance was a good standard that could be compared with itself to assure the quality of the ELISA sandwich assay.

10.2.4 VXD-001 P04 control in Western blot determination

For the last three years, in each western blot performed to study the Acinetovax vaccine, the control was aliquoted of drug substance that has been used as a standard. Routine western blot was performed with two monoclonal antibodies that recognize each different protein, N1, and N5.

As mentioned before (section 6.1), these monoclonal antibodies were obtained from immunized mice and recognize proteins that have developed part of the immune response produced by Acinetovax.

Antibody N1 recognizes a protein at 22 kDa, and antibody N5 recognizes a protein around 40 kDa. An example of this western blot of an assay performed in January 2021 is shown hereafter:
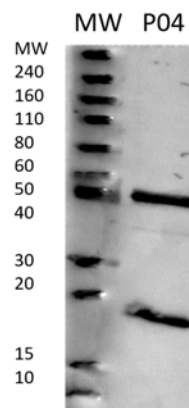
Figure 40. Western blot results of drug substance P04 incubated with antibodies N1 and N5.

Figure 40 shows the result of a western blot performed in January 2021 demonstrating that the technique was able to identify immune-dominant proteins present in the vaccine two years after having produced the drug substance VXD-001 (P04).

The capacity of antibodies to still recognize protein Omp22, one of the immunodominant protein of the vaccine, was not degraded and could still produce a protective immune response, as demonstrated in section 10.2.1.

10.3 First galenical approach based on Vaxdyn procedure:

The first Acinetovax batch produced consisted of a replication of Vaxdyn procedure performed *in-situ* to immunize the mice. This procedure involved mixing the drug substance with the adjuvant in a 1:2 preparation and afterward lyophilizing it to improve its stability.

As mentioned earlier, aluminum hydroxide degrades when it is exposed to frozen temperatures, and to perform the lyophilization, it was necessary to freeze the drug product.

Two cryoprotectants were tested that were trehalose and sucrose, to achieve lyophilization (154). The first produced batches were: batch 1 that was an exact replication of Vaxdyn procedure, batch 2 contained trehalose apart from bacteria and adjuvant as a

cryoprotectant, and batch 3 contained sucrose as cryoprotectant. In the following table, the composition of batches 1, 2, and 3 can be found.

Table 31. Composition of batches 1, 2, and 3.

Batch	Usage	VXD-001	Aluminum quantity	Trehalose	Sucrose
1	Mice	1 x10^{10} bacteria	5 mg	-	-
2	Mice	1 x10^{10} bacteria	5 mg	55 mg	-
3	Mice	1 x10^{10} bacteria	5 mg	-	55 mg

Differential Scanning Calorimetry (DSC):

After the design of the formulation, a DSC assay method was performed to study the thermal characteristics of the product. This method avoided trial-error analysis because it determined the exact temperatures at which the product was affected by different thermal events. Results of the three batches of table 31 can be found in figure 41.

DSC analysis of batches 1, 2 and 3
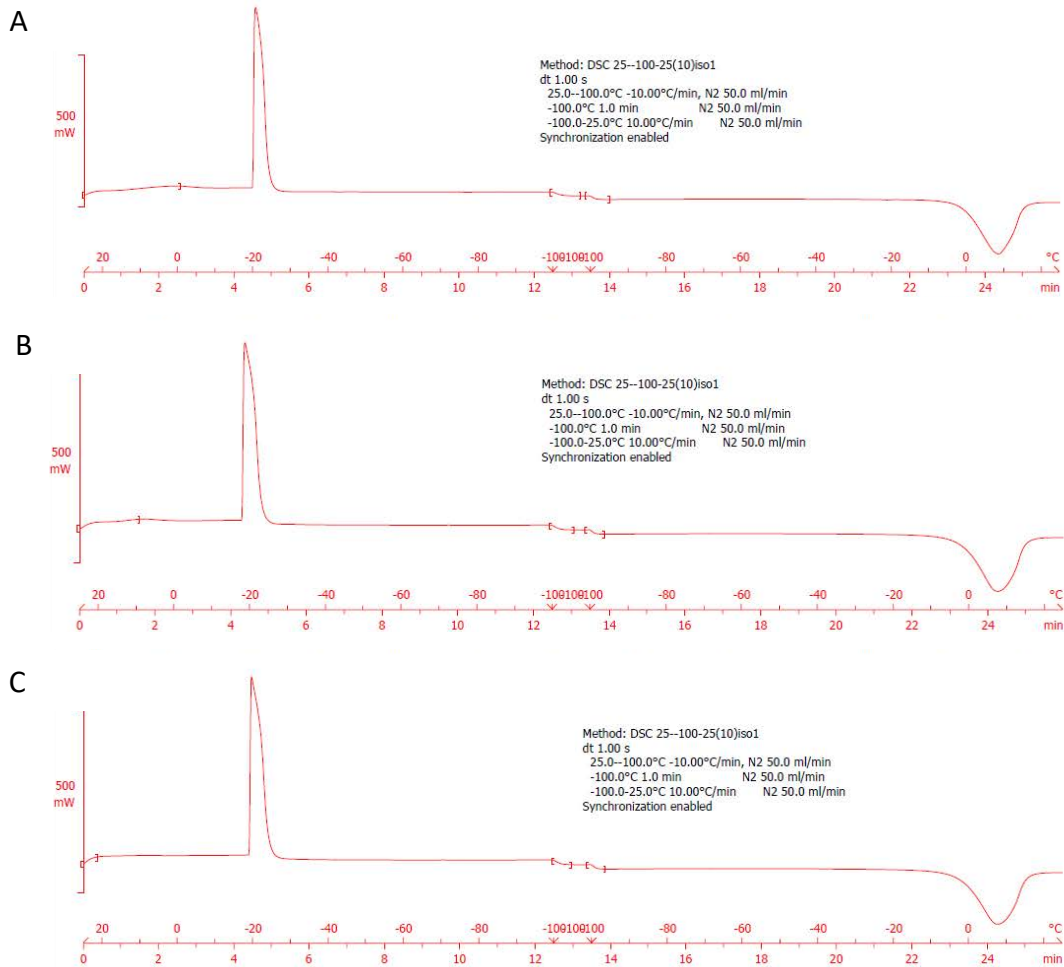
Figure 41. Complete DSC result for batches 1 (A), 2 (B), and 3 (C).

Figure 41 shows the DSC energy analysis result, facing necessary energy to change 10ºC of temperatures per minute against temperature/time. The three batches showed similar results in which the curve showed a significant exotherm corresponding to ice formation.

Afterwads a zoom of thus graphic during product melting was performed and can be found hereafter:

DSC analysis of batches 1, 2 and 3 (thermal events)

A

Step   -24.17e-03 Wg^-1
              -0.73 mW
Onset   -34.59 °C
Inflect. Pt. -28.18 °C
Endset   -26.28 °C
Midpoint   -31.39 °C

0.1
Vg^-1

Integral   -15.49 mJ
  normalized -0.51 Jg^-1
Onset   -23.36 °C
Peak   -21.39 °C
Endset   -19.84 °C

B

Step   -6.19e-03 Wg^-1
              -0.20 mW
Onset   -58.88 °C
Inflect. Pt. -54.29 °C
Endset   -50.20 °C
Midpoint   -54.10 °C

Integral   14.55 mJ
  normalized 0.46 Jg^-1
Onset   -48.64 °C
Peak   -41.15 °C
Endset   -36.03 °C

0.05
Wg^-1

C

Step   -4.60e-03 Wg^-1
              -0.14 mW
Onset   -54.36 °C
Inflect. Pt. -49.29 °C
Endset   -48.58 °C
Midpoint   -51.37 °C

Integral   10.61 mJ
  normalized 0.34 Jg^-1
Onset   -45.54 °C
Peak   -38.65 °C
Endset   -34.93 °C

0.05
Wg^-1

Figure 42. Thermal events were detected in DSC results for batches 2 (A), 2 (B), and 3 (C).

The results show thermic events showing up when drug product was melting. Batch 1 showed an endothermic event at 23.36ºC (T onset). In batches 2 and 3, the behavior was similar. A glass transition was observed at -45.54ºC (T onset) in batch 2 and was found at -48.64ºC (T onset) in batch 3. Also, the ice melting endotherm event is shown (T onset).

In practical terms, the thermal events indicated by the DSC were the limits of temperatures at which the lyophilization method should not work. It was important to work some degrees below these limits. These events occur at atmosphere pressures and therefore, when the void was activated, the risk to suffer the thermal events was dramatically reduced (167). After activating the void, the temperature can be increased avoiding the thermal events.

Lyophilization:

Following DSC results, the recipe was designed, and parameters were set to perform the lyophilization of batches 1-3.

The freezing temperature was established at -50ºC because thermal events were detected between -45ºC and -48ºC in DSC. Afterward, the void was activated with the vacuum, and thanks to this, the DP temperature could be increased to reach primary drying temperature avoiding thermal events. The events could be produced in specific pressure conditions. Thermal events should be avoided because they could cause the product loss of stability or degradation while producing the primary drying. Then, the product was heated until -15ºC, where the primary drying was performed for 48 hours. Then, the secondary drying was performed at 35ºC for 15 hours. A summary of the recipe can be founded hereafter:

Table 32. Batches 1, 2, and 3 lyophilization recipe.

Step	Temperature	Time
Freezing	-50ºC	Eight h
Primary drying	-15ºC	48 h
Secondary drying	30ºC	15 h

Once vials were extracted from the lyophilizer, they were encapsulated and stored at 5±3ºC until stability started. The visual aspect of vials can be found hereafter:
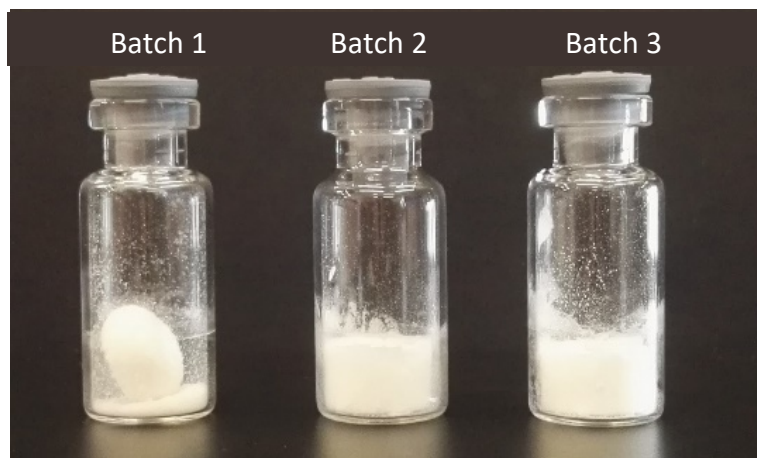
Figure 43 Visual aspect of batches 1, 2, and 3.

As shown, batches 2 and 3 produced a stable tablet, while batch 1 created a non-stable tablet. This event might probably be related to the cryoprotectants introduced in batches 2 and 3.

In vivo:

From the three previous formulas, batch 1 was discarded because it could not produce a suitable lyophilization product. Between trehalose and sucrose, trehalose was selected because some other products in Reig Jofre are produced with this cryoprotectant, and the experience working with this product was more extensive than with sucrose. Therefore, the trehalose formulation from previous batches was selected (batch 2).

Batch 2 was selected as the best formulation, and an immunization *in vivo* assay was performed to study its response against bacteria. The analysis was performed with the following doses in different animal groups (M1 – M5). Group M1 was vaccinated with an *in situ* control of Acinetovax (positive control), M2 with batch 2 of Acinetovax, M3 with irradiated batch 2 of Acinetovax, M4 with aluminum hydroxide (adjuvant) and M5 was a naïve group of animals:

Table 33. Composition of vaccine administered to each animal group in the *in vivo* assay of batch LP0281_02.

Group	Bacteria	Aluminum hydroxide (Aluminum mg)	Trehalose	Lyophilization	Irradiation	Number of animals
M1: Positive control	2E+09 bacteria	1 mg	-	No	-	5
M2: batch 2	2E+09 bacteria	1 mg	11 mg	Yes	-	10
M3: batch 2 irradiated	2E+09 bacteria	1 mg	11 mg	Yes	25 kGy	5
M4: Adjuvant	-	1 mg	-	No	-	5
M5: Naïve	-	-	-	No	-	5

In vivo assay was performed as described in section 6.3 of chapter 1. Survival of immunized mice against sepsis model is shown hereafter:

In vivo analysis of batch 2 (n = 5)
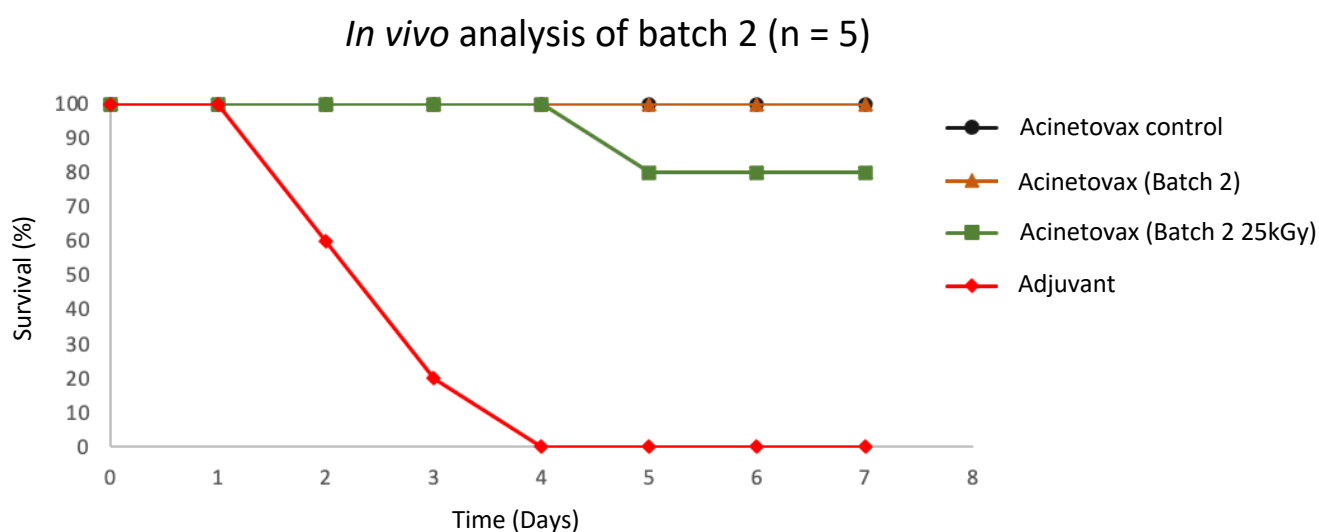
Figure 44. *In vivo* results of groups of mice vaccinated batches a positive control, batch 2, irradiated batch 2, and negative controls (n = 5).

Figure 44 show that positive control in an *in vivo* method and batch 2 had identical results: 100% survival in both cases. Irradiated batch 2 was treated with 25 kGy to mimic the final sterilization process that happens in industrial production processes. This batch condition had an 80% of survival, which means that one mouse died in the process. Meanwhile, adjuvant and naïve control had a 0% survival rate. All results obtained suggest that the vaccines produce significant protection.

These results showed that irradiation could be a proper technique to achieve the final sterilization of the drug product which did not reduce the protection elicited. Although, these results had to be confirmed (see section 10.10).

Sera of animals were obtained at day 21 from all animals. Spleens were obtained from M2 and M4 groups. These samples were used to perform the study of the cellular response of the Acinetovax. Results and analysis can be found in chapter 3.

10.4 Stability study of the drug product:

After batch 2 success, the next objective consisted of obtaining more information about drug product stability while the analytical methods were developed in parallel.

Therefore, the trehalose formulation from previous batches was selected (batch 2), and batch 4, identical to batch 2 was performed to study stability with this formula.

Table 34. Composition of batch 4

Batch	Dosage	VXD-001	Aluminum quantity	Trehalose
4	Mice	1×10^{10} bacteria	5 mg	55 mg

Lyophilization:

Following DSC results of batch 2 (section 10.3), the recipe was constructed to be identical to previous batches, and parameters were set to perform the lyophilization of batches 1-3. The freezing time was extended for 8 hours due to a problem with the vacuum of the lyophilizer. The final recipe is described hereafter:

Table 35. Batch 4 lyophilization recipe.

Step	Temperature	Time
Freezing	-50ºC	16 h
Primary drying	-15ºC	48 h
Secondary drying	30ºC	15 h

The freezing temperature was established at -50ºC for 16 hours. Then the vacuum to induce the void was activated and the product was heated until -15ºC, where the primary drying was performed for 48 hours. Then, the secondary drying was performed at 35ºC for 15 hours.

Stability:

The batch 4 was studied under a stability assay with different analysis steps. The formula was studied at 5 ± 3ºC, 25 ± 5ºC, and 40 ± 2ºC at a relative humidity in the last two temperatures of 75 ± 5% RH. Vaxdyn confirmed the 5 ± 3ºC condition as the temperature at which the drug substance was stable. The 25 ± 5ºC condition was performed to study the product's behavior at room temperature, and 40 ± 2ºC is known as an accelerated condition to force the degradation of the product. A summary of the stability can be found in table 36.

Table 36. Stability of the drug product batch 4.

Conditions		1 month	3 months	6 months	9 months
5 ± 3°C	Time 0 analysis	C	C	C	X
25°± 5ºC/75 ± 5% RH		C	C	C	X
40 ± 2ºC/75 ± 5% RH		C	C	C	X

C = ELISA, WB, µBCA, visual aspect

X =No further analysis

Stability summary

The stability started, and the drug product was analyzed with the methods specified in table 37. In this document, just the most relevant events are going to be described.

At one month of stability, visual aspect results were vital to determine that batch 4 at 40 ± 5ºC started producing non-reconstitute precipitates. Also, conditions of stability 5 ± 3ºC and 25 ± 5ºC showed this same problem at three months. At six months of stability and observing that the problem was increasing, stability was stopped.

Also, probably because of drug degradation, the results obtained showed high variability, especially the ELISA method used to quantify Omp22 regarding drug substance.

As mentioned, the stability was early stopped due to production issues and new formulations were proposed. At first sight, it was thought that the trehalose was not protecting aluminum hydroxide from low temperature. Therefore, some other

cryoprotectants were tested, but none of them could produce a homogeneous tablet as trehalose formulas did.

Then, the lyophilization of batch 4 was re-evaluated, and it was discovered that the product was treated under freezing conditions for eight extra hours than expected. As aluminum hydroxide was sensible to freezing temperatures, it was thought that this elongated step might have caused the damage, despite a cryoprotectant as trehalose was used.
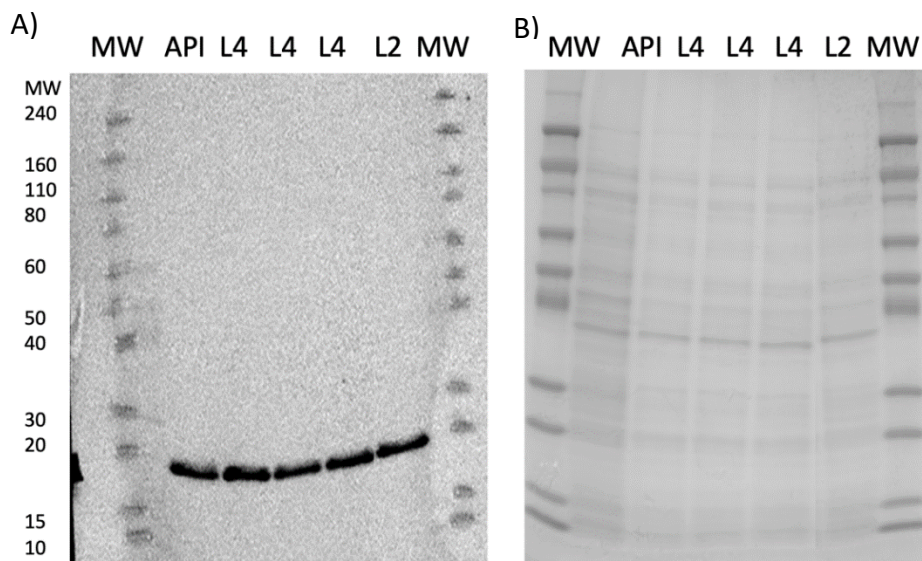
Figure 45. Initial stability western blot results analyzing batch 4 (L4), VXD-001 (API), and a drug product control Batch (L2). **A.** Western blot. **B.** Coomassie staining
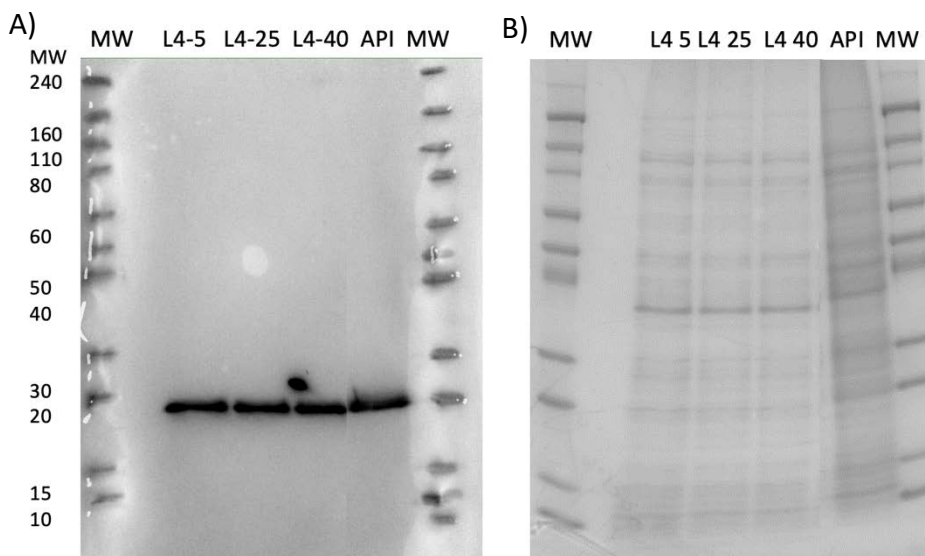
Figure 46. Three months stability western blot results analyzing batch 4 (L4), VXD-001 (API), and drug product control (batch 2 (L2)). A. Western blot. B. Coomassie staining

Coomassie Blue staining and western blot were the methods producing the most valuable information. Coomassie staining showed a difference between VXD-001 and Acinetovax in figures 45 and 46 and it can be observed that the drug substance had more intensity than drug product.

Afterward, it was confirmed that this issue was related to the aluminum hydroxide adjuvant (section 10.5). This same result was obtained at 3 and 6 months of stability (data not shown). Meanwhile, western blot detected an immunodominant protein Omp22, with the same result at T0 and 6M of stability and between all conditions tested meaning that the stability of this immunodominant protein was conserved.

ELISA results could not be analyzed because variability was higher than expected and no conclusions could be obtained, µBCA results helped show bacterial quantity (see annex 2), and the response was maintained throughout the time, which means that the method was helpful in measure bacterial load.

10.5 Effect of aluminum hydroxide of SDS PAGE Coomassie staining and Western blot

An assay was performed to study the electrophoretic profile of 7 concentrations of aluminum hydroxide mixed with the same bacterial concentration to study the effect of aluminum hydroxide in the electrophoresis. Two gels were performed, one was used to perform a Coomassie Blue staining and the other one to perform a western blot with antibodies N1 and N5. The exact concentrations can be found hereafter:

Table 37. Western blot sample preparation.

Sample	VXD-001 (µL)	Al(OH)$_3$ (µL)	Water volume (µL)	Bacteria concentration (bacteria/mL)	Al(OH)$_3$ concentration (mg aluminum/mL)
C1	40	0	60	6.32E+09	0
C2	40	10	50	6.32E+09	1
C3	40	20	40	6.32E+09	2
C4	40	30	30	6.32E+09	3
C5	40	40	20	6.32E+09	4
C6	40	50	10	6.32E+09	5
C7	40	60	0	6.32E+09	6

Samples were treated as explained in section 6.6, and the results can be observed hereafter:
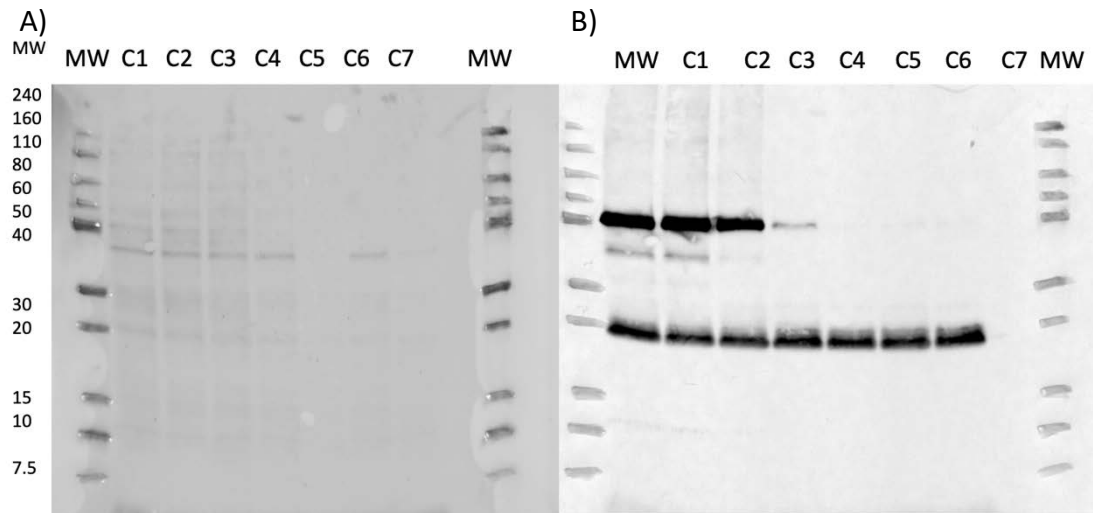
Figure 47. Coomassie staining and western blot results studying the effect of aluminum hydroxide. A. Western blot. B. Coomassie staining

Results show that the staining intensity of the proteins was reduced with the increment of aluminum hydroxide in Coomassie Blue staining, but western blot suggests something else.

While the protein detected by antibody N5 disappeared from the gel with the increment of aluminum hydroxide, the protein Omp22 detected by antibody N1 shows up with no interference. The effect observed in WB and Coomassie analysis starts in C3 concentration and increases in C4-C7.

The hypothesis to explain this effect was that proteins with low molecular weight (MW) do not bind to aluminum hydroxide as strong as it does with high MW protein, and the denaturing conditions to introduce proteins in the gel separates small weight proteins but does no separate high MW proteins. As aluminum hydroxide has a positive charge, it does not flow with the proteins inside the gel pulling the proteins with it.

10.6 *In vivo* dose/response:

An *in vivo* assay was performed to check the best dose for animals due to the bacterial dose reduction. Results and discussion about this analytical assay can be found in section 7.1.1.

10.7 Study of the influence of freezing time on lyophilized drug substance:

In this section, several parameters were measured. First, previous formulas were designed to be delivered in mice, but the final formulation was meant to be injected in humans. Volume for human injections is different from mice volume.

Even though the mice formula has been tested in an *in vivo* assay and has shown protection capacity, the human formula could not be tested in any animal model. Therefore, it was decided to carry in parallel a human dosage and a mice dosage. When any change was implemented on the human dose, the same changes were transferred to the mice formula to check if the changes affected the *in vivo* response.

Second, two options were carried out to study the new formula, a formula with aluminum hydroxide (batch 18) and a formula without aluminum hydroxide (batch 19). This second option was included to check the viability of a formula with no aluminum hydroxide as a possible option to avoid different problems related to the adjuvant an the lyophilization.

Third, this study measured the effect of extra 8 hours during the freezing step in lyophilization. The mice and human doses were included to check if both formulas behaved similar regarding the extra 8 hours. Batch 20 contained the human formula, and batch 21 contained the mice formula. Comparison between batch 20 and 18 was used to check the effect of the eight extra hours exposed to freezing temperatures.

Table 38. Composition of batches 18, 19, 20, and 21.

Batch	Dosage	VXD-001	Aluminum quantity	Trehalose
18	Human	1×10^9 bacteria	0.85 mg	27.5 mg
19	Human	1×10^9 bacteria	-	27.5 mg
20*	Human	1×10^{10} bacteria	5 mg	55 mg
21*	Mice	1×10^{10} bacteria	5 mg	55 mg
*The lyophilization of these batches contained eight extra hours at freezing temperature.				

DSC:

Lyophilization parameters for batch 20 and 21 were established based on DSC performed for batches 1-3 (section 10.3).

For batches 18 and 19, a new DSC was performed because some formulation changes were produced from previous formulas. The DSC results can be found hereafter:

DSC analysis of batches 18 and 19
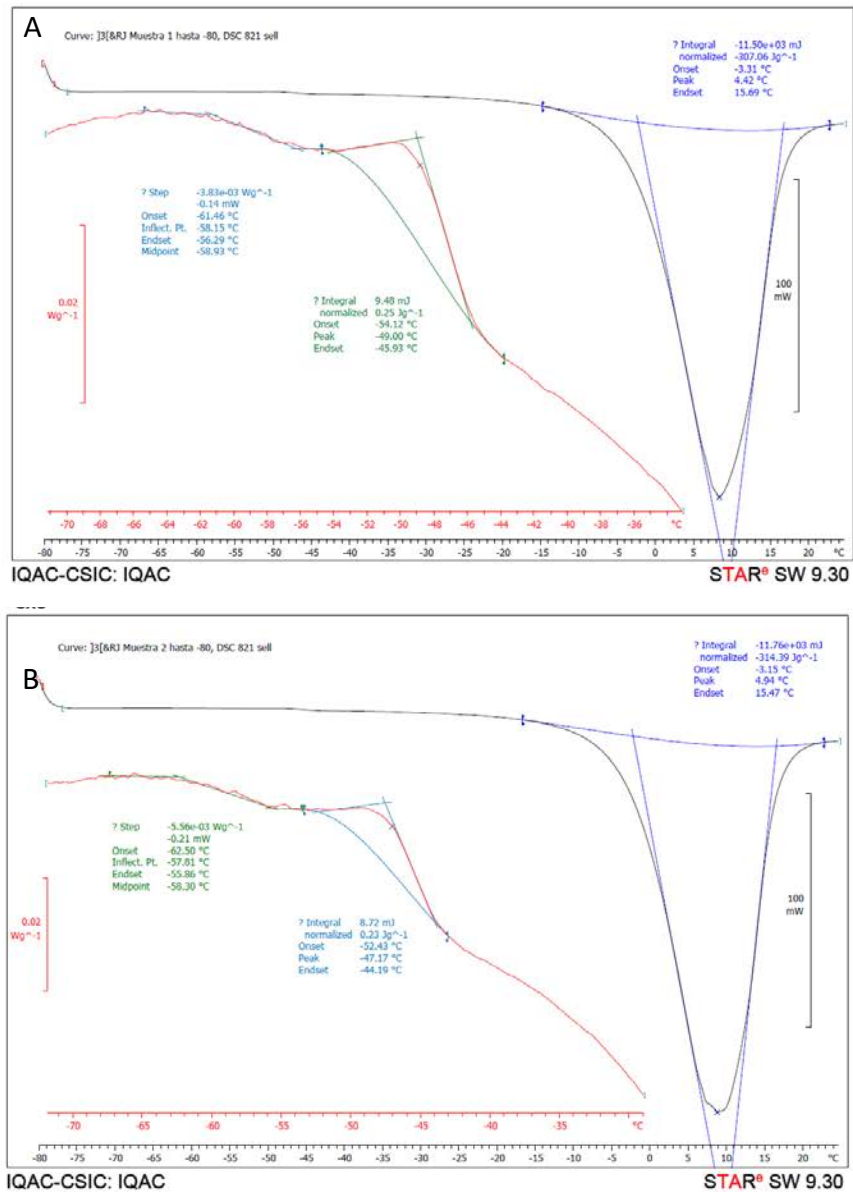
Figure 48. DSC results of batches 18 (A) and 19 (B) showing thermal events during drug product melting.

The results show events that show up when drug product was melting, around -54ºC, meaning that the freezing temperature at which void was produced before starting primary drying should be below -54ºC. The risk of suffering thermal events was reduced once the void is produced. This event happens due to a combination of temperature and pressure (167).

Lyophilization:

Lyophilization of batches 20 and 21 was identical to batch 4 recipe. Results of DSC for batches 18 and 19 had a slight differentiation in primary drying. During this stage, the freezing temperature was established at -100ºC. Then the product was heated until -65ºC, where the primary drying was performed for 48 hours. Afterwards, the secondary drying was performed at 30ºC for 15 hours.

Formulation changes in batches 18 and 19 produced a thermal variation from the previous DSC. This change might be related to the increase of NaCl in the formula as the bacteria diluent. NaCl showed a negative effect on lyophilization processes. The primary drying temperature was lower than in previous batches (-65ºC) because thermal events produced in the sample were between -62.5 and -45.9 ºC. These thermal events are produced during the sample heating process at atmospheric pressure. The void produced during lyophilization allows avoiding the collapse of the formula when the temperature is changed to primary drying temperature at -25ºC. Recipe for lyophilization can be found hereafter:

Table 39. Batches 18 and 19 lyophilization recipe.

Step	Temperature	Time
Freezing	-100ºC	16 h
Primary drying	-65ºC	48 h
Secondary drying	30ºC	15 h

Batches 18 and 19

Batch 18 was performed correctly, and the tablet was stable. Although, batch 19 could not obtain a proper tablet because it did not have enough mass to produce it since aluminum hydroxide was removed. It would be necessary to have more mass added to stabilize the tablet, probably administered with trehalose.

Batches 18 and 19 stabilities were tested at 40ºC to force the degradation of the product and check if the precipitate appeared in these formulas with extra lyophilization time. Each batch contained nine vials, 3 of each were reconstituted at T0, one month, and three months.

Table 40. Stability of the drug product batches 18 and 19.

Conditions	Time 0 analysis	1 month	3 months
Batch 18 40 ± 2ºC/75 ± 5% RH	C	C	C
Batch 19 40 ± 2ºC/75 ± 5% RH	C	C	C

C = Visual appearance after reconstitution

The results of batches 18 and 19 regarding visual appearance are summarized hereafter (table 41). Complete results can be found in annex 2 but the most critical parameters will be summarized hereafter.

Table 41. Stability results of the drug product batches 18 and 19.

Batch	Conditions	Time 0 analysis	1 month	3 months
18	40 ± 2ºC/75 ± 5% RH	Non precipitated product	Non precipitated product	Non precipitated product
19		Non precipitated product	Precipitated product	Precipitated product

The most important result was that neither batch 18 nor batch 19 produced precipitations after three months of stability, assuring that the product was not degraded when exposition to freezing temperatures was controlled.

Another parameter offering some information was that Coomassie staining and western blot showed the same effect of aluminum tested in section 10.5. Samples were inserted in the gel by triplicate, and results can be observed hereafter.
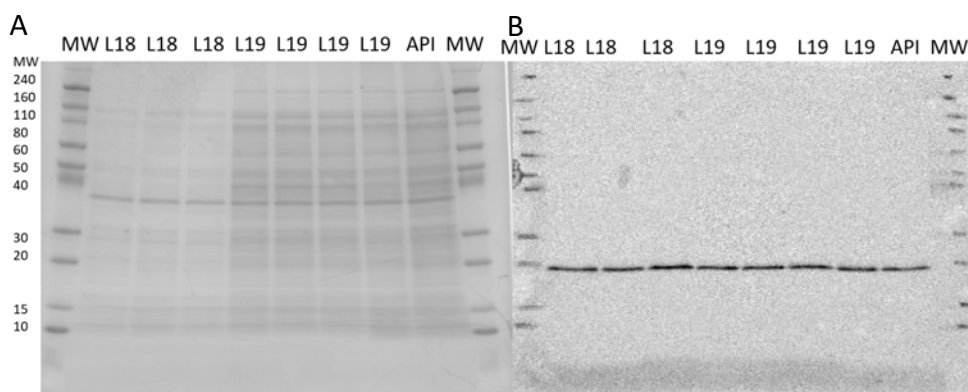
Figure 49. Coomassie staining and western blot comparing batches 18, 19 and control containing VXD-001 (API). **A.** Coomassie staining **B.** Western blot

As observed before in previous assays, aluminum hydroxide in batch 18 produces a reduction of proteins entering the gel, but this effect was not observed in western blot revealed with antibody N1. This effect was not observed in batch 19 results.

Batches 20 and 21

Batches 20 and 21 were tested in the stability at 40±2ºC to force the degradation of the product. They were produced with extra 8 hours of freezing temperatures during lyophilization. Each batch contained nine vials, 3 of each were reconstituted at T0, one month, and three months.

Table 42. Stability of the drug product batches 20 and 21.

Conditions	Time 0 analysis	1 month	3 months
Batch 20 40 ± 2ºC/75 ± 5% RH	C	C	C
Batch 21 40 ± 2ºC/75 ± 5% RH	C	C	C

C = Visual appearance after reconstitution

The results obtained are summarized hereafter:

Table 43. Stability results of the drug product batches 20 and 21.

Batch	Conditions	Time 0 analysis	1 month	3 months
20	40 ± 2ºC/75 ± 5% RH	Non precipitated product	Non precipitated product	Non precipitated product
21		Non precipitated product	Precipitated product	Precipitated product

Results showed in figure 50 are the drug product batch 21 started producing precipitates. These precipitates were part of the process of degradation of aluminum hydroxide after being affected by freezing temperatures.(167).

Figure 50. Non-reconstitutable precipitates were produced in batch 21 marked with red circles.

Meanwhile, batch 20 did not show this effect, maybe because of the reduction of aluminum dose in the total volume of the drug product.

This result confirmed that the extra 8 hours of freezing time in drug products was critical, especially in high dose batches such as batch 4.

Results of batch 18 confirmed that the lyophilization could be performed over a batch with aluminum and trehalose. The trehalose was still considered the main cryoprotectant of the formulation. Also, formula with no aluminum was observed a possible candidate to develop the vaccine. Finally, the control of the freezing temperature during lyophilization was extremely necessary to assure the stability of the product.

10.8 Comparison of liquid and lyophilized formulas:

Based on previous results, formulations were proposed; batches 26 and 30 were prepared with a human dose, and batches 27 and 29 had mice dose. Batches 26 and 27 were lyophilized following the previous working pathway, while batches 29 and 30 were liquid.

The liquid condition was purposed to check the stability of liquid formulation. Liquid formulas are cheaper than lyophilized ones in industrial production processes. In the case both options, liquid and lyophilized, worked similarly, liquid option would be selected.

Furthermore, all four formulas were irradiated at three different irradiation doses (8 kGy, 15 kGy, and 25 kGy), all tested to study their capacity to sterilize the batches and the effect produced by irradiation in the drug product. All these formulas had a final volume of 0.5 mL, and their composition is summarized hereafter:

Table 44. Composition of batches 26, 27, 29 and 30.

Batch	Usage	VXD-001 (bacteria /vial)	Aluminum (Al^{3+}mg/vial)	Trehalose (mg/vial)	NaCl (mg/vial)	Final volume	Lyophilized
26	Human	1 x10^9	0.83	25.4	1.8	0.5 mL (after reconstitution)	Yes
27	Mice	2.5 x10^9	2.1	25.4	0.63	0.5 mL (after reconstitution)	Yes
29	Mice	2.5 x10^9	2.1	-	-	0.5 mL	No
30	Human	1 x10^9	0.83	-	4.06	0.5 mL	No

DSC:

The DSC performed to analyze batches 18 and 19 (section 2.2.5) was selected as the base to produce lyophilization of batches 26 and 27.

Lyophilization:

Batches 26 and 27 were produced following the same recipe used in section 10.8.

Sterility:

Sterility was studied measuring the possible growth of colony-forming units (CFUs). This parameter was studied following section 9.2. Samples were observed for 14 days to look for the possible evolution of any contaminant microorganism. Results are presented in the following table.

Table 45. Sterility results of batch 27 incubated in TSB and TG media culture.

Culture media	Batch number (irradiation dose)	Days of incubation													
		1	2	3	4	5	6	7	8	9	10	11	12	13	14
TSB	27(25 kGy)	N	-	-	-	N	N	N	N	-	-	N	N	N	N
	27(15 kGy)	N	-	-	-	N	N	N	N	-	-	N	N	N	N
	27(8 kGy)	N	-	-	-	N	N	N	N	-	-	N	N	N	N
	Negative control	N	-	-	-	N	N	N	N	-	-	N	N	N	N
TG	27(25 kGy)	N	-	-	-	N	N	N	N	-	-	N	N	N	N
	27(15 kGy)	N	-	-	-	N	N	N	N	-	-	N	N	N	N
	27(8 kGy)	N	-	-	-	N	N	N	N	-	-	N	N	N	N
	Negative control	N	-	-	-	N	N	N	N	-	-	N	N	N	N

N = Negative

P = Positive

Results suggest that all conditions treated with irradiation were sterilized, and no microorganism grew in the process. TSG is a media used to study the growth of multiple microorganisms but especially aerobic bacteria, fungus, and yeast. USP and European pharmacopeia had accepted this media to study sterility (168,169). Meanwhile, TG was used for aerobic and non-aerobic bacteria(168,169).

With these results it was concluded that 8 kGy dose of irradiation was enough to achieve sterility of the drug product. Higher irradiation doses were unnecessary and had the risk to provoke damage in proteins and in the bacteria.

Stability:

Batch 26 was studied at 5±3ºC, but batches 27, 29 and 30 were also studied at 25±5ºC:

Table 46. Stability of the drug product 26, 27, 29, and 30.

Batch	Conditions		Non-irradiated	T0	1M	3M	6M	9M
26	5±3ºC	8kGy	C	C	C	C	C	C
		15kGy	C	C	C	X	X	X
		25kGy	C	C	C	X	X	X
27	5±3ºC and 25±5ºC	8kGy	C	C	C	C	C	C
		15kGy	C	C	C	X	X	X
		25kGy	C	C	C	X	X	X
29	5±3ºC and 25±5ºC	8kGy	C	C	C	C	C	C
		15kGy	C	C	C	X	X	X
		25kGy	C	C	C	X	X	X
30	5±3ºC and 25±5ºC	8kGy	C	C	C	C	C	C
		15kG	C	C	C	X	X	X
		25kGy	C	C	C	X	X	X

C = ELISA, WB, µBCA, reconstitution time, pH, osmolarity and visual aspect

X = No further analysis

Stability showed much information at different levels. The samples were analyzed following table 46 indications, and many conclusions were obtained. Result tables can be found in annex 2, but the most critical parameters will be summarized hereafter.

<u>Western blot</u>

Western blot emerged as the central technique in this stability. ELISA test was discarded to study the method's potency until it was improved to reduce variability, so western blot was the only assay that could measure the interaction between an antibody produced by immunized mice (N1) and protein Omp22 related with the immune response.

T0 results showed that the formulation changes which involved reducing bacterial dose from 2E+09 to 1E+09 bacteria/dose and aluminum hydroxide from 1 to 0.85 mg of aluminum changed the rate aluminum/ bacteria almost duplicating aluminum hydroxide dose. This methodology change, produced a reduction of visibility of the proteins in the Coomassie staining and western blot, as mentioned earlier (see figure 47), and almost no protein above 30 kDa could be observed in the Coomassie staining (see figures 51 and 52).

In Western blot, Omp22 protein could be detected, but the protein of 40 kDa could not be observed. It was therefore decided to incubate the bacteria western blot exclusively with antibody N1. Results of these assays at starting of stability can be found hereafter:
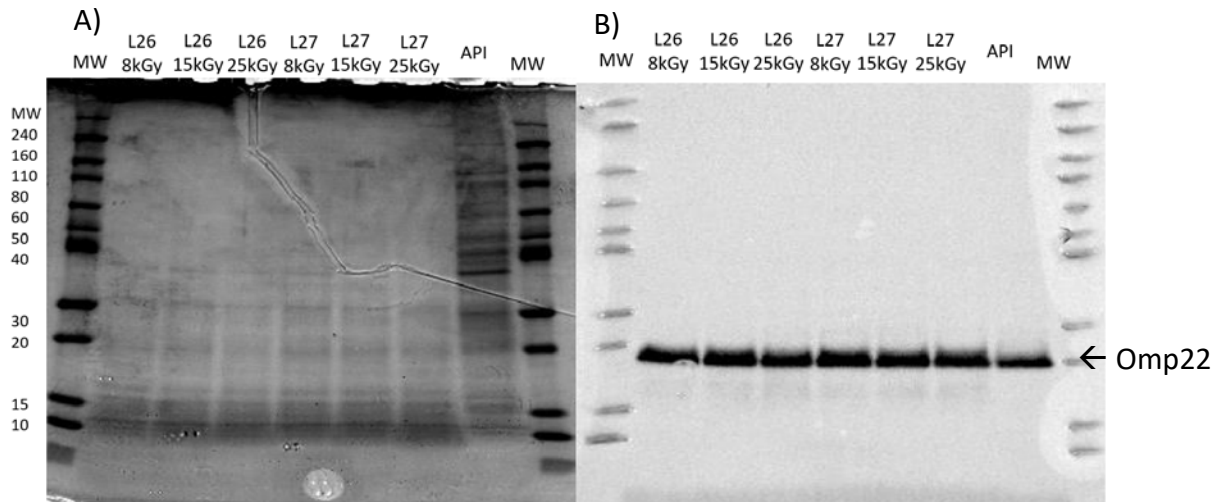
Figure 51. Coomassie Blue staining and western blot starting time stability result of batches 26, 27, VXD-001 (API), and molecular weight control. Batches 26 y 27 were analyzed at three different irradiation doses (8 kGy, 15 kGy, and 25 kGy). **A.** Coomassie staining **B.** Western blot
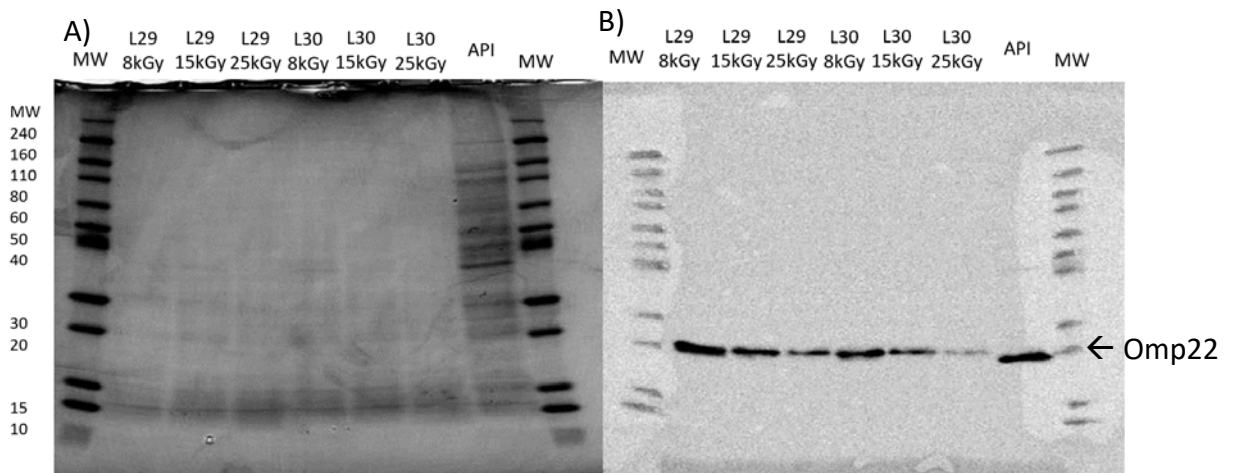
Figure 52. Coomassie Blue staining and western blot starting time stability result of batches 29 and 30, VXD-001 (API) and molecular weight control. Batches 29 and 30 were analyzed at three different irradiation doses (8 kGy, 15 kGy, and 25 kGy). **A.** Coomassie staining **B.** Western blot

At T0, a reduction of the western blot response related to the increase of irradiation dose in liquid formulas was observed (see figure 52). The higher the irradiation dose, the lower the western blot response. Although, lyophilized formulas were not affected by irradiation (see figure 52).

At three months of stability, the degradation of liquid formulas increased. This effect showed a remarkable increase in stabilities at 25ºC, which means that these formulas were more sensitive to irradiation effect and higher temperature conditions, concerning antibody recognition than lyophilized ones.
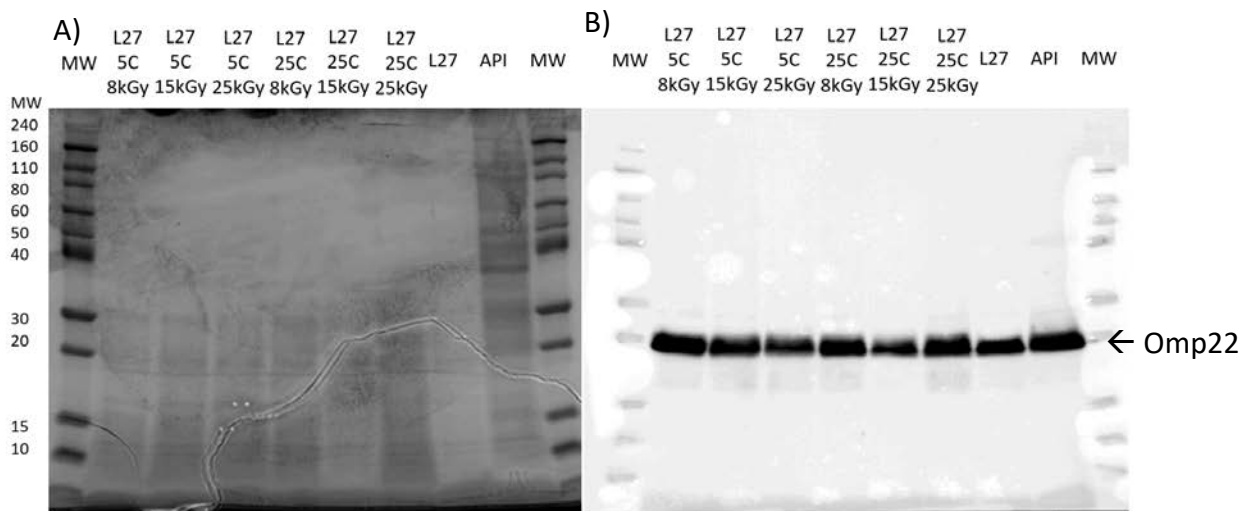
Figure 53. Coomassie Blue staining and western blot at three months of stability result of batch 27, VXD-001 (API), and molecular weight control. Batch 27 was analyzed at three different irradiation doses (8 kGy, 15 kGy, and 25 kGy) and different temperatures (5ºC and 25ºC). **A.** Coomassie staining **B.** Western blot
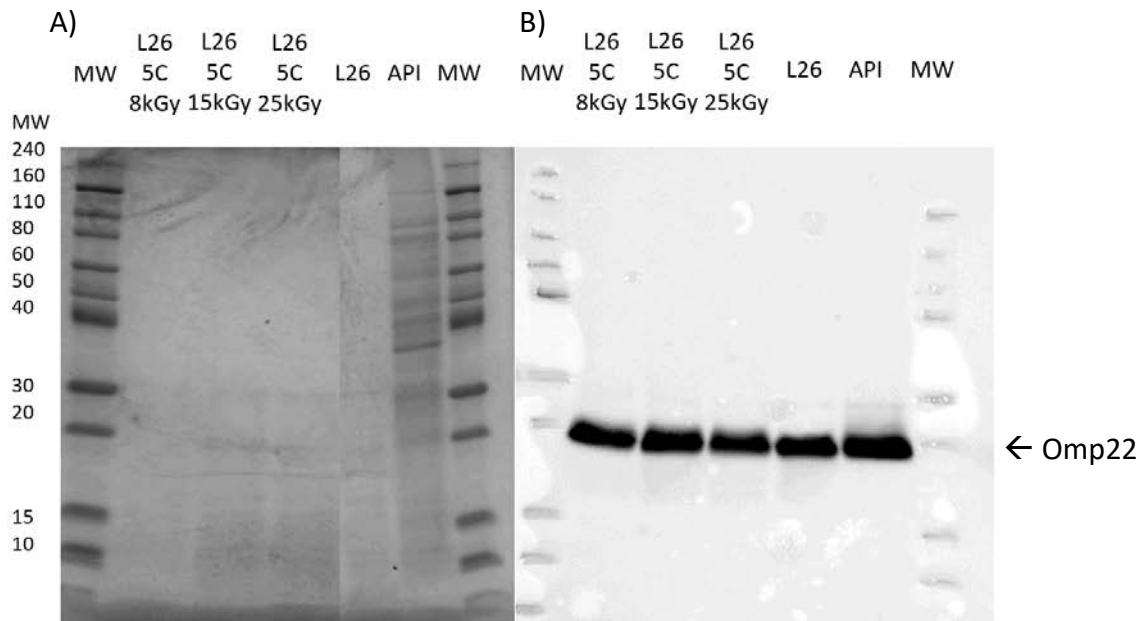
Figure 54. Coomassie Blue staining and western blot at three months of stability result of batch 26, VXD-001 (API), and molecular weight control. Batch 26 was analyzed at three different irradiation doses (8 kGy, 15 kGy, and 25 kGy). **A.** Coomassie staining **B.** Western blot
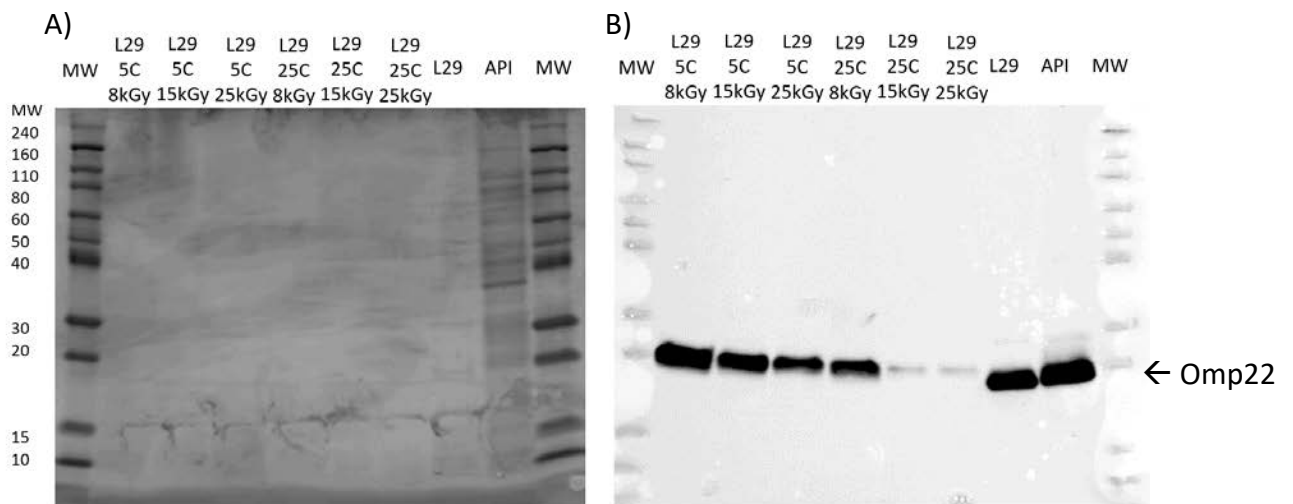
Figure 55. Coomassie Blue staining and western blot at three months of stability result of batch 29, VXD-001 (API), and molecular weight control. Batch 29 was analyzed at three different irradiation doses (8 kGy, 15 kGy, and 25 kGy) and different temperatures (5ºC and 25ºC). **A.** Coomassie staining **B.** Western blot
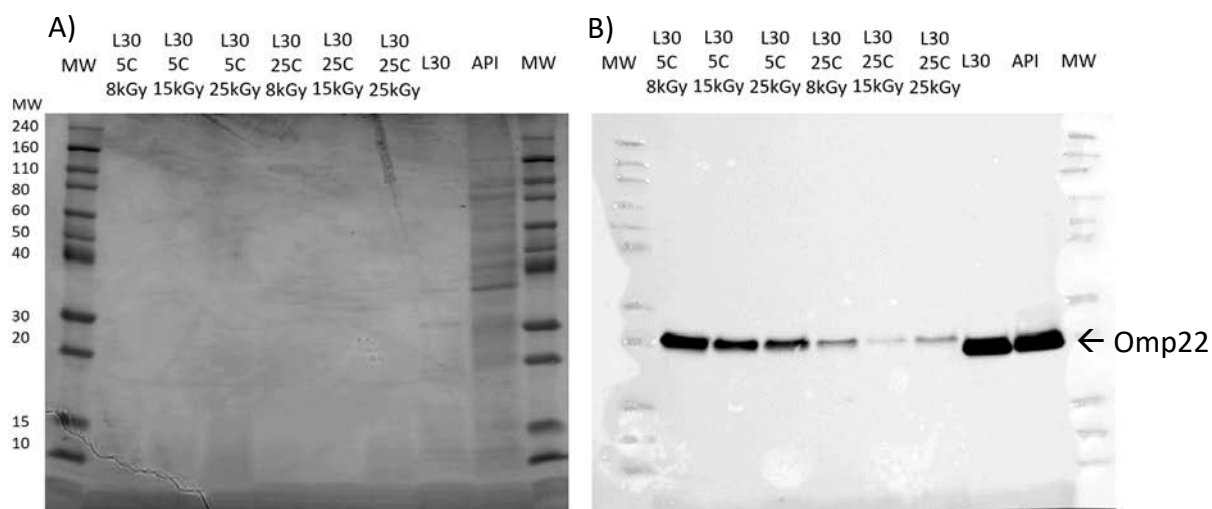
Figure 56. Coomassie staining and western blot at three months of stability result of batch 30 VXD-001 (API) and molecular weight control. Batch 30 was analyzed at three different irradiation doses (8 kGy, 15 kGy, and 25 kGy) and different temperatures (5ºC and 25ºC). **A.** Coomassie staining **B.** Western blot

Results of figures 54, 55 and 56 suggest that protein Omp22 was degraded in liquid formulas and could not be detected in western blot, while there was no problem detecting it in lyophilized formulas. High temperatures enhance this effect.

After these results, two decisions were made. First, all 15 kGy and 25 kGy irradiation doses were eliminated from stability and discarded. It was demonstrated that 8 kGy could produce sterile products (see section 10.8), and a higher irradiation dose could cause problems (see figures 55 and 56). Also, 25ºC conditions were stopped in liquid formulas. The rest of the stability continued with no further degradation of any of the formulas, liquid of lyophilized ones until nine months of stability, that stability was stopped.

µBCA:

Protein quantity determined by µBCA was assessed at different times during the stability. Plates were performed as described in section 6.5.1 of chapter 1. The analysis also contained an VXD-001 control to verify the results and compare samples with the original preparation.

Also, controls of all plates performed during the stability of batches 26, 27, 29, and 30 have been represented hereafter to show that they produce the expected µBCA response in all plates, and therefore, previous results are trustworthy.

VXD-001 (P04) µBCA evolution
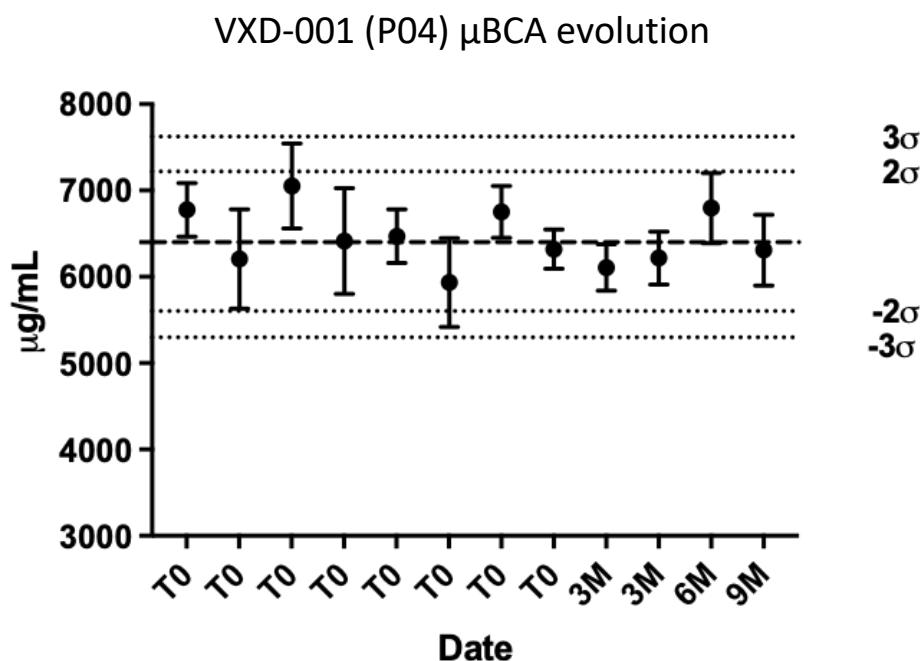
Figure 57. µBCA drug substance controls that were analyzed with drug product in the stability. The protein content of the drug substance is faced against the different time samples were analyzed. Mean ± SD

As it can be observed in figure 57, all controls could be found around the historical mean value of 6400 µg/mL distributed parametrically. Results suggest that showed plates were satisfactory performed. Results of Acinetovax batches 26, 27, 29 and 30 increased the response to µBCA when were analyzed due to irradiation and therefore, the results have been excluded.

Physic-chemical parameters:

Physic-chemical parameters such as osmolarity, reconstitution time, and visual aspect were constant throughout the whole process. Osmolarity, designed to be around 0.300 Osmol/L, was influenced by neither irradiation nor time. Reconstitution time was not influenced by stability either. This parameter was around 5 seconds during the whole process. The visual

aspect was observed to assure that no precipitates showed up, and they did not. These three parameters showed that, at the physic-chemical level, the product was stable.

Turbiscan:

During the formulation study, it was observed that the precipitation time after the mix of bacteria and aluminum hydroxide was fast. While drug substances had a visual precipitation time measured in days, drug product precipitation could be observed in around 15 minutes. After this time, the drug product was separated into two different phases. This effect was firstly measured in these batches (26, 27, 29, and 30).

To evaluate this effect with a more refined technique, the turbiscan analysis method was performed. With this technique, the precipitation time of different analytes was determined.

These samples were sent as representations of different parameters that wanted to be studied. M1 contained the bacterial vial that would conform the final formulation with bacteria, trehalose, and NaCl 0.9% at the determined osmolarity. M2 contained the actual formula with bacteria and aluminum hydroxide. M3 contained the drug substance with no added product as a control of the best possible situation, bearing in mind that the drug substance contained a bacterial suspension that precipitated. Visual phase separation was observed hereafter at 1 and 3 hours after being homogenized.
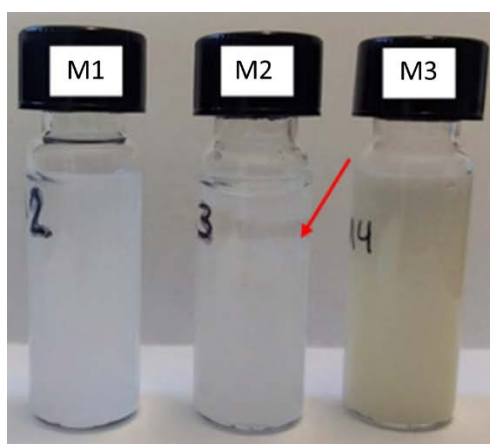
Figure 58. The visual aspect of samples sent to be analyzed through turbiscan. A red arrow signals in vial M2 at 24 hours the height at which separation between liquid phases can be found.

As observed in figure 59, sample containing bacteria and aluminum hydroxide (M2) precipitated. It seems there was a vast difference between the proposed formula (M1) and the actual formula (M2). Thanks to the turbiscan methodology, this observation was studied deeply, and hereafter is shown the transmission (ΔT) of four samples at different heights of the vial and at different times.

Samples were studied for 120 minutes and 24 hours. 120 minutes graphic contains readings every 5 minutes until 120 minutes, and the 24 hours graphic contains reads every hour. Analysis results can be observed in figures 60, 61, and 62.

Turbiscan results (M1)
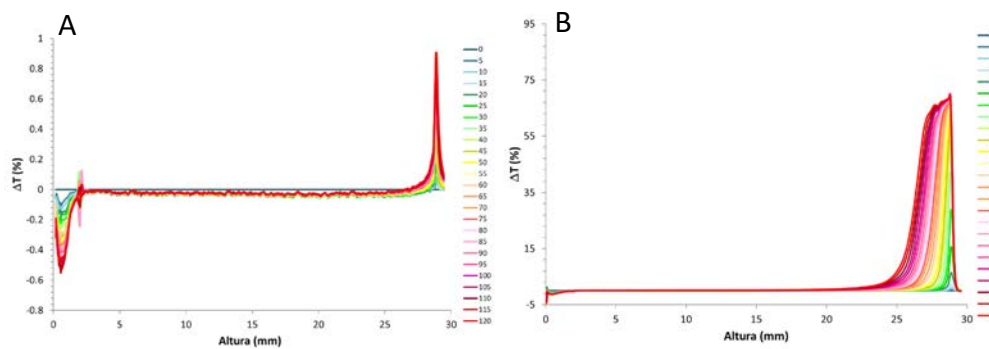
Figure 59. Light transmission at different heights on sample M1 vial. The lines with different colors represent transmission evolution throughout 120 minutes (A) and 24 hours.

Turbiscan results (M2)
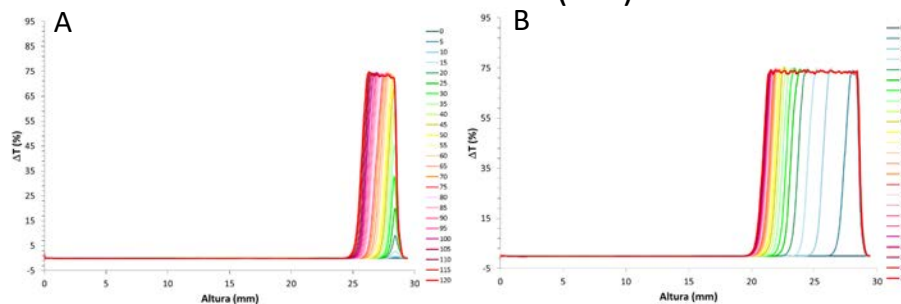
Figure 60. Light transmission at different heights on sample M2 vial. The lines with different colors represent transmission evolution throughout 120 minutes (A) and 24 hours.

Turbiscan results (M3)
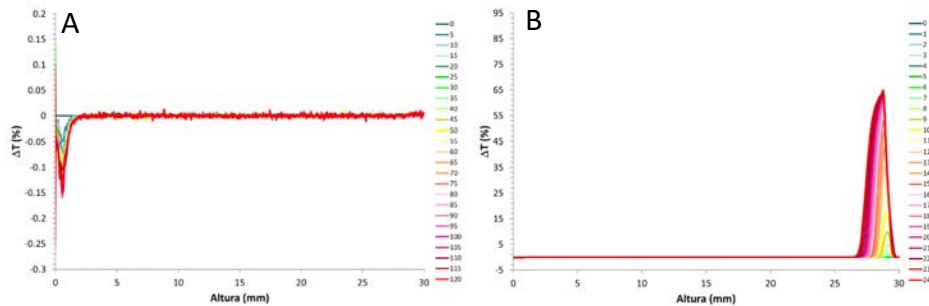
Figure 61. Light transmission at different heights on sample M3 vial. The lines with different colors represent transmission evolution throughout 120 minutes (A) and 24 hours.

The main conclusion was that all samples presented sedimentation processes that was monitored and a progressive increase of ΔT was detected in the top of the vial. This effect was due to a clarification on the upper part of the vial. The region clarification samples reached maximum values of $\Delta T = 73 - 75\%$ for samples M1 and M2 and a value of $\Delta T = 65\%$ for sample M3 at 24 hours. These values indicated a lower sedimentation speed for M3.

It was also observed that the height at which interphase ($\Delta T = 0$) was formed was M1 = 22 mm, M2 = 20 mm, and M3 27 mm. This result is probably linked with the number of particles present in the sample.

Also, results suggest that M1 and M3 had similar behaviors. M3 was more stable than M1 because almost no clarity increased at 2 hours of analysis, and M1 increased of ΔT of 1% at the top vial. This increase of ΔT was an acceptable value for industrial scalability of Acinetovax (M3) because it was an increase on the precipitation time offering few hours in which the product did not precipitate and allowed us to fabricate the vaccine. The difference between M1 and M3 regarding its composition was that M3 had a 1.58E+10 bacteria/mL concentration while M1 had a concentration of 2E+09 bacteria/mL. This suggests that there was an inverse correlation in which the higher the bacterial dose, the slower the precipitation time. Meanwhile, M2 had an increase of ΔT of 75% after two hours, observed in the top 5 mm of the vial, meaning that it was by far the most unstable option.

At 30 minutes, M2 reached a clarification of 30%, entirely inadequate for an industrial process.

This technique confirmed that the formula proposed separated bacteria and aluminum hydroxide was more feasible in terms of industrial production processes than the original formula with bacteria with adjuvant. It was decided then to perform subsequent batches with this formulation. The selected option avoids the effect of aluminum hydroxide in all the analytical techniques.

10.9 New buffers for separated vial drug product perspective:

Subsequent batches were produced without aluminum hydroxide, and this adjuvant was stored in a separated vial.

This change produced some advantages. For example, the aluminum hydroxide would not interact with the analytical methods. Also, the suspension of batches described in section 10.8 was compared to the stability of suspension of the product separated in two different vials, one for the bacteria and another one for the aluminum hydroxide.

Results showed that the scalability to industrial batches would be more accessible when separating bacteria and aluminum hydroxide.

Therefore, several different formulation options were considered for the development of this formulation. Several possible options for possible buffer formulations were selected. Different buffers were tested to stabilize the vaccine formula in a pH of 6.

For these formulations in batches 31-36, the possible buffer composition to control the pH of the formula was decided, and two formulations, one for the mice and another for human use, were developed. Formulas of the components per vial are shown in table 47:

Table 47. Composition of batches 31 - 36.

Batch	Usage	VXD-001 (bacteria/vial)	Trehalose (mg/vial)	L-Histidine HCl (mg/vial)	L-Histidine base (mg/vial)	Tris (mg/vial)	Glycine (mg/vial)	NaCl (mg/vial)	Final volume
31	Human	1×10^9 bacteria	25.4 mg	0.28 mg	0.18 mg	-	-	1.46 mg	500 mL
32	Mice	2.5×10^9 bacteria	25.4 mg	0.28 mg	0.18 mg	-	-	0.56 mg	500 mL
33	Human	1×10^9 bacteria	25.4 mg	-	-	1.2 mg	7.2 mg	-	500 mL
34	Mice	2.5×10^9 bacteria	25.4 mg	-	-	1.2 mg	7.2 mg	-	500 mL
35	Human	1×10^9 bacteria	25.4 mg	-	-	-	-	-	500 mL
36	Mice	2.5×10^9 bacteria	25.4 mg	-	-	-	-	-	500 mL

*Water for injection

DSC:

Batches 31-36 were studied in a new DSC because some formulation changes were produced. Analysis was performed in DSC equipment. Approximately around 30 mg of sample were introduced in aluminum pans and were sealed before the analysis. An experimental condition such as temperature ranges were selected. First, the temperature of the study decreased to measure the freezing point of the sample from 25ºC until -80ºC with a temperature change of -10ºC per minute. Afterward, samples were maintained at -80ºC for one minute. Then samples were heated from -80ºC until -25ºC with a temperature change of 10ºC per minute. The results of DSC determination are shown hereafter:

DSC results of batches 31-37

A

B

C
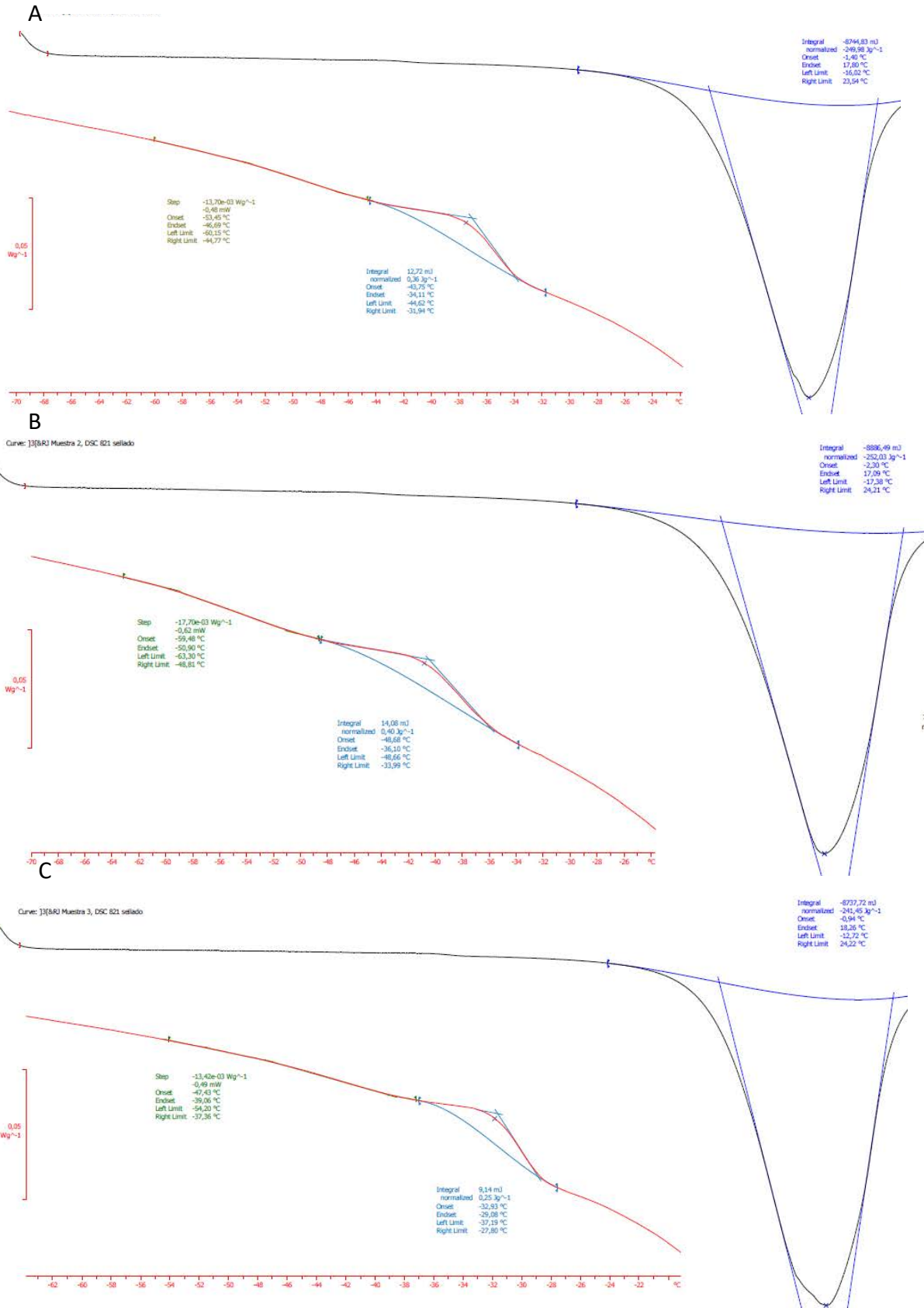
Figure 62. DSC results of batches 31-32(A), 33-34 (B), and 35-36 (C) during the drug product melting process.

Thermal events were found between -53.45ºC and -46.69ºC in histidine buffer formula, between -59.48ºC and -50.9ºC in tris-glycine buffer formula, and between -47.43ºC and -39.06ºC in the non-buffered formula. These thermal events obliged the formula to freeze at -60ºC until the void was produced to proceed to primary drying afterward.

Lyophilization

Due to DSC results, the recipe was determined as observed hereafter:

Table 48.Lyophilization recipe of batches 31-36.

Step	Temperature	Time
Freezing	-60ºC	8 h
Primary drying	-25ºC	48 h
Secondary drying	35ºC	15 h

The freezing temperature was established below thermal events, and void was produced afterward before primary drying. The absence of pressure allows the primary step to be performed without the risk of suffering thermal events that could produce a collapse in the product.

All six batches were produced correctly, and no problems with the final tablet were detected although no aluminum hydroxide was added to the formula.

Analysis of the batch:

These formulations were studied with several analysis methods, and the most remarkable formula was the histidine formula (batches 31 and 32) because it was closer to pH 6.

Further analyses were performed, and several hypotheses were confirmed. For example, it was confirmed that liquid drug products were more susceptible to irradiation than lyophilized drug products.

Just batch 31 is shown in figure 64 to simplify the results, but the rest of the batches behaved similarly. The conditions presented are irradiated, non-irradiated, lyophilized, and non-lyophilized all combined. Hereafter, western blot results show the effect of irradiation:
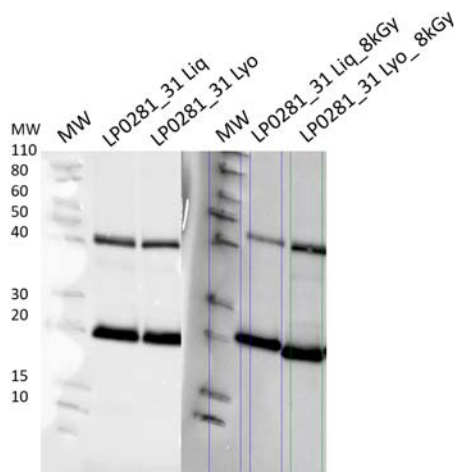
Figure 63. Western blot results of batch 31 liquid (LP0281_31 Liq) and lyophilized (LP0281_31 Lyo) and, in both cases, irradiated and non-irradiated.

Western blot result shows at figure 64 the irradiated formulas and the non-irradiated formulas. In non-irradiated conditions, lyophilized and non-lyophilized formulas behaved equally, but when Acinetovax was irradiated, liquid formula response to western blot reacted differently. The protein detected by the antibody N1 in irradiated liquid and lyophilized conditions was different. This difference was probably produced due to aggregation induced by irradiation on liquid formula, while this event did not occur in lyophilized condition. Also, it was observed that the protein detected by antibody N5 at 40 kDa was fading away in the irradiated and liquid formula.

10.10 Final formulation

The last manufactured batch was the batch 37, it contained a similar formula as the batch 32. This batch was produced and introduced into a stability study and it is still ongoing. The objective of this batch was to work with the buffer selected in the previous step and study its behavior with the different developed techniques. Hereafter, the composition of the batch is shown:

Table 49. Composition of batch LP281_37.

Batch	Usage	VXD-001 bacteria/vial	Trehalose mg/vial	L-Histidine HCl mg/vial	L-Histidine base mg/vial	Tris mg/vial	Glycine mg/vial	NaCl mg/vial	WFI volume
37	Mice	2.5 x10⁹ bacteria	25.4 mg	0.28 mg	0.18 mg	-	-	0.56 mg	500 mL

DSC

The DSC results of section 10.9 were used to create the recipe for batch 37.

Stability

The stability of this batch was studied in two conditions, non-irradiated and irradiated with 8 kGy. Previously, this irradiation dose was proven to be enough to produce sterility in previous batches (section 10.8). Both forms were studied at 5 ± 3°C ºC and 25 ± 5°C ºC. A summary of the stability can be found hereafter:

Table 50. Stability of the drug product batch 37.

Condition	Gamma-irradiation	Date of analysis						
		0	3 months	6 months	9 months	12 months	18 months	24 months
5±3°C	0	C	C	C	C/V	C	C	C
	8 kGy)	C	C	C	C/V	C	C	C
25±5°C/60%±5% RH	0	C	C	C	C/V	C	C	C
	8 kGy	C	C	C	C/V	C	C	C

C: Reconstitution time/ Visual appearance/ELISA (antigen Omp22 content)/ µBCA (Protein content)/ pH/ Osmolarity;
V: *In vivo* assay.

The results regarding ELISA, µBCA, pH, osmolarity and reconstitution time were stable throughout the stability. The complete results can be found in annex 2. The stability has not been finished yet.

In vivo:

Batch 37 was tested in an *in vivo* assay to study the immunological response elicited by the vaccine to protect mice against an infection produced by *A. baumannii* ATCC19606 at 9 months of stability. The assay contained an adjuvant control, a positive control performed *in situ* by Vaxdyn and the batch 37 non-irradiated and irradiated at 8 kGy. The different groups tested can be found in the following table:

Table 51. Composition of each administration injected for every immunization for each animal.

Group	Number of Bacteria	Aluminum hydroxide (Aluminum mg)	Irradiation	Number of animals
Adjuvant control	-	0.83 mg	-	8
Acinetovax positive control	1×10^9	0.83 mg	-	8
Batch 37	1×10^9	0.83 mg	-	8
Irradiated batch 37	1×10^9	0.83 mg	8 kGy	8

Lyophilized vials of batch 37 were reconstituted with 500 mL containing aluminum hydroxide with a content of 4,2 mg of Al^{3+} per mL. Animals were immunized with a final dose of 1E+09 bacteria and 0.83 mg of Al^{3+} and afterwards infected following section 6.3. The survival results obtained from the assay can be found hereafter:
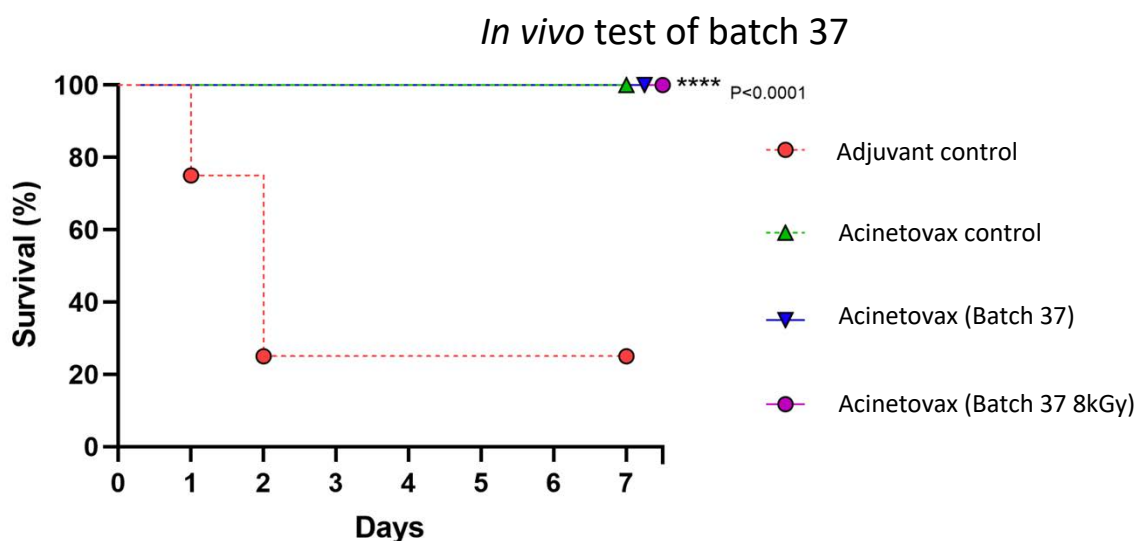
Figure 64. *In vivo* results of groups of mice vaccinated batches a positive control, batch 2, irradiated batch 2, and negative controls (n = 8).

As presented in the figure 65, positive control, irradiated and non-irradiated batch 37 showed a 100% of protection in the survival assay. Which means that neither the lyophilization, nor the irradiation produced decrease in the protection elicited by the vaccine developed. Meanwhile, adjuvant control showed a 25% of survival, this difference between study and control groups was significant ($p<0.0001$). These results also suggest

that the control, composed by VXD-001 drug substance batch P04, after 3 years of being fabricated produced a protective response.

Moreover, the results suggest that the batch 37 was stable after 9 months of stability and that the formulation developed in this thesis was effective to protect from an *A. baumannii* infection in a murine sepsis model, which were the 2 main objective in this chapter.

The results obtained in this section were a perfect conclusion for the optimization of the formula. Lyophilization is an essential process to improve the stability of the drug product and the survival analysis show it did not reduce the capacity to elicit protection of the vaccine.

As observed in section 10.8, lyophilization also protected the drug product at molecular level from irradiation, an essential treatment to sterilize the drug product. Since the vaccine Acinetovax could not be sterilize by filtration or heat, irradiation was the only alternative to obtain a sterile vaccine. Proving that irradiation did not reduce the capacity of the vaccine to promote a protective response was essential for the project.

The batch 37 is still being tested and its stability will be studied in Reig Jofre.

10.11 Summary of chapter 2

After 37 batches with different excipients, fill and finish and production methods, the vaccine Acinetovax was significantly improved in terms of stability through a lyophilization process and has conserved its efficacy. Further, all the work summarized in this chapter helped to improve the production, making it more scalable to produce bigger batches in an industrial environment and has increased the knowledge about the product. Meanwhile, the analytical techniques were improved and adapted to the requirements of the drug product optimization.

These results confirmed that the objective of the chapter was achieved and therefore, the hypothesis was validated.

10.12 Technical achievements

-The pharmaceutical formulation of the vaccine Acinetovax was optimized, characterized, and improved to obtain a more stable product.

- The formulation was designed to have a lyophilization process and it has been demonstrated that improves its stability.
- The formula was optimized to control the final pH, avoid damage by irradiation and improve its scalability.
- The formula maintains the protection capacity of the vaccine showed initially by the non-formulated vaccine.

Chapter 3. Humoral and cellular response of the vaccine Acinetovax in a mice sepsis model

11. Introduction

Vaccines are pharmaceutical products based on the capacity of our immune cells to remember antigens present on pathogens that might cause infections. Afterward, when the pathogen infects the host, the adaptive response may develope more rapidly than in a non-vaccinated person. Therefore, it is essential to know the undelaying humoral and cellular response behind the administration of a vaccine.

11.1 *A. baumannii* immune response

Regarding the innate immune response against *A. baumannii*, neutrophils play an essential role in infection clearance (170,171) as indicated by a high infection prevalence in neutropenic patients (172). This effect has also been observed in mouse models of infection (173).

Neutrophil's role in pneumonia was evaluated (170) and it was determined that neutrophils were rapidly recruited to the site of infection at 4 hours and reached the highest frequency at 24 hours. Increased lethality was observed in neutrophil-depleted hosts (170)(174). Early production of chemokines and cytokines acting on neutrophils is essential for *A. baumannii* infection clearing (171). Neutrophils are crucial to fight *A. baumannii* bacteremia, septicemia, and skin infections in mouse models (175–177).

Neutrophils have several bactericidal mechanisms. Oxidative burst is the primary defense against *A. baumannii*. At the molecular level, the role of Nicotinamide Adenine Dinucleotide Phosphate oxidase (NADPH oxidase) is also indispensable to avoid dissemination and replication of *A. baumannii* (178,179).

As mentioned before, the adaptive immune response to *A. baumannii* has not been thoroughly studied, but the humoral immune response has been explored to develop several vaccines against *A. baumannii*. Some of these vaccines are based on different *A. baumannii* membrane proteins. For example, a vaccine based on the outer membrane protein A (OmpA) showed Th2 immune response (74). As neutrophils are activated during Th17-mediated immune responses. Therefore, maybe *A. baumannii* induces Th17 response in mice resulting on the recruitment and activation of neutrophils.

11.2 Acinetovax vaccine immune response

The base of a vaccine is its capacity of eliciting a protective immune response, and one of the milestones of the project was to demonstrate the capacity of the vaccine to induce a protective response that can be maintained thanks to memory cell response. For this reason, one of the main objectives of the thesis consisted of studying the immune response induced by the vaccine Acinetovax.

Some crucial statements determined by Vaxdyn regarding its protective capacity are the basis for this thesis (72). The vaccine Acinetovax, elicited a protective immune response increasing mice survival in a murine sepsis model of wild type (ATCC 19606) and LPS(-) clinical isolate (Ab-154) *A. baumannii,* as shown in Figure 3.

Vaxdyn proved that vaccines based on whole LPS(-) *A. baumannii* cells could protect mice in a murine sepsis model produced by *A. baumannii* LPS(+) and LPS(-) infections. In both cases, the vaccine produced a 100% survival in animals vaccinated and 0% in the case of non-vaccinated animals (see figure 3 on introduction).

This same study determined that the vaccine elicited a protective immune response with specific IgG and IgM production and these results can be found in the figure 66 (72).

Ig determination in mice *serum*
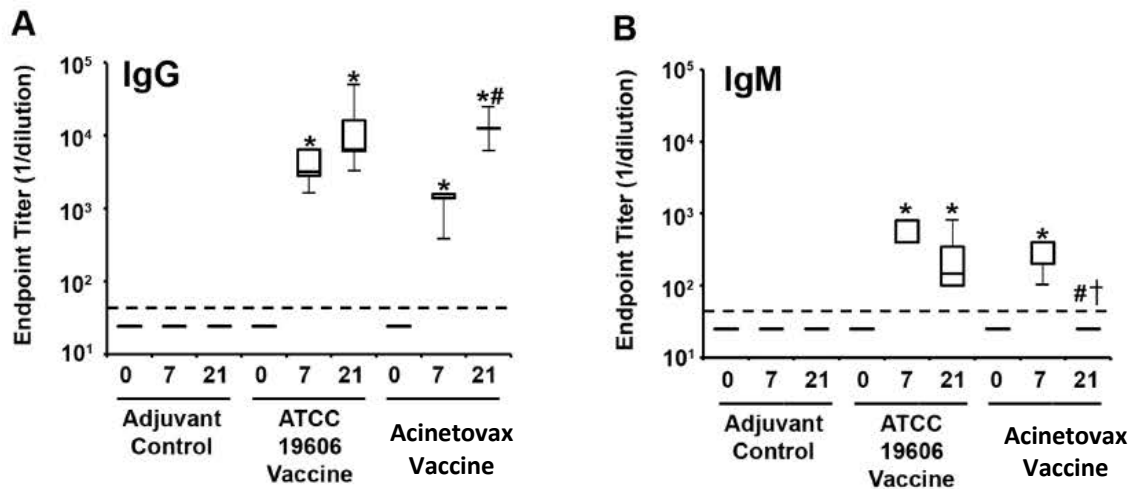
Figure 65. IgG (A) and IgM (B) production by animals vaccinated with ATCC 19606 LPS(+) isolate vaccine Acinetovax at 0, 7, and 21 days after immunization. *p<0.05 compared to levels in control mice at the same point. #p<0.05 compared to 7-day samples from the same experimental group. †p<0.05 compared to the 21-day sample in ATCC 19606 vaccinated mice.

IgG and IgM production results show a significant response of vaccinated mice both with ATCC 19606 and IB010 vaccines, meaning that the protection elicited by the immunization is supported by a strong antibody production (72).

Acinetovax vaccine is based in the cell strain IB010, which is an LPS(-) *A. baumannii* strain.

11.3 Aluminum hydroxide response

Aluminum hydroxide is a molecule used in many vaccines as an adjuvant to increase the immune response induced. As mentioned previously, aluminum hydroxide is used mainly in single protein-based vaccines to boost the immune response that is otherwise limited (142).

Aluminum hydroxide has been reported to induce different T cell responses such as Th2 (180) or Th1 responses (181) depending on the antigen. The immune response induced also depends on vaccine's inoculation site (181). Therefore, the adjuvant might just simply enhance the response induced by the immunogen, which is the effect looked for (181).

11.4 Flow cytometry

Flow cytometry is a technology that allows the analysis of single cells suspended in a buffered salt-based solution under a laminar flux. Each cell is analyzed by visible light and several fluorescence detectors. The visible light analysis is performed in forward and side directions, that indicate the size of the cell (forward scatter analysis, FCS) and the the complexity or granularity of the cell (side scatter, SSC), respectively. (182).

Afterward, samples can be prepared to be analyzed through immunofluorescence staining with several different methods to stain cells that express a certain membrane or intracellular protein of interest, or other kind of analysis (182).

Cell staining is usually performed using monoclonal antibodies specific for cell expressed proteins. These antibodies are conjugated to fluorochrome molecules that when excited by a laser beam produce light emissions at different length waves. Flow cytometer's fluorochrome detectors captures the light pulses and transform them on a digital pulse.. A general scheme of the analysis by flow cytometry (182) is showed in the next illustration.
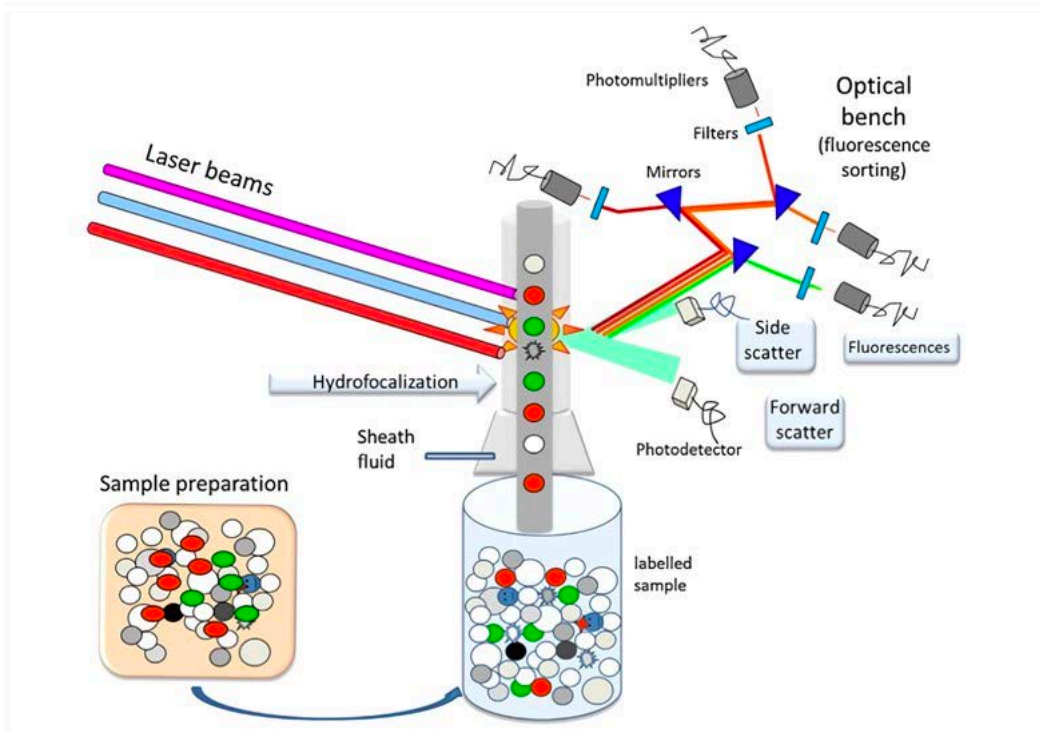
Figure 66. Flow cytometry light detection (183).

Cytometers nowadays can analyze more than 30 colors, but the most used ones are blue (488 nm), violet (405 nm), green (532 and 552 nm), green-yellow (561 nm), red (640 nm,) and ultraviolet (355 nm) (182). The emission spectra of the different fluorochromes sometimes overlap, and this is one of the main issues that have to be taken into account when using flow cytometry (182).
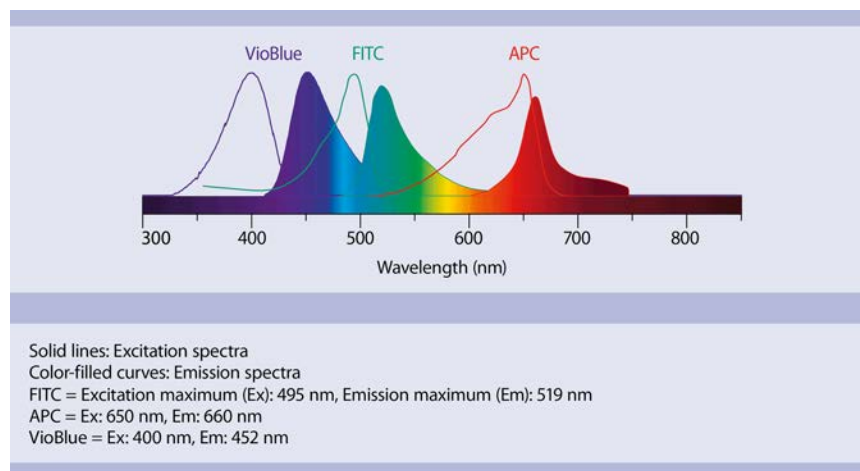
Figure 67. Spectra of different fluorophores used in flow cytometry.

This characteristic can be solved thanks to the variety of fluorochromes to label the antibodies that can be used. The number is continuously growing throughout the years and this allow scientist to obtain more accurate methods to analyze samples.

11.5 Hypothesis:

The immune response induced by Acinetovax is a Th17 response, and it is protective in a murine sepsis model of *A. baumannii* infection.

11.6 Technical objectives:

Analyze humoral and cellular responses induced by Acinetovax formulation manufactured in Reig Jofre.

- Perform an *in vivo* assay to compare the protection elicited by the designed formula to the original formulation.
- Develop an indirect ELISA assay to study the antibody subtypes produced by the B cells of immunized mice as a mean to propose the T helper population that underlays the humoral response that could be further used in clinical assays.
- Develop a flow cytometry methodology to study cytokines generated by splenocytes stimulated with different conditions.
- Develop a positive control with PMA and ionomycin to activate IL2, TNF- α, IFN- γ, IL4, IL13, and IL17 production.
- Develop an incubation assay with splenocytes with VXD-001 and study production of IL2, TNF-α, IFN-γ, IL4, IL13, and IL17 cytokines.

12. Material and methods

12.1 Material

12.1.1 Material and equipment

The required material used for chapter 3 analysis can be found in the following table:

Table 52. Specific material used for chapter 3

Cell stimumlation and flow cytometry		
Product	*Reference*	*Brand*
70 μm pore size mesh	CLS431751	Merk, Darmstadt, Germany
RPMI medium	21875042	Thermo Fisher, Waltham, USA
Trypan Blue	T8154	Merk, Darmstadt, Germany
Neubauer	Z359629	Merk, Darmstadt, Germany
FBS	A4766801	Thermo Fisher; Waltham
Streptomycin/Penicillin	63689	Merk, Darmstadt, Germany
Ionomycin	I0634-1MG	Sigma-Aldrich, San Luis, USA
PMA	P-8139	Sigma-Aldrich, San Luis, USA
Brefeldin A	B7651	Sigma-Aldrich, San Luis, USA
MACS Inside Stain	130-090-477	Myltenyi, Bergisch Gladbach, Germany
Viobility 488/520 Fixable Dye	130-109-812	Myltenyi, Bergisch Gladbach, Germany
FC blocking solution	130-092-575	Myltenyi, Bergisch Gladbach, Germany
Sodium azide	S2002	Myltenyi, Bergisch Gladbach, Germany
ELISA reagents		
Product	*Reference*	*Brand*
Antibody anti-mouse IgG1	13401582	Fisher Scientific, Hampton, USA
Antibody anti-mouse IgG2a	553388	Fisher Scientific, Hampton, USA
Antibody anti-mouse IgG2b	550333	Fisher Scientific, Hampton, USA
Antibody anti-mouse IgG3	553406	Fisher Scientific, Hampton, USA

Furthermore, a collection of antibodies was used to perform the cytometry studies with different reagents.

Most of the used antibodies were recombinant antibodies (REA) quality. REA antibodies were produced by genetic modifications on B cells and do not attach to Fc receptors. All

antibodies were IgG1 to reduce the complexity of the assays because they share the isotype control for each color.

A table with the mouse-specific antibodies necessary to perform the flow cytometry analysis can be found hereafter:

Table 53. Flow cytometry reagents

Monoclonal antibodies	Reference	Brand	Antibody isotype
Anti-IL-4-PE, Clone BVD4-1D11	130-102-435	Myltenyi, Bergisch Gladbach, Germany	-
Anti-IL-17A-PE, REA660	130-112-009		-
Anti-IFN-g-APC, REA638	130-123-283		-
Anti-TNF-a-APC, RE636	130-123-277		-
CD4-APC-Vio770, Clone REA604	130-119-132		-
CD3-PerCP-Vio700, Clone REA641	130-120-826		-
Anti-IL-2 PE-Cy 7, Clone JES6-5H4	25-7021-82	Thermo Fisher, Waltham, USA	IgG2b, kappa
Anti-IL13 PE, CloneeBio13A	12-7133-82		IgG1, kappa
Rat IgG2b-PE	130-102-663	Myltenyi, Bergisch Gladbach, Germany	-
REA Control-PE, Clone REA293	130-113-450		-
REA Control-APC, Clone REA293	130-113-446		-
REA Control-APC, Clone REA293	130-113-446		-
REA Control-APC, Clone REA293	130-113-446		-
REA Control-APC-Vio770, Clone REA293	130-113-447		-
REA Control-PerCP-Vio700, Clone REA293	130-113-453		-
Rat IgG2b kappa PE-Cy7, CloneeB149/10H5	25-4031-82	Thermo Fisher, Waltham, USA	IgG2b, kappa
Rat IgG1 kappa PE, Clone eBRG1	12-4301-82		IgG1, kappa

The necessary equipment used for chapter 3 can be found in the following table:

Table 54. Chapter 3 equipment

Equipment	Brand
FACS canto II	BD Biosciences, San Jose, USA
Centrifuge 5084/5084	Eppendorf, Hamburg, Germany
CO_2 cell incubator	Cell expert, Hamburg, Germany

12.1.2 Acinetovax vaccine

Vaccine formulations used in the immunization are those described in:

-Drug substance is described in section 9.1.1

12.2 *In vivo* method assay

In vivo method assay material and method are explained in section 6.3.

12.2.1 Infection model

On day 21 after administering the first dose of vaccine, 1E+08 CFU/mL of the clinical isolate Ab-154 (134) of *A. baumannii* were intravenously injected into five animals of groups M1 to M4. Mice survival was monitored for seven days (135).

12.2.2 Sample organization

<u>*Sera samples*</u>:

Sera samples were obtained from the animals at 7 and 21 days post vaccination and preserved at -80ºC until the analysis. *Sera* samples were obtained from the cava vein of mice with a syringe and left in a 1.5 mL eppendorf tube at room temperature for 30 minutes. Next, the tube was centrifuged at 10000 rpm for 10 minutes at 4ºC. Then samples were frozen at -80ºC and were sent to Reig Jofre facilities.

<u>Spleen:</u>

Spleens were collected from mice on day 22 after the first immunization. Afterward, they were processed. Animal immunization and spleen sample collection was performed in the CNM in Madrid.

Spleens were mechanically disrupted in a flux cabinet. Inside a sterile *petri* plate, spleens were smashed between the frosted ends of two sterile microscope slides. The disaggregated tissue was passed through a 70 μm pore size mesh to discard clumps and debris. The mesh was washed with PBS buffer to collect the cells on a 15 mL falcon tube. Afterward, cells were washed twice with 10 mL of RPMI + 10% FBS and were centrifuged at 600 rpm for 3 minutes both times. After the second wash, samples were reconstituted with 10 mL of RPMI and were counted. To count the cells, they were diluted in Trypan Blue in a 1:2 proportion, then, cells were counted in a Neubauer chamber. Later, cells were resuspended with 10% DMSO 90% FBS solution at the desired concentration and immediately frozen at -80ºC. For long-term storage, cells were maintained in liquid nitrogen.

12.3 Cytokine analysis by flow cytometry:

Cytokines produced by the splenocytes obtained from vaccinated and non-vaccinated mice, mainly regarding the memory T cell population, were analyzed. The cytokines associated with the different T helper cell populations were selected to perform the analysis. The cytokines selected to study T helper response Th1 were TNFα and IFNγ. For Th2 cells, IL-4 and IL-13. For Th17 cells, IL17A (88).

12.3.1 Splenocyte cultures

Cryovials containing frozen splenocytes were thawed quickly by gently swirling the vial. To achieve the rapid thawing, RPMI complete media (10% FBS, 1 % streptomycin/penicillin, 30mM 2-mercaptoetanol) at 37ºC was added dropwise to the cells. Cell solution was immediately centrifuged to eliminate DMSO as fast as possible. The cell pellet was resuspended in 1 mL of RPMI complete media, filtered through a 70 μm mesh, washed as previously described, collected, and counted. In the culture, 2E+06 live cells were incubated in a different stimulus specified for every experiment in the results section.

12.3.2 Flow cytometry

Splenocytes cultured (section 12.3.1) for the designated period under the different stimuli conditions (positive control, negative control, and treatment) were collected, filtered through a 70 μm mesh, washed twice with PBSA (PBS, 2% FBS) (3 minutes at 650 rpm), and counted. Cells (2E+05 per well) were resuspended with 50μL of the live dead reagent diluted in PBSA at a 1:50 dilution and incubated for 15 minutes. Afterward, cells were washed with PBSA (650 rpm, 3 minutes). Fc receptors present on the membranes of cell samples were blocked with Miltenyi blocking solution ((1:50 dilution in PBSA) and incubated for 10 minutes. Cells were washed twice as described, resuspended in 200 μL of PBS, and incubated either with anti-CD3 and anti-CD4 antibodies or isotype controls. Cells were washed twice with PBSB (2% FBS, 0,1% sodium azyde) (650 rpm, 3 minutes). Samples were fixed and permeabilized with Miltenyi fixation and permeabilization kit. 50 μL of fixation reagent was added for 10 minutes. Then, a washing step was performed with PBSB (650 rpm, 3 minutes) twice. Then, permeabilization solution was added for 20 minutes. Afterward, cells were labeled with cytokine-specific antibodies: anti-IL2, anti-IL4, anti-IL13, anti-TNFα, anti-IFNγ, and anti-IL17A diluted in permeabilization buffer for 30 minutes at 5ºC (antibody concentration will be described in the results section). Cells labeled with the isotype control were added for each condition containing isotype control for each fluorochrome. Cells were washed twice with PBSB (3 minutes at 650 rpm), resuspended in 200 μL of PBS, and analyzed on the flow cytometer.

Gating strategy for flow cytometry data analysis

The route of analysis followed to analyze the samples is the one explained hereafter. First, single cells (singlets) were selected to eliminate cell aggregates. Afterward, the hole population cells were represented, showing Forward Scatter (FSC) vs. Side Scatter (SSC) from where lymphocytes were selected. In this representation, the cells were found in the region selected in the graphic (See graphic figure 69 A).

Flow cytometry scheme of analysis
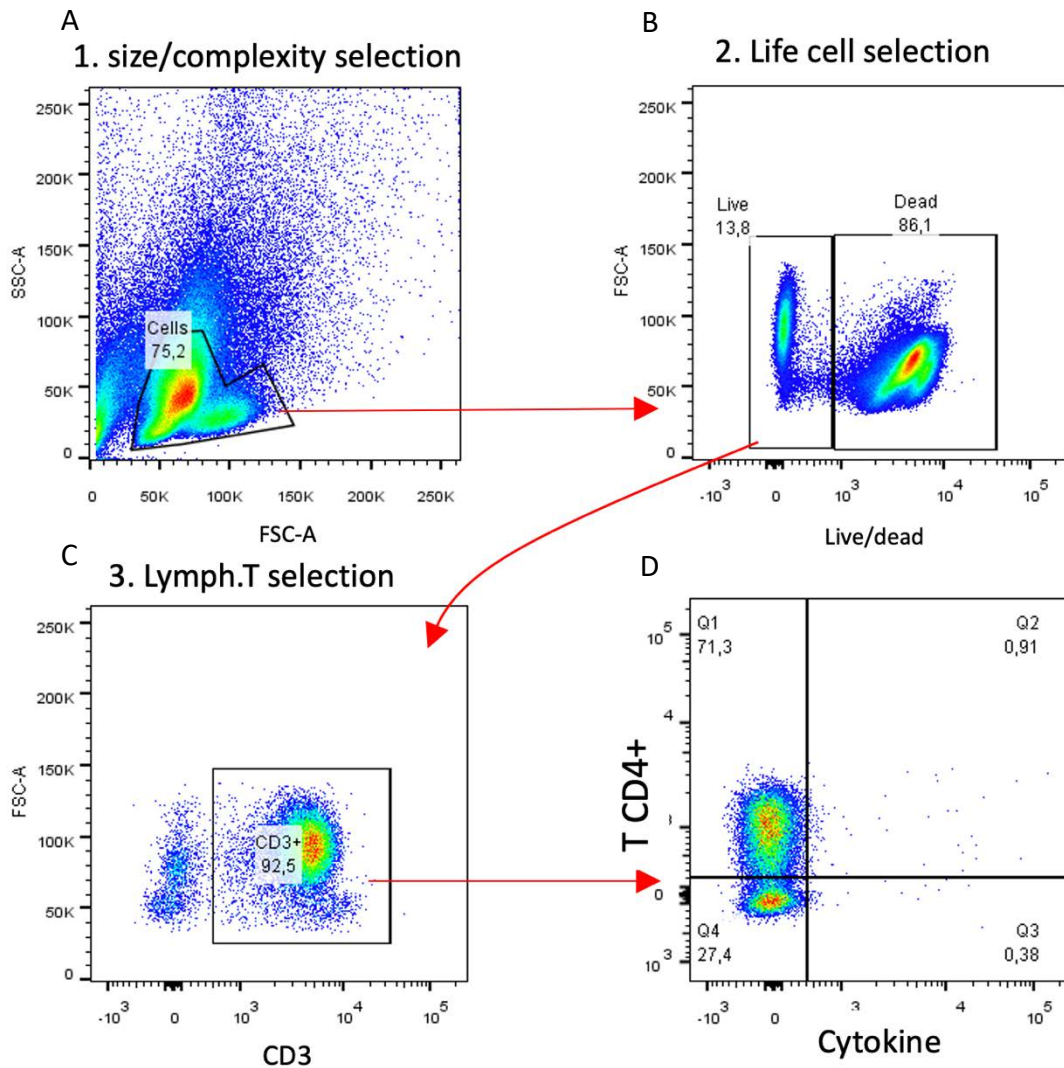
Figure 68. Example of flow cytometry gating strategy performed in each analysis. **A.** Selection of complete splenocytes among the whole cell population. **B.** Selection of alive cells. **C.** Selection of CD3+ cells among alive cells. **D.** Separation of CD3+ cells in 4 categories, positive and negative for CD4 and the cytokine of interest, in this case, IL2.

A dot-plot showing FSC-A and the fluorochrome FITC (gfigure 69B) was used to select live cells from the selected region. Further steps on the analysis were performed, studying the live cell population that expressed CD3 representing most of the living cells of the total population (figure 69C).

Afterward, cytokine production was analyzed on cells selected in figure 69C chart ploting CD4+ and IL2+ cell populations, in figure 69D. In every assay, the result of the isotype control of each color was subtracted to the rest of the samples to obtain the real data.

12.4 IgG detection in *sera* by ELISA

ELISA serum method can be found in section 6.4. Specific reagents used for this ELISA were biotinylated anti-mouse IgG1, IgG2a, IgG2b and IgG3 antibodies described in table 52.

12.4.1 IgG isotype ELISA analysis

ELISA analysis consisted on the subtraction of blanks of the ELISA plate. Then, the mean of the triplicate for each sample was calculated . Afterwards, the absorbance of the 6 different plates were used to perform the Grubb's test, which was applied to eliminate possible outliers. The Schapiro Wilk test confirmed the normality of the data that allowed to perform an ANOVA test between all conditions. Then, an ANOVA assay was performed to compare the same IgG isotype production between the ELISA results of animals vaccinated with different conditions, and with IgG response between different isotypes of the same group of animals.

13. Results and discussion

13.1 *In vivo* assay

13.1.1 Survival

During Acinetovax formulation development, an *in vivo* assay was performed to test the effect of lyophilization and irradiation on vaccine's batch 2 following the method described in section 10.3.

Sera samples were obtained 21days after immunization of the animals, and the studies performed with them can be found in section 10.3.

13.1.2 Study of the humoral response induced by Acinetovax

One of the most critical areas during the production of a vaccine is understanding the immune response induced. The immune response to Acinetovax was separated into two areas, the humoral and cellular response. This section was centered on the humoral response induced by Acinetovax, studying IgG isotype antibody production. Antibody isotype determination also helped to determine which could be the cellular response to the vaccine.

As explained previously, it has been demonstrated that IL4 produced by Th2-type T helper follicular cells promote the isotype switch to low affinity IgG1. Instead, IFNγ secreted by Th1 induces the production of IgG2a. Th17-secreted IL17 has been shown to induce the switch to IgG2a and IgG3 and also to IgG2b (88,90,184,185).

Thus, to study the humoral immune response induced, the isotype of the IgG antibodies specific for *A. baumannii* produced were analyzed in the *sera* samples of mice from the different immunization groups (M1-M5). *Sera* of animals were collected as described in section 6.3 and the method and the results obtained on the *in vivo* study were described in section 10.3. The ELISA plates were coated with 100 µL/well of *A. baumannii* (5E+08 bacteria/mL), the strain composing the vaccine Acinetovax.

IgG isotypes present in mice *sera* after immunization with Acinetovax (batch 2)
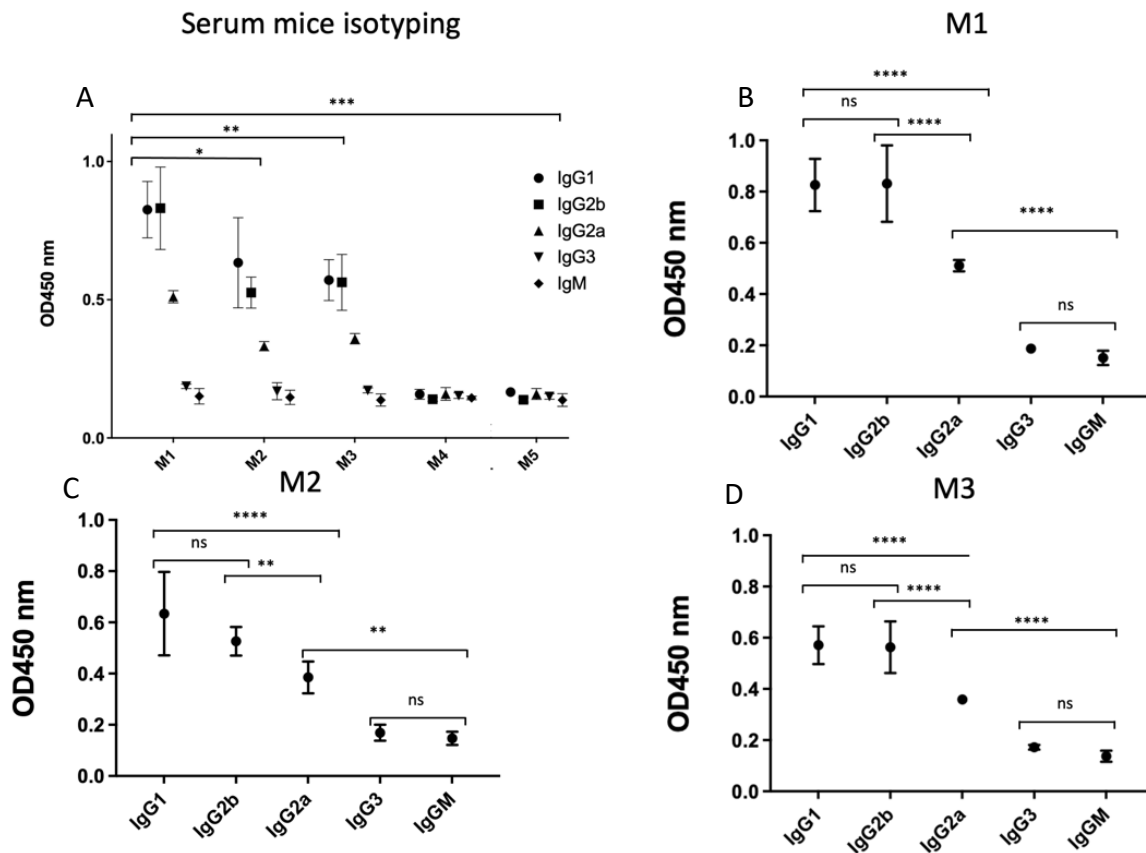
Figure 69. Comparison of the IgG subtypes abundance in the *serum* of immunized mice of groups M1, M2, M3, M4 and M5. **A**. General comparison of IgG production from animals M1-M5. **B**. Detail of graphic A with differences between isotype production of sample M1. **C**. Detail of graphic A with differences between isotype production of sample M2. **D**. Detail of graphic A with differences between isotype production of sample M3. *$p<0.05$; **$p<0.005$; ***$p<0.0005$; ****$p<0.00005$.

The results of figure 70 confirmed that mice vaccinated with Acinetovax developed an immune response with the production of IgG antibodies specific for the *A. baumannii* strain composing the vaccine of groups M1-M3. Meanwhile, these antibodies could not be detected in adjuvant treated nor in naïve mice. These data confirm that the vaccine was effective and there was a specific humoral immune response against the target pathogen *A. baumannii*.

Further, the comparison of the production of the different IgG subisotypes showed statistically significant differences. The complete results of the analysis that can be found in the annex 3 and conclusions are collected hereafter:

-Groups M1, M2 and M3 produced high levels of IgG1, IgG2a and IgG2b compared to the control groups M4 and M5 and the differences were significantly different ($p<0.0001$). However, there were differences on the level of IgG3 or IgM between these groups. These results indicated that the response to *A. baumannii* was predominantly mediated by IgG1, IgG2b and IgG2a.

-There were statistically significant differences between the production of IgG1, IgG2a and IgG2b in group M1 and groups M2/M3. Mice from group M1 produced significantly higher levels of these three isotypes in response to the vaccine. However, as previously shown, this difference did not result on a lower protection in front of *A. baumannii,* as *shown in* the *in vivo* assay, between groups M1 and M2 and only a slight difference in the case of M3 (see graphic 69).

-There were no significant differences in antibody production between groups M2 and M3, which indicate that even though the irradiation had some influence in the stability of the vaccine (see section 10.8), it had no impact on the humoral immune response induced.

-There was no difference in IgM response in groups M1-M5. This suggest that IgM antibodies are not the predominant isotype in theresponse elicited by the vaccine. The *serum* was analyzed on day 21 after immunization and therefore only the predominant switched isotypes were increased.

-IgG3 production was low in in all the animals tested regardless of the treatment group.

The abundance of the different isotypes produced in immunized mice was as follows: IgG1 = IgG2b >> IgG2a > IgG3 = IgM. In 6-month-old C57BL/6 mice immunized with Acinetovax, the most abundant isotype were IgG1 and IgG2b followed by IgG2a and much lower concentrations of IgM and IgG3. IgM is usually produced at the first days of the infection

when the adaptive immune response is being developed meaning that the vaccination has developed correctly a protective humoral immune response.(81)

Regarding the T helper response, Th1 and Th2 response produce respectively isotypes antibodies IgG2a and IgG1 and these responses are mutually exclusive, therefore, having both antibodies present with suggest that a response different than Th1 and Th2 was happening (186).

Based on these results we can suggest that the vaccine Acinetovax induced a Th17 response. As mentioned above, Th17 response elicits the production of IgG1, IgG2a, IgG2b and IgG3 (88) and the humoral response produced by the vaccine produced 3 out of 4 of these antibody isotypes. Also, to explain the absence of IgG3, this subtype of antibody is mainly produced against bacterial polysaccharides (187). So, probably, since bacteria used in this vaccine formulation were devoid of LPS and polysaccharides in the membrane, this would explain the lack of IgG3 production.

13.2 Analysis of the T cell response

Mice splenocytes were phenotypically characterized by flow cytometry.

13.2.1 Analysis of Cell viability

As splenocytes were cryopreserved right after being collected, when they were thawed their cell viability was assessed. Before starting the cell culture, the percentage of alive cells was around 30-50% in all the samples analyzed.

Also, viability during the cytometry analysis was evaluated and results showed that in all animals and all conditions studied, most of the cells were dead. Hereafter, viability, $CD3^+$ cells and $CD3^+CD4^+$ cells of each animal tested in this thesis were summarized.

Table 55. Summary of live/dead, CD3 and CD4 cells recovered from vaccinated and non-vaccinated mice (animals from M2 and M5 groups, respectively).

	Population of splenocytes %			
	Non vaccinated		Vaccinated	
	Mean	CV	Mean	CV
Live/dead	6	35%	9	10%
CD3	42	60%	49	48%
CD3 CD4	5	85%	20	62%

Results suggest that a small percentage of cells (6 - 9%) survived to freezing, transport and culture and flow cytometry procedures. Also, it can be observed that there were 95% of $CD3^+CD8^+$ cells and 5% of $CD3^+CD4^+$ indicating a high dominance of CD8 cells over CD4 cells.

Vaccinated mice, had significantly higher levels of $CD3^+CD4^+$ cells compared to non-vaccinated mice, suggesting an ongoing T helper response in vaccinated mice. These cells, that were proposed to be Th17, might be directing the protective immune response described in the *in vivo* assay (see section 10.3) and thus leading to the production of the specific antibodies described above (see section 13.2.1).

13.2.2 Membrane and intracellular staining set up conditions

Intracellular cytokine production by T cells was set up to analyze the cellular immune response induced by Acinetovax in the mice sepsis model described above.

First, a positive control was set up with splenocytes from immunized mice. Splenocytes were divided in two groups that were cultured for 6 hours either with phorbol 12-myristate 13-acetate (PMA) (25 ng/mL), ionomycin(1 µg/mL) and brefeldin A (10 µg/mL) as the positive control or with brefeldin A (10 µg/mL) alone and considered the negative control (95).

PMA/ionomycin was used to induce a potent non-specific stimulation resulting on the production of most of the T cell cytokines without the intervention of APCs or antigen (95). Brefeldin A was used as inhibitor of cell exocytosis as it inhibits the transport between endoplasmic reticulum and Golgi organelles and consequently cytokine secretion (188). Used together PMA, ionomycin and brefeldin A, stimulates cytokine production by activated T cells that accumulate in the cytoplasm and can be detected using cytokine specific monoclonal antibodies (95). This activation was meant to be used as a positive control.

After the 6 h culture, cells were stained with antibody anti-CD3-Percp-Cy5, anti-CD4-APC-Cy7, anti-IL2-PE-Cy7 or the corresponding isotype controls. The results are shown hereafter (figure 71) analyzed following the gating strategy described above..

CD3 and CD4 in splenocytes (flow cytometry)
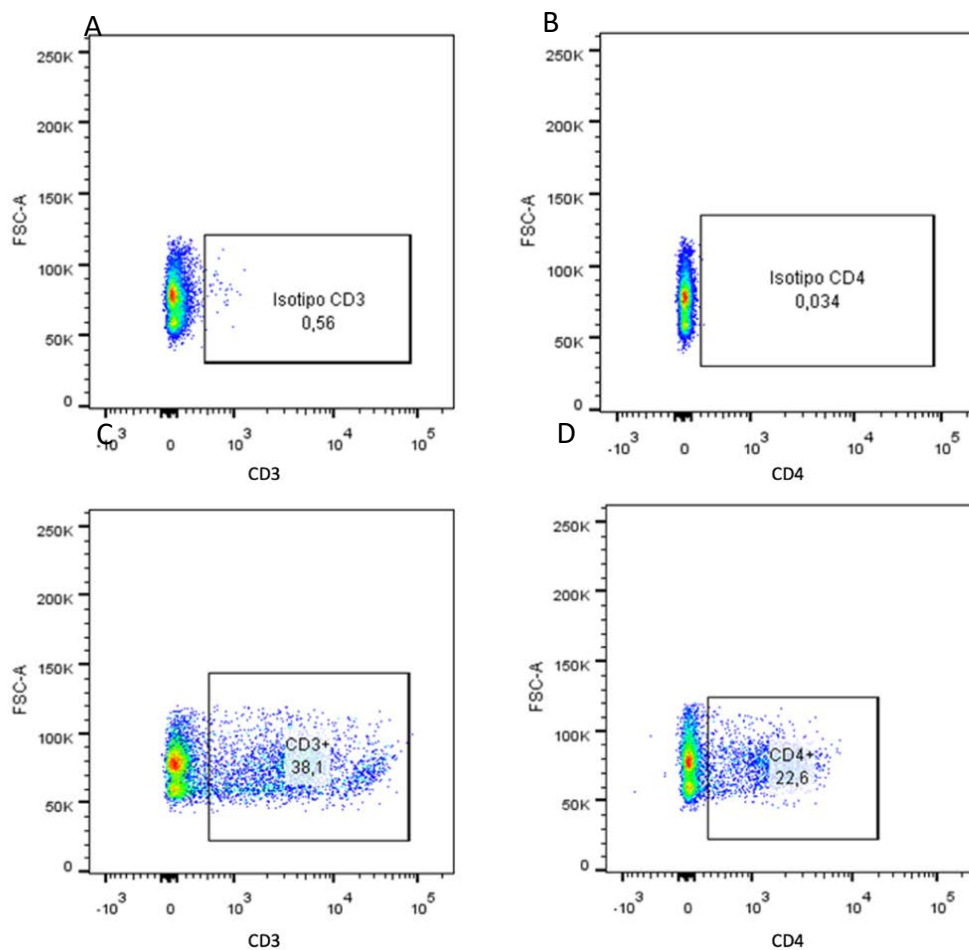
Figure 70. Flow cytometry gating comparing positive control splenocytes stained with anti-CD3 and CD4 antibodies and splenocytes stained with the corresponding isotype controls. Dot plots show FSC-A (cell size) and the cells stained with anti-CD3 and anti-CD4. **A.** Isotype CD3- gate. **B.** Isotype CD4- gate. **C.** positive control CD3$^+$ gate. **D.** positive control CD4$^+$ gate.

Results suggest that the staining procedure with anti-CD3 and anti-CD4 antibodies was performed properly. The antibodies used were specific, and non-specific background could not be detected.

Figure 69 shows an example of the staining analysis. In this case, the 38% of the splenocytes were CD3$^+$ and out of them a 22.6% were CD4$^+$. Both molecules combined indicated that the cell was a T helper lymphocyte (81).

Cells were also stained intracellularly with an anti-IL2 antibody. Results showing IL2 production by alive CD3$^+$ CD4$^+$ cells can be observed hereafter:

IL2 production in splenocytes (flow cytometry)
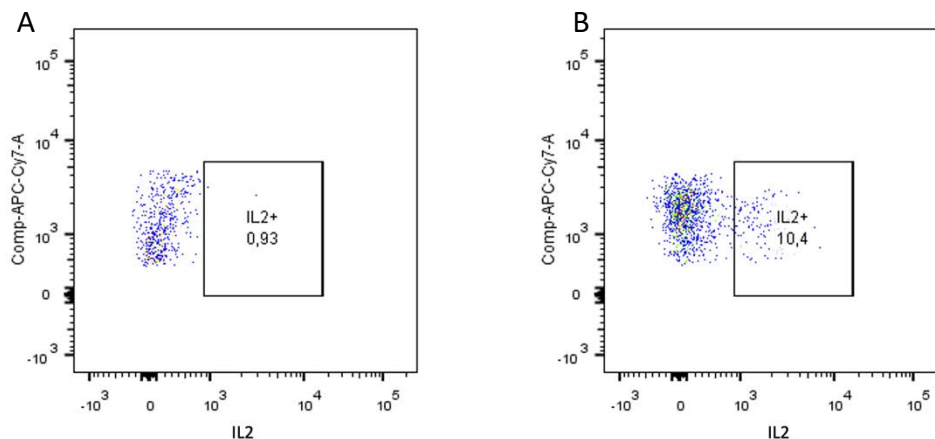
Figure 71. Flow cytometry gating performed to study IL2 produced by CD4 T cells stimulated with PMA and Ionomycin (**B**) and the isotype control (**A**).

Cell gating strategy used for the analysis was described in figure 69. Figure 72B shows IL2 staining in the CD3$^+$ CD4$^+$ cells. Isotype control was used to setup the region for IL2 producing cells. The isotype control was used to stablish the lower limit of the analysis and then study the positive control. The positive control produced a clear and activated population due to the action of PMA-ionomycin. In the positive control, incubated with PMA-ionomycin, we detected a 10.4% of IL2$^+$ CD4$^+$ T cells.

These results suggest that the positive control was set up properly for IL2.

13.2.3 Titration of cytokine-specific antibodies

As described before, the T helper cell populations secrete different cytokines. It was important to understand what type of T cell response was induced in the immunized mice.

Cytokine production was analyzed with cytokine-specific antibodies labeled with different fluorochroms as described in section 12.1.1. Cytokine-specific antibodies were titrated testing different concentrations as follows: antibodies anti-TNFα, IFNγ and IL2 were tested at 0.3, 0.15 and 0.03 µg/mL. Anti IL13 at 2.0, 1.0 and 0.2 µg/mL and anti-IL4 at 0.5, 0.1 and 0.02 µg/mL.

The isotype control for each antibody was used at the highest concentration to confirm their specificity at the highest titer..

Isotype controls were used to set the window to study the cytokine production. The results of the cells stimulated with PMA, ionomycin and brefeldin A are shown in the following table.

Table 56. Flow cytometry results of titration of antibodies anti IL2, IL4, IL13, TNFa, IFNg , IL17A PE and IL17A APC. The percentage shown represents the number of CD4^{+} cells that are also positive for each of these cytokines (n = 1).

		Percentage of CD3^{+}CD4^{+} splenocytes		
	Isotype	Antibody concentration		
		High	Medium	Low
IL2	1.20%	29.10%	**17.50%**	15.50%
IL4	1.00%	5.50%	**4.40%**	3.40%
IL13	1.00%	12.30%	**3.80%**	5%
TNFα	1.20%	40.50%	**37.50%**	24.30%
IFNγ	1.20%	28.10%	26%	**26.20%**
IL17	1.00%	**2.70%**	0.90%	0.20%

Cytokines produced by live, CD3^{+}CD4^{+} cells were studied following the gating strategy describe in figure 69.

Table 56 shows in bold green letters the selected antibody concentration that was used in the successive assays. The medium concentration was selected for IL-2 and IL-13 because even though high concentration produced higher response, most of this response could be non-specific leading to higher background noise. Meanwhile, IL-4 or TNFα positive cell numbers did not show differences between medium and high concentrations, so medium concentration was also selected. For IL-17, the highest concentration was selected because medium, and low concentrations did not show any cell staining.

Thanks to this assay, it was determined that all cytokine production was induced with this stimulation protocol and could be detected by flow cytometry. Also, the best antibody concentrations were selected.

13.2.4 Set up of *A. baumannii*-specific T cell response analysis

The next step consisted of the study the T cell response in *A. baumannii* stimulated splenocytes. The objective was to analyze if the culture of splenocytes with the *A. baumannii* strain contained in the vaccine formulation, could induce an IL2 response *in vitro*.

Splenocytes (2E+06 cells) of vaccinated mice were seeded in a 24 well plate with 2E+07 or 2E+05 bacteria/well and were cultured for 7, 20 and 24 hours to assess different cytokine production kinetics. Also, a positive and negative control were performed as previously explained in section 13.2.2.

IL2 production was measured as described on live CD3$^+$CD4$^+$ splenocytes acquiring 20.000 cells/sample in the flow cytometer.:

Analysis of incubation of splenocytes with *A. baumannii*
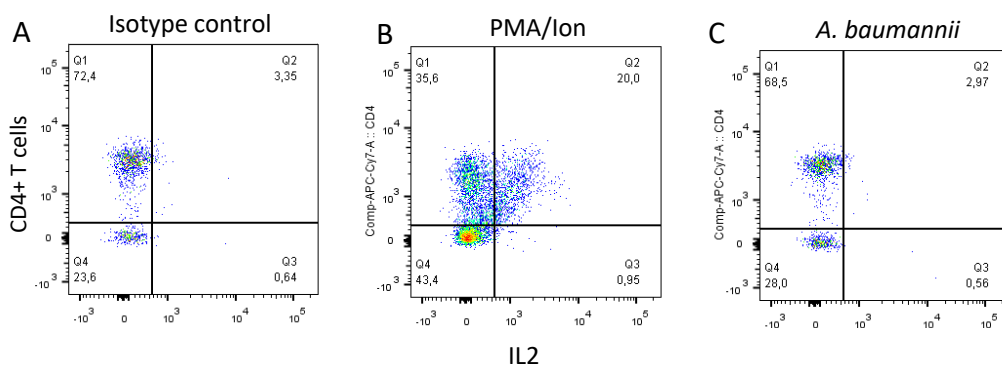
Figure 72. Flow cytometry gating performed to compare splenocytes stained with anti-CD4 and anti-IL2 antibody. Gating is performed facing APC-Cy7-A (anti-CD4) against PE-Cy7-A (anti-IL2). **A.** Positive control with PMA, Ionomycin and brefeldin A. **B.** PE-Cy7-A isotype antibody of positive control cells. **C.** Splenocytes incubated with 2E+07 bacteria for 24 hours.

As it can be observed, the stimulation of splenocytes with *A. baumannii* for 24h did not induce the production of IL2 (Figure 74C). However, a 20% of the CD3$^+$CD4$^+$ splenocytes cultured with PMA/Ionomycin did produce the cytokine IL2 (Figure 74B). This result indicates that stimulation with *A. baumannii* was not sufficient to activate the CD4$^+$ T cells. These cells were functional as they were clearly able to produce IL2 in the presence of a strong stimulus such as PMA and Ionomycin. (Figure 74). This was true at all the stimulation times and different concentrations of bacteria tested. Results suggest a response against *A. baumannii* with no IL2 production or an incubation that was not able to reproduce cell activation *in vitro*. However, a clear antibody-mediated response to the immunogen was described in section 13.1.2. Thus, technical issues such as timing, splenocytes viability or the *A. baumannii* stimulus used might have been responsible for the absence of IL2 response by CD4 T cells. A summary of the data is shown in table 57.

As mentioned before, no condition was able to activate the cells apart from positive control. IL2 is a molecule that indicates antigen T cell stimulation because is produced mainly by Lymphocyte T CD4$^+$ cells (189–191). A negative result of IL2 expression means that non-antigen presentation was on-going, which was not the case because the vaccine produced a protective response (section 10.3). Probably the method simply did not achieve the activation of cells due to other reasons.

Table 57. Results of staining positive control incubated 4 hours with PMA, Ionomycin and brefeldin A and splenocytes incubated with 2 doses of VXD-001 drug substance (2E+07 and 2E+05 bacteria) for 7, 20 and 24 hours. Results showed in the table are % of CD4$^+$ and IL2$^+$ cells. (n = 1)

% of CD3$^+$CD4$^+$IL2$^+$ cells			
time / stimulus	PMA/Ion	2E+07 bacteria	2e+05 bacteria
4h	20	-	-
7h	-	2	2
20h	-	0	2
24h	-	4	3

13.2.5 Stimulation condition set up with PMA and ionoyicin

The T cell response induced by *A. baumannii* was studied with the incubation of lymphocytes with *A. baumannii* bacteria. The incubation time was modified from 4 to 16 hours to extend the stimulation time. The objective consisted in increasing the incubation time to gather inside the cells cytokines which might be produced by T cells between 4 and 18 hours of incubation. Therefore, a comparation between the initial stimulation time (4 hours) with PMA, Ionomycin and Brefeldin A and the extended time (16 hours) was done to obtain a positive control of 16 hours.

To perform this assay, splenocytes from vaccinated mice were cultured in the presence of reduced concentrations of PMA, ionomycin and Brefeldin A to avoid cell toxicity. The selected final concentrations were 10 ng/mL for PMA, 250 ng/mL for Ionomycin and 5 µg/mL of Brefeldin A. This change also allowed cytokine detection produced at different times during exposition to the stimuli. Results after subtracting the isotype control value from all samples are shown hereafter:

Table 58. Flow cytometry results showing percentage of CD3$^+$-CD4$^+$ cells that are also positive to cytokine production detected with antibodies anti IL2, IL4, IL13, TNFα, IFNγ , IL17A PE and IL17A APC titration results.

	Percentage of cytokine positive T CD4$^+$ splenocytes (%)					
	IL2	IL4	TNFα	IFNγ	IL13	IL17A PE
C- 4H	0	0	3	3	0	0
C- 16H	0	0	3	3	0	0
4H	12	1	33	9	10	7
16H	15	1	29	3	16	8

Table 58 suggest that IL2, TNF α, IL17A and IL13 were similarly produced upon 4 or 16 hours of stimulation. IL4 was also produced at the two stimulation conditions but the percentage of IL4$^+$ cells was low in both cases. From these results it was also observed that the number of IFN-γ^+ TCD4 cells was higher at 4 hours. The conclusion of this assay was that both activations were comparable and non-significant differences could be found between 4 and 16 hours of incubation with PMA, ionomycin and brefeldin A. This result means that the time increase did not affect the results obtained from the assay.

13.2.6 Study of cytokine production in response to *A. baumannii*

To determine if there was a predominant subpopulation of CD4$^+$ T cells responding to the vaccine, a comparison between positive control cells and cells incubated with *A. baumannii* bacteria for 16 hours was set up. The concentration of PMA and ionomycin for positive control and Brefeldin A used in this assay were described in section 12.3.2.

The assay was performed 3 times with splenocytes of 3 different vaccinated mice. Isotype results were subtracted to the rest of the samples. The results of the different conditions can be observed hereafter.

Table 59. Flow cytometry percentage of T CD4+ cells positive for cytokine production detected with antibodies anti IL2, IL4, IL13, TNFα, IFNγ IL17A PE and IL17A APC. Samples studied were a negative control isotype, positive control with PMA and ionomycin and Brefeldin A, splenocytes incubated 16 hours with 2E+07 bacteria and a negative control of splenocytes incubated exclusively with brefeldin A. These results are the mean of 3 different assays (n = 3).

| | Cytokine produced by T CD4+ cells (%) | | | | | | | | | | | |
| | IL2 | | IL4 | | TNFα | | IFNγ | | IL13 | | IL17A PE | |
	Mean	SD	Mean	SD	Mean	SD	Mean	SD	Mean	SD	Mean	SD
PMA/Ion	22	3	0	0	42	3	3	0	9	6	1	1
Bacteria 16h	3	2	0	0	2	2	1	1	1	1	0	0
w/o stimulation	1	0	0	0	3	5	3	4	0	0	0	0

As observed, PMA/Ionomycin results were positive in all conditions tested except for IL4. Splenocytes stimulated with bacteria produced low levels of IL2, TNFα, IFNγ, IL17 and IL13 but not IL4 compared to those of the PMA/Ion stimulated cells. However, only the expression of IL2, IL17 and IL13 was higher to that of non-stimulated splenocytes from the same sample.

The conclusions obtained from this assay was that probably the positive control was not perfectly stablished because it was supposed to work activating non-specifically all cytokines capable of being produced by a lymphocyte. Also, it was determined that incubation with bacteria might be producing a slight response, activating IL2 cytokines, even though, this result was low and was produced with high standard deviation results.

13.2.7 Comparison of cytokine production between vaccinated and non-vaccinated mice

Bearing in mind the difficulties to obtain a T specific response for *A. baumannii*, we wanted to check if a predominant CD4 T cell could be activated *in vitro* being incubated with PMA, ionomycin and Brefeldin A.

Splenocytes of vaccinated and non-vaccinated mice were incubated during 24 hours with PMA, ionomycin and Brefeldin A to obtain the maximum cytokine production. The determination was performed in 7 different assays in which vaccinated and non-vaccinated mice were compared.

Also, a group of splenocytes were cultured in the presence of Brefeldin A alone and were used as control. Also, isotype control was used, and its result was subtracted to the rest of the samples.

These cells were stained with the antibodies specific for IL2, IL4, TNFα, IFNγ, IL17A and IL13 and the results can be observed in the following table:

Table 60. Flow cytometry results in a percentage of CD4$^+$ cells that were also positive to cytokine production detected with antibodies anti IL2, IL4, IL13, TNFα, IFNγ and IL17A. Samples studies were a positive control with PMA and ionomycin A for vaccinated and non-vaccinated cells, and a negative control of splenocytes incubated exclusively with brefeldin A. Isotype result has been subtracted from the rest of the data. These results are the mean of 7 different assays.

	Percentage of activated CD3$^+$ CD4$^+$ splenocytes (n = 7)											
	IL2		IL4		TNFα		IFNγ		IL17A		IL13	
	Mean	SD	Mean	SD	Mean	SD	Mean	SD	Mean	SD	Mean	SD
C+ vac	7,7	4,2	-0,8	0,5	23,5	17,0	3,6	3,6	1,9	3,9	11,0	15,9
C+ No vac	7,2	4,5	-0,7	0,3	20,8	11,9	2,2	2,9	-1,2	3,1	9,8	13,5
C- vac	1,5	1,8	-0,9	0,3	1,6	3,4	9,0	10,1	7,5	11,0	0,9	2,6
C- No vac	0,8	1,0	1,9	3,1	0,1	3,0	-1,2	1,8	-0,8	2,3	2,8	6,0

Results show the seven assays had a substantial standard deviation between them. This is due to the difference of activation between samples in the different assays. Some cytokines were produced in the positive control, such as IL2, TNFα, or IL13. The rest of the cytokines could not be detected in these assays.

Trying to obtain more information from these results and study the difference between vaccinated and non-vaccinated results, a comparison dividing vaccinated C+ by non-vaccinated C+ results was performed. Results value close to 1 suggest no differences between vaccinated and non-vaccinated C+.

Table 61. Mean and standard deviation from the seven flow cytometry assays after dividing positive and negative controls of vaccinating results by positive and negative controls of non-vaccinated results.

	IL2		IL4		TNFα		IFNγ		IL17A APC		IL13	
	Mean	SD	Mean	SD	Mean	SD	Mean	SD	Mean	SD	Mean	SD
C+ vac/ c+ no vac	1,7	1,5	1,8	1,8	1,1	0,8	1,8	2,3	0,2	0,6	1,1	1,0
C- vac/ c- no vac	0,6	5,8	0,4	1,0	0,9	4,5	3,4	6,4	0	6,3	0,7	0,3

Results show that in most cases, there were no differences between samples from vaccinated and non-vaccinated animals because the obtained values were close to 1. Some cytokines, such as IL2 or IFNγ, showed higher percentage values, but the biggest problem was the standard deviation was too high for reaching any conclusion. This might mean the assay was not set up correctly to study these samples, and no conclusions could be obtained.

14. Technical achievements

- The humoral response produced by the vaccine Acinetovax has been characterized:
    - A potent IgG response has been described against *A. baumannii*.
    - The IgG subtypes produced suggested that the T helper cell was Th17
    - The vaccinated and non-vaccinated mice had different levels of CD4 activated cells.
    - The positive control for most of the cytokines was set up, although no activation could be achieved with bacteria.

15. Technical general summary

This thesis project has been performed in a multidisciplinary environment, using techniques from knowledge fields such as immunology, pharmacology, molecular biology, or physic-chemistry. The test battery developed and used for this project was crucial to achieving the main final goal: producing a vaccine successful in its pre-clinical stage.

15.1 Chapter one

Part of the humoral response was characterized thanks to the use of different analytical techniques. The vaccine's efficacy was studied through the *in vivo* assay, which showed a potent IgG humoral response. Also, this assay (see figure 13) helped determine the optimal vaccine dose.

Furthermore, the humoral response produced in the *in vivo* assay showed that the vaccine could produce an IgG response specific against *A. baumannii* that can protect the animals from the infection.

Then, splenocytes from immunized mice were used to develop hybridomas from a list of antibodies. Afterward, the antibodies were screened, and eight antibodies were selected. The most suitable antibodies to develop an ELISA and WB analytical techniques were antibodies 1 and 7. The protein detected by them was the protein Omp22, characterized by MALDI TOF/TOF and it was determined through TEM analysis that the protein Omp22 can be found on the bacterial membrane. Thanks to this assay, this protein was found to be one of the immunodominant proteins of the vaccine.

Also, different analytical techniques required to measure the quality of the vaccine were developed and optimized. An ELISA assay was used to quantify the protein Omp22 on the bacterial surface was developed and validated following ICH international guidelines. The assay complied with all characteristics previously determined to study the precision, accuracy, linearity, or robustness.

Another analytical method was developed to quantify the number of bacteria present in the drug product, known as µBCA.

Some other techniques, such as Western blot and Coomassie staining, were developed to study the identity of the vaccine detecting Omp22 and other proteins in the pharmaceutical product.

With the information showed in chapter one, the methods selected to study the vaccine have been proved accurate enough to study the quality of the drug product throughout the time.

15.2 Chapter two

The pharmaceutical formulation was optimized in several parameters. It was demonstrated that processes as lyophilization and irradiation do not affect the vaccine efficacy. Also, the formula was optimized by selecting the best components for the vaccine, ensuring lyophilization is the process that improves the stability of the vaccine, testing the sterility and studying the formula in stability studies.

Different cryoprotectants were tested and rehalose was chosen because it has been demonstrated to protect aluminum hydroxide from degradation and produced a stable tablet. Also, the sterility of the product was assured.

Furthermore, sterility was tested in two separated batches, but also, drug product exposed to non-sterile production process has demonstrated to avoid contamination of the sample.

Besides, it was determined that lyophilized formula was more stable than a liquid formula with or without aluminum hydroxide.

Also, the precipitation time helped redefine the formula and separated bacteria and aluminum hydroxide in two different vials, allowing the industrial scalability of the product.

In vivo performed with batch 37, was the culmination of the thesis. This result suggested that all the work performed to develop and optimize the vaccine was recompensed. The optimized formula and it could elicit a protection of 100 % both in irradiated and non-irradiated formulas.

15.3 Chapter three

In this chapter, the main result obtained was the characterization of the cellular response produced by the vaccine. It was suggested that Acinetovax induced a Th17 response. This suggestion was performed because, Th17 response elicits the production of IgG1, IgG2a, IgG2b, and IgG3 (88), but the result of this analysis was that the four isotypes were produced, but not IgG3.

The explanation for the lack of an IgG3 subtype production might be that this subtype of antibody was mainly produced against polysaccharides of the pathogens that elicited the immune response (187). So, maybe, since the bacteria used in this vaccine was LPS- and did not have polysaccharides in the membrane, the immune response produced might have been Th17 but did not produce IgG3 due to the lack of polysaccharides.

Furthermore, it was demonstrated that humoral response production between vaccinated and non-vaccinated mice was significantly different (see figure 70). Vaccinated mice produce B cell response that besides the survival assay demonstrated to be a protective response.

Also, it was determined that even though Vaxdyn and Reig Jofre's formulas behaved slightly different regarding the IgG subtype, *in vivo* protection capacity was similar. With ELISA results, it was also observed that no significant differences could be found between irradiated and non-irradiated formulas.

Meanwhile, flow cytometry results showed no relevant results due to the procedure's variability and incapacity to produce or detect some cytokines. Although, the analysis

performed enhanced the immunological characterization thanks to the study of splenocyte populations.

For example, significant differences could be detected between cells from vaccinated and non-vaccinated mice, showing vaccinated mice as having higher number CD4$^+$ T cells. This suggested that the protective vaccination induced significant changes in mice spleens that might be supporting mice protection as observed in the *in vivo* assay. Further, the *serum* IgG response support that the optimized vaccine formulation was effective and induced a potent humoral response. These results were confirmed afterwards with the *in vivo* assay performed with batch 37.

16. General conclusions

Observing the results obtained in chapters 1, 2, and 3, it could be determined that most of the objectives from the thesis have been achieved:

- The selection, development, and validation of analytical techniques required to characterize the vaccine and its study in the pharmaceutical development environment has been completed successfully.

- The obtention of a pharmaceutical formulation that is effective, scalable, and stable has also been achieved.

- The vaccine has been immunologically characterized, understanding part of the humoral response production and studying the protective capacity of the vaccine.

Apart from these objectives, it should be noted that the work performed in this thesis has allowed the recruitment of external investors that ensures the continuation of the development of the vaccine until reaching the clinical stage.

17. Bibliography

1.   Risou J, Pebrot AR. Studies on bacterial taxonomy. X. The revision of species under Acromobacter group. Ann Inst Pasteur (Paris). 1954;86(6):722–8.

2.   Juni E. Interspecies transformation of Acinetobacter: genetic evidence for a ubiquitous genus. J Bacteriol. 1972;112(2):917–31.

3.   Henriksen SD. Moraxella, neisseria and branhamella. Annu Rev Microbiol. 1976;63–83.

4.   Bouvet PJM, Grimont PAD. Taxonomy of the genus Acinetobacter with the recognition of Acinetobacter baumannii sp. nov., Acinetobacter haemolyticus sp. nov., Acinetobacter johnsonii sp. nov., and Acinetobacter junii sp. nov. and emended descriptions of Acinetobacter calcoaceticus and Acinetobacter lwoffii. Int. J. Syst. Bacteriol. 1986; 36:228-240.

5.   Rossau R, Van Landschoot A, Gillis M D ley J. Taxonomy of Moraxellaceae fam. nov., a New Bacterial Family To Accommodate the Genera Moraxella, Acinetobacter, and Psychrobacter and Related Organisms. Int J Syst BACTERIOLO. 1991;41 (2):309-310.

6.   Piperaki ET, Tzouvelekis LS, Miriagou V, *et al*. Carbapenem-resistant Acinetobacter baumannii: in pursuit of an effective treatment. Clin Microbiol Infect. 2019;25(8):951–957.

7.   Touchon M, Cury J, Yoon EJ, Krizova L, *et al*. The genomic diversification of the whole Acinetobacter genus: Origins, mechanisms, and consequences. Genome Biol Evol. 2014;6(10):2866–2882.

8.   Baumann P. Isolation of Acinetobacter from soil and water. J Bacteriol. 1968;96(1):39–42.

9.   List of Prokaryotic names with Standing in Nomenclature (LPSN). Acinetobacter [Internet]. 2021. [cited 2021 Nov 4]. Available from: https://www.bacterio.net/genus/acinetobacter.

10. Alsan M, Klompas M. Acinetobacter baumannii: An emerging and important pathogen. J Clin Outcomes Manag. 2010;17(8):27–35.

11. Bennett MD, John E, Dolin MD, *et al.* Principles and Practice of Infectious Diseases. Elsevier. 2014;2.

12.   Towner KJ. The Genus Acinetobacter. Prokaryotes. 2006;6:197–214.

13.   Peleg AY, Seifert H, Paterson DL. Acinetobacter baumannii: Emergence of a successful pathogen. Clin Microbiol Rev. 2008;21(3):538–582.

14.   Seifert H, Dijkshoorn L, Gerner-Smidt P, *et al,*. Distribution of Acinetobacter species on human skin: Comparison of phenotypic and genotypic identification methods. J Clin Microbiol. 1997;35(11):2819–25.

15.   La Scola B, Raoult D. Acinetobacter baumannii in human body louse. Emerg Infect Dis. 2004;10(9):1671-3.

16.   Nira Rabin N, Yue Zheng, Opoku-Temeng C, *et al.* Biofilm formation mechanisms and targets for developing antibiofilm agents. Future Med Chem. 2015;7(4):493–512.

17.   Constanze E, Dietze B, Dietz E, Runden H. Acinetobacter Outbreaks, 1977–2000. Infect Control Hosp Epidemiol. 1997;1394–1397.

18.   Moubareck CA, Halat DH. Insights into Acinetobacter baumannii: A review of microbiological, virulence, and resistance traits in a threatening nosocomial pathogen. Antibiotics. 2020;9(3):119.

19.   Fukuta Y, Muder RR, Agha ME, *et al*. Risk factors for acquisition of multidrug-resistant Acinetobacter baumannii among cancer patients. Am J Infect Control. 2013;41(12):1249–1252.

20.   Lynch JP, Zhanel GG, Clark NM. Infections Due to Acinetobacter baumannii in the ICU: Treatment Options. Semin Respir Crit Care Med. 2017;38(3):311–25.

21.   Chen W. Host Innate Immune Responses to Acinetobacter baumannii Infection. Front Cell Infect Microbiol. 2020;10(September):1–16.

22.   Joly-Guillou ML. Clinical impact and pathogenicity of Acinetobacter. Clin Microbiol Infect. 2005;11(11):868–873.

23.   Jones CL, Clancy M, Honnold C, *et al*. Fatal Outbreak of an Emerging Clone of Extensively Drug-Resistant Acinetobacter baumannii with Enhanced Virulence. Clin Infect Dis. 2015;61(2):145–54.

24.   García-Garmendia JL, Garnacho-Montero J, Ortiz-Leyba C, *et al.* Risk factors for acinetobacter baumannii (AB) nosocomial bacteremia in critically ill patients: A cohort study. Crit Care Med. 1999;27(1):939–946.

25. Talbot GH, Bradley J, Edwards JE, Gilbert D, Scheld M, Bartlett JG. Bad bugs need drugs: An update on the development pipeline from the Antimicrobial Availability Task Force of the Infectious Diseases Society of America. Chemother J. 2006;15(4):97–105.

26. Spellberg B, Rex JH. The value of single-pathogen antibacterial agents. Nat Rev Drug Discov. 2013;12(12):963–964.

27. Falagas ME, Karveli EA. The changing global epidemiology of Acinetobacter baumannii infections: A development with major public health implications. Clin Microbiol Infect. 2007;13(2):117–119.

28. Fournier PE, Richet H. The epidemiology and control of Acinetobacter baumannii in health care facilities. Clin Infect Dis. 2006;42(5):6692–6929.

29. Ribera A, Vila J, Pascual A. Clinical features and Epidemiology of A. baumannii. 2004;(5):183–191.

30. Dijkshoorn L, Nemec A, Seifert H. An increasing threat in hospitals: Multidrug-resistant Acinetobacter baumannii. Nat Rev Microbiol. 2007;5(12):939–951.

31. Ferrara AM. Potentially multidrug-resistant non-fermentative Gram-negative pathogens causing nosocomial pneumonia. Int J Antimicrob Agents. 2006;27(3):183–195.

32. Bissell MG. Nosocomial Bloodstream Infections in US Hospitals: Analysis of 24,179 Cases From a Prospective Nationwide Surveillance Study. Yearb Pathol Lab Med. 2006;2006(4):285–6.

33. Wood GC, Mueller EW, Croce MA, *et al.* Evaluation of a clinical pathway for ventilator-associated pneumonia: Changes in bacterial flora and the adequacy of empiric antibiotics over a three-year period. Surg Infect (Larchmt). 2005;6(2):203–13.

34. Falagas ME, Bliziotis IA, Siempos II. Attributable mortality of Acinetobacter baumannii infections in critically ill patients: a systematic review of matched cohort and case-control studies. Crit Care. 2006;10(2):48.

35. Wu CL, Yang DI, Wang NY, et al. Quantitative culture of endotracheal aspirates in the diagnosis of ventilator-associated pneumonia in patients with treatment

failure. Chest. 2002;122(2):662–668.

36.   Jones RN. Microbial etiologies of hospital-acquired bacterial pneumonia and ventilator-associated bacterial pneumonia. Clin Infect Dis. 2010. 1;51 (1):81-87.

37.   Garnacho J, Sole-Violan J, Sa-Borges M, *et al*. Clinical impact of pneumonia caused by Acinetobacter baumannii in intubated patients: A matched cohort study. Crit Care Med. 2003;31(10):2478–2482.

38.   Wong T, Student M, City I, Schlichting AB, *et al*. No Decrease in Early Ventilator-Associated Pneumonia After Early Use of Chlorhexidine. 2017;25(2):173–171.

39.   Garnacho-Montero J, Ortiz-Leyba C, Fernández-Hinojosa E, *et al*. Acinetobacter baumannii ventilator-associated pneumonia: Epidemiological and clinical findings. Intensive Care Med. 2005;31(5):649–655.

40.   Bergogne-Bérézin E, Towner KJ. Acinetobacter spp. as nosocomial pathogens: Microbiological, clinical, and epidemiological features. Clin Microbiol Rev. 1996;9(2):148–165.

41.   Cisneros JM, Rodriguez-Baño J. Nosocomial bactermia due to Acinetobacter baumannii: Epidemiology, clinical features and treatment. Clin Microbiol Infect. 2002;8(11):687–693.

42.   Cisneros JM, Reyes MJ, Pachón J, Becerril B, Caballero FJ, García-Garmendía JL, *et al*. Bacteremia due to Acinetobacter baumannii: Epidemiology, clinical findings, and prognostic features. Clin Infect Dis. 1996;22(6):1026–1032.

43.   Wisplinghoff H, Paulus T, Lugenheim M, *et al*. Nosocomial bloodstream infections due to Acinetobacter baumannii, Acinetobacter pittii and Acinetobacter nosocomialis in the United States. J Infect. 2012;64(3):282–290.

44.   Valero C, Fariñas MC, García Palomo D, *et al.* Endocarditis due to Acinetobacter lwoffi on native mitral valve. Int J Cardiol. 1999;69(1):97–99.

45.   Chopra T, Marchaim D, Awali RA, *et al.* Epidemiology of bloodstream infections caused by Acinetobacter baumannii and impact of drug resistance to both carbapenems and ampicillin-sulbactam on clinical outcomes. Antimicrob Agents Chemother. 2013;57(12):6270–6275.

46.   Gaynes R, Edwards JR. Overview of nosocomial infections caused by gram-negative bacilli. Clin Infect Dis. 2005;41(6):848–854.

47.   Jiménez-Mejías ME, Pachón J, *et al*. Treatment of multidrug-resistant
       Acinetobacter baumannii meningitis with ampicillin/sulbactam. Clin Infect Dis.
       1997;24(5):932–935.

48.   Metan G, Alp E, Aygen B, Sumerkan B. Acinetobacter baumannii meningitis in post-
       neurosurgical patients: Clinical outcome and impact of carbapenem resistance [17].
       J Antimicrob Chemother. 2007;60(1):197–199.

49.   Falagas ME, Karveli EA. The changing global epidemiology of Acinetobacter
       baumannii infections: A development with major public health implications. Clin
       Microbiol Infect. 2007;13(2):117–119.

50.   Manchanda V, Sinha S, Singh N. Multidrug resistant Acinetobacter. J Glob Infect
       Dis. 2010;2(3):291.

51.   Fournier PE, Vallenet D, Barbe V, *et al.* Comparative genomics of multidrug
       resistance in Acinetobacter baumannii. PLoS Genet. 2006;2(1):62–72.

52.   Santajit S, Indrawattana N. Mechanisms of Antimicrobial Resistance in ESKAPE
       Pathogens. Biomed Res Int. 2016; 2016: 2475067.

53.   Viehman JA, Nguyen MH, Doi Y. Treatment options for carbapenem-resistant and
       extensively drug-resistant Acinetobacter baumannii infections. Drugs.
       2014;74(12):1315–1333.

54.   Hsueh PR, Teng LJ, Chen CY, *et al.* Pandrug-resistant Acinetobacter baumannii
       causing nosocomial infections in a University Hospital, Taiwan. Emerg Infect Dis.
       2002;8(8):827-832.

55.   Shrivastava SR, Shrivastava PS, Ramasamy J. World health organization releases
       global priority list of antibiotic-resistant bacteria to guide research, discovery, and
       development of new antibiotics. JMS - J Med Soc. 2018;32(1):76–77.

56.   Antunes LCS, Visca P, Towner KJ. Acinetobacter baumannii: Evolution of a global
       pathogen. Pathog Dis. 2014;71(3):292–301.

57.   Shlaes DM, Bradford PA. Antibiotics—From There to Where? Pathog Immun.
       2018;3(1):19.

58.   Queenan AM, Pillar CM, Deane J, et al. Multidrug resistance among Acinetobacter
       spp. in the USA and activity profile of key agents: Results from CAPITAL Surveillance

2010. Diagn Microbiol Infect Dis [Internet]. 2012;73(3):267–270.

59. Owen RJ, Li J, Nation RL, *et al.* In vitro pharmacodynamics of colistin against Acinetobacter baumannii clinical isolates. J Antimicrob Chemother. 2007;59(3):473–477.

60. Perez F, Hujer AM, Hujer KM, et al,. Global challenge of multidrug-resistant Acinetobacter baumannii. Antimicrob Agents Chemother. 2007;51(3471):84.

61. Marques MB, Brookings ES, Moser SA, *et al.* Comparative in vitro antimicrobial susceptibilities of nosocomial isolates of Acinetobacter baumannii and synergistic activities of nine antimicrobial combinations. Antimicrob Agents Chemother. 1997;41:881–885.

62. Reddy T, Chopra T, Marchaim D, *et al.* Trends in antimicrobial resistance of Acinetobacter baumannii isolates from a Metropolitan Detroit health system. Antimicrob Agents Chemother. 2010;54(5):2235–2238.

63. Oethinger M, Kern W V., Jellen-Ritter AS, *et al.* Ineffectiveness of topoisomerase mutations in mediating clinically significant fluoroquinolone resistance in Escherichia coli in the absence of the AcrAB efflux pump. Antimicrob Agents Chemother. 2000;44(1):10–13.

64. Piddock LJ. Multidrug Resistance Efflux Pumps in Bacteria. Clin Microbiol. 2006;19(2):382–402.

65. Queenan AM, Bush K. Carbapenemases: The versatile β-lactamases. Clin Microbiol Rev. 2007;20(3):440–458.

66. Sievert DM, Ricks P, Edwards JR, *et al.* Antimicrobial-Resistant Pathogens Associated with Healthcare-Associated Infections Summary of Data Reported to the National Healthcare Safety Network at the Centers for Disease Control and Prevention, 2009–2010. Infect Control Hosp Epidemiol. 2013;34(1):1–14.

67. Mussi, Maria A, Limansky AS, Viale AM. Acquisition of Resistance to Carbapenems in Multidrug-Resistant Clinical Strains of. Society. 2005;49(4):1432–40.

68. Yahav D, Farbman L, Leibovici L, *et al.* Colistin: New lessons on an old antibiotic. Clin Microbiol Infect. 2012;18(1):18–29.

69. Moffatt JH, Harper M, Harrison P, *et al.* Colistin resistance in Acinetobacter baumannii is mediated by complete loss of lipopolysaccharide production.

Antimicrob Agents Chemother. 2010;54(12):4971–4977.

70.   Needham BD, Trent MS. Fortifying the barrier: The impact of lipid A remodelling on bacterial pathogenesis. Nat Rev Microbiol. 2013;11(7):467–481.

71.   Bertani B, Ruiz N. Function and Biogenesis of Lipopolysaccharides. EcoSal Plus. 2018;8(1):1–33.

72.   García-Quintanilla M, Pulido MR, Pachón J, *et al.* Immunization with lipopolysaccharide-deficient whole cells provides protective immunity in an experimental mouse model of Acinetobacter baumannii infection. PLoS One. 2014;9(12):1–14.

73.   McConnell MJ, Domínguez-Herrera J, Smani Y, *et al.* Vaccination with outer membrane complexes elicits rapid protective immunity to multidrug-resistant acinetobacter baumannii. Infect Immun. 2011;79(1):518–526.

74.   Luo G, Lin L, Ibrahim AS, *et al.* Active and passive immunization protects against lethal, extreme drug resistant-Acinetobacter baumannii infection. PLoS One. 2012;7(1):e29446.

75.   Fattahian Y, Rasooli I, Mousavi Gargari SL, *et al.* Protection against Acinetobacter baumannii infection via its functional deprivation of biofilm associated protein (Bap). Microb Pathog. 2011;51(6):402–406.

76.   Bentancor L V., Routray A, Bozkurt-Guzel C, *et al.* Evaluation of the trimeric autotransporter ata as a vaccine candidate against Acinetobacter baumannii infections. Infect Immun. 2012;80(10):3381–3388.

77.   McConnell MJ, Rumbo C, Bou G, *et al*. Outer membrane vesicles as an acellular vaccine against Acinetobacter baumannii. Vaccine. 2011;29(34):5705–5710.

78.   McConnell MJ, Pachón J. Active and passive immunization against Acinetobacter baumannii using an inactivated whole cell vaccine. Vaccine 2010;29(1):1–5.

79.   Park BS, Lee JO. Recognition of lipopolysaccharide pattern by TLR4 complexes. Exp Mol Med. 2013;45(12):66-69.

80.   Kaur BP, Secord E. Innate Immunity. Pediatr Clin North Am [Internet]. 2019;66(5):905–911.

81.   Abbas AK, Lichtman AH Pillai S. Basic immunology. ELSEVIER. 2016.

82.   Al-Shehri SS. Reactive oxygen and nitrogen species and innate immune response.

Biochimie. 2021;181:52–64.

83.   Papenfuss TL, Rebelatto MC, Bolon B. Toxicologic Pathology for Non-Pathologists. 355-395.

84.   Chaplin DD. Overview of the immune response. J Allergy Clin Immunol. 2010;125(2):S3-23.

85.   Cronkite DA, Strutt TM. The regulation of inflammation by innate and adaptive lymphocytes. J Immunol Res. 2018; 2018:1467538.

86.   Lumen. B Lymphocytes and Humoral Immunity [Internet]. 2021 [cited 2021 Nov 4]. Available from: https://courses.lumenlearning.com/microbiology/chapter/b-lymphocytes-and-humoral-immunity/.

87.   Budzynska P. Regulation of B Cell Development by Transcription Factors IRF4 and BACH2 [Internet]. 2017. [cited 2021 Nov 4]. Available from: https://www.semanticscholar.org/paper/Regulation-of-B-cell-development-by-transcription-Budzy%C5%84ska/b07e8c08d6349a6c61ff6ac45a0e61bc552ead30

88.   Mitsdoerffer M, Lee Y, Jäger A, Kim HJ, Korn T, Kolls JK, et al. Proinflammatory T helper type 17 cells are effective B-cell helpers. Proc Natl Acad Sci U S A. 2010;107(32):14292–14297.

89.   Deenick EK, Hasbold J, Hodgkin PD. Switching to IgG3, IgG2b, and IgA is division linked and independent, revealing a stochastic framework for describing differentiation. J Immunol. 1999; 163(9):4707–4714.

90.   Snapper CM, Mond JJ. Towards a comprehensive view of immunoglobulin class switching. Immunol Today. 1993;14(1):15–17.

91.   Ando M, Ito M, Srirat T, Kondo T, *et al.* Memory T cell, exhaustion, and tumor immunity. Immunol Med [Internet]. 2020;43(1):1–9.

92.   British Society for immunology editors. BSI. T-cell activation. [Internet]. 2021. [cited 2021 Nov 4]. Available from: https://www.immunology.org/public-information/bitesized-immunology/systems-and-processes/t-cell-activation

93.   Perdue S, Humphrey J. Immune system [Internet]. 2020. [cited 2021 Oct 28]. Available from: https://www.britannica.com/science/immune-system/T-cell-antigen-receptors

94.   Sallusto F, Lanzavecchia A. Heterogeneity of CD4+ memory T cells: functional

modules for tailored immunity. Eur J Immunol. 2009; 39(8):2076–82.

95. Ai W, Li H, Song N, *et al.* Optimal method to stimulate cytokine production and its use in immunotoxicity assessment. Int J Environ Res Public Health. 2013;10(9):3834–3842.

96. Wang W, Sung N, Gilman-Sachs A, *et al.* Helper (Th) Cell Profiles in Pregnancy and Recurrent Pregnancy Losses: Th1/Th2/Th9/Th17/Th22/Tfh Cells. Front Immunol. 2020;11:1–14.

97. Hsieh CS, Macatonia SE, Tripp CS, *et al.* Development of TH1 CD4+ T cells through IL-12 produced by Listeria-induced macrophages. Science. 1993; 260(5107):547–549.

98. Constant SL, Bottomly K. Induction of Th1 and Th2 CD4+ T cell responses: the alternative approaches. Annu Rev Immunol. 1997;15:297–322.

99. Gajewski TF, Fitch FW. Anti-proliferative effect of IFN-gamma in immune regulation. I. IFN-gamma inhibits the proliferation of Th2 but not Th1 murine helper T lymphocyte clones. J Immunol. 1988; 140(12):4245–4252.

100. Swain SL, Weinberg AD, English M, *et al.* IL-4 directs the development of Th2-like helper effectors. J Immunol. 1990; 145(11):3796–3806.

101. Korn T, Bettelli E, Oukka M, *et al.* IL-17 and Th17 Cells. Annu Rev Immunol. 2009;27:485–517.

102. Mangan PR, Harrington LE, O'Quinn DB, *et al.* Transforming growth factor-beta induces development of the T(H)17 lineage. Nature. 2006;441(7090):231-234.

103. Infante-Duarte C, Horton HF, Byrne MC, *et al.* Microbial lipopeptides induce the production of IL-17 in Th cells. J Immunol. 2000; 165(11):6107-6115.

104. Ye P, Rodriguez FH, Kanaly S, *et al.* Requirement of interleukin 17 receptor signaling for lung CXC chemokine and granulocyte colony-stimulating factor expression, neutrophil recruitment, and host defense. J Exp Med. 2001;194(4):519-527.

105. Chung DR, Kasper DL, Panzo RJ, *et al.* CD4+ T cells mediate abscess formation in intra-abdominal sepsis by an IL-17-dependent mechanism. J Immunol. 2003; 170(4):1958–1963.

106. Khader SA, Bell GK, Pearl JE, *et al*. IL-23 and IL-17 in the establishment of protective pulmonary CD4+ T cell responses after vaccination and during Mycobacterium

tuberculosis challenge. Nat Immunol. 2007; 8(4):369–377.

107. Rudner XL, Happel KI, Young EA, *et al.* Interleukin-23 (IL-23)-IL-17 cytokine axis in murine Pneumocystis carinii infection. Infect Immun. 2007; 75(6):3055–3061.

108. Huang W, Na L, Fidel PL, Schwarzenberger P. Requirement of interleukin-17A for systemic anti-Candida albicans host defense in mice. J Infect Dis. 2004;190(3):624–631.

109. Aggarwal S, Gurney AL. IL-17: prototype member of an emerging cytokine family. J Leukoc Biol. 2002;71(1):1–8.

110. Sigal LJ. Activation of CD8 T Lymphocytes during Viral Infections. Elsevier. 2016;4(3):286–290.

111. Nielsen M, Lund O, Buus S, *et al.* MHC Class II epitope predictive algorithms. Immunology. 2010;130(3):319–328.

112. Agencia Española de Medicamentos y Productos Sanitarios (AEMPS). Good manufacturing practicies. [Internet]. 2021 [cited 2021 Nov 4]. Available from: https://www.aemps.gob.es/industria-farmaceutica/guia-de-normas-de-correcta-fabricacion/

113. International Council for Harmonisation of Technical Requirements for Pharmaceuticals for Human Use(ICH). [Internet]. 2021 [cited 2021 Nov 4] Available from: https://www.ich.org/page/ich-guidelines

114. Huang W, Yao Y, Wang S, *et al.* Immunization with a 22-kDa outer membrane protein elicits protective immunity to multidrug-resistant Acinetobacter baumannii. Sci Rep [Internet]. 2016;6(2):1–12.

115. Britannica The Editors of Encyclopaedia. "Antibody" [Internet]. Encyclopedia Britannica. 2020. [cited 2021 Nov 4]Available from: https://www.britannica.com/science/antibody.

116. Choi D, Tsang RSW, Ng MH. Sandwich capture ELISA by a murine monoclonal antibody against a genus-specific LPS epitope for the detection of different common serotypes of salmonellas. J Appl Bacteriol. 1992;72(2):134–8.

117. Tomita M, Tsumoto K. Hybridoma technologies for antibody production. Immunotherapy. 2011;3(3):371–80.

118. Coons AH, Creech HJ, Jones RN. Immunological Properties of an Antibody

Containing a Fluorescent Group. Proc Soc Exp Biol Med. 1941;47(2):200–202.

119. Aydin S. A short history, principles, and types of ELISA, and our laboratory experience with peptide/protein analyses using ELISA. Peptides [Internet]. 2015;72:4–15.

120. Van Weemen BK, Schuurs AH. Immunoassay using antigen-enzyme conjugation. J Opioid Manag. 2019;15(6):445-555.

121. Engvall E, Perlmann P. Enzyme-linked immunosorbent assay (ELISA). Quantitative assay of immunoglobulin G. Immunochemistry. 1971;8(9):871–874.

122. Lindström P, Wager O. IgG autoantibody to human serum albumin studied by the ELISA-technique. Scand J Immunol. 1978;7(5):419–425.

123. Kato K, Hamaguchi Y, Okawa S, *et al.* Use of rabbit antiboty IgG bound onto plain and aminoalkylsilyl glass surface for the enzyme-linked sandwich immunoassay. J Biochem. 1977;82(1):261–266.

124. Cortés-Ríos J, Zárate AM, Figueroa JD, *et al.* Protein quantification by bicinchoninic acid (BCA) assay follows complex kinetics and can be performed at short incubation times. Anal Biochem. 2020;608.

125. Smith PK, Krohn RI, Hermanson GT, *et al.* Measurement of protein using bicinchoninic acid. Anal Biochem. 1985;150(1):76–85.

126. Gornall AG, Bardawill CJ, David MM. Determination of serum proteins by means of the biuret reaction. J Biol Chem. 1949;177(2):751–766.

127. Lowry OH, Rosebrough NH, Farr AL. Protein measurement with the Folin phenol reagent. J Biol Chem. 1951;193:265–275.

128. Hnasko R. ELISA: Methods and Protocols. ELISA Methods Protoc. 2015;1318:1–216.

129. Towbin H, Staehelin T, Gordon J. Electrophoretic transfer of proteins from polyacrylamide gels to nitrocellulose sheets: procedure and some applications. Proc Natl Acad Sci U S A. 1979;76(9):4350–4354.

130. Mahmood T, Yang P-C. Western blot: technique, theory, and trouble shooting. N Am J Med Sci. 2012;4(9):429–434.

131. Carretero-Ledesma M, García-Quintanilla M, *et al.* Phenotypic changes associated with colistin resistance due to lipopolysaccharide loss in acinetobacter baumannii. Virulence. 2018;9(1):930–942.

132. Fernández-Cuenca F, Pascual Á, Ribera A, *et al.* Diversidad clonal y sensibilidad a los antimicrobianos de Acinetobacter baumannii aislados en hospitales españoles. Estudio multicéntrico nacional: proyecto GEIH-Ab 2000. Enferm Infecc Microbiol Clin. 2004;22(5):267–271.

133. Fernández-Cuenca F, Tomás-Carmona M, Caballero-Moyano F, *et al.* Actividad de 18 agentes antimicrobianos frente a aislados clínicos de Acinetobacter baumannii: segundo estudio nacional multicéntrico (proyecto GEIH-REIPI-Ab 2010). Enferm Infecc Microbiol Clin. 2013;31(1):4–9.

134. Garcia-Quintanilla M, Pulido M, McConnell M. First Steps Towards a Vaccine against Acinetobacter baumannii. Curr Pharm Biotechnol. 2014;14(10):897–902.

135. Rodríguez-Hernández MJ, Pachón J, Pichardo C, *et al.* Imipenem, doxycycline and amikacin in monotherapy and in combination in Acinetobacter baumannii experimental pneumonia. J Antimicrob Chemother. 2000;45(4):493–501.

136. Sthilaire PM, Lowary TL, Meldal M. Oligosaccharide mimetics obtained by novel, rapid screening of carboxylic acid encoded glycopeptide libraries. J Am Chem Soc. 1998;120(51):13312–13320.

137. Woehrle GH, Brown LO, Hutchison JE. Thiol-functionalized, 1.5-nm gold nanoparticles through ligand exchange reactions: Scope and mechanism of ligand exchange. J Am Chem Soc. 2005;127(7):2172–2183.

138. Ron H, Rubinstein I. Self-assembled monolayers on oxidized metals. 3. Alkylthiol and dialkyl disulfide assembly on gold under electrochemical conditions. J Am Chem Soc. 1998;120(51):13444–13452.

139. Spriano S, Sarath Chandra V, Cochis A, *et al.* How do wettability, zeta potential and hydroxylation degree affect the biological response of biomaterials? Mater Sci Eng C. 2017;74:542–555.

140. Bukšek H, Luxbacher T, Petrinić I. Zeta potential determination of polymeric materials using two differently designed measuring cells of an electrokinetic analyzer. Acta Chim Slov. 2010;57(3):700–706.

141. Uniprot. Omp22 [Internet]. 2021. [cited 2021 Nov 4] Available from: https://www.uniprot.org/uniprot/V5VG76

142. He P, Zou Y, Hu Z. Advances in aluminum hydroxide-based adjuvant research and

its mechanism. Vol. 11, Human Vaccines and Immunotherapeutics. 2015:477–488.

143.   Treanor JJ, Campbell JD, Zangwill KM, *et al.* Safety and immunogenicity of an inactivated subvirion influenza A (H5N1) vaccine. N Engl J Med. 2006;354(13):1343–1351.

144.   Kuroda E, Coban C, Ishii KJ. Particulate adjuvant and innate immunity: past achievements, present findings, and future prospects. Int Rev Immunol. 2013;32(2):209–220.

145.   Brewer JM. (How) do aluminium adjuvants work? Immunol Lett. 2006;102(1):10–15.

146.   Aucouturier J, Dupuis L, Ganne V. Adjuvants designed for veterinary and human vaccines. Vaccine. 2001;19(17–19):2666–2672.

147.   de Titta A, Ballester M, Julier Z, *et al*. Nanoparticle conjugation of CpG enhances adjuvancy for cellular immunity and memory recall at low dose. Proc Natl Acad Sci U S A. 2013;110(49):19902–19907.

148.   Hussain MJ, Wilkinson A, Bramwell VW, *et al.* Th1 immune responses can be modulated by varying dimethyldioctadecylammonium and distearoyl-sn-glycero-3-phosphocholine content in liposomal adjuvants. J Pharm Pharmacol. 2014;66(3):358-366.

149.   Joshi MD, Unger WJ, Storm G, *et al.* Targeting tumor antigens to dendritic cells using particulate carriers. J Control Release. 2012;161(1):25-37.

150.   Petrovsky N. Novel human polysaccharide adjuvants with dual Th1 and Th2 potentiating activity. Vaccine. 2006;24(2):S2-26–9.

151.   Tritto E, Mosca F, De Gregorio E. Mechanism of action of licensed vaccine adjuvants. Vaccine. 2009;27(25–26):3331-3334.

152.   Hogenesch H. Mechanism of immunopotentiation and safety of aluminum adjuvants. Front Immunol. 2012;3:406.

153.   HogenEsch H, O'Hagan DT, Fox CB. Optimizing the utilization of aluminum adjuvants in vaccines: you might just get what you want. npj Vaccines [Internet]. 2018;3(1):1–11.

154.   Li X, Thakkar SG, Ruwona TB, *et al.* A method of lyophilizing vaccines containing aluminum salts into a dry powder without causing particle aggregation or

decreasing the immunogenicity following reconstitution. J Control Release [Internet]. 2015;204:38–50.

155.   Wang W, Singh M. Selection of Adjuvants for Enhanced Vaccine Potency. World J Vaccines. 2011;01(02):33–78.

156.   National Institute of Infectious Diseases (NIID). Minumum requirements for biological products [Internet]. 2006. [cited 2021 Nov 4] Available from: https://www.niid.go.jp/niid/images/qa/seibutuki/MRBP_english/mrbp_2006.pdf

157.   Federal drug administration (FDA). Sterile Drug Products Current Good Manufacturing Practice Guidance for Industry. Filtration [Internet]. 2004 [cited 2021 Nov 4];(9):1–63. Available from: http://www.fda.gov/downloads/Drugs/GuidanceComplianceRegulatoryInformation/Guidances/ucm070342.pdf

158.   Hasanain F, Guenther K, Mullett WM, *et al.* Gamma sterilization of pharmaceuticals--a review of the irradiation of excipients, active pharmaceutical ingredients, and final drug product formulations. PDA J Pharm Sci Technol. 2014;68(2):113–137.

159.   Denyer P, Hodges N, Gorman G. Pharmaceutical product gammairradiation with Cobalt 60. Vol. 8, Pahtaceutical Microbiology. 2011. 365-367.

160.   Di Pretoro A, Manenti F. Freeze Drying/Lyophilization of Pharmaceutical and Biological Products. Vol. 206, SpringerBriefs in Applied Sciences and Technology. 2020. 59-64.

161.   Harring TR, Deal NS, Kuo DC. Disorders of sodium and water balance. Emerg Med Clin North Am. 2014;32(2):379-401.

162.   Rasouli M. Basic concepts and practical equations on osmolality: Biochemical approach. Clin Biochem. 2016;49(12):936-941.

163.   Deardorff DL. Osmotic strength, osmolality, and osmolarity. Am J Hosp Pharm. 1980;37(4):504-509.

164.   Pansare SK, Patel SM. Lyophilization Process Design and Development: A Single-Step Drying Approach. J Pharm Sci [Internet]. 2019;108(4):1423–1433.

165.   Gaidhani KA, Harwalkar M, Deepak B. LYOPHILIZATION / FREEZE DRYING – A REVIEW. World J Pharm Res. 2015;4.

166. Clua Palau G. Application of quality by design and near infrared spectroscopy in manufacturing and control of freeze-dried drug products. TDX (Tesis Dr en Xarxa).

167. Horn J, Friess W. Detection of collapse and crystallization of saccharide, protein, and mannitol formulations by optical fibers in lyophilization. Front Chem. 2018;6(1):1-9.

168. Editors European Pharmacopeia. European Pharmacopeia.

169. Editors United States Pharmacopeia. United States Pharmacopeia.

170. Van Faassen H, KuoLee R, Harris G, *et al.* Neutrophils play an important role in host resistance to respiratory infection with Acinetobacter baumannii in mice. Infect Immun. 2007;75(12):5597-5608.

171. Qiu H, KuoLee R, Harris G, *et al.* High susceptibility to respiratory Acinetobacter baumannii infection in A/J mice is associated with a delay in early pulmonary recruitment of neutrophils. Microbes Infect. 2009;11(12):946-955.

172. Karim M, Khan W, Farooqi B, *et al.* Bacterial isolates in neutropenic febrile patients. J Pak Med Assoc. 1991;41(2):35-37.

173. Joly-Guillou ML, Wolff M, Pocidalo JJ, *et al.* Use of a new mouse model of Acinetobacter baumannii pneumonia to evaluate the postantibiotic effect of imipenem. Antimicrob Agents Chemother. 1997;41(2):345-351.

174. Tsuchiya T, Nakao N, Yamamoto S, *et al.* NK1.1(+) cells regulate neutrophil migration in mice with Acinetobacter baumannii pneumonia. Microbiol Immunol. 2012;56(2):107–116.

175. Breslow JM, Meissler J, Hartzell RR, *et al*. Innate immune responses to systemic acinetobacter baumannii infection in mice: Neutrophils, but not interleukin-17, mediate host resistance. Infect Immun. 2011;79(8):3317–3327.

176. Bruhn KW, Pantapalangkoor P, Nielsen T, *et al*. Host fate is rapidly determined by innate effector-microbial interactions during Acinetobacter baumannii bacteremia. J Infect Dis. 2015;211(8):1296–1305.

177. Grguric-Smith LM, Lee HH, Gandhi JA, *et al*. Neutropenia exacerbates infection by Acinetobacter baumannii clinical isolates in a murine wound model. Front Microbiol. 2015;6(10):1–11.

178. García-Patiño MG, García-Contreras R, Licona-Limón P. The immune response

against Acinetobacter baumannii, an emerging pathogen in nosocomial infections. Front Immunol. 2017;8.

179. Qiu H, Kuolee R, Harris G, *et al.* Role of NADPH phagocyte oxidase in host defense against acute respiratory Acinetobacter baumannii infection in mice. Infect Immun. 2009;77(3):1015-1021.

180. Marrack P, McKee AS, Munks MW. Towards an understanding of the adjuvant action of aluminium. Nat Rev Immunol. 2009;9(4):287-93.

181. Hu Z, Zhu F, He P, *et al*. Study on the kinesis of cellular immunity in adults vaccinated with recombinant hepatitis B vaccine. Zhonghua Liu Xing Bing Xue Za Zhi. 2007;28(4):326–330.

182. McKinnon KM. Flow cytometry: an overview. Cell Vis. 1998;5(1):56–61.

183. Depince-Berger A-E, Aanei C, Iobagiu C, *et al*. New tools in cytometry. Morphologie. 2016;100(331):199–209.

184. Toellner KM, Luther SA, Sze DM, *et al*. T helper 1 (Th1) and Th2 characteristics start to develop during T cell priming and are associated with an immediate ability to induce immunoglobulin class switching. J Exp Med. 1998;187(8):1193–1204.

185. Olatunde AC, Hale JS, Lamb TJ. Cytokine-skewed Tfh cells: functional consequences for B cell help. Trends Immunol [Internet]. 2021;42(6):536-50.

186. Azuma M, Yagita H. Co-signal Molecules in T Cell Activation. Vol. 1189, Advances in Experimental Medicine and Biology. 2019. 156-166.

187. McLay J, Leonard E, Petersen S, *et al.* Gamma 3 gene-disrupted mice selectively deficient in the dominant IgG subclass made to bacterial polysaccharides. II. Increased susceptibility to fatal pneumococcal sepsis due to absence of anti-polysaccharide IgG3 is corrected by induction of anti-polys. J Immunol. 2002 ;168(7):3437-3443.

188. Nylander S, Kalies I. Brefeldin A, but not monensin, completely blocks CD69 expression on mouse lymphocytes: Efficacy of inhibitors of protein secretion in protocols for intracellular cytokine staining by flow cytometry. J Immunol Methods. 1999;224(1–2):69–76.

Annex 1

ELISA Validation

Plate 1 190522_Placa 1_Validación ELISA   105254   23/05/2019
EP0281_01   N.P.   Carlos Berrio
A10659   105254

RAW data												
	1	2	3	4	5	6	7	8	9	10	11	12
A	2.108	2.18	2.202	2.143	2.194	1.593	1.032	1.011	0.036	0.038	0.032	0.028
B	2.172	1.983	2.112	2.39	2.321	1.527	1.053	1.128	0.040	0.042	0.043	0.036
C	1.804	1.888	1.801	2.202	2.352	1.657	1.124	1.049	0.039	0.038	0.037	0.035
D	1.579	1.559	1.476	2.386	2.262	1.738	1.071	1.034	0.038	0.039	0.038	0.037
E	1.316	1.291	1.783	2.266	1.767	1.739	1.041	0.039	0.039	0.045	0.038	0.036
F	0.987	0.945	0.885	2.148	1.714	1.703	0.983	0.039	0.039	0.040	0.038	0.036
G	0.665	0.667	0.654	2.261	1.716	1.626	1.000	0.040	0.040	0.038	0.038	0.035
H	0.335	0.36	0.344	2.278	1.679	1.588	1.052	0.037	0.037	0.041	0.037	0.034

Blank	0.038	0.0013	3%

Blank substraction												
	1	2	3	4	5	6	7	8	9	10	11	12
A	2.070	2.142	2.164	2.105	2.156	1.555	0.994	0.973	0.0	0.0	0.0	0.0
B	2.134	1.945	2.074	2.352	2.283	1.489	1.015	1.090	0.0	0.0	0.0	0.0
C	1.766	1.850	1.763	2.164	2.314	1.619	1.086	1.011	0.0	0.0	0.0	0.0
D	1.541	1.521	1.438	2.348	2.224	1.700	1.033	0.996	0.0	0.0	0.0	0.0
E	1.278	1.253	1.745	2.228	1.729	1.701	1.003	0.0	0.0	0.0	0.0	0.0
F	0.949	0.907	0.847	2.110	1.676	1.665	0.945	0.0	0.0	0.0	0.0	0.0
G	0.627	0.629	0.616	2.223	1.678	1.588	0.962	0.0	0.0	0.0	0.0	0.0
H	0.297	0.322	0.306	2.240	1.641	1.550	1.014	0.0	0.0	0.0	0.0	0.0

Fit standard curve by least squares						
	Mean	SD	CV%	Concentration (bacteria/mL)		
C1	2.125	0.049	2%	1.27E+07		
C2	2.051	0.097	5%	1.11E+07		
C3	1.793	0.049	3%	9.53E+06		
C4	1.500	0.055	4%	7.94E+06		
C5	1.266	0.018	1%	6.35E+06		
C6	0.901	0.051	6%	4.76E+06		
C7	0.624	0.007	1%	3.18E+06		
C8	0.308	0.013	4%	1.59E+06		

Standard curve	
Intersection axis	0.101
Slope	0.000
R2	0.99

Standard curve plate 1

Precision calculation									
	Mean C1, C2 and C3 No blank substraction (Tabla 9 report)			Mean C1, C2 and C3 Blank substaction			Original concentration calculation (bacterias/mL)		Method precision calculation (bacterias/mL)
	Mean	SD	CV%	Mean	SD	CV%			
MC1	2.267	0.085	4%	2.229	0.085	4%	1.25E+07	MC1	1.77E+10
MC2	1.671	0.073	4%	1.633	0.073	4%	8.97E+06	MC2	1.78E+10
MC3	1.010	0.044	4%	1.010	0.044	4%	5.32E+06	MC3	1.76E+10
								Media	1.77E+10
								Desvest	9.90E+07
								CV%	1%

Specificity											
Absence of capture Ab			Absence of detection Ab			Absence of sample			Abscence of streptavidine		
Mean	SD	CV%	Mean	SD	CV%	Mean	SD	CV%	Mean	SD	CV%
0.039	0.001	4%	0.040	0.002	6%	0.038	0.003	8%	0.035	0.003	8%

Linearity					
	Result		CV% Recta		
	0.99	Residuales	Limit CV	Reults	
				2%	C1
				5%	C2
				3%	C3
			10%	4%	C4
				1%	C5
				6%	C6
				1%	C7
				4%	C8

Sistem suitability

Resultado

Plate 1

E P 0 2 8 1 _ 0 1 _ P l a c a 1

bacteria/mL	OD		
X	Y1	Y2	Y3
1.27e+007	2.070	2.142	2.164
1.11e+007	2.134	1.945	2.074
9.53e+006	1.766	1.850	1.763
7.94e+006	1.541	1.521	1.438
6.35e+006	1.278	1.253	~~1.745~~
4.76e+006	0.949	0.907	0.847
3.18e+006	0.627	0.629	0.616
1.59e+006	0.297	0.322	0.306

190620_Placa 2_Validación ELISA   105254   21/06/2019
EP0281_01   N.P.   Carlos Berrio

Plate 2 (A1D1)

A10359   105254
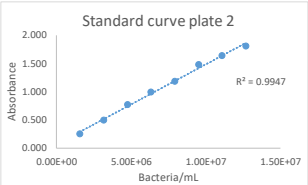
RAW data												
	1	2	3	4	5	6	7	8	9	10	11	12
A	1.803	1.838	1.875	0.029	0.031	0.033	0.032	0.030	0.030	0.034	0.037	0.035
B	1.668	1.718	1.617	1.614	1.592	1.471	1.352	1.833	1.844	1.630	1.644	0.035
C	1.509	1.532	1.503	1.591	1.509	1.449	1.332	1.817	1.695	1.624	1.601	0.031
D	1.233	1.197	1.233	1.208	1.230	0.988	1.004	1.286	1.346	1.273	1.235	0.034
E	1.004	1.051	1.024	1.113	1.129	1.017	0.922	1.271	1.280	1.221	1.201	0.036
F	0.813	0.768	0.816	0.729	0.738	0.640	0.667	0.775	0.812	0.739	0.701	0.035
G	0.546	0.537	0.503	0.731	0.703	0.650	0.605	0.817	0.768	0.759	0.706	0.034
H	0.276	0.286	0.286	0.031	0.037	0.035	0.036	0.035	0.032	0.031	0.031	0.032

	Blank	0.033	0.003	8%

Blank subtraction												
	1	2	3	4	5	6	7	8	9	10	11	12
A	1.770	1.805	1.842	N.P.	N.P.	N.P.	N.P.	N.P.	N.P.	N.P.	N.P.	N.P.
B	1.635	1.685	1.584	1.581	1.559	1.438	1.319	1.800	1.811	1.597	1.611	N.P.
C	1.476	1.499	1.470	1.558	1.476	1.416	1.299	1.784	1.662	1.591	1.568	N.P.
D	1.200	1.164	1.200	1.175	1.197	0.955	0.971	1.253	1.313	1.240	1.202	N.P.
E	0.971	1.018	0.991	1.080	1.096	0.984	0.889	1.238	1.247	1.188	1.168	N.P.
F	0.780	0.735	0.783	0.696	0.705	0.607	0.634	0.742	0.779	0.706	0.668	N.P.
G	0.513	0.504	0.470	0.698	0.670	0.617	0.572	0.784	0.735	0.726	0.673	N.P.
H	0.243	0.253	0.253	N.P.	N.P.	N.P.	N.P.	N.P.	N.P.	N.P.	N.P.	N.P.

Fit standard curve by least squares							
	Mean	SD	CV%	Concentration (bacteria/mL)		Recta	
C1	1.806	0.036	2%	1.27E+07	Axis intersection	0.063	
C2	1.635	0.051	3%	1.11E+07	Slope	0.000	
C3	1.482	0.015	1%	9.53E+06	R2	0.99	
C4	1.188	0.021	2%	7.94E+06			
C5	0.994	0.024	2%	6.35E+06			
C6	0.766	0.027	4%	4.76E+06			
C7	0.496	0.023	5%	3.18E+06			
C8	0.250	0.006	2%	1.59E+06			

Standard curve plate 2

$R^2 = 0.9947$

Method precision calculation											
	Sample 1			Sample 2			Sample 3			Sample 4		
	Mean	SD	CV%	Mean	SD	CV%	Mean	SD	CV%	Mean	SD	CV%
C1	1.544	0.046	3%	1.368	0.069	5%	1.765	0.069	4%	1.592	0.018	1%
C2	1.137	0.058	5%	0.950	0.042	4%	1.263	0.034	3%	1.200	0.030	3%
C3	0.693	0.015	2%	0.608	0.026	4%	0.760	0.025	3%	0.694	0.028	4%

Concentration calculation (bacteria/mL)					Concentration calculation (bacteria/mL)			
	Sample 1	Sample 2	Sample 3	Sample 4		Sample 1	Sample 2	Sample 3	Sample 4
C1	1.04E+07	9.19E+06	1.20E+07	1.08E+07	C1	1.48E+10	1.30E+10	1.70E+10	1.53E+10
C2	7.57E+06	6.25E+06	8.45E+06	8.01E+06	C2	1.50E+10	1.24E+10	1.68E+10	1.59E+10
C3	4.43E+06	3.84E+06	4.91E+06	4.44E+06	C3	1.47E+10	1.27E+10	1.62E+10	1.47E+10
					Media	1.48E+10	1.27E+10	1.67E+10	1.53E+10
					Desvest	1.78E+08	3.17E+08	3.84E+08	6.01E+08
					CV%	1%	2%	2%	4%
					Recovery	94%	80%	105%	97%

Specificity	
Trehalose specificity	Sucrose specificity
Mean	Mean
0.034	0.034

Method precision			
Media	Desvest	Varianza	CV%
1.49E+10	1.64E+09	2.32E+18	11%
	limit CV %	Result	
	15%	11%	

Linearity					
R2		Residuales	CV% Standard curve		
Limit R2	Result		Limit CV	Reults	
0.98	0.99			2%	C1
				3%	C2
				1%	C3
			10%	2%	C4
				2%	C5
				4%	C6
				5%	C7
				2%	C8

Acuracy of the media of samples			
Cncentración teórica	1.58E+10	Limit recovery	
		125%	1.98E+10
		75%	1.19E+10
Media of samples	Recovery		
1.49E+10	94%		

Sistem suitability

10. Method precision ≤ 15%

Plate 2 (A1D1)

E P 0 2 8 1 _ 0 1 _ P l a c a 2

N o n l i n f i t o f E P 0 2 8 1 _ 0 1 _ P l a c a 2
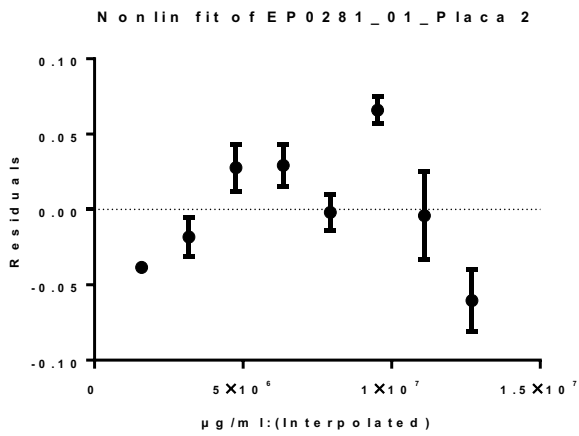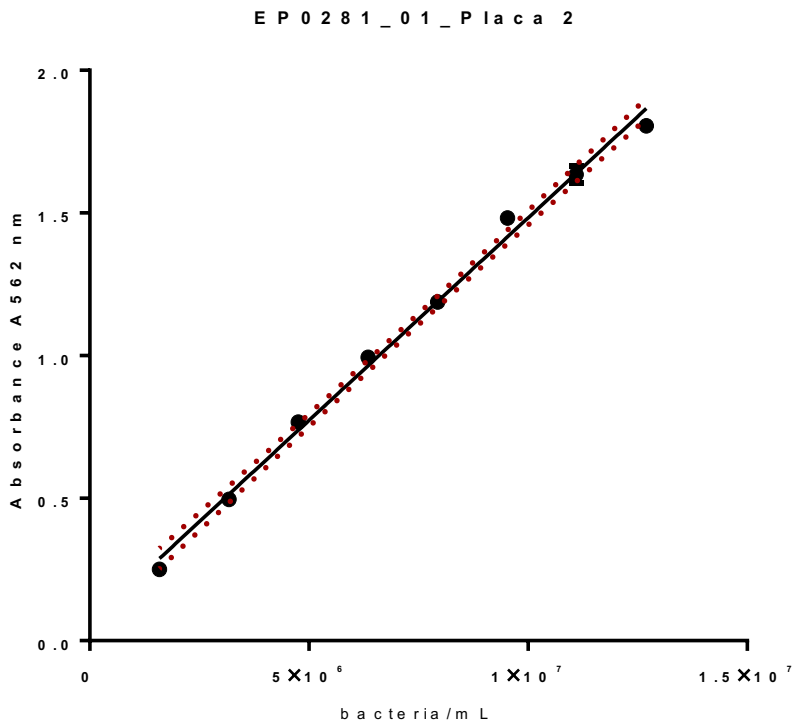
bacteria/mL	OD		
X	Y1	Y2	Y3
1.27e+007	1.770	1.805	1.842
1.11e+007	1.635	1.685	1.584
9.53e+006	1.476	1.499	1.470
7.94e+006	1.200	1.164	1.200
6.35e+006	0.971	1.018	0.991
4.76e+006	0.780	0.735	0.783
3.18e+006	0.513	0.504	0.470
1.59e+006	0.243	0.253	0.253

Plate 3 (A2D1)

190620_Plate 3_Validación ELISA   105254   21/06/2019
EP0281_01   N.P.   Montse Plaza
A10659   105254
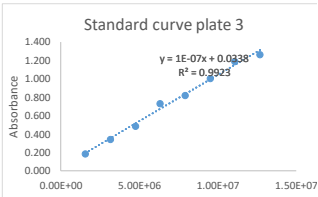
RAW data

	1	2	3	4	5	6	7	8	9	10	11	12
A	1.367	1.245	1.285	0.031	0.034	0.036	0.035	0.031	0.030	0.030	0.033	0.030
B	1.274	1.196	1.196	1.351	1.379	1.564	1.552	1.404	1.258	1.315	1.313	0.033
C	1.104	0.990	1.009	1.266	1.270	1.482	1.407	1.299	1.280	1.376	1.225	0.034
D	0.927	0.809	0.819	1.130	1.026	1.278	1.155	1.025	0.992	1.053	1.022	0.031
E	0.817	0.759	0.723	1.078	0.980	1.182	1.154	0.970	0.924	1.055	0.970	0.034
F	0.559	0.489	0.510	0.658	0.662	0.843	0.795	0.704	0.667	0.694	0.663	0.032
G	0.403	0.376	0.352	0.624	0.588	0.780	0.725	0.657	0.622	0.675	0.635	0.031
H	0.218	0.214	0.216	0.032	0.032	0.032	0.034	0.031	0.031	0.031	0.030	0.033

	Blank	0.0321	0.0018	6%

Blank subtraction

	1	2	3	4	5	6	7	8	9	10	11	12
A	1.335	1.213	1.253	N.P.	N.P.	N.P.	N.P.	N.P.	N.P.	N.P.	N.P.	N.P.
B	1.242	1.164	1.164	1.319	1.347	1.532	1.520	1.372	1.226	1.283	1.281	N.P.
C	1.072	0.958	0.977	1.234	1.238	1.450	1.375	1.267	1.248	1.344	1.193	N.P.
D	0.895	0.777	0.787	1.098	0.994	1.246	1.123	0.993	0.960	1.021	0.990	N.P.
E	0.785	0.727	0.691	1.046	0.948	1.150	1.122	0.938	0.892	1.023	0.938	N.P.
F	0.527	0.457	0.478	0.626	0.630	0.811	0.763	0.672	0.635	0.662	0.631	N.P.
G	0.371	0.344	0.320	0.592	0.556	0.748	0.693	0.625	0.590	0.643	0.603	N.P.
H	0.186	0.182	0.184	N.P.	N.P.	N.P.	N.P.	N.P.	N.P.	N.P.	N.P.	N.P.

Cálculo recta patron

	Mean	SD	CV%	Concentration (bact/mL)
C1	1.267	0.062	5%	1.27E+07
C2	1.190	0.045	4%	1.11E+07
C3	1.002	0.061	6%	9.53E+06
C4	0.820	0.065	8%	7.94E+06
C5	0.734	0.047	6%	6.35E+06
C6	0.487	0.036	7%	4.76E+06
C7	0.345	0.026	7%	3.18E+06
C8	0.184	0.002	1%	1.59E+06

Standard curve	
Axis intersection	0.034
Slope	0.000
R2	0.99

Standard curve plate 3

$y = 1E-07x + 0.0338$
$R^2 = 0.9923$

Method precision calculation

	Sample 1			Sample 2*			Sample 3			Sample 4		
	Mean	SD	CV%	Mean	SD	CV%	Mean	SD	CV%	Mean	SD	CV%
C1	1.284	0.057	4%	1.469	0.072	5%	1.278	0.065	5%	1.275	0.062	5%
C2	1.021	0.065	6%	1.160	0.059	5%	0.946	0.042	4%	0.993	0.040	4%
C3	0.601	0.035	6%	0.754	0.049	6%	0.630	0.034	5%	0.635	0.025	4%

Sample concentration calculation(bacterias/mL)

	Sample 1	Sample 2*	Sample 3	Sample 4
C1	1.24E+07	1.42E+07	1.23E+07	1.23E+07
C2	9.80E+06	1.12E+07	9.05E+06	9.52E+06
C3	5.63E+06	7.14E+06	5.92E+06	5.96E+06

Sample concentration calculation(bacterias/mL)

	Sample 1	Sample 2*	Sample 3	Sample 4
C1	1.76E+10	2.02E+10	1.75E+10	1.75E+10
C2	1.94E+10	2.22E+10	1.80E+10	1.89E+10
C3	1.86E+10	2.36E+10	1.96E+10	1.97E+10
Media	1.85E+10	2.20E+10	1.83E+10	1.87E+10
Desvest	9.30E+08	1.73E+09	1.09E+09	1.14E+09
CV%	5%	8%	6%	6%
Recovery	117%	139%	116%	118%

Specificity

Trehalose specificity	Sucrose specificity
Media	Media
0.032	0.033

Method precision

Media	Desvest	Varianza	CV%
1.85E+10	1.74E+09	3.63E+18	9%
limit CV %	Result		
15%	9%		

Linearity

R2		Residuales	CV% Recta		
Limit R2	Result		Limit CV	Reults	
0.98	0.99			5%	C1
				4%	C2
				6%	C3
			10%	8%	C4
				6%	C5
				7%	C6
				7%	C7
				1%	C8

Acuracy of the media of samples

Cncentración teórica	1.58E+10	Limit recovery	
		125%	1.98E+10
		75%	1.19E+10
Media of samples	Recovery		
1.85E+10	117%		

Sistem suitability

Plate 3 (A2D1)

EP0281_01_Placa 3

Nonlin fit of EP0281_01_Placa 3
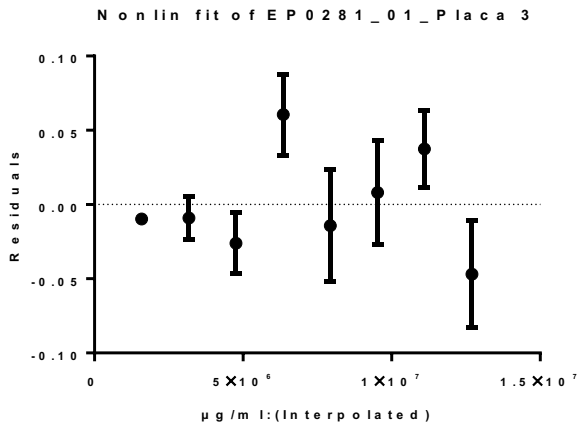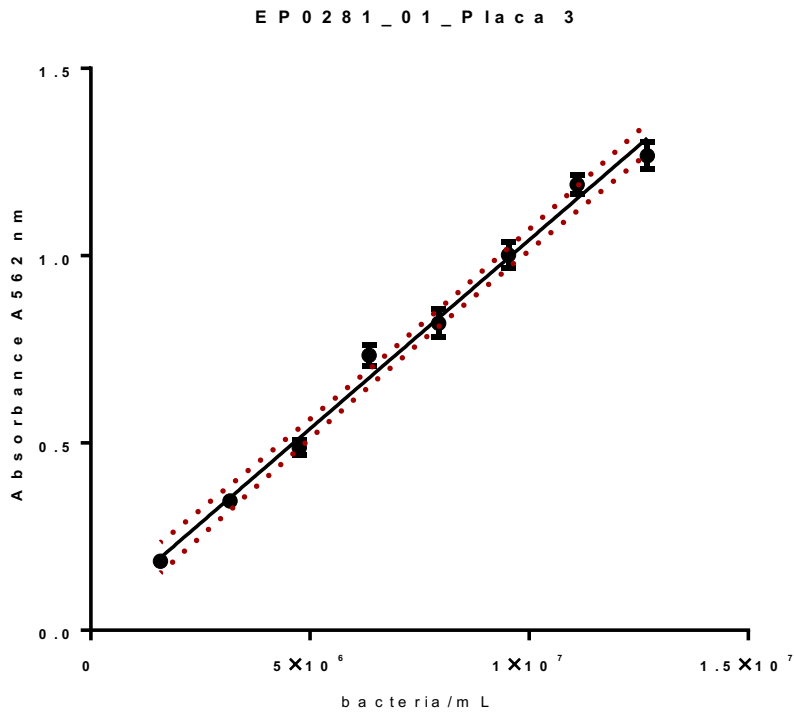
bacteria/mL	OD		
X	Y1	Y2	Y3
1.27e+007	1.335	1.213	1.253
1.11e+007	1.242	1.164	1.164
9.53e+006	1.072	0.958	0.977
7.94e+006	0.895	0.777	0.787
6.35e+006	0.785	0.727	0.691
4.76e+006	0.527	0.457	0.478
3.18e+006	0.371	0.344	0.320
1.59e+006	0.186	0.182	0.184

190522_Placa 4_Validación ELISA   105254   22/05/2019
EP0281_01   N.P.   Carlos Berrio
Analisis   105254

Plate 4 (A1:D2)

RAW data

	1	2	3	4	5	6	7	8	9	10	11	12
A	2.370	2.155	2.099	0.035	0.034	0.034	0.029	0.037	0.030	0.029	0.032	0.038
B	1.923	2.075	1.812	1.738	1.818	1.919	1.902	1.956	2.027	2.370	2.435	0.038
C	1.849	1.793	1.612	1.753	1.813	1.908	1.996	2.050	1.959	2.432	2.388	0.039
D	1.570	1.582	1.424	1.345	1.417	1.451	1.484	1.502	1.557	1.761	1.740	0.039
E	1.232	1.209	1.180	1.294	1.335	1.415	1.369	1.466	1.443	1.743	1.713	0.040
F	0.918	0.920	0.930	0.810	0.831	0.841	0.821	0.838	0.891	1.103	1.134	0.040
G	0.623	0.639	0.596	0.861	0.823	0.865	0.840	0.894	0.897	1.137	1.036	0.040
H	0.338	0.336	0.323	0.038	0.039	0.038	0.039	0.038	0.039	0.039	0.039	0.050

Blanco	0.0356	0.0038	11%

Blank subtraction

	1	2	3	4	5	6	7	8	9	10	11	12
A	2.334	2.119	2.063	N.P.	N.P.	N.P.	N.P.	N.P.	N.P.	N.P.	N.P.	N.P.
B	1.887	2.039	1.776	1.702	1.782	1.883	1.866	1.920	1.991	2.334	2.399	N.P.
C	1.813	1.757	1.576	1.717	1.777	1.872	1.960	2.014	1.923	2.396	2.352	N.P.
D	1.534	1.546	1.388	1.309	1.381	1.415	1.448	1.466	1.521	1.725	1.704	N.P.
E	1.196	1.173	1.144	1.258	1.299	1.379	1.333	1.430	1.407	1.707	1.677	N.P.
F	0.882	0.884	0.894	0.774	0.795	0.805	0.785	0.802	0.855	1.067	1.098	N.P.
G	0.587	0.603	0.560	0.825	0.787	0.829	0.804	0.858	0.861	1.101	1.000	N.P.
H	0.302	0.300	0.287	N.P.	N.P.	N.P.	N.P.	N.P.	N.P.	N.P.	N.P.	N.P.

Fit standard curve to least squares

	Mean	SD	CV%	Concentration (bact/mL)
C1	2.172	0.143	7%	1.27E+07
C2	1.901	0.132	7%	1.11E+07
C3	1.716	0.124	7%	9.53E+06
C4	1.490	0.088	6%	7.94E+06
C5	1.171	0.026	2%	6.35E+06
C6	0.887	0.006	1%	4.76E+06
C7	0.584	0.022	4%	3.18E+06
C8	0.297	0.008	3%	1.59E+06

Standard curve	
Axis intersection	0.071
Slope	0.000
R2	1.00

Standard curve plate 4

$R^2 = 0.9951$

Method precision calculation

	Sample 1			Sample 2			Sample 3			Sample 4		
	Media	Desvest	CV%	Media	Desvest	CV%	Media	Desvest	CV%	Media	Desvest	CV%
C1	1.745	0.041	2%	1.896	0.044	2%	1.962	0.048	2%	2.371	0.032	1%
C2	1.312	0.051	4%	1.394	0.049	4%	1.456	0.050	3%	1.704	0.020	1%
C3	0.796	0.022	3%	0.806	0.018	2%	0.844	0.028	3%	1.067	0.047	4%

Sample concentration calculation (bacteria/mL)

	Sample 1	Sample 2	Sample 3	Sample 4
C1	9.91E+06	1.08E+07	1.12E+07	1.36E+07
C2	7.35E+06	7.84E+06	8.20E+06	9.67E+06
C3	4.29E+06	4.35E+06	4.58E+06	5.90E+06

Sample concentration calculation (bacteria/mL)

	Sample 1	Sample 2	Sample 3	Sample 4
C1	1.40E+10	1.53E+10	1.59E+10	1.93E+10
C2	1.46E+10	1.55E+10	1.63E+10	1.92E+10
C3	1.42E+10	1.44E+10	1.51E+10	1.95E+10
Media	1.43E+10	1.51E+10	1.58E+10	1.93E+10
Desvest	2.77E+08	6.07E+08	5.73E+08	1.63E+08
CV%	2%	4%	4%	1%
Recovery	90%	95%	100%	122%

Specificity

Trehalose specificity	Sucrose specificity
Media	Media
0.039	0.043

Method precision

Media	Desvest	Varianza	CV%
1.61E+10	2.23E+09	4.21E+18	14%
		limit CV %	Result
		15%	14%

Linearity

R2		Residuales	CV% Recta		
Limit R2	Result		Limit CV	Reults	
0.98	1.00			7%	C1
				7%	C2
				7%	C3
			10%	6%	C4
				2%	C5
				1%	C6
				4%	C7
				3%	C8

Acuracy of the media of samples

Cncentración teórica	1.58E+10	Limit recovery	
		125%	1.98E+10
		75%	1.19E+10
Media of samples	Recovery		
1.61E+10	102%		

Sistem suitability

Plate 4 (A1D2)

E P 0 2 8 1 _ 0 1 _ P l a c a   4

N o n l i n   f i t   o f   E P 0 2 8 1 _ 0 1 _ P l a c a   4
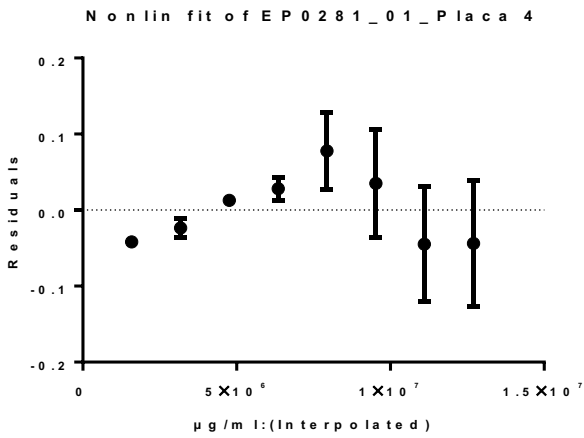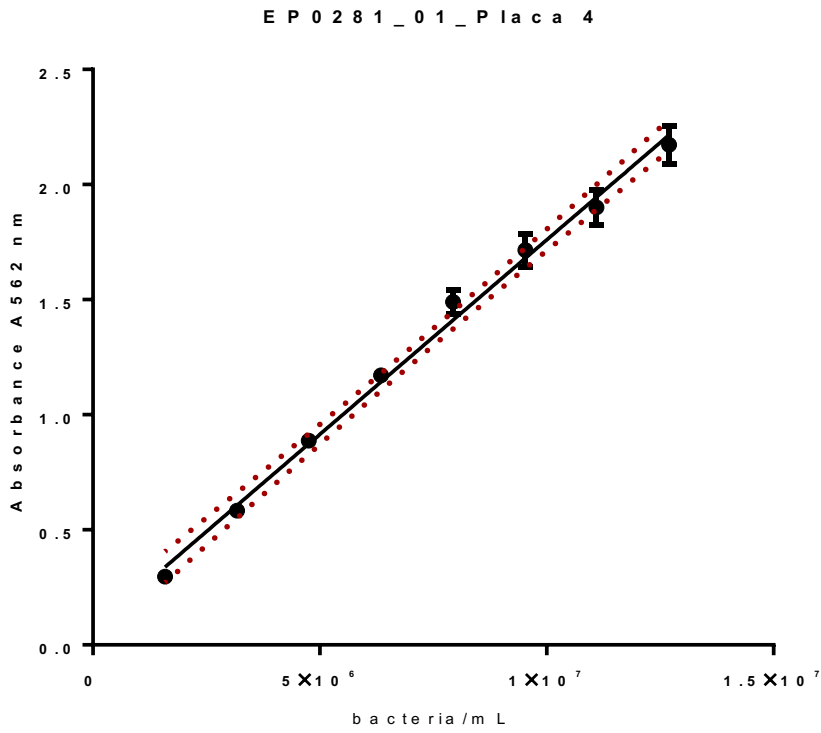
bacteria/mL	OD		
X	Y1	Y2	Y3
1.27e+007	2.334	2.119	2.063
1.11e+007	1.887	2.039	1.776
9.53e+006	1.813	1.757	1.576
7.94e+006	1.534	1.546	1.388
6.35e+006	1.196	1.173	1.144
4.76e+006	0.882	0.884	0.894
3.18e+006	0.587	0.603	0.560
1.59e+006	0.302	0.300	0.287

Plate 5

190514_EP0281_01_Placa 5   105254   15/05/2019
EP0281_01   N.P   Carlos Berrio
A10659   105254

RAW data	1	2	3	4	5	6	7	8	9	10	11	12
A	1.109	0.973	1.042	0.037	0.035	0.037	1.297	1.257	1.178	0.040	0.039	0.033
B	1.057	0.931	0.960	0.977	0.975	0.038	1.271	1.182	1.163	1.216	1.130	0.041
C	0.986	0.808	0.890	0.895	0.923	0.039	1.028	1.066	0.973	1.162	1.148	0.041
D	0.728	0.706	0.702	0.658	0.734	0.039	0.898	0.864	0.829	0.846	0.851	0.039
E	0.676	0.573	0.609	0.652	0.739	0.039	0.718	0.732	0.680	0.797	0.829	0.041
F	0.474	0.458	0.441	0.415	0.439	0.038	0.516	0.514	0.490	0.485	0.534	0.039
G	0.340	0.305	0.329	0.398	0.403	0.040	0.349	0.364	0.346	0.487	0.488	0.035
H	0.193	0.178	0.179	0.033	0.033	0.039	0.208	0.209	0.193	0.034	0.033	0.034

	Blanco	0.037	0.002	6%

Blank subtraction	1	2	3	4	5	6	7	8	9	10	11	12
A	1.072	0.936	1.005	N.P.	N.P.	N.P.	1.260	1.220	1.141	N.P.	N.P.	N.P.
B	1.020	0.894	0.923	0.940	0.938	N.P.	1.234	1.145	1.126	1.179	1.093	N.P.
C	0.949	0.771	0.853	0.858	0.886	N.P.	0.991	1.029	0.936	1.125	1.111	N.P.
D	0.691	0.669	0.665	0.621	0.697	N.P.	0.861	0.827	0.792	0.809	0.814	N.P.
E	0.639	0.536	0.572	0.615	0.702	N.P.	0.681	0.695	0.643	0.760	0.792	N.P.
F	0.437	0.421	0.404	0.378	0.402	N.P.	0.479	0.477	0.453	0.448	0.497	N.P.
G	0.303	0.268	0.292	0.361	0.366	N.P.	0.312	0.327	0.309	0.450	0.451	N.P.
H	0.156	0.141	0.142	N.P.	N.P.	N.P.	0.171	0.172	0.156	N.P.	N.P.	N.P.

Standard curve

Recta patrón 7 minutos

	Mean	SD	CV%	Concentración (bact/mL)
C1	1.004	0.068	7%	1.27E+07
C2	0.945	0.066	7%	1.11E+07
C3	0.812	0.058	7%	9.53E+06
C4	0.675	0.014	2%	7.94E+06
C5	0.582	0.052	9%	6.35E+06
C6	0.420	0.017	4%	4.76E+06
C7	0.287	0.018	6%	3.18E+06
C8	0.146	0.008	6%	1.59E+06

Recta	
Axis intersection	0.043
Slope	0.000
R2	0.99

Recta patrón 9 minutos

	Mean	SD	CV%	Concentración (bact/mL)
C1	1.240	0.028	2%	1.27E+07
C2	1.168	0.058	5%	1.11E+07
C3	0.985	0.047	5%	9.53E+06
C4	0.826	0.035	4%	7.94E+06
C5	0.673	0.027	4%	6.35E+06
C6	0.469	0.014	3%	4.76E+06
C7	0.316	0.010	3%	3.18E+06
C8	0.166	0.009	5%	1.59E+06

Recta	
Axis intersection	0.008
Slope	0.000
R2	0.99

Standard curve plate 5 7 minutes — R² = 0.9931

Standard curve plate 5 9 minutes — R² = 0.9948

Sample analysis

	7 minutes			9 minutes		
	Mean	SD	CV%	Mean	SD	CV%
C1	0.905	0.040	4%	1.127	0.037	3%
C2	0.658	0.047	7%	0.793	0.024	3%
C3	0.376	0.018	5%	0.461	0.024	5%
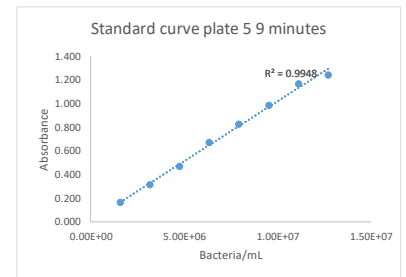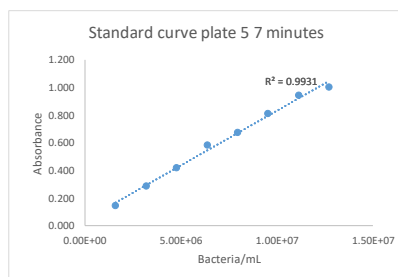
Sample concentration calculation		
	7 minutes	9 minutes
C1	1.09E+07	1.11E+07
C2	7.77E+06	7.77E+06
C3	4.21E+06	4.48E+06

Sample concentration calculation (bacteria/mL)		
	7 minutes	9 minutes
C1	1.54E+10	1.57E+10
C2	1.54E+10	1.54E+10
C3	1.39E+10	1.48E+10
Media	1.49E+10	1.53E+10
Desvest	8.67E+08	4.43E+08
CV%	6%	3%

Plate 5 recovery		
	7 minutes	9 minutes
Theoretical value	1.58E+10	1.58E+10
Experimental value	1.49E+10	1.53E+10
Recovery	94%	97%

Sistem suitability

E P 0 2 8 1 _ 0 1 _ P l a c a 5 a

N o n l i n f i t o f E P 0 2 8 1 _ 0 1 _ P l a c a 5 a
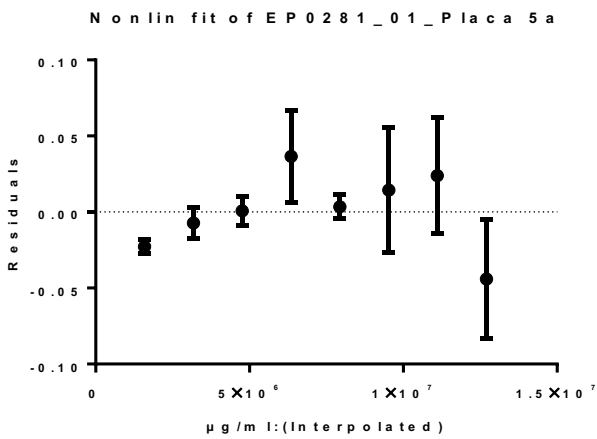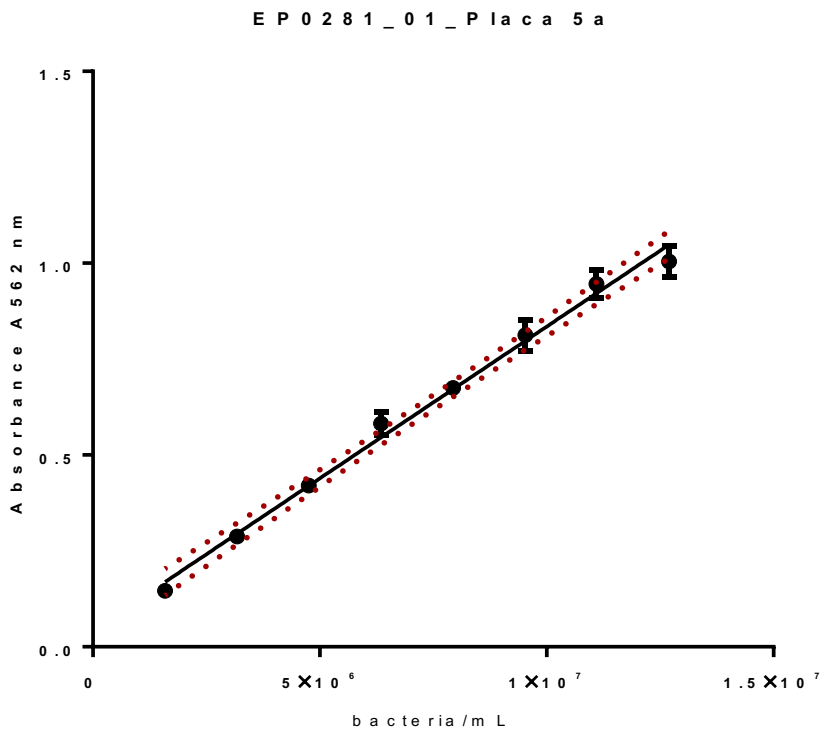
bacteria/mL	OD		
X	Y1	Y2	Y3
1.27e+007	1.072	0.936	1.005
1.11e+007	1.020	0.894	0.923
9.53e+006	~~0.949~~	0.771	0.853
7.94e+006	0.691	0.669	0.665
6.35e+006	0.639	0.536	0.572
4.76e+006	0.437	0.421	0.404
3.18e+006	0.303	0.268	0.292
1.59e+006	0.156	0.141	0.142

E P 0 2 8 1 _ 0 1 _ P l a c a 5 b
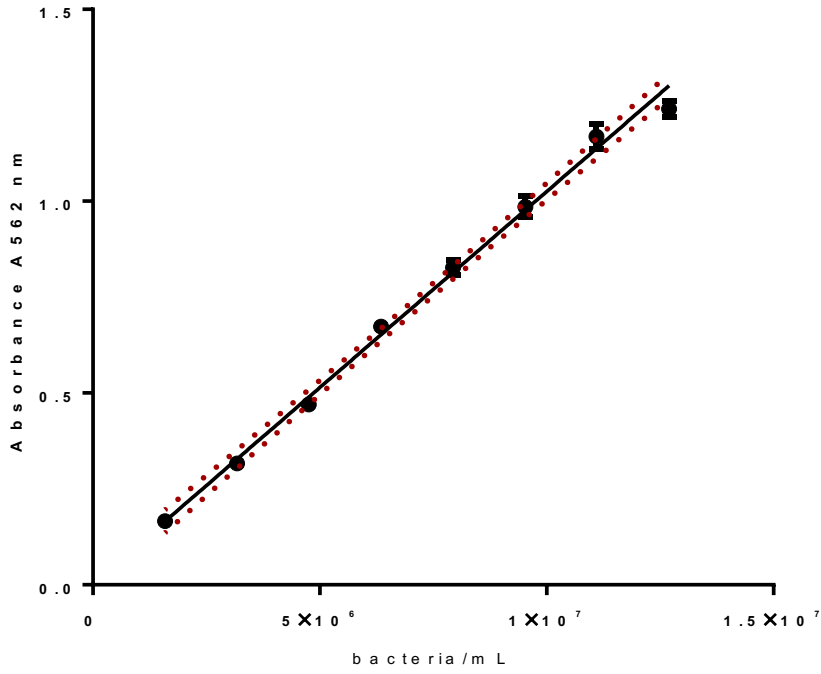
N o n l i n f i t o f E P 0 2 8 1 _ 0 1 _ P l a c a 5 b
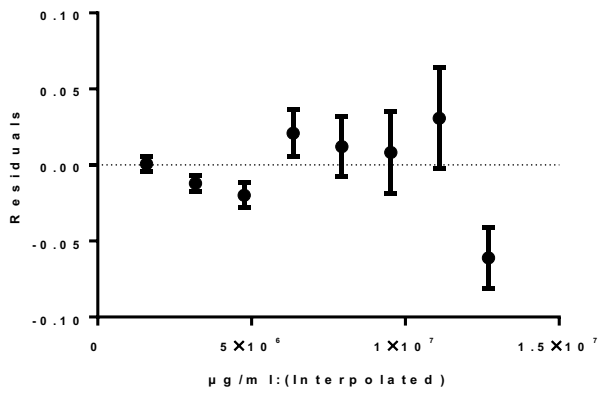
bacteria/mL	OD		
X	Y1	Y2	Y3
1.27e+007	1.260	1.220	1.141
1.11e+007	1.234	1.145	1.126
9.53e+006	0.991	1.029	0.936
7.94e+006	0.861	0.827	0.792
6.35e+006	0.681	0.695	0.643
4.76e+006	0.479	0.477	0.453
3.18e+006	0.312	0.327	0.309
1.59e+006	0.171	0.172	0.156

Plate 6

190514_EP0281_01_Placa 6	105254	15/05/2019
EP0281_01	N.P	Carlos Berrio
A10659	105254	

RAW data

	1	2	3	4	5	6	7	8	9	10	11	12
A	0.964	0.957	0.974	0.035	0.034	0.038	0.670	0.676	0.666	0.036	0.037	0.037
B	0.896	0.897	0.904	1.048	0.959	0.038	0.688	0.616	0.634	0.721	0.789	0.038
C	0.799	0.783	0.737	1.007	1.012	0.038	0.569	0.539	0.553	0.739	0.785	0.037
D	0.709	0.644	0.655	0.760	0.737	0.038	0.470	0.496	0.476	0.538	0.621	0.038
E	0.542	0.524	0.537	0.729	0.693	0.038	0.367	0.388	0.364	0.549	0.641	0.037
F	0.411	0.391	0.430	0.456	0.422	0.038	0.300	0.322	0.287	0.356	0.360	0.038
G	0.249	0.248	0.254	0.437	0.443	0.037	0.194	0.205	0.190	0.329	0.358	0.038
H	0.159	0.154	0.153	0.038	0.039	0.037	0.117	0.118	0.117	0.033	0.030	0.032

Blanco	0.037	0.002	5%

Blank subtraction

	1	2	3	4	5	6	7	8	9	10	11	12
A	0.927	0.920	0.937	N.P.	N.P.	N.P.	0.633	0.639	0.629	N.P.	N.P.	N.P.
B	0.859	0.860	0.867	1.011	0.922	N.P.	0.651	0.579	0.597	0.684	0.752	N.P.
C	0.762	0.746	0.700	0.970	0.975	N.P.	0.532	0.502	0.516	0.702	0.748	N.P.
D	0.672	0.607	0.618	0.723	0.700	N.P.	0.433	0.459	0.439	0.501	0.584	N.P.
E	0.505	0.487	0.500	0.692	0.656	N.P.	0.330	0.351	0.327	0.512	0.604	N.P.
F	0.374	0.354	0.393	0.419	0.385	N.P.	0.263	0.285	0.250	0.319	0.323	N.P.
G	0.212	0.211	0.217	0.400	0.406	N.P.	0.157	0.168	0.153	0.292	0.321	N.P.
H	0.122	0.117	0.116	N.P.	N.P.	N.P.	0.080	0.081	0.080	N.P.	N.P.	N.P.

Standard curve

Recta patrón 7 minutos

	Mean	SD	CV%	Concentración (bact/mL)
C1	0.928	0.009	1%	1.27E+07
C2	0.862	0.004	1%	1.11E+07
C3	0.723	0.033	4%	9.53E+06
C4	0.633	0.035	5%	7.94E+06
C5	0.498	0.009	2%	6.35E+06
C6	0.374	0.020	5%	4.76E+06
C7	0.214	0.003	2%	3.18E+06
C8	0.119	0.003	3%	1.59E+06

Recta patrón 5 minutos

	Mean	SD	CV%	Concentración (bact/mL)
C1	0.636	0.004	1%	1.27E+07
C2	0.609	0.037	6%	1.11E+07
C3	0.517	0.015	3%	9.53E+06
C4	0.444	0.014	3%	7.94E+06
C5	0.336	0.013	4%	6.35E+06
C6	0.266	0.018	7%	4.76E+06
C7	0.160	0.008	5%	3.18E+06
C8	0.081	0.001	1%	1.59E+06

Recta	
Axis intersection	0.003
Slope	0.000
R2	0.99

Recta	
Axis intersection	0.006
Slope	0.000
R2	0.99

Standard curve Plate 6, 7 minutes

Standard curve plate 6, 5 minute
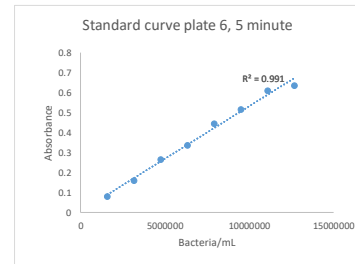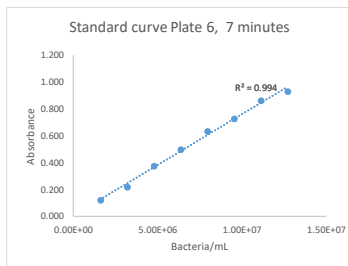
Sample analysis

	7 minutes			5 minutes		
	Mean	SD	CV%	Mean	SD	CV%
C1	0.970	0.037	4%	0.722	0.034	5%
C2	0.693	0.028	4%	0.551	0.051	9%
C3	0.403	0.014	4%	0.314	0.015	5%

Sample concentration		
	7 minutes	5 minutes
C1	1.28E+07	1.36E+07
C2	9.12E+06	1.04E+07
C3	5.28E+06	5.86E+06

Sample concentration		
	7 minutes	5 minutes
C1	1.81E+10	1.93E+10
C2	1.81E+10	2.06E+10
C3	1.75E+10	1.94E+10
Media	1.79E+10	1.98E+10
Desvest	3.64E+08	7.05E+08
CV%	2%	4%

Plate 6 recovery		
	7 minutes	5 minutes
Theoretical value	1.58E+10	1.58E+10
Experimental value	1.79E+10	1.98E+10
Recovery	113%	125%

Sistem suitability

	Resultado	Conforme
1. r2 coeficiente de determinación de Pearson ≥ 0.98. Recta 7 minutos	0.99	Conforme
2. r2 coeficiente de determinación de Pearson ≥ 0.98. Recta 9 minutos	0.99	Conforme
3. Recta estándar realizada con mínimo 6 puntos. No pueden despreciarse dos valores consecutivos. 7 minutos	8	Confome
4. Recta estándar realizada con mínimo 6 puntos. No pueden despreciarse dos valores consecutivos. 9 minutos	8	Confome
5. CV Sample 7 minutos ≤ 10%	2%	Conforme
6. CV Sample 9 minutos ≤ 10%	4%	Conforme
7. Recovery of 7 minutes	113%	Conforme
8. Recovery of 9 minutes	125%	Conforme

E P 0 2 8 1 _ 0 1 _ P l a c a 6 a
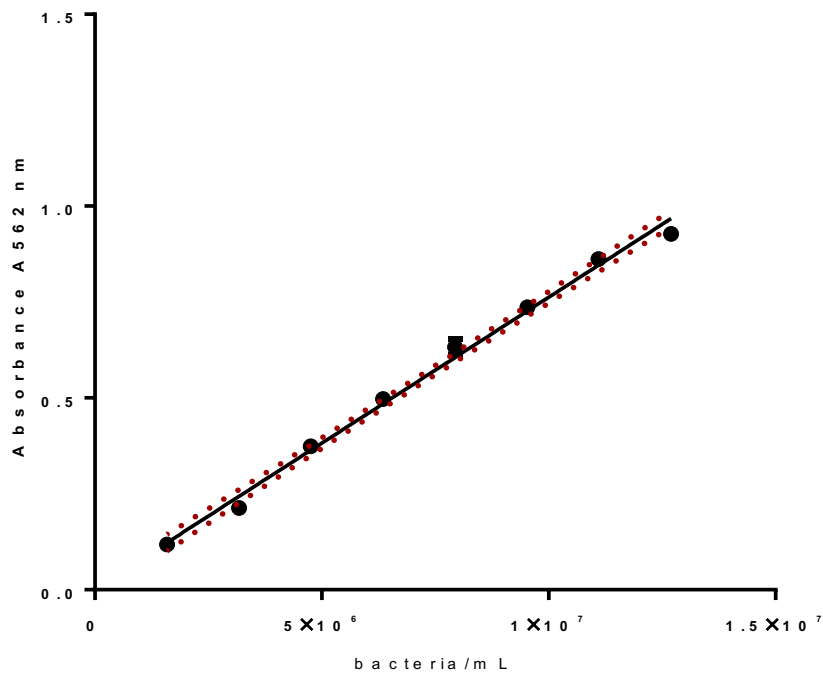
N o n l i n fit o f E P 0 2 8 1 _ 0 1 _ P l a c a 6 a
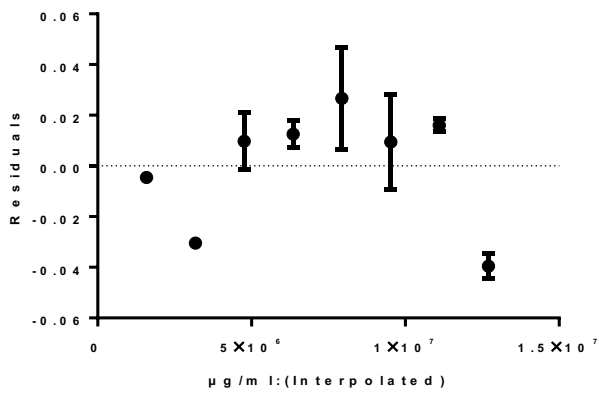
bacteria/mL	OD		
X	Y1	Y2	Y3
1.27e+007	0.927	0.920	0.937
1.11e+007	0.859	0.860	0.867
9.53e+006	0.762	0.746	0.700
7.94e+006	0.672	0.607	0.618
6.35e+006	0.505	0.487	0.500
4.76e+006	0.374	0.354	0.393
3.18e+006	0.212	0.211	0.217
1.59e+006	0.122	0.117	0.116

E P 0 2 8 1 _ 0 1 _ P l a c a 6 b
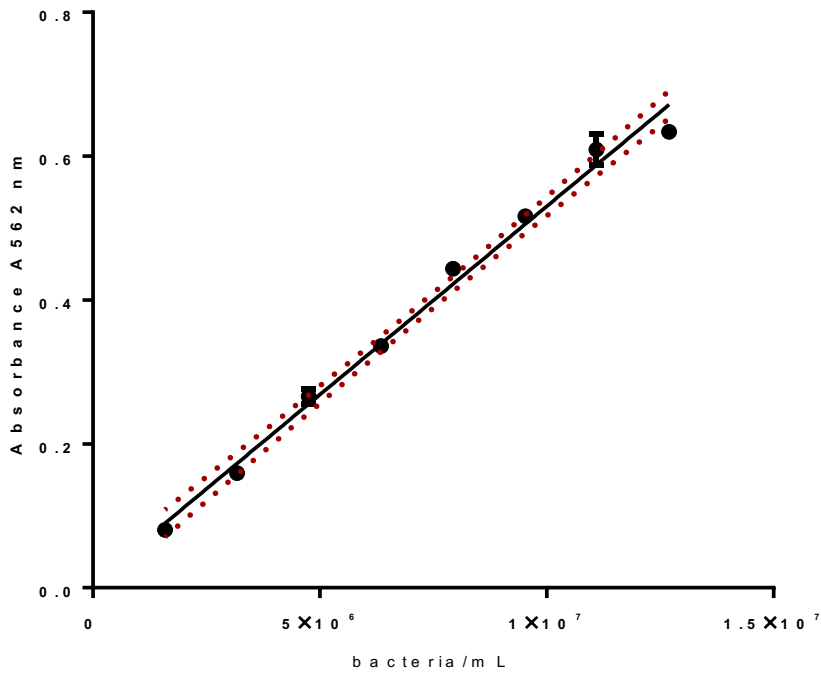
N o n l i n f i t o f E P 0 2 8 1 _ 0 1 _ P l a c a 6 b
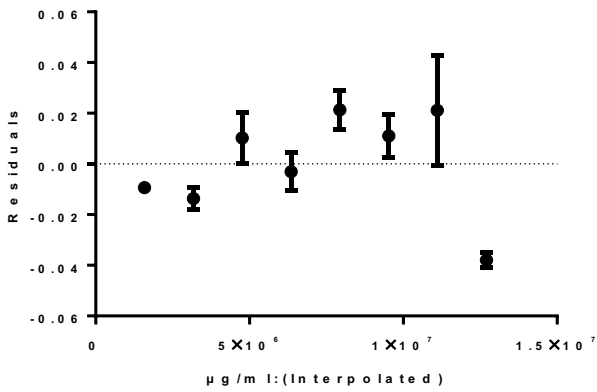
bacteria/mL	OD		
X	Y1	Y2	Y3
1.27e+007	0.633	0.639	0.629
1.11e+007	0.651	0.579	0.597
9.53e+006	0.532	0.502	0.516
7.94e+006	0.433	0.459	0.439
6.35e+006	0.330	0.351	0.327
4.76e+006	0.263	0.285	0.250
3.18e+006	0.157	0.168	0.153
1.59e+006	0.080	0.081	0.080

µBCA Validation

Plate 1

105254   Fecha   16/07/2019

RAW DATA

0.639	0.634	0.654	0.421	0.419	0.281	0.664	0.664	0.668	0.112	0.115	0.525
0.580	0.577	0.569	0.422	0.420	0.281	0.482	0.478	0.487	0.113	0.116	0.537
0.541	0.542	0.531	0.418	0.414	0.283	0.439	0.446	0.443	0.113	0.117	0.552
0.457	0.461	0.453	0.417	0.418	0.283	0.411	0.421	0.403	0.112	0.118	0.524
0.381	0.387	0.381	0.415	0.286	0.288	0.381	0.389	0.377	0.116	0.119	0.539
0.322	0.323	0.322	0.415	0.282	0.290	0.330	0.323	0.315	0.113	0.114	0.541
0.258	0.261	0.259	0.425	0.279	0.286	0.281	0.291	0.279	0.114	0.119	0.542
0.190	0.187	0.187	0.428	0.284	0.286	0.242	0.230	0.230	0.117	0.118	0.538

	Media	Desvest	CV%
Blank	0.114	0.00183225	2%

Rest the blank to absorbances

0.525	0.520	0.540	0.307	0.305	0.167	0.550	0.550	0.554	N.P.	N.P.	0.411
0.466	0.463	0.455	0.308	0.306	0.167	0.368	0.364	0.373	N.P.	N.P.	0.423
0.427	0.428	0.417	0.304	0.300	0.169	0.325	0.332	0.329	N.P.	N.P.	0.438
0.343	0.347	0.339	0.303	0.304	0.169	0.297	0.307	0.289	N.P.	N.P.	0.410
0.267	0.273	0.267	0.301	0.172	0.174	0.267	0.275	0.263	N.P.	N.P.	0.425
0.208	0.209	0.208	0.301	0.168	0.176	0.216	0.209	0.201	N.P.	N.P.	0.427
0.144	0.147	0.145	0.311	0.165	0.172	0.167	0.177	0.165	N.P.	N.P.	0.428
0.076	0.073	0.073	0.314	0.170	0.172	0.128	0.116	0.116	N.P.	N.P.	0.424

Estándar curve

Strandard curve

µg/mL proteina	Media	Desvest	CV%
32	0.529	0.010	2%
28	0.462	0.006	1%
24	0.424	0.006	1%
20	0.343	0.004	1%
16	0.269	0.003	1%
12	0.209	0.001	0%
8	0.146	0.002	1%
4	0.074	0.002	2%

Sandar curve

Axis intesection	0.01
Slope	0.02
R2	1.00

BSA Standard curve plate 1 µBCA

R² = 0.9969

VXD-001 curve
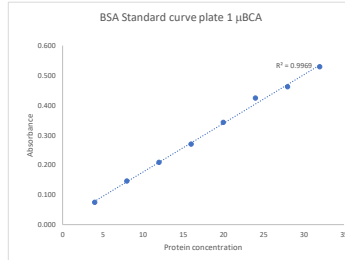
VXD-001 curve

Concentración API	Media	Desvest	CV%
1.00E+08	0.552	0.002	0%
6.25E+07	0.369	0.005	1%
5.47E+07	0.329	0.004	1%
4.69E+07	0.298	0.009	3%
3.91E+07	0.269	0.006	2%
3.13E+07	0.209	0.008	4%
2.34E+07	0.170	0.006	4%
1.56E+07	0.120	0.007	6%

VXD-001 curve

Intersección eje	0.07
Pendiente	0.00
R2	1.00

Linearity sample VXD-001 µBCA

R² = 0.9954
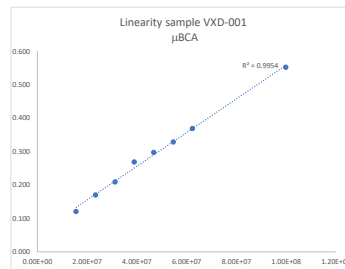
Sample analisis

	Instrumental precision				Passing the samples though standard curve			
	Media	Desvest	CV%	Concentración		µg/mL	bact/mL	µg/mL teoricos
C1	0.31	0.00	1%	5.00E+07	C1	17.9	5.00E+07	20.25
C2	0.17	0.00	2%	2.50E+07	C2	9.6	2.50E+07	10.12

Paso de la muestra por la recta			µg/mL calculation		Normalización 1E+09
C1	5644		Promedio	5854	371
C2	6065		Desvest	298	
			CV%	5%	

Sistem suitability

	Promedio	Desviación estandar	CV			Concentración experimental µg/mL	Concentración teórica µg/mL	
Control QC3	0.424	0.009	2%		Control QC3	25.1	24.0	

Specificity

Blanco NaCl				Blanco Trehalosa				Blanco Sacarosa		
Media OD	Desviación estandar	CV%		Media OD	Desviación estandar	CV%		Media OD	Desviación estandar	CV%
0.114	0.002	2%		0.117	0.001	1%		0.118	0.002	2%

Sistem suitability

	Resultado	Conforme
1. OD562 NaCl 0.9% ≤ 0.15	0.11	Conforme
2. OD562 Blanco trehalosa ≤ 0.15	0.12	Conforme
3. OD562 Blanco sacarosa ≤ 0.15	0.12	Conforme
4. r2 coeficiente de determinación de Pearson estandar ≥ 0.98.	1.00	Conforme
5. r2 coeficiente de determinación de Pearson muestra ≥ 0.98.	1.00	Conforme
6. CV maximo recta patrón≤ 10%	2%	Conforme
7. CV maximo recta muestra ≤ 10%	6%	Conforme
8. Recta estándar realizada con mínimo 6 puntos. No pueden despreciarse dos valores consecutivos.	8	Conforme
9. Recta estándar muestra con mínimo 6 puntos. No pueden despreciarse dos valores consecutivos.	8	Conforme
10. CV Intrumental precision C1 ≤ 10%	1%	Conforme
11. CV Intrumental precision C2 ≤ 10%	2%	Conforme
12. Instrumental precisión C1, C2 ≤ 10%	5%	Conforme
13. Sistem suitability ≥ 20.4 µg/mL y ≤ 27.6 µg/mL	25.1	Conforme

Plate 1 BSA linearity

	μg/mL	Standard curve linearity		
	X	Mean	SD	N
C1	32.00	0.530000	0.010000	3
C2	28.00	0.460000	0.010000	3
C3	24.00	0.420000	0.010000	3
C4	20.00	0.340000	0.000000	3
C5	16.00	0.270000	0.000000	3
C6	12.00	0.210000	0.000000	3
C7	8.00	0.150000	0.000000	3
C8	4.00	0.070000	0.000000	3

Standard curve BSA
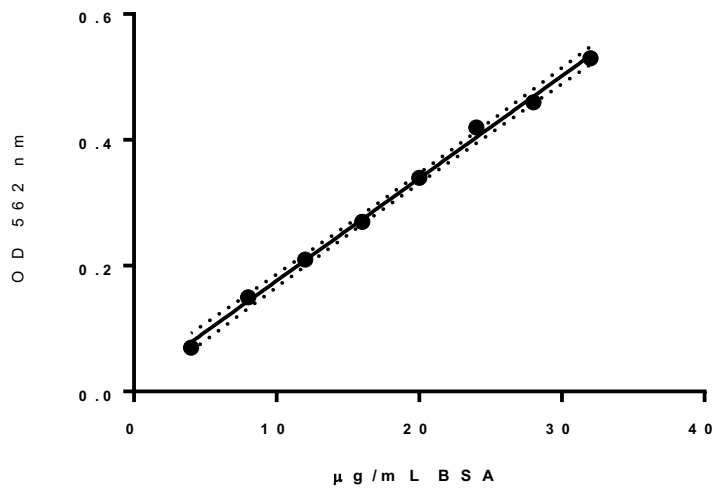
Residuals of Standard curve
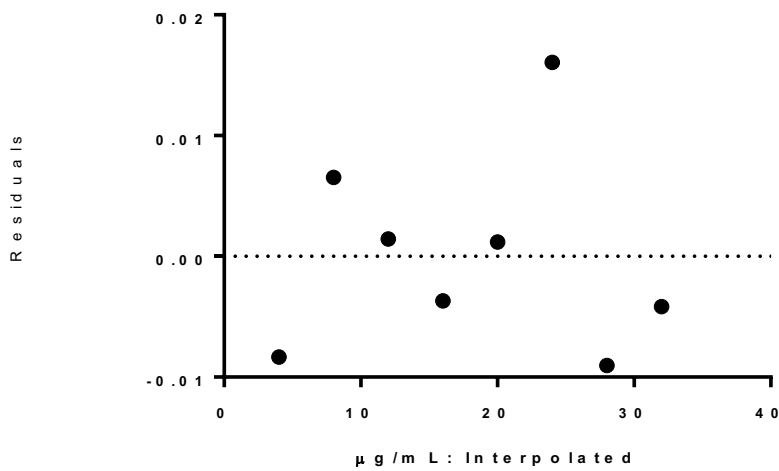
Plate 1 VXD-001 linearity

	Bacteria/mL	VXD-001 Linearity		
	X	Mean	SD	N
C1	1.00e+008	0.550000	0.000000	3
C2	6.25e+007	0.370000	0.000000	3
C3	5.47e+007	0.330000	0.000000	3
C4	4.69e+007	0.300000	0.010000	3
C5	3.91e+007	0.270000	0.010000	3
C6	3.13e+007	0.210000	0.010000	3
C7	2.34e+007	0.170000	0.010000	3
C8	1.56e+007	0.120000	0.010000	3

V X D - 0 0 1   L i n e a r i t y

R e s i d u a l s   o f   S t a n d a r d   c u r v e

Plate 2 (A1D1) 1.5 h

| | 105254 | | | | | | Fecha | 16/07/2019 |
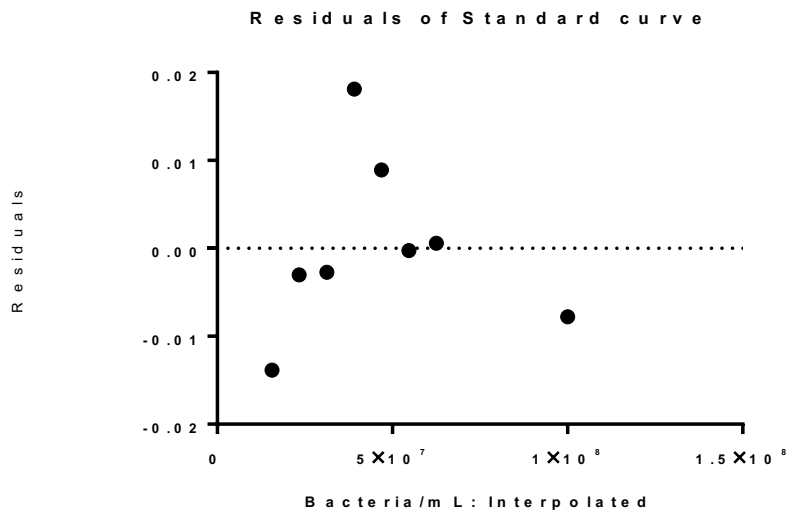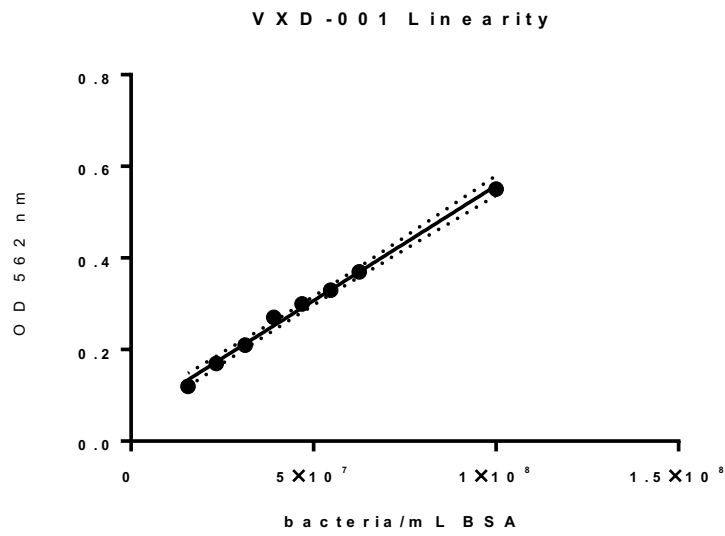
RAW DATA

0.560	0.555	0.557	0.101	0.101	0.104	0.102	0.105	0.104	0.107	0.105	0.492
0.516	0.515	0.522	0.367	0.384	0.379	0.382	0.381	0.384	0.42	0.418	0.495
0.458	0.451	0.455	0.241	0.253	0.248	0.257	0.257	0.261	0.418	0.409	0.513
0.402	0.403	0.406	0.376	0.373	0.388	0.372	0.376	0.381	0.362	0.366	0.485
0.348	0.346	0.348	0.245	0.248	0.255	0.256	0.259	0.261	0.364	0.367	0.481
0.293	0.289	0.289	0.371	0.371	0.390	0.382	0.374	0.382	0.312	0.314	0.499
0.240	0.235	0.240	0.256	0.251	0.259	0.255	0.261	0.257	0.318	0.313	0.5
0.177	0.176	0.174	0.104	0.107	0.111	0.110	0.109	0.107	0.109	0.107	0.503

	Media	Desviación estandar	CV%
Blanco	0.106	0.003	3%

Absorbancias

µg/mL proteina												
32	0.454	0.449	0.451	N.P.	N.P.	N.P.	N.P.	N.P.	N.P.	N.P.	N.P.	0.386
28	0.410	0.409	0.416	0.261	0.278	0.273	0.276	0.275	0.278	0.314	0.312	0.389
24	0.352	0.345	0.349	0.135	0.147	0.142	0.151	0.151	0.155	0.312	0.303	0.407
20	0.296	0.297	0.300	0.270	0.267	0.282	0.266	0.270	0.275	0.256	0.260	0.379
16	0.242	0.240	0.242	0.139	0.142	0.149	0.150	0.153	0.155	0.258	0.261	0.375
12	0.187	0.183	0.183	0.265	0.265	0.284	0.276	0.268	0.276	0.206	0.208	0.393
8	0.134	0.129	0.134	0.150	0.145	0.153	0.149	0.155	0.151	0.212	0.207	0.394
4	0.071	0.070	0.068	N.P.	N.P.	N.P.	N.P.	N.P.	N.P.	N.P.	N.P.	0.397

Recta patrón

RP				Recta	
Media	Desvest	CV%		Intersección eje	0.02
0.452	0.003	1%		Pendiente	0.01
0.412	0.004	1%		R2	1.00
0.349	0.004	1%			
0.298	0.002	1%			
0.242	0.001	0%			
0.185	0.002	1%			
0.133	0.003	2%			
0.070	0.002	2%			

Standard curve plate 2 1.5h µBCA

$R^2 = 0.9987$

Análisis muestras

Sample 1

	Media	Desvest	CV%	Concentración
C1	0.27	0.01	2	5.00E+07
C2	0.14	0.01	4	2.50E+07

Sample 1

	µg/mL	bact/mL	µg/mL teóricos
C1	18.0	5.00E+07	20.25
C2	9.0	2.50E+07	10.12

Sample 2

	Media	Desvest	CV%	Concentración
C1	0.28	0.01	2	5.00E+07
C2	0.15	0.00	3	2.50E+07

Sample 2

	µg/mL	bact/mL	µg/mL teóricos
C1	18.7	5.00E+07	20.25
C2	9.4	2.50E+07	10.12

Sample 3

	Media	Desvest	CV%	Concentración
C1	0.27	0.00	1	5.00E+07
C2	0.15	0.00	1	2.50E+07

Sample 3

	µg/mL	bact/mL	µg/mL teóricos
C1	18.5	5.00E+07	20.25
C2	9.7	2.50E+07	10.12

Paso por la recta de las muestras

	Sample 1	Sample 2	Sample 3
C1	5682	5877	5819
C2	5649	5924	6123

Concentración proteica en 1.58E+10 bacterias/mL

	Sample 1	Sample 2	Sample 3
Promedio	5665	5900	5971
Desvest	23.0	33.8	214.7
CV%	0%	1%	4%

Media muestras	Desviacion estandar	Varianza	CV%
5846	160	25591	3%

Normalización 1E+09 bacterias

Sample 1	Sample 2	Sample 3
358.6	373.4	377.9

Media	Desviación estandar	CV%	Varianza
370.0	10.12	3%	103

Sistem suitability

	Promedio	Desviación estandar	CV			Concentración experimental µg/mL	Concentración teórica µg/mL	
Control QC3	0.390	0.010	3%		Control QC3	26.9	24.0	

Sistem suitability

	Resultado	Conforme
1. OD562 NaCl 0.9% ≤ 0.15	0.11	Conforme
2. r2 coeficiente de determinación de Pearson estandar ≥ 0.98.	1.00	Conforme
3. Recta estándar realizada con mínimo 6 puntos. No pueden despreciarse dos valores consecutivos.	8	Confome
4. CV máximo de los distintos puntos de la recta ≤ 10%	2%	Conforme
5. Method precision ≤ 15%	3%	Conforme
6. Sistem suitability ≤ 27.6 µg/mL y ≥ 20.4 µg/mL	26.9	Conforme

Plate 2 (A1D1) 2 h

BP0261_04   Condición   105254 / 2 horas revelado   Fecha 16/07/2019   Carlos Berrio

RAW DATA

0.614	0.610	0.613	0.108	0.109	0.112	0.110	0.113	0.112	0.114	0.113	0.537
0.567	0.567	0.576	0.407	0.425	0.420	0.424	0.422	0.425	0.464	0.46	0.544
0.503	0.498	0.504	0.267	0.280	0.275	0.285	0.284	0.289	0.463	0.451	0.565
0.443	0.445	0.449	0.418	0.414	0.431	0.412	0.418	0.423	0.401	0.404	0.537
0.383	0.381	0.385	0.271	0.274	0.282	0.283	0.287	0.289	0.403	0.405	0.525
0.322	0.318	0.318	0.412	0.411	0.432	0.424	0.415	0.423	0.345	0.346	0.547
0.262	0.257	0.265	0.282	0.276	0.285	0.282	0.287	0.283	0.351	0.344	0.547
0.192	0.192	0.190	0.112	0.114	0.119	0.119	0.116	0.115	0.117	0.114	0.548

	Media	Desviación estandar	CV%
Blanco	0.114	0.003182635	3%

Absorbancias

µg/mL proteina												
32	0.500	0.496	0.499	N.P.	N.P.	N.P.	N.P.	N.P.	N.P.	N.P.	N.P.	0.423
28	0.453	0.453	0.462	0.293	0.311	0.306	0.310	0.308	0.311	0.350	0.346	0.430
24	0.389	0.384	0.390	0.153	0.166	0.161	0.171	0.170	0.175	0.349	0.337	0.451
20	0.329	0.331	0.335	0.304	0.300	0.317	0.298	0.304	0.309	0.287	0.290	0.423
16	0.269	0.267	0.271	0.157	0.160	0.168	0.169	0.173	0.175	0.289	0.291	0.411
12	0.208	0.204	0.204	0.298	0.297	0.318	0.310	0.301	0.309	0.231	0.232	0.433
8	0.148	0.143	0.151	0.168	0.162	0.171	0.168	0.173	0.169	0.237	0.230	0.433
4	0.078	0.078	0.076	N.P.	N.P.	N.P.	N.P.	N.P.	N.P.	N.P.	N.P.	0.434

Recta patrón

RP				Recta	
Media	Desvest	CV%		Intersección eje	0.024
0.50	0.00	0%		Pendiente	0.015
0.46	0.01	1%		R2	1.00
0.39	0.00	1%			
0.33	0.00	1%			
0.27	0.00	1%			
0.21	0.00	1%			
0.15	0.00	3%			
0.08	0.00	1%			

Standard curve plate 2 2 h µBCA — R² = 0.9984

Análisis muestras

Sample 1

	Media	Desvest	CV%	Concentración			µg/mL	bact/mL	µg/mL teóricos
C1	0.30	0.01	2	5.00E+07		C1	18.3	5.00E+07	20.25
C2	0.16	0.01	3	2.50E+07		C2	9.1	2.50E+07	10.12

Sample 2

	Media	Desvest	CV%	Concentración			µg/mL	bact/mL	µg/mL teóricos
C1	0.31	0.01	2	5.00E+07		C1	18.9	5.00E+07	20.25
C2	0.17	0.00	2	2.50E+07		C2	9.5	2.50E+07	10.12

Sample 3

	Media	Desvest	CV%	Concentración			µg/mL	bact/mL	µg/mL teóricos
C1	0.31	0.00	1	5.00E+07		C1	18.7	5.00E+07	20.25
C2	0.17	0.00	1	2.50E+07		C2	9.8	2.50E+07	10.12

Paso por la recta de las muestras / Concentración proteica en 1.58E+10 bacterias/mL

	Sample 1	Sample 2	Sample 3			Sample 1	Sample 2	Sample 3
C1	5751	5944	5885		Promedio	5731	5973	6037
C2	5712	6002	6189		Desvest	27	41	215
					CV%	0%	1%	4%

Media muestras	Desviación estandar	Varianza	CV%
5914	161	26063	3%

Normalización 1E+09 bacterias

Sample 1	Sample 2	Sample 3
362.7	378.1	382.1

Media	Desviación estandar	CV%	Varianza
374.3	10.22	3%	104

Sistem suitability

	Promedio	Desviación estandar	CV			Concentración experimental µg/mL	Concentración teórica
Control QC3	0.430	0.011548036	3%		Control QC3	26.8	24,0 µg/mL

Accuracy

Media OD accuracy / OD pasada por la recta accuracy

	Media	Desvest	CV%	Concentración			µg/mL	bact/mL
C1	0.35	0.01	2	2.50E+07		C1	21.2	2.50E+07
C2	0.29	0.00	1	2.50E+07		C2	17.5	2.50E+07
C3	0.23	0.00	1	2.50E+07		C3	13.8	2.50E+07

Recovery (se resta concentración experimental)

	Concentración experimental	Concentración teórica	Recovery
C1	11.7	12	98%
C2	8.0	8	101%
C3	4.3	4	108%

Sistem suitability

	Resultado	Conforme
1. OD562 NaCl 0.9% ≤ 0.15	0.11	Conforme
2. r2 coeficiente de determinación de Pearson estandar ≥ 0.98.	1.00	Conforme
3. Recta estándar realizada con mínimo 6 puntos. No pueden despreciarse dos valores consecutivos.	8	Conforme
4. Recovery 12 µg/mL	98%	Conforme
5. Recovery 8 µg/mL	101%	Conforme
6. Recovery 4 µg/mL	108%	Conforme
7. CV máximo de los distintos puntos de la recta ≤ 10%	3%	Conforme
8. Method precision ≤ 15%	3%	Conforme
9. Sistem suitability ≤ 27.6 µg/mL y ≥ 20.4 µg/mL	26.8	Conforme

Plate 2 (A1D1) 2.5 h
EP0281_04

		Condición	105254				Fecha	16/07/2019
			2.5 horas de revelado				Analista	Carlos Berrio

RAW DATA

0.651	0.647	0.650	0.112	0.113	0.115	0.114	0.116	0.116	0.118	0.116	0.566
0.601	0.599	0.610	0.431	0.452	0.445	0.449	0.446	0.450	0.49	0.487	0.576
0.534	0.526	0.534	0.283	0.297	0.291	0.302	0.300	0.306	0.49	0.477	0.593
0.470	0.471	0.475	0.443	0.439	0.457	0.438	0.443	0.449	0.424	0.428	0.563
0.405	0.403	0.407	0.287	0.290	0.299	0.300	0.304	0.305	0.427	0.429	0.553
0.341	0.336	0.337	0.436	0.436	0.458	0.450	0.439	0.447	0.365	0.365	0.575
0.277	0.272	0.280	0.298	0.292	0.302	0.298	0.303	0.299	0.371	0.364	0.576
0.203	0.203	0.199	0.116	0.118	0.123	0.123	0.120	0.118	0.121	0.119	0.576

	Media	Desviación estandar	CV%
Blanco	0.117	0.003263434	3%

Absorbancias

µg/mL proteina												
32	0.534	0.530	0.533	N.P.	N.P.	N.P.	N.P.	N.P.	N.P.	N.P.	N.P.	0.449
28	0.484	0.482	0.493	0.314	0.335	0.328	0.332	0.329	0.333	0.373	0.370	0.459
24	0.417	0.409	0.417	0.166	0.180	0.174	0.185	0.183	0.189	0.373	0.360	0.476
20	0.353	0.354	0.358	0.326	0.322	0.340	0.321	0.326	0.332	0.307	0.311	0.446
16	0.288	0.286	0.290	0.170	0.173	0.182	0.183	0.187	0.188	0.310	0.312	0.436
12	0.224	0.219	0.220	0.319	0.319	0.341	0.333	0.322	0.330	0.248	0.248	0.458
8	0.160	0.155	0.163	0.181	0.175	0.185	0.181	0.186	0.182	0.254	0.247	0.459
4	0.086	0.086	0.082	N.P.	N.P.	N.P.	N.P.	N.P.	N.P.	N.P.	N.P.	0.459

Recta patrón

RP				Recta	
Media	Desvest	CV%		Intersección eje	0.03
0.53	0.00	0%		Pendiente	0.02
0.49	0.01	1%		R2	1.00
0.41	0.00	1%			
0.35	0.00	1%			
0.29	0.00	1%			
0.22	0.00	1%			
0.16	0.00	3%			
0.08	0.00	3%			

Standard curve Plate 2 2.5 h µBCA — $R^2 = 0.9984$

Análisis muestras

Sample 1

	Media	Desvest	CV%	Concentración			µg/mL	bact/mL	µg/mL teóricos
C1	0.32	0.01	2	5.00E+07		C1	18.3	5.00E+07	20.25
C2	0.17	0.01	3	2.50E+07		C2	9.1	2.50E+07	10.12

Sample 2

	Media	Desvest	CV%	Concentración			µg/mL	bact/mL	µg/mL teóricos
C1	0.33	0.01	2	5.00E+07		C1	18.9	5.00E+07	20.25
C2	0.18	0.00	2	2.50E+07		C2	9.6	2.50E+07	10.12

Sample 3

	Media	Desvest	CV%	Concentración			µg/mL	bact/mL	µg/mL teóricos
C1	0.33	0.00	1	5.00E+07		C1	18.7	5.00E+07	20.25
C2	0.19	0.00	2	2.50E+07		C2	9.8	2.50E+07	10.12

Paso por la recta de las muestras

	Sample 1	Sample 2	Sample 3
C1	5765	5960	5885
C2	5732	6025	6188

Concentración proteica en 1.58E+10 bacterias/mL

	Sample 1	Sample 2	Sample 3
Promedio	5748	5993	6036
Desvest	23	46	214
CV%	0%	1%	4%

Media muestras	Desviacion estandar	Varianza	CV%
5926	155	24112	3%

Normalización 1E+09 bacterias

Sample 1	Sample 2	Sample 3
363.8	379.3	382.1

Media	Desviacion estandar	CV%	Varianza
375.0	9.83	3%	97

Sistem suitability

	Promedio	Desviación estandar	CV			Concentración experimental µg/mL	Concentración teórica
Control QC3	0.455	0.011804963	3%		Control QC3	26.5	24,0 µg/mL

Sistem suitability

	Resultado	Conforme
1. OD562 NaCl 0.9% ≤ 0.15	0.12	Conforme
2. r2 coeficiente de determinación de Pearson estandar ≥ 0.98.	1.00	Conforme
3. Recta estándar realizada con mínimo 6 puntos. No pueden despreciarse dos valores consecutivos.	8	Confome
4. CV máximo de los distintos puntos de la recta ≤ 10%	3%	Conforme
5. Method precision ≤ 15%	3%	Conforme
6. Sistem suitability ≤ 27.6 µg/mL y ≥ 20.4 µg/mL	26.5	Conforme

Plate 2 (A1D1) ANOVA robustness

ANOVA Robustness			
Data sets analyzed	A : 1,5 h	B : 2 h	C : 2,5 h

ANOVA summary	
F	0.3067
P value	0.7404
P value summary	ns
Significant diff. among means (P < 0.05)?	No
R square	0.03929

ANOVA robustness of plate 2

Plate 3 (A2D1)

	EP0281_04			Condición	105254 N.P.			Fecha Analista	17/07/2019 Carlos Berrio		
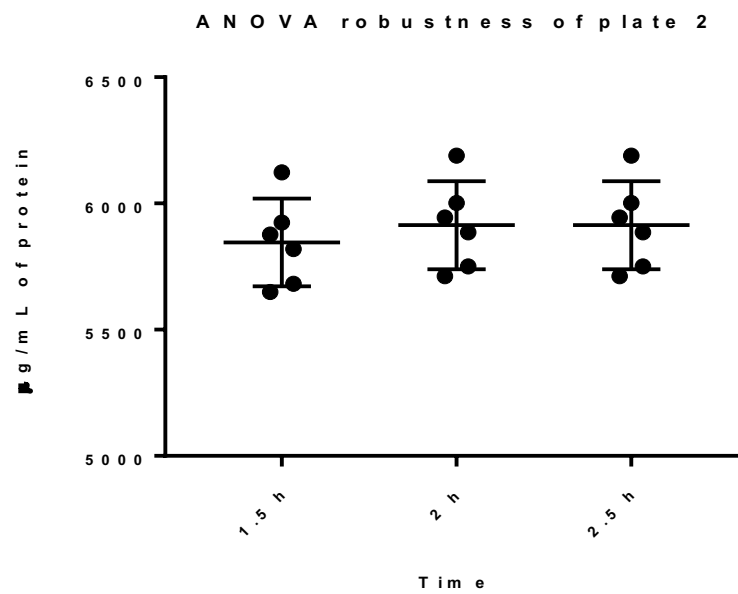
RAW DATA

0.569	0.593	0.587	0.105	0.106	0.101	0.104	0.109	0.106	0.107	0.107	0.483
0.545	0.538	0.542	0.429	0.430	0.416	0.435	0.411	0.436	0.475	0.474	0.506
0.486	0.492	0.503	0.273	0.284	0.280	0.278	0.277	0.284	0.462	0.466	0.529
0.419	0.430	0.435	0.430	0.434	0.432	0.429	0.441	0.429	0.415	0.411	0.512
0.366	0.375	0.362	0.288	0.283	0.282	0.283	0.283	0.281	0.394	0.403	0.501
0.304	0.310	0.306	0.429	0.431	0.435	0.427	0.431	0.429	0.347	0.351	0.508
0.239	0.245	0.245	0.280	0.283	0.275	0.279	0.289	0.283	0.348	0.355	0.514
0.179	0.181	0.183	0.105	0.109	0.110	0.111	0.111	0.112	0.113	0.113	0.486

	Media	Desviación estandar	CV%
Blanco	0.108	0.003492253	3%

Absorbancias

µg/mL proteina												
32	0.461	0.485	0.479	N.P.	N.P.	N.P.	N.P.	N.P.	N.P.	N.P.	N.P.	0.375
28	0.437	0.430	0.434	0.321	0.322	0.308	0.327	0.303	0.328	0.367	0.366	0.398
24	0.378	0.384	0.395	0.165	0.176	0.172	0.170	0.169	0.176	0.354	0.358	0.421
20	0.311	0.322	0.327	0.322	0.326	0.324	0.321	0.333	0.321	0.307	0.303	0.404
16	0.258	0.267	0.254	0.180	0.175	0.174	0.175	0.175	0.173	0.286	0.295	0.393
12	0.196	0.202	0.198	0.321	0.323	0.327	0.319	0.323	0.321	0.239	0.243	0.400
8	0.131	0.137	0.137	0.172	0.175	0.167	0.171	0.181	0.175	0.240	0.247	0.406
4	0.071	0.073	0.075	N.P.	N.P.	N.P.	N.P.	N.P.	N.P.	N.P.	N.P.	0.378

Recta patrón

RP		
Media	Desvest	CV%
0.475	0.012	0.026
0.434	0.004	0.008
0.386	0.009	0.022
0.320	0.008	0.026
0.260	0.007	0.026
0.199	0.003	0.015
0.135	0.003	0.026
0.073	0.002	0.027

Recta	
Intersección eje	0.02
Pendiente	0.01
R2	1.00

Standard curve plate 3 µBCA

$R^2 = 0.9965$

Análisis muestras

Sample 1				
	Media	Desvest	CV%	Concentración
C1	0.32	0.00	1	5.00E+07
C2	0.17	0.01	3	2.50E+07

Sample 1			
	µg/mL	bact/mL	mg/mL teóricos
C1	20.6	5.00E+07	20.25
C2	10.4	2.50E+07	10.12

Sample 2				
	Media	Desvest	CV%	Concentración
C1	0.32	0.01	2	5.00E+07
C2	0.17	0.00	2	2.50E+07

Sample 2			
	µg/mL	bact/mL	mg/mL teóricos
C1	20.4	5.00E+07	20.25
C2	10.3	2.50E+07	10.12

Sample 3				
	Media	Desvest	CV%	Concentración
C1	0.32	0.01	3	5.00E+07
C2	0.17	0.00	2	2.50E+07

Sample 3			
	µg/mL	bact/mL	mg/mL teóricos
C1	20.5	5.00E+07	20.25
C2	10.5	2.50E+07	10.12

Paso por la recta de las muestras			
	Sample 1	Sample 2	Sample 3
C1	6473	6440	6451
C2	6561	6461	6604

Concentración proteica en 1.58E+10 bacterias/mL			
	Sample 1	Sample 2	Sample 3
Promedio	6517	6451	6528
Desvest	62.5	14.5	108.1
CV%	1%	0%	2%

Media muestras	Desviacion estandar	Varianza	CV%
6498	42	1736	1%

Normalización 1E+09 bacterias

Sample 1	Sample 2	Sample 3
412.5	408.3	413.1

Media	Desviación estandar	CV%	Varianza
411.3	2.64	1%	7

Sistem suitability

	Promedio	Desviación estandar	CV			Concentración experimental µg/mL	Concentración teórica µg/mL
Control QC3	0.397	0.015	4%		Control QC3	25.6	24,0 µg/mL

Accuracy

Media OD accuracy				
	Media	Desvest	CV%	Concentración
C1	0.36	0.01	1.7	2.50E+07
C2	0.30	0.01	3.1	2.50E+07
C3	0.24	0.00	1.5	2.50E+07

OD pasada por la recta accuracy		
	µg/mL	bact/mL
C1	23.2	2.50E+07
C2	18.9	2.50E+07
C2	15.1	2.50E+07

Recovery (se resta concentración experimental)		
	Concetntración experimental	Concentración teórica	Recovery
C1	12.8	12.0	107%
C2	8.5	8.0	106%
C3	4.7	4.0	117%

Sistem suitability

	Resultado	Conforme
1. OD562 NaCl 0.9% ≤ 0.15	0.11	Conforme
2. r2 coeficiente de determinación de Pearson estandar ≥ 0.98.	1.00	Conforme
3. Recta estándar realizada con mínimo 6 puntos. No pueden despreciarse dos valores consecutivos.	8	Confome
4. Recovery 12 µg/mL	107%	Conforme
5. Recovery 8 µg/mL	106%	Conforme
6. Recovery 4 µg/mL	117%	Conforme
7. CV máximo de los distintos puntos de la recta ≤ 10%	3%	Conforme
8. Method precision ≤ 15%	1%	Conforme
9. Sistem suitability ≤ 27.6 µg/mL y ≥ 20.4 µg/mL	25.6	Conforme

Plate 4 (A1D2)

			Condición	105254 N.P.			Fecha	17/07/2019			
EP0281_04							Analista	Mariona Canyellas			

RAW DATA

0.605	0.608	0.574	0.111	0.107	0.104	0.104	0.105	0.108	0.109	0.106	0.512
0.536	0.543	0.541	0.435	0.418	0.412	0.410	0.410	0.411	0.452	0.456	0.504
0.499	0.494	0.530	0.279	0.284	0.270	0.270	0.275	0.271	0.461	0.457	0.479
0.423	0.427	0.403	0.429	0.430	0.412	0.411	0.415	0.415	0.392	0.407	0.501
0.359	0.370	0.357	0.283	0.283	0.270	0.269	0.274	0.278	0.399	0.399	0.506
0.304	0.304	0.302	0.422	0.421	0.411	0.409	0.420	0.405	0.328	0.337	0.511
0.243	0.248	0.252	0.286	0.277	0.273	0.269	0.274	0.274	0.35	0.34	0.505
0.200	0.261	0.183	0.111	0.113	0.110	0.108	0.115	0.109	0.11	0.111	0.514

	Media	Desviación estandar	CV%
Blanco	0.109	0.003	3%

Absorbancias

µg/mL proteina												
32	0.496	0.499	0.465	N.P.	N.P.	N.P.	N.P.	N.P.	N.P.	N.P.	N.P.	0.403
28	0.427	0.434	0.432	0.326	0.309	0.303	0.301	0.301	0.302	0.343	0.347	0.395
24	0.390	0.385	0.421	0.170	0.175	0.161	0.161	0.166	0.162	0.352	0.348	0.370
20	0.314	0.318	0.294	0.320	0.321	0.303	0.302	0.306	0.306	0.283	0.298	0.392
16	0.250	0.261	0.248	0.174	0.174	0.161	0.160	0.165	0.169	0.290	0.290	0.397
12	0.195	0.195	0.193	0.313	0.312	0.302	0.300	0.311	0.296	0.219	0.228	0.402
8	0.134	0.139	0.143	0.177	0.168	0.164	0.160	0.165	0.165	0.241	0.231	0.396
4	0.091	0.152	0.074	N.P.	N.P.	N.P.	N.P.	N.P.	N.P.	N.P.	N.P.	0.405

RP

Media	Desvest	CV%
0.487	0.019	4%
0.431	0.004	1%
0.399	0.020	5%
0.309	0.013	4%
0.253	0.007	3%
0.195	0.001	1%
0.139	0.005	3%
0.106	0.041	39%

Recta patrón

Recta	
Intersección eje	0.02
Pendiente	0.01
R2	0.99

Standard curve plate 4 µBCA — $R^2 = 0.9965$

Análisis muestras

Sample 1

	Media	Desvest	CV%	Concentración
C1	0.32	0.01	2	5.00E+07
C2	0.17	0.00	2	2.50E+07

Sample 1

	µg/mL	bact/mL	mg/mL teóricos
C1	20.1	5.00E+07	20.25
C2	10.4	2.50E+07	10.12

Sample 2

	Media	Desvest	CV%	Concentración
C1	0.30	0.00	0	5.00E+07
C2	0.16	0.00	1	2.50E+07

Sample 2

	µg/mL	bact/mL	mg/mL teóricos
C1	19.1	5.00E+07	20.25
C2	9.6	2.50E+07	10.12

Sample 3

	Media	Desvest	CV%	Concentración
C1	0.30	0.01	2	5.00E+07
C2	0.17	0.00	1	2.50E+07

Sample 3

	µg/mL	bact/mL	mg/mL teóricos
C1	19.2	5.00E+07	20.25
C2	9.9	2.50E+07	10.12

Paso por la recta de las muestras

	Sample 1	Sample 2	Sample 3
C1	6320	6002	6041
C2	6538	6036	6213

Concentración proteica en 1.58E+10 bacterias/mL

	Sample 1	Sample 2	Sample 3
Promedio	6429	6019	6127
Desvest	154.1	24.1	121.6
CV%	2%	0%	2%

Media muestras	Desviación estandar	Varianza	CV%
6191	213	45196	3%

Normalización 1E+09 bacterias

Sample 1	Sample 2	Sample 3
406.9	380.9	387.8

Media	Desviación estandar	CV%
391.9	13.5	3%

Sistem suitability

	Promedio	Desviación estandar	CV
Control QC3	0.395	0.01103242	3%

	Concentración experimental µg/mL	Concentración teórica µg/mL
Control QC3	25.3	24.0

Accuracy

Media OD accuracy

	Media	Desvest	CV%	Concentración
C1	0.35	0.00	1	2.50E+07
C2	0.29	0.01	2	2.50E+07
C3	0.23	0.01	4	2.50E+07

OD pasada por la recta accuracy

	µg/mL	bact/mL
C1	22.1	2.50E+07
C2	18.3	2.50E+07
C2	14.2	2.50E+07

Recovery (se resta concentración experimental)

	Concentración experimental	Concentración teórica	Recovery
C1	12.2	12.0	102%
C2	8.3	8.0	104%
C3	4.3	4.0	106%

Sistem suitability

	Resultado	Conforme
1. OD562 NaCl 0.9% ≤ 0.15	0.11	Conforme
2. r2 coeficiente de determinación de Pearson estandar ≥ 0.98.	0.99	Conforme
3. Recta estándar realizada con mínimo 6 puntos. No pueden despreciarse dos valores consecutivos.	7	Confome
4. Recovery 12 µg/mL	102%	Conforme
5. Recovery 8 µg/mL	104%	Conforme
6. Recovery 4 µg/mL	106%	Conforme
7. CV máximo de los distintos puntos de la recta ≤ 10%	5%	Conforme
8. Method precision ≤ 15%	3%	Conforme
9. Sistem suitability ≤ 27.6 µg/mL y ≥ 20.4 µg/mL	25.3	Conforme

Annex 2

Batch 4 5ºC

Parameter	Acceptance criteria	INITIAL	1 MONTH	3 MONTHS	6 MONTHS
APPEARANCE					
Visual Appearance	White freeze dried form. Incomplete reconstitution	Normal		Lumps	Lumps
IDENTITY					
Protein ID. by Molecular Size SDS-PAGE	Report the value	Comply		Comply	Comply
Protein ID. by WB SDS-PAGE-r / nr	Electrophoretic mobility of band recognized by the mAb anti-*A baumannii* comparable to RS	Comply		Comply	Comply
ASSAY					
Total Protein	Report the value	4773 mg/mL		4762 µg/mL	4038 µg/mL
ELISA Potency	Report the value	1.1E+10 bacteria/mL		7.7E+09 bacteria/mL Reanalysis: 1.1E+10 bacteria/mL	2.5E+10 bacteria/mL
PHYSCHEM & CHARACTERIZATION					
Residual Moisture	Report the value	1.9% H20			2.0% H20

Batch 5 25ºC

Parameter	SOP	Acceptance criteria	INITIAL	1 MONTH	3 MONTHS	6 MONTHS
APPEARANCE						
Visual Appearance	NA	White freeze-dried form. Incomplete reconstitution	Normal	Lumps	Lumps	Lumps
IDENTITY						
Protein ID. by Molecular Size SDS-PAGE	NA	Report the value	Comply	Comply	Comply	Comply
Protein ID. by WB SDS-PAGE-r / nr	NA	Electrophoretic mobility of band recognized by the mAb anti-*A baumannii* comparable to RS	Comply	Comply	Comply	Comply
ASSAY						
Total Protein	NA	Report the value	4773 µg/mL	4228µg/mL	4721 µg/mL	4113 µg/mL
ELISA Potency	NA	Report the value	1.1E+10 bacteria/mL	1.2E+10 bacteria/mL	7.2E+09 bacteria/mL Reanalysis: 1.3E+10 bacteria/mL	1.93E+10 bacteria/mL
PHYSCHEM & CHARACTERIZATION						
Residual Moisture	NA	Report the value	1.9% H20	1.7% H20		2.4% H20

Batch 4 40ºC

Parameter	SOP	Acceptance criteria	INITIAL	1 MONTH	3 MONTHS	6 MONTHS
APPEARANCE						
Visual Appearance	NA	White freeze-dried form. Incomplete reconstitution	Normal	Lumps	Lumps	Lumps
IDENTITY						
Protein ID. by Molecular Size SDS-PAGE	NA	Report the value	Comply	Comply	Comply	Comply
Protein ID. by WB SDS-PAGE-r / nr	NA	Electrophoretic mobility of band recognized by the mAb anti-*A baumannii* comparable to RS	Comply	Comply	Comply	Comply
ASSAY						
Total Protein	NA	Report the value	4773µg/mL	4302 µg/mL	4823 µg/mL	4110 µg/mL
ELISA Potency	NA	Report the value	1.1E+10 bacteria/mL	1.3E+10 bacteria/mL	7.2E+09 bacteria/mL Reanalysis: 1.2E+10 bacteria/mL	2.2E+10 bacteria/mL
PHYSCHEM & CHARACTERIZATION						
Residual Moisture	NA	Report the value	1.9% H2O	2.2% H2O	2.2% H2O	3.3% H2O

Batch 18 5ºC

Parameter	SOP	Acceptance criteria	INITIAL	1 MONTH	Theoretical
			Date: 11/03/2019	Date: 23/04/2019	
APPEARANCE					
Visual Appearance	NA	White freeze-dried form. Incomplete reconstitution	Normal	Normal	Normal
IDENTITY					
Protein ID. by Molecular Size SDS-PAGE	NA	Report the value	Comply	Comply	Comply
Protein ID. by WB SDS-PAGE-r / nr	NA	Electrophoretic mobility of band recognized by the mAb anti-*A baumannii* comparable to RS	Comply	Comply	Comply
ASSAY					
Total Protein	NA	Report the value	313.4 µg/mL	303.2 µg/mL	404 mg/mL
ELISA Potency	NA	Report the value	7.35E+08 bacteria/mL	8.82E+08 bacteria/mL	7,90E+08
PHYSCHEM & CHARACTERIZATION					
Residual Moisture	NA	Report the value	6.7% H2O	8.5% H2O	N.P.

Batch 18 40ºC

Parameter	SOP	Acceptance criteria	INITIAL Date: 11/03/2019	1 MONTH Date: 23/04/2019	Theoretical
APPEARANCE					
Visual Appearance	NA	White freeze-dried form. Incomplete reconstitution	Normal	Normal	Normal
IDENTITY					
Protein ID. by Molecular Size SDS-PAGE	NA	Report the value	Comply	Comply	Comply
Protein ID. by WB SDS-PAGE-r / nr	NA	Electrophoretic mobility of band recognized by the mAb anti-*A baumannii* comparable to RS	Comply	Comply	Comply
ASSAY					
Total Protein	NA	Report the value	313.4 µg/mL	294.7 µg/mL	404.0 mg/mL
ELISA Potency	NA	Report the value	7.35+08 bacteria/mL	8.01E+08 bacteria/mL	7.90E+08
PHYSCHEM & CHARACTERIZATION					
Residual Moisture	NA	Report the value	6.7% H2O	8.5% H2O	N.P.

Batch 19 5ºC

Parameter	SOP	Acceptance criteria	INITIAL	1 MONTH
				Date:
APPEARANCE				
Visual Appearance	NA	White freeze-dried form. Incomplete reconstitution	Normal	Normal
IDENTITY				
Protein ID. by Molecular Size SDS-PAGE	NA	Report the value	Lower than expected	Normal
Protein ID. by WB SDS-PAGE-r / nr	NA	Electrophoretic mobility of band recognized by the mAb anti-*A baumannii* comparable to RS	Comply	Comply
ASSAY				
Total Protein	NA	Report the value	307.3 µg/mL	303.4 µg/mL
ELISA Potency	NA	Report the value	4.38E+08 bacteria/mL	6.39E+08 bacteria/mL
PHYSCHEM & CHARACTERIZATION				
Residual Moisture	NA	Report the value	7.5% H2O	10.1% H2O

Batch 19 40ºC

Parameter	SOP	Acceptance criteria	INITIAL	1 MONTH
				Date:
APPEARANCE				
Visual Appearance	NA	White freeze-dried form. Incomplete reconstitution	Normal	Normal
IDENTITY				
Protein ID. by Molecular Size SDS-PAGE	NA	Report the value	Comply	Comply
Protein ID. by WB SDS-PAGE-r / nr	NA	Electrophoretic mobility of band recognized by the mAb anti-*A baumannii* comparable to RS	Comply	Comply
ASSAY				
Total Protein	NA	Report the value	307.3 µg/mL	315.5 µg/mL
ELISA Potency	NA	Report the value	4.38E+08 bacteria/mL	7.29+08 bacteria/mL
PHYSCHEM & CHARACTERIZATION				
Residual Moisture	NA	Report the value	7.5% H2O	No measurable

Batch 26 5ºC 8kGy

Parameter	SOP	Acceptance criteria	Non irradiated	First analysis	INITIAL	1 MONTH	3 MONTHS	6 MONTHS	9 MONTHS
			14/10/19	25/11/19	Date: 17/02/2020		Date: 17/05/2020	Date: 17/08/2020	Date: 25/11/2020
APPEARANCE									
Visual Appearance	NA	White suspension*	White lyophilizate	White lyophilizate	White lyophilizate		White lyophilizate	White lyophilizate	White lyophilizate
IDENTITY									
Protein ID. by Molecular Size SDS-PAGE	NA	Accordant to pre-validation information	Comply	Comply	Comply		Comply	Comply	Comply
Protein ID. by WB SDS-PAGE-r / nr	NA	Accordant to pre-validation information	Comply	Comply	Comply		Comply	Comply	Comply
ASSAY									
Total Protein (µg/mL)	NA	Report the value	861 (105%)	1087 (127%)	1194 (140%)		1033 (134%)	1100 (128%)	987 (128%)
µBCA Potency (bacteria/mL)	NA	Report the value	2.05E+07	2.51E+09	2.52E+09		2.60E+09	2.43E+09	2.37E+09 (118%)
PHYSCHEM & CHARACTERIZATION									
Ph	NA	Report the value	6.3	5.81	6.06		6.1	6.33	6.1
Osmolarity (Osmol/L)	NA	Report the value	0.307	0.307	0.363		0.314	0.306	0.302
Reconstitution time (seconds)	NA	Report the value	5	8.3	5		5	5	5
Residual water content (%H20)	NA	Report the value	N.P.	4.0%	4.2%		N.P.	N.P.	NP

Batch 26 5ºC 15kGy

Parameter	SOP	Acceptance criteria	Non irradiated 14/10/19	First analysis 25/11/19	INITIAL Date: 17/02/2020	1 MONTH	3 MONTHS Date: 17/05/2020
APPEARANCE							
Visual Appearance	NA	White suspension (when it stands it separates in two phases that can be resuspended after shaking)	White lyophilizate	White lyophilizate	White lyophilizate		White lyophilizate
IDENTITY							
Protein ID. by Molecular Size SDS-PAGE	NA	Accordant to pre-validation information	Comply	Comply	Comply		Comply
Protein ID. by WB SDS-PAGE-r / nr	NA	Accordant to pre-validation information	Comply	Comply	Comply		Comply
ASSAY							
Total Protein (µg/mL)	NA	Report the value	861 (105%)	1173 (145%)	1268 (148%)		1072 (139%)
µBCA Potency (bacteria/mL)	NA	Report the value	2.05E+07	2.63E+09	2.93E+09		2.71E+09
PHYSCHEM & CHARACTERIZATION							
Ph	NA	Report the value	6.3	5.9	6.0		6.03
Osmolarity (Osmol/L)	NA	Report the value	0.307	0.301	0.342		0.308
Reconstitution time (seconds)	NA	Report the value	5	4.7	5		5
Residual water content (%H20)	NA	Report the value	N.P.	3.7%	3.7%		N.P.

Batch 26 5ºC 25kGy

Parameter	SOP	Acceptance criteria	Non irradiated 14/10/19	First analysis 25/11/19	INITIAL Date: 17/02/2020	1 MONTH	3 MONTHS Date: 17/05/2020
APPEARANCE							
Visual Appearance	NA	White lyophilizate	White lyophilizate	White lyophilizate	White lyophilizate		White lyophilizate
IDENTITY							
Protein ID. by Molecular Size SDS-PAGE	NA	Accordant to pre-validation information	Comply	Comply	Comply		Comply
Protein ID. by WB SDS-PAGE-r / nr	NA	Accordant to pre-validation information	Comply	Comply	Comply		Comply
ASSAY							
Total Protein (µg/mL)	NA	Report the value	861 (105%)	1332 (164%)	1503 (176%)		1438 (186%)
µBCA Potency (bacteria/mL)	NA	Report the value	2.05E+07	3.25E+09	3.54E+09		3.76E+09
PHYSCHEM & CHARACTERIZATION							
Ph	NA	Report the value	6.3	6.5	6.0		5.9
Osmolarity (Osmol/L)	NA	Report the value	0.307	0.302	0.348		0.31
Reconstitution time (seconds)	NA	Report the value	5	5	5		5
Residual water content (%H20)	NA	Report the value	N.P.	2.6%	2.6%		N.P.

Batch 27 5ºC 8kGy

Parameter	SOP	Acceptance criteria		First analysis	INITIAL	1 MONTH	3 MONTHS	6 MONTHS	9 MONTHS

			Non-irradiated	25/11/19	Date: 28/01/2020		Date: 17/05/2020	Date: 17/08/2020	Date: 17/11/2020
APPEARANCE									
Visual Appearance	NA	White lyophilizate	White lyophilizate	White lyophilizate	White lyophilizate		White lyophilizate	White lyophilizate	White lyophilizate
IDENTITY									
Protein ID. by Molecular Size SDS-PAGE	NA	Accordant to pre-validation information	Comply	Comply	Comply		Comply	Comply	Comply
Protein ID. by WB SDS-PAGE-r / nr	NA	Accordant to pre-validation information	Comply	Comply	Comply		Comply	Comply	Comply
ASSAY									
Total Protein (µg/mL)	NA	Report the value	2076 (102%)	2448 (125%)	2611 (122%)		2223 (113%)	2364 (110%)	1987 (99%)
µBCA Potency (bacteria/mL)	NA	Report the value	4.92E+09	6.22E+09	5.87E+09		5.35E+09	5.04E+09	4.51E+09 (90%)
PHYSCHEM & CHARACTERIZATION									
Ph	NA	Report the value	6.4	5.8	6.3		6.28	6.34	6.29
Osmolarity (Osmol/L)	NA	Report the value	0.297	0.291	0.329		0.285	0.284	0.287
Reconstitution time (seconds)	NA	Report the value	5	3	7		5	5	5
Residual water content (%H20)	NA	Report the value	N.P.	2.4%	2.0%		N.P.	N.P.	NP

Batch 27 25ºC 8kGy

Parameter	SOP	Acceptance criteria		First analysis	INITIAL	1 MONTH	3 MONTHS	6 MONTHS	9 MONTHS

			Non-irradiated	Date: 25/11/19	Date: 28/01/2020	Date: 17/03/2020	Date: 17/05/2020	Date: 17/08/2020	Date: 17/11/2020
APPEARANCE									
Visual Appearance	NA	White lyophilizate	White lyophilizate	white lyophilizate	white lyophilizate		white lyophilizate	white lyophilizate	white lyophilizate
IDENTITY									
Protein ID. by Molecular Size SDS-PAGE	NA	Accordant to pre-validation information	Comply	Comply	Comply		Comply	Comply	Comply
Protein ID. by WB SDS-PAGE-r / nr	NA	Accordant to pre-validation information	Comply	Comply	Comply		Comply	Comply	Comply
ASSAY									
Total Protein (µg/mL)	NA	Report the value	2076 (102%)	2448 (125%)	2611 (122%)		2255 (115%)	2613 (122%)	2323 (116%)
µBCA Potency (bacteria/mL)	NA	Report the value	4.92E+09	6.22E+09	5.87E+09		4.96E+09	5.71E+09	5.5E+09 (110%)
PHYSCHEM & CHARACTERIZATION									
Ph	NA	Report the value	6.4	5.8	6.3		6.28	6.20	6.27
Osmolarity (Osmol/L)	NA	Report the value	0.297	0.291	0.329		0.287	0.286	0.291
Reconstitution time (seconds)	NA	Report the value	5	3	7		5	5	5
Residual water content (%H20)	NA	Report the value	N.P.	2.4%	2.0%		N.P	N.P	N.P

Batch 27 5ºC 15 kGy

Parameter	SOP	Acceptance criteria	Non-irradiated	First analysis 25/11/19	INITIAL Date: 28/01/2020	1 MONTH Date: 17/03/2020	3 MONTHS Date: 17/05/2020
APPEARANCE							
Visual Appearance	NA	White lyophilizate	White lyophilizate	white lyophilizate	white lyophilizate		white lyophilizate
IDENTITY							
Protein ID. by Molecular Size SDS-PAGE	NA	Accordant to pre-validation information	Comply	Comply	Comply		Comply
Protein ID. by WB SDS-PAGE-r / nr	NA	Accordant to pre-validation information	Comply	Comply	Comply		Comply
ASSAY							
Total Protein (µg/mL)	NA	Report the value	2076 (102%)	2730 (135%)	2704 (127%)		2285 (116%)
µBCA Potency (bacteria/mL)	NA	Report the value	4.92E+09	6.86E+09	6.11E+09		5.53E+09
PHYSCHEM & CHARACTERIZATION							
Ph	NA	Report the value	6.4	6.0	6.4		6.3
Osmolarity (Osmol/L)	NA	Report the value	0.30	0.29	0.33		0.287
Reconstitution time (seconds)	NA	Report the value	5	3	4		5
Residual water content (%H20)	NA	Report the value	N.P.	2.1%	2.0%		N.P.

Batch 27 25ºC 15 kGy

Parameter	SOP	Acceptance criteria	Non-irradiated	First analysis 25/11/19	INITIAL Date: 28/01/2020	1 MONTH Date: 17/03/2020	3 MONTHS Date: 17/05/2020
APPEARANCE							
Visual Appearance	NA	White lyophilizate	White lyophilizate	white lyophilizate	white lyophilizate		white lyophilizate
IDENTITY							
Protein ID. by Molecular Size SDS-PAGE	NA	Accordant to pre-validation information	Comply	Comply	Comply		Comply
Protein ID. by WB SDS-PAGE-r / nr	NA	Accordant to pre-validation information	Comply	Comply	Comply		Comply
ASSAY							
Total Protein (µg/mL)	NA	Report the value	2076 (102%)	2730 (135%)	2704 (127%)		2352 (120%)
µBCA Potency (bacteria/mL)	NA	Report the value	4.92E+09	6.86E+09	6.11E+09		5.72E+09
PHYSCHEM & CHARACTERIZATION							
Ph	NA	Report the value	6.4	6.0	6.4		6.23
Osmolarity (Osmol/L)	NA	Report the value	0.297	0.29	0.334		0.284
Reconstitution time (seconds)	NA	Report the value	5	3	4		5
Residual water content (%H20)	NA	Report the value	N.P.	2.1%	2.0%		N.P

Batch 27 5ºC 25 kGy

Parameter	SOP	Acceptance criteria	Non-irradiated	First analysis 25/11/19	INITIAL Date: 28/01/2020	1 MONTH Date: 17/03/2020	3 MONTHS Date: 17/05/2020
APPEARANCE							
Visual Appearance	NA	White lyophilizate	White lyophilizate	White lyophilizate	White lyophilizate		White lyophilizate
IDENTITY							
Protein ID. by Molecular Size SDS-PAGE	NA	Accordant to pre-validation information	Comply	Comply	Comply		Comply
Protein ID. by WB SDS-PAGE-r / nr	NA	Accordant to pre-validation information	Comply	Comply	Comply		Comply
ASSAY							
Total Protein (µg/mL)	NA	Report the value	2076 (102%)	2724 (134%)	2915 (136%)		2692 (137%)
µBCA Potency (bacteria/mL)	NA	Report the value	4.92E+09	7.24E+09	6.66E+09		6.69E+09
PHYSCHEM & CHARACTERIZATION							
Ph	NA	Report the value	6.4	6.0	6.4		6.21
Osmolarity (Osmol/L)	NA	Report the value	0.297	0.285	0.328		0.285
Reconstitution time (seconds)	NA	Report the value	5	3	4		5
Residual water content (%H20)	NA	Report the value	N.P.	3.1%	3.0%		N.P.

Batch 27 25ºC 25 kGy

Parameter	SOP	Acceptance criteria	Non-irradiated	First analysis 25/11/19	INITIAL Date: 28/01/2020	1 MONTH Date: 17/03/2020	3 MONTHS Date: 17/05/2020
APPEARANCE							
Visual Appearance	NA	White lyophilizate	White lyophilizate	white lyophilizate	white lyophilizate		white lyophilizate
IDENTITY							
Protein ID. by Molecular Size SDS-PAGE	NA	Accordant to pre-validation information	Comply	Comply	Comply		Comply
Protein ID. by WB SDS-PAGE-r / nr	NA	Accordant to pre-validation information	Comply	Comply	Comply		Comply
ASSAY							
Total Protein (µg/mL)	NA	Report the value	2076 (102%)	2724 (134%)	2915 (136%)		2955 (150%)
µBCA Potency (bacteria/mL)	NA	Report the value	4.92E+09	7.24E+09	6.66E+09		7.49E+09
PHYSCHEM & CHARACTERIZATION							
Ph	NA	Report the value	6.4	6.0	6.4		6.21
Osmolarity (Osmol/L)	NA	Report the value	0.297	0.285	0.328		0.286
Reconstitution time (seconds)	NA	Report the value	5	3	4		5
Residual water content (%H20)	NA	Report the value	N.P.	3.1%	3.0%		N.P.

Batch 29 5ºC 8 kGy

Parameter	SOP	Acceptance criteria	Non irradiated Date: 16/12/2019	INITIAL Date: 28/01/2020	1 MONTH Date: 17/03/2020	3 MONTHS Date: 17/05/2020	6 MONTHS Date: 17/08/2020	9 MONTHS Date: 17/11/2020
APPEARANCE								
Visual Appearance	NA	White suspension (when it stands it separates in two phases that can be resuspended after shaking)	Comply	Comply		Comply	Comply	Comply
IDENTITY								
Protein ID. by Molecular Size SDS-PAGE	NA	Accordant to pre-validation information	Comply	Comply		Comply	Comply	Comply
Protein ID. by WB SDS-PAGE-r / nr	NA	Accordant to pre-validation information	Comply	Comply		Comply	Comply	Comply
ASSAY								
Total Protein (µg/mL)	NA	Report the value	2321 (120%)	2801 (131%)		2548 (118%)	2766 (129%)	2597 (130%)
µBCA Potency (bacteria/mL)	NA	Report the value	5.96E+09	6.36E+09		5.81E+09	6.13E+09	2.51E+09 (125%)
PHYSCHEM & CHARACTERIZATION								
Ph	NA	Report the value	6.73	5.2		6.0	6.12	6.14
Osmolarity (Osmol/L)	NA	Report the value	0.276	0.275		0.277 (CV = 0%)	0.278	0.277

Batch 29 25ºC 8 kGy

Parameter	SOP	Acceptance criteria	Non irradiated	INITIAL	1 MONTH	3 MONTHS
			Date: 16/12/2019	Date: 28/01/2020	Date: 17/03/2020	Date: 17/05/2020
APPEARANCE						
Visual Appearance	NA	White suspension (when it stands it separates in two phases that can be resuspended after shaking)	Comply	Comply		Comply
IDENTITY						
Protein ID. by Molecular Size SDS-PAGE	NA	Accordant to pre-validation information	Comply	Comply		Comply
Protein ID. by WB SDS-PAGE-r / nr	NA	Accordant to pre-validation information	Comply	Comply		Comply
ASSAY						
Total Protein (µg/mL)	NA	Report the value	2321 (120%)	2801 (131%)		2445 (113%)
µBCA Potency (bacteria/mL)	NA	Report the value	5.96E+09	6.36E+09		5.23E+09
PHYSCHEM & CHARACTERIZATION						
Ph	NA	Report the value	6.7	5.2		5.72
Osmolarity (Osmol/L)	NA	Report the value	0.276	0.275		0.279 (CV = 0%)

Batch 29 5ºC 15 kGy

Parameter	SOP	Acceptance criteria	Non irradiated Date: 16/12/2019	INITIAL Date: 28/01/2020	1 MONTH Date: 17/03/2020	3 MONTHS Date: 17/05/2020
APPEARANCE						
Visual Appearance	NA	White suspension (when it stands it separates in two phases that can be resuspended after shaking)	Comply	Comply		Comply
IDENTITY						
Protein ID. by Molecular Size SDS-PAGE	NA	Accordant to pre-validation information	Comply	Comply		Comply
Protein ID. by WB SDS-PAGE-r / nr	NA	Accordant to pre-validation information	Comply	Comply		Comply
ASSAY						
Total Protein (µg/mL)	NA	Report the value	2321 (120%)	2773 (129%)		2455 (113%)
µBCA Potency (bacteria/mL)	NA	Report the value	5.96E+09	6.28E+09		5.26E+09
PHYSCHEM & CHARACTERIZATION						
Ph	NA	Report the value	6.7	5.2		5.9
Osmolarity (Osmol/L)	NA	Report the value	0.276	0.277		0.278 (CV = 0%)

Batch 29 25ºC 15 kGy

Parameter	SOP	Acceptance criteria	Non irradiated	INITIAL	1 MONTH	3 MONTHS
			Date: 16/12/2019	Date: 28/01/2020	Date: 17/03/2020	Date: 17/05/2020
APPEARANCE						
Visual Appearance	NA	White suspension (when it stands it separates in two phases that can be resuspended after shaking)	Comply	Comply		Comply
IDENTITY						
Protein ID. by Molecular Size SDS-PAGE	NA	Accordant to pre-validation information	Comply	Comply		Comply
Protein ID. by WB SDS-PAGE-r / nr	NA	Accordant to pre-validation information	Comply	Comply		Comply
ASSAY						
Total Protein (µg/mL)	NA	Report the value	2321 (120%)	2773 (129%)		2660 (123%)
µBCA Potency (bacteria/mL)	NA	Report the value	5.96E+09	6.28E+09		5.81E+09
PHYSCHEM & CHARACTERIZATION						
Ph	NA	Report the value	6.7	5.2		5.9
Osmolarity (Osmol/L)	NA	Report the value	0.276	0.277		0.279 (CV = 1%)

Batch 29 5ºC 25 kGy

Parameter	SOP	Acceptance criteria	Non irradiated	INITIAL	1 MONTH	3 MONTHS

			Date: 16/12/2019	Date: 28/01/2020	Date: 17/03/2020	Date: 17/05/2020
APPEARANCE						
Visual Appearance	NA	White suspension (when it stands it separates in two phases that can be resuspended after shaking)	Comply	Comply		Comply
IDENTITY						
Protein ID. by Molecular Size SDS-PAGE	NA	Accordant to pre-validation information	Comply	Comply		Comply
Protein ID. by WB SDS-PAGE-r / nr	NA	Accordant to pre-validation information	Comply	Comply		Comply
ASSAY						
Total Protein (μg/mL)	NA	Report the value	2321 (120%)	2824 (132%)		2569 (119%)
μBCA Potency (bacteria/mL)	NA	Report the value	5.96E+09	6.42E+09		5.57E+09
PHYSCHEM & CHARACTERIZATION						
Ph	NA	Report the value	6.7	5.8		5.6
Osmolarity (Osmol/L)	NA	Report the value	0.276	0.293		0.281 (CV% = 1%)

Batch 29 25ºC 25 kGy

Parameter	SOP	Acceptance criteria	Non irradiated Date: 16/12/2019	INITIAL Date: 28/01/2020	1 MONTH Date: 17/03/2020	3 MONTHS Date: 17/05/2020
APPEARANCE						
Visual Appearance	NA	White suspension (when it stands it separates in two phases that can be resuspended after shaking)	Comply	Comply		Comply
IDENTITY						
Protein ID. by Molecular Size SDS-PAGE	NA	Accordant to pre-validation information	Comply	Comply		Comply
Protein ID. by WB SDS-PAGE-r / nr	NA	Accordant to pre-validation information	Comply	Comply		Comply
ASSAY						
Total Protein (µg/mL)	NA	Report the value	2321 (120%)	2824 (132%)		2500 (116%)
µBCA Potency (bacteria/mL)	NA	Report the value	5.96E+09	6.42E+09		5.38E+09
PHYSCHEM & CHARACTERIZATION						
Ph	NA	Report the value	6.7	5.8		6.2
Osmolarity (Osmol/L)	NA	Report the value	0.276	0.293		0.281 (CV = 2%)

Batch 30 5ºC 8 kGy

Parameter	SOP	Acceptance criteria	Non irradiated Date: 16/12/2019	INITIAL Date: 14/01/2020	1 MONTH Date: 17/03/2020	3 MONTHS Date: 17/05/2020	6 MONTHS Date: 17/08/2020	9 MONTHS Date: 17/11/2020
APPEARANCE								
Visual Appearance	NA	White suspension (when it stands it separates in two phases that can be resuspended after shaking)	Comply	Comply		Comply	Comply	Comply
IDENTITY								
Protein ID. by Molecular Size SDS-PAGE	NA	Accordant to pre-validation information	Comply	Comply		Comply	Comply	Comply
Protein ID. by WB SDS-PAGE-r / nr	NA	Accordant to pre-validation information	Comply	Comply		Comply	Comply	Comply
ASSAY								
Total Protein (µg/mL)	NA	Report the value	899 (126%)	1174		1012	1201 (140%)	1036 (130%)
µBCA Potency (bacteria/mL)	NA	Report the value	2.31E+09	2.39E+09		2.42E+09	2.71E+09	2.51E+09 (125%)
PHYSCHEM & CHARACTERIZATION								
Ph	NA	Report the value	6.3	5.2		5.7	5.9	5.9
Osmolarity (Osmol/L)	NA	Report the value	0.307	0.308		0.306 (CV = 0%)	0.306	0.280

Batch 30 25ºC 8 kGy

Parameter	SOP	Acceptance criteria	Non irradiated Date: 16/12/2019	INITIAL Date: 14/01/2020	1 MONTH Date: 17/03/2020	3 MONTHS Date: 17/05/2020
APPEARANCE						
Visual Appearance	NA	White suspension (when it stands it separates in two phases that can be resuspended after shaking)	Comply	Comply		Comply
IDENTITY						
Protein ID. by Molecular Size SDS-PAGE	NA	Accordant to pre-validation information	Comply	Comply		Comply
Protein ID. by WB SDS-PAGE-r / nr	NA	Accordant to pre-validation information	Comply	Comply		Comply
ASSAY						
Total Protein (µg/mL)	NA	Report the value	899 (126%)	1174		1016
µBCA Potency (bacteria/mL)	NA	Report the value	2.31E+09	2.39E+09		2.43E+09
PHYSCHEM & CHARACTERIZATION						
Ph	NA	Report the value	6.3	5.2		6.0
Osmolarity (Osmol/L)	NA	Report the value	0.307	0.308		0.311 (CV = 2%)

Batch 30 5ºC 15 kGy

Parameter	SOP	Acceptance criteria	Non irradiated Date: 16/12/2019	INITIAL Date: 14/01/2020	1 MONTH Date: 17/03/2020	3 MONTHS Date: 17/05/2020
APPEARANCE						
Visual Appearance	NA	White suspension (when it stands it separates in two phases that can be resuspended after shaking)	Comply	Comply		Comply
IDENTITY						
Protein ID. by Molecular Size SDS-PAGE	NA	Accordant to pre-validation information	Comply	Comply		Comply
Protein ID. by WB SDS-PAGE-r / nr	NA	Accordant to pre-validation information	Comply	Comply		Comply
ASSAY						
Total Protein (μg/mL)	NA	Report the value	899 (126%)	1098		2083
μBCA Potency (bacteria/mL)	NA	Report the value	2.31E+09	2.65E+09		2.62E+09
PHYSCHEM & CHARACTERIZATION						
Ph	NA	Report the value	6.3	5.0		5.5
Osmolarity (Osmol/L)	NA	Report the value	0.307	0.306		0.306 (CV = 0%)

Batch 30 25ºC 15 kGy

Parameter	SOP	Acceptance criteria	Non irradiated	INITIAL	1 MONTH	3 MONTHS
			Date: 16/12/2019	Date: 14/01/2020	Date: 17/03/2020	Date: 17/05/2020
APPEARANCE						
Visual Appearance	NA	White suspension (when it stands it separates in two phases that can be resuspended after shaking)	Comply	Comply		Comply
IDENTITY						
Protein ID. by Molecular Size SDS-PAGE	NA	Accordant to pre-validation information	Comply	Comply		Comply
Protein ID. by WB SDS-PAGE-r / nr	NA	Accordant to pre-validation information	Comply	Comply		Comply
ASSAY						
Total Protein (μg/mL)	NA	Report the value	899 (126%)	1098		865
μBCA Potency (bacteria/mL)	NA	Report the value	2.31E+09	2.65E+09		1.98E+09
PHYSCHEM & CHARACTERIZATION						
Ph	NA	Report the value	6.3	5.0		5.7
Osmolarity (Osmol/L)	NA	Report the value	0.307	0.306		0.308 (CV = 0%)

Batch 30 5ºC 25 kGy

Parameter	SOP	Acceptance criteria	Non irradiated	INITIAL	1 MONTH	3 MONTHS
			Date: 16/12/2019	Date: 28/01/2020	Date: 17/03/2020	Date: 17/05/2020
APPEARANCE						
Visual Appearance	NA	White suspension (when it stands it separates in two phases that can be resuspended after shaking)	Comply	Comply		Comply
IDENTITY						
Protein ID. by Molecular Size SDS-PAGE	NA	Accordant to pre-validation information	Comply	Comply		Comply
Protein ID. by WB SDS-PAGE-r / nr	NA	Accordant to pre-validation information	Comply	Comply		Comply
ASSAY						
Total Protein (µg/mL)	NA	Report the value	899 (126%)	988		975
µBCA Potency (bacteria/mL)	NA	Report the value	2.31E+09	2.20E+09		2.31E+09
PHYSCHEM & CHARACTERIZATION						
Ph	NA	Report the value	6.3	5.2		5.3
Osmolarity (Osmol/L)	NA	Report the value	0.307	0.309		0.306 (CV = 0%)

Batch 30 25ºC 25 kGy

Parameter	SOP	Acceptance criteria	Non irradiated	INITIAL	1 MONTH	3 MONTHS
			Date: 16/12/2019	Date: 14/01/2020	Date: 17/03/2020	Date: 17/05/2020
APPEARANCE						
Visual Appearance	NA	White suspension (when it stands it separates in two phases that can be resuspended after shaking)	Comply	Comply		Comply
IDENTITY						
Protein ID. by Molecular Size SDS-PAGE	NA	Accordant to pre-validation information	Comply	Comply		Comply
Protein ID. by WB SDS-PAGE-r / nr	NA	Accordant to pre-validation information	Comply	Comply		Comply
ASSAY						
Total Protein (µg/mL)	NA	Report the value	899 (126%)	988		915
µBCA Potency (bacteria/mL)	NA	Report the value	2.31E+09	2.20E+09		2.13E+09
PHYSCHEM & CHARACTERIZATION						
Ph	NA	Report the value	6.3	5.2		5.6
Osmolarity (Osmol/L)	NA	Report the value	0.307	0.309		0.309 (CV = 0%)

Batch 37 5ºC

Parameter	SOP	Acceptance criteria	INITIAL	3 MONTHS	6 MONTHS	9 MONTHS
			4/12/20	20/3/21	30/6/21	14/9/21
APPEARANCE						
Visual Appearance	NA	White lyophilizate	White lyophilizate	White lyophilizate	White lyophilizate	White lyophilizate
IDENTITY						
Protein ID. by Molecular Size SDS-PAGE	NA	Accordant to pre-validation information	Comply	-	Comply	-
Protein ID. by WB SDS-PAGE-r / nr	NA	Accordant to pre-validation information	Comply	-	Comply	-
ASSAY						
Total Protein (µg/mL)	NA	Report the value	2332	2069	2204	2094
ELISA Potency (bacteria/mL)	NA	Report the value	3.21E+09*	5.50E+09	4.58E+09	4.94E+09
PHYSCHEM & CHARACTERIZATION						
pH	NA	Report the value	6.5	6.1	6.1	
Osmolarity (Osmol/L)	NA	Report the value	0.300	0.287	0.281	
Reconstitution time (seconds)	NA	Report the value	5	5	5	
Residual water content (%H20)	NA	Report the value	2.1%	-	5.1%	

Batch 37 5ºC 8 kGy

Parameter	SOP	Acceptance criteria	INITIAL	3 MONTHS	6 MONTHS	9 MONTHS
			4/12/20	20/3/21	30/6/21	14/9/21
APPEARANCE						
Visual Appearance	NA	White lyophilizate	White lyophilizate	White lyophilizate	White lyophilizate	White lyophilizate
IDENTITY						
Protein ID. by Molecular Size SDS-PAGE	NA	Accordant to pre-validation information	Comply	-	Comply	-
Protein ID. by WB SDS-PAGE-r / nr	NA	Accordant to pre-validation information	Comply	-	Comply	-
ASSAY						
Total Protein (μg/mL)	NA	Report the value	2217	2084	2274	2268
ELISA Potency (bacteria/mL)	NA	Report the value	3.40 E+09*	6.94E+09	6.46E+09	6.17E+09
PHYSCHEM & CHARACTERIZATION						
pH	NA	Report the value	6.4	6.1	6.1	
Osmolarity (Osmol/L)	NA	Report the value	0.293	0.292	0.280	
Reconstitution time (seconds)	NA	Report the value	5	5	5	
Residual water content (%H20)	NA	Report the value	3.2%	-	7.3%	

Batch 37 25ºC

Parameter	SOP	Acceptance criteria	INITIAL	3 MONTHS	6 MONTHS	9 MONTHS
			4/12/20	20/3/21	30/6/21	14/9/21
APPEARANCE						
Visual Appearance	NA	White lyophilizate	White lyophilizate	White lyophilizate	White lyophilizate	White lyophilizate
IDENTITY						
Protein ID. by Molecular Size SDS-PAGE	NA	Accordant to pre-validation information	Comply	-	Comply	-
Protein ID. by WB SDS-PAGE-r / nr	NA	Accordant to pre-validation information	Comply	-	Comply	-
ASSAY						
Total Protein (µg/mL)	NA	Report the value	2332	1982	2134	2150
ELISA Potency (bacteria/mL)	NA	Report the value	3.21E+09*	5.38E+09	5.40E+09	5.22E+09
PHYSCHEM & CHARACTERIZATION						
pH	NA	Report the value	6.5	6.0	6.1	
Osmolarity (Osmol/L)	NA	Report the value	0.300	0.286	0.280	
Reconstitution time (seconds)	NA	Report the value	5	5	5	
Residual water content (%H20)	NA	Report the value	2.1%	-	5.8%	

Batch 37 25ºC 8 kGy

Parameter	SOP	Acceptance criteria	INITIAL	3 MONTHS	6 MONTHS	9 MONTHS
			4/12/20	20/3/21	30/6/21	14/9/21
APPEARANCE						
Visual Appearance	NA	White lyophilizate	White lyophilizate	White lyophilizate	White lyophilizate	White lyophilizate
IDENTITY						
Protein ID. by Molecular Size SDS-PAGE	NA	Accordant to pre-validation information	Comply	-	Comply	-
Protein ID. by WB SDS-PAGE-r / nr	NA	Accordant to pre-validation information	Comply	-	Comply	-
ASSAY						
Total Protein (µg/mL)	NA	Report the value	2217	2236	2323	2296
ELISA Potency (bacteria/mL)	NA	Report the value	3.40 E+09*	6.89E+09	6.45E+09	6.61E+09
PHYSCHEM & CHARACTERIZATION						
pH	NA	Report the value	6.4	6.0	6.0	
Osmolarity (Osmol/L)	NA	Report the value	0.293	0.288	0.280	
Reconstitution time (seconds)	NA	Report the value	5	5	5	
Residual water content (%H20)	NA	Report the value	3.2%	-	10.1%	

Annex chapter 3

ANOVA analysis of IgG isotype analysis of section 13.1.2:

IgG1				IgG2a				IgG2b			
Sample	Significant	Summary	*p* value	Sample	Significant	Summary	*p* value	Sample	Significant	Summary	*p* value
M1 vs. M2	Yes	*	0.0112	M1 vs. M2	Yes	****	<0,0001	M1 vs. M2	Yes	****	<0.0001
M1 vs. M3	Yes	***	0.0006	M1 vs. M3	Yes	****	<0.0001	M1 vs. M3	Yes	****	<0.0001
M1 vs. M4	Yes	****	<0.0001	M1 vs. M4	Yes	****	<0.0001	M1 vs. M4	Yes	****	<0.0001
M1 vs. M5	Yes	****	<0.0001	M1 vs. M5	Yes	****	<0.0001	M1 vs. M5	Yes	****	<0.0001
M2 vs. M3	No	ns	0.7633	M2 vs. M3	No	ns	0.1774	M2 vs. M3	No	ns	0.9396
M2 vs. M4	Yes	****	<0.0001	M2 vs. M4	Yes	****	<0.0001	M2 vs. M4	Yes	****	<0.0001
M2 vs. M5	Yes	****	<0.0001	M2 vs. M5	Yes	****	<0.0001	M2 vs. M5	Yes	****	<0.0001
M3 vs. M4	Yes	****	<0.0001	M3 vs. M4	Yes	****	<0.0001	M3 vs. M4	Yes	****	<0.0001
M3 vs. M5	Yes	****	<0.0001	M3 vs. M5	Yes	****	<0.0001	M3 vs. M5	Yes	****	<0.0001
M4 vs. M5	No	ns	0.9999	M4 vs. M5	No	ns	>0.9999	M4 vs. M5	No	ns	>0.9999

IgG3				IgM			
Sample	Significant	Summary	*p* value	Sample	Significant	Summary	*p* value
M1 vs. M2	No	ns	0.3287	M1 vs. M2	No	ns	0.9979
M1 vs. M3	No	ns	0.5065	M1 vs. M3	No	ns	0.8151
M1 vs. M4	Yes	**	0.0098	M1 vs. M4	No	ns	0.99
M1 vs. M5	Yes	**	0.0045	M1 vs. M5	No	ns	0.8151
M2 vs. M3	No	ns	0.9975	M2 vs. M3	No	ns	0.9365
M2 vs. M4	No	ns	0.4435	M2 vs. M4	No	ns	0.9999
M2 vs. M5	No	ns	0.2786	M2 vs. M5	No	ns	0.9365
M3 vs. M4	No	ns	0.2786	M3 vs. M4	No	ns	0.971
M3 vs. M5	No	ns	0.1604	M3 vs. M5	No	ns	>0.9999
M4 vs. M5	No	ns	0.9975	M4 vs. M5	No	ns	0.971

M1				M2				M3		
	Significant	Summary	*p* value		Significant	Summary	*p* value		Significant	Summary	*p* value
IgG1 vs. IgG2a	Yes	****	<0.0001	IgG1 vs. IgG2a	Yes	****	<0.0001	IgG1 vs. IgG2a	Yes	****	<0.0001
IgG1 vs. IgG2b	No	ns	>0.9999	IgG1 vs. IgG2b	No	ns	0.1622	IgG1 vs. IgG2b	No	ns	0.9992
IgG1 vs. IgG3	Yes	****	<0.0001	IgG1 vs. IgG3	Yes	****	<0.0001	IgG1 vs. IgG3	Yes	****	<0.0001
IgG1 vs. IgM	Yes	****	<0.0001	IgG1 vs. IgM	Yes	****	<0.0001	IgG1 vs. IgM	Yes	****	<0.0001
IgG2a vs. IgG2b	Yes	****	<0.0001	IgG2a vs. IgG2b	Yes	**	0.0024	IgG2a vs. IgG2b	Yes	****	<0.0001
IgG2a vs. IgG3	Yes	****	<0.0001	IgG2a vs. IgG3	Yes	*	0.0123	IgG2a vs. IgG3	Yes	****	<0.0001
IgG2a vs. IgM	Yes	****	<0.0001	IgG2a vs. IgM	Yes	**	0.0038	IgG2a vs. IgM	Yes	****	<0.0001
IgG2b vs. IgG3	Yes	****	<0.0001	IgG2b vs. IgG3	Yes	****	<0.0001	IgG2b vs. IgG3	Yes	****	<0.0001
IgG2b vs. IgM	Yes	****	<0.0001	IgG2b vs. IgM	Yes	****	<0.0001	IgG2b vs. IgM	Yes	****	<0.0001
IgG3 vs. IgM	No	ns	0.9405	IgG3 vs. IgM	No	ns	0.9886	IgG3 vs. IgM	No	ns	0.8287